

# **THERMAL DEPOLYMERIZATION OF SCRAP TIRES INTO LIQUID FUELS: UPGRADATION AND UTILIZATION IN DIESEL ENGINE**

Thesis

Submitted in partial fulfillment of the requirements for the Degree of

**DOCTOR OF PHILOSOPHY**

by

**AKHIL MOHAN**



**DEPARTMENT OF MECHANICAL ENGINEERING  
NATIONAL INSTITUTE OF TECHNOLOGY KARNATAKA,  
SURATHKAL, MANGALORE – 575025  
DECEMBER, 2021**

# **THERMAL DEPOLYMERIZATION OF SCRAP TIRES INTO LIQUID FUELS: UPGRADATION AND UTILIZATION IN DIESEL ENGINE**

Thesis

Submitted in partial fulfillment of the requirements for the Degree of

**DOCTOR OF PHILOSOPHY**

by

**AKHIL MOHAN**

Under the guidance of

**Dr. VASUDEVA MADAV**

**Dr. SAIKAT DUTTA**  
**(Dept. of Chemistry)**



**DEPARTMENT OF MECHANICAL ENGINEERING  
NATIONAL INSTITUTE OF TECHNOLOGY KARNATAKA,  
SURATHKAL, MANGALORE – 575025  
DECEMBER, 2021**

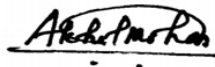
## DECLARATION

I hereby declare that the research thesis entitled “**THERMAL DEPOLYMERIZATION OF SCRAP TIRES INTO LIQUID FUELS: UPGRADATION AND UTILIZATION IN DIESEL ENGINE**” which is being submitted to the **National Institute of Technology Karnataka, Surathkal** in partial fulfillment of the requirements for the award of the degree of **Doctor of Philosophy in Mechanical Engineering** is a *bonafide report of the research work carried out by me*. The material contained in this research thesis has not been submitted to any other Universities or Institutes for the award of any degree.

Register Number: **177076ME001**

Name of the Research Scholar: **AKHIL MOHAN**

Signature of the Research Scholar:



(Department of Mechanical Engineering)

Place: NITK, Surathkal

Date : 27-12-2021

**CERTIFICATE**

This is to certify that the research thesis entitled **“THERMAL DEPOLYMERIZATION OF SCRAP TIRES INTO LIQUID FUELS: UPGRADATION AND UTILIZATION IN DIESEL ENGINE”** submitted by **Mr. AKHIL MOHAN (Register Number: 177076ME001)** as the record of the research work carried out by him, *is accepted as the research thesis submission in partial fulfillment of the requirements for the award of the degree of Doctor of*



**Dr. VASUDEVA MADAV**

Research Guide

Date: 27/12/2021



**Dr. SAIKAT DUTTA**

(Dept. of Chemistry)

Research Co-guide

Date: 27/12/2021



**Chairman, DRPC**

Date: 27/12/2021

**Dr. SATYABODH M. KULKARNI**

Professor & Head

Dept. of Mechanical Engineering  
National Institute of Technology Karnataka, Surathika,  
Srinivasnagar - 575 025, Mangalore (INDIA)



## ACKNOWLEDGMENT

I want to thank **Dr. Vasudeva Madav**, Assistant Professor, Department of Mechanical Engineering, and **Dr. Saikat Dutta**, Assistant Professor, Dept. of Chemistry, for their guidance, understanding, patience, constructive criticism, moral support, and friendly guidance throughout the course of research work at National Institute of Technology, Karnataka, Surathkal. Accurate planning with systematic implementation is a valuable tool to succeed in life, which I have learned. They encouraged me to grow as an experimentalist and as an instructor, and an independent thinker. They have been a great source of inspiration for me, and I remain indebted to them.

I extend my sincere thanks to **Dr. Satyabodh M. Kulkarni**, Professor, HOD Mechanical, for his support and providing the facilities required to complete research work. I take this opportunity to acknowledge former HOD of Mechanical Engineering, **Dr. Narendranath S.**, for his timely support and encouragement.

I am incredibly grateful to **Dr. Kumar G.N.**, Department of Mechanical Engineering, and **Dr. Ravishankar K.S.** for accepting to be members of the Research Progress Assessment Committee (RPAC) and their valuable suggestions during the RPAC meeting.

I wish to express my sincere gratitude to **Prof. Shuichi Torri**, Kumamoto University, Japan and **Prof. Srinivas Seethamraju**, IIT Bombay for evaluating my thesis and their valuable suggestions. I am sincerely thankful to my DTAC Members Dr. Anish S, Dr. Ravishankar K S for their valuable suggestions during Defense seminar.

Special thanks to MHRD, Govt. of India, which helped me to pursue a Ph.D. Program.

Technical support for conducting pilot-scale experiments in a 10-ton rotating autoclave reactor at Mandakan Energy Products is gratefully acknowledged. Their contribution towards waste management of scrap tires as a business model is genuinely inspiring and provides immense motivation to come with the problem statement.

I am forever indebted to all teaching and non-teaching staff of the Department of Mechanical Engineering and Department of Chemistry, NITK, Surathkal, for their friendly support and encouragement. Thanks to **Mr. Chandrasekhar K., Mr. Jayanth, Mr. Yatin, Mr. Vinayraj, Mr. Yashpal** of Internal Combustion Engines Research Laboratory for their help experiments on a single-cylinder diesel engine.

Thanks to SAIF IIT Bombay and SAIF, IIT Madras, Italab, and Chennai to support fuel testing. I am grateful to **Mr. Swarup Banerjee**, LECO, to conduct 2D GC×GC TOF-MS analysis and

process the data using LECO Chroma software. Special appreciation to Dr. Saravanan Balusamy, IIT Hyderabad, for the fruitful discussions on IC Engines and support in conducting fuel property analysis.

I want to thank B-tech students, fellow research scholars, and lab mates for their cheerful cooperation, motivational talks, and encouragement.

Thanks to my mother, **Smt. Jayasree G.**, beloved father, **Shri. Mohanan Pillai S** and my brother Mr. Amal Mohan. Your blessings together have made it possible for me to complete this work, and I am grateful. Finally, I would like to thank my wife, **Mrs. Reshma Babu**, for her unconditional love, encouragement, and patience in completing the research study. I thank Reshma's parents, **Smt. Sreedevi Babu** and **Babu O. N.**, her brother **Rahul Babu** and her sister **Radhika Babu** for their motivation and support.

Many thanks to everybody in my family and my native place and friends for all your love and generous support these years. Every year when I visit home, I am recharged with your smile and your encouraging words.

**AKHIL MOHAN**

## ABSTRACT

Conversion of scrap tire into fuel oils has attracted commercial attention since revenue can be generated from inexpensive and abundant feedstock while easing waste management issues. Globally, 1.5 billion scrap tires are generated every year. Environmental accumulation of tire waste is a global problem, and one way to control the problem is to convert them into fuels and specialty chemicals. There are various approaches for recycling scrap tires, such as re-treading, reclaiming useful products for playgrounds, open incineration, pyrolysis, gasification, and illegal dumping. Illegal dumping often provides a site for breeding mosquitoes, rodents, and larvae formation. Open burning releases a thick black plume of smoke with 1,3-butadiene, nitrogen, carbon, and sulfur oxides with the release of hazardous polyaromatic hydrocarbons. Out of the approaches mentioned above to recycle tires, pyrolysis is an interesting energy recovery process due to the formation of solid (carbon black) and steel wires (in the case of the tire), pyro-gas, along oil products. Production of crude tire pyrolysis oil from scrap tires is a promising approach by thermal depolymerization at an oxygen starved atmosphere and a temperature of 400-600 °C.

The primary objective of present study is to refine CTPO by the principle of selective adsorption and preferential solubility using cost-effective adsorbent and solvent and utilization as a fuel in a single-cylinder diesel engine. A field study was conducted in a 10-ton rotating autoclave reactor to optimize scrap tire pyrolysis parameters (400 °C, 10 °C/min, 0.2 bar, 4 rpm), and investigate the existing problems in the industry with a special focus on applying CTPO in diesel engines. Crude tire pyrolysis oil (CTPO) is a dark brown to black colored syrupy liquid with C<sub>6</sub>-C<sub>24</sub> organic compounds with various classes such as paraffin, olefins, terpenes, aromatics, nitrogen, and sulfur-containing compounds, oxygen-containing compounds. The major challenge for utilizing CTPO in engine or furnace is the inferior fuel properties such as low heat content, low flash point, high acidity, low cetane index, creaming or phase separation in storage tanks, pungent smell due to the presence of dibenzothiophenes and mercaptans. However, thermal distillation is widely used as an upgradation technology implemented in most of the small scale tire pyrolysis units. Distillation needs huge capital investment and energy, making the process less attractive and unsuitable for the long-term run.

In the present study, a straightforward, robust, inexpensive, and scalable up-gradation strategy for refining CTPO by preferential solubility and selective adsorption to utilize single-cylinder direct-injected stationary engines is formulated. A limited study has been attempted for the up-gradation of CTPO using adsorbents and solvents. The present study also envisages extensive

characterization of CTPO, StTPO and diesel to comprehend the fuel chemistry in terms of physical, thermal, and chemical analysis through various analytical techniques. GC×GC TOF-MS analysis showed that sulfur, benzene derivatives, naphthalene's and polyaromatic hydrocarbons were lowered by 48.86%, 25.68%, 43.69%, and 27.79%, respectively. The batch scale process's oil yield is improved by 95% compared to the laboratory scale upgradation strategy. Experimental results found that StTPO40 is a binary optimal blend in terms of performance, combustion, and emissions. The emissions from StTPOxx were significantly improved after upgradation by silica gel as adsorbent and petroleum ether as a diluent.

Furthermore, ethyl levulinate, a potential bio-diluent with high oxygenate, was also utilized as an additive to StTPOxx blends to scrutinize performance, combustion, and emissions of single-cylinder, direct-injected stationary diesel engine, which is another novelty of the present study. The emission components are significantly dropped down after the upgradation of CTPO, but the performance was slightly lowered after the refining process. The nitrous oxide emission from StTPO40 and StTPO40EL10 was significantly reduced by 43.09% and 44.54%, respectively. Heat release from StTPOxx and StTPOxxEL10 were higher than diesel due to the high amount of polyaromatics hydrocarbons, naphthalenes, and benzene derivatives. StTPO40EL10 is a ternary optimal blend in terms of performance, combustion, and emission, with EL as a potential diesel additive.

It can be concluded that the StTPOxx and StTPOxxEL10 can be fully utilized in a diesel engine without any modifications and operational failures. In short, the lower blend percentage of StTPO40EL10 and StTPO40 can be used as an alternative fuel for a single-cylinder direct-injected diesel engine. In contrast, the higher blend percentage (StTPO60EL10, StTPO80EL10, StTPO90EL10, StTPO60, StTPO80, and StTPO100) can be utilized in boilers, furnaces, burners and marine engines.

**Keywords:** CTPO, Upgradation, StTPO, Engine, Performance, Combustion, Emissions, Ethyl levulinate



	<b>Page No.</b>
<b>CONTENTS</b>	
<b>DECLARATION</b>	
<b>CERTIFICATE</b>	
<b>ACKNOWLEDGEMENT</b>	
<b>ABSTRACT</b>	
<b>CONTENTS</b>	i
<b>LIST OF FIGURES</b>	ii
<b>LIST OF TABLES</b>	iii
<b>NOMENCLATURE</b>	iv
<b>CHAPTER 1</b>	
<b>INTRODUCTION</b>	<b>1</b>
1.1 Background	1
1.2 Problem with scrap tires	2
1.3 Typical composition in a scrap tire	2
1.4 Recycling methods for scrap tire	5
1.5 Thermal pyrolysis of scrap tires	7
1.6 Upgradation of CTPO	8
1.7 Fuel additives	8
1.8 The organization of the report	9
<b>CHAPTER 2</b>	
<b>LITERATURE REVIEW</b>	<b>12</b>
2.1 Thermal depolymerization of scrap tires	12
2.2 Characterization of CTPO using various analytical instruments	20
2.3 Various refining strategies for upgradation of CTPO	25
2.4 CTPO and upgraded pyrolysis oil as an alternate fuel in diesel engine	30
2.5 Use of EL as a biofuel additive	33
2.6 Mechanism of diesel spray development in diesel engines	37
2.7 Combustion in diesel engines	39
2.8 Mechanism of NO <sub>x</sub> formation in diesel engines	40
2.9 Summary of literature review	43
2.10 Research gap	45
2.11 Objectives of present investigation	45
2.12 Scope of the work or results expected	46
<b>CHAPTER 3</b>	
<b>EXPERIMENTAL METHODOLOGY</b>	<b>47</b>
3.1 Materials	47
3.2 Thermal depolymerisation of scrap tire into CTPO	48
3.3 Batch scale upgrading experiments	52
3.4 Physicochemical characteristics of liquid fuel samples	52
3.5 Surface tension measurements	53
3.6 Calculated cetane index analysis	54
3.7 Elemental analysis	54
3.7.1 CHNS/O analyzer	54
3.7.2 ICP-AES	55
3.8 FT-IR	56

3.9	GC-HRMS	57
3.10	2D GC×GC TOF-MS	57
3.10.1	2D GC×GC TOF-MS optimization	58
3.11	Thermal analysis by DSC Spectrometer	59
3.12	Fluorescence property analysis	59
3.13	Engine testing and instrumentation	64
<b>CHAPTER 4</b>	<b>CHARACTERIZATION AND PYROLYTIC LIQUEFACTION OF SCRAP TIRE IN A 10-TON ROTATING AUTOCLAVE REACTOR</b>	<b>69</b>
4.1	Introduction	69
4.2	Thermal pyrolysis of worn tire into CTPO	69
4.3	Physicochemical properties of CTPO	75
4.4	FTIR analysis	77
4.5	NMR spectroscopy	78
4.6	GC HRMS analysis	78
4.7	TGA analysis	79
4.8	Oxidation stability	80
4.9	Conclusions	81
<b>CHAPTER 5</b>	<b>VARIOUS UPGRADATION STRATEGIES FOR REFINING CTPO</b>	<b>82</b>
5.1	Introduction	82
5.2	Upgradation of CTPO using column chromatography	82
5.3	Upgradation of CTPO using a magnetic stirrer	82
5.4	Effect of upgrading on the physicochemical and thermal properties of upgraded tire pyrolysis oil	83
5.5	Elemental analysis and chemical composition	84
5.6	Comparative study on fuel properties of CTPO, CoTPO, and StTPO with diesel	86
5.7	FTIR analysis	89
5.8	NMR analysis	91
5.9	1D GC-MS analysis	93
5.10	TGA analysis	96
5.11	Oxidation stability	97
5.12	Recovery and regeneration of used adsorbent and solvent	98
5.13	Batch scale upgradation process	99
5.14	Effect of batch scale upgradation on oil quality and yield	100
5.15	Fuel property analysis	102
5.16	Boiling point determination	107
5.17	Stability analysis	108
5.18	2D GC×GC TOFMS analysis	110
5.19	DSC analysis	122
5.20	Scale up strategy of upgraded tire pyrolysis oil in a continuous regime	124
5.21	Conclusion	125
<b>CHAPTER 6</b>	<b>EXPERIMENTAL PERFORMANCE, STUDIES ON COMBUSTION AND</b>	<b>126</b>

		<b>EMISSION OF A SINGLE CYLINDER DIESEL ENGINE FUELLED WITH UPGRADED TIRE PYROLYSIS OIL AND ITS BLEND WITH DIESEL</b>	
	6.1	Introduction	126
6.2		Performance characteristics	126
	6.2.1	BTE	126
	6.2.2	BSEC	129
6.3		Combustion analysis	130
	6.3.1	In-cylinder pressure	130
	6.3.2	Net heat release	132
	6.3.3	Rate of pressure rise	135
	6.4	Emission characteristics	137
	6.4.1	NO <sub>x</sub> emissions	137
	6.4.2	CO emissions	140
	6.4.3	CO <sub>2</sub> emissions	141
	6.4.4	UBHC emissions	142
6.5		Conclusion	144
<b>CHAPTER 7</b>		<b>EXPERIMENTAL STUDY ON EFFECT OF EL ON SINGLE CYLINDER DIESEL ENGINE FUELLED WITH UPGRADED TIRE PYROLYSIS OIL DIESEL TERNARY BLENDS</b>	<b>145</b>
	7.1	Introduction	145
	7.2	Fuel properties of StTPOxxEL10 blends	145
	7.3	Performance characteristics	147
	7.3.1	Variation of BTE with load	147
7.4		Combustion characteristics	148
	7.4.1	Variation of in-cylinder pressure with load	148
	7.4.2	Variation of net heat release with load	149
7.5		Emission characteristics	151
	7.5.1	Variation of NO <sub>x</sub> emission with load	151
	7.5.2	Variation of oxides of carbon with load	153
	7.5.3	Variation of unburned hydrocarbon emission with load	154
7.6		Effect of EL on the performance, combustion, and emissions from diesel engine fuelled with StTPOxxEL10 blends	156
7.7		Conclusion	158
<b>CHAPTER 8</b>		<b>SUMMARY AND CONCLUSIONS</b>	<b>160</b>
		<b>Scope of future work</b>	<b>163</b>
		<b>REFERENCES</b>	<b>165</b>
		<b>APPENDICES</b>	<b>185</b>
		Appendix I: Photographs of the experimental setup used in the present study	185
		Appendix II: List of Tables	188
		Appendix III: List of Figures	191
		<b>LIST OF PUBLICATIONS BASED ON Ph.D. RESEARCH WORK</b>	<b>192</b>
		<b>BIODATA</b>	<b>194</b>

<b>Fig. No.</b>	<b>LIST OF FIGURES</b>	<b>Page No.</b>
1.1	Section of a radial tire and essential parts	3
1.2	Life of a tire from production to end of service life	4
1.3	Various application of tires	6
1.4	Road map of research work in the present study	11
2.1	Various types of slow pyrolysis reactors used for production of tire derived fuels	13
2.2	Various types of fast pyrolysis reactors	14
2.3	Mechanism of diesel development and break up	37
2.4	Various modes of liquid disintegration	38
2.5	Various mechanism of NO <sub>x</sub> formation	42
3.1	Basic layout of pyrolysis of tires	49
3.2	Process scheme for 10-ton tire pyrolysis industry layout	51
3.3	Batch scale upgradation strategy	52
3.4	Schematic representation of drop shape analyzer	54
3.5	Basic working of CHNS/O analyser	55
3.6	Basic working principle of ICP-AES	56
3.7	Working principle of FT-IR Spectroscopy	56
3.8	Basic principle of GC-HRMS	57
3.9	Schematic of instrumentation of 2D GC×GC TOF-MS	59
3.10	Instrumentation of fluorescence spectrometry	60
3.11	Overview of present research study	62
3.12	The methodology proposed in the present study	63
3.13	Schematic layout of the single-cylinder engine test rig	66
4.1	Products from pyrolysis of scrap tires	70
4.2	Characterization techniques used in the analysis of CTPO	71
4.3	Schematic of methodologies used in the preliminary investigations on CTPO	72
4.4	FT-IR spectra of CTPO	78
4.5	NMR spectra of CTPO	78
4.6	1D GC-MS chromatogram of CTPO	79
4.7	TGA of CTPO	80
4.8	The gummy deposit formed during storage of CTPO	81
5.1	Upgradation of CTPO using the bed of silica in a column	83
5.2	Upgradation of CTPO using a magnetic stirrer	83
5.3	FT-IR spectra of CTPO, CoTPO, and StTPO	90
5.4	NMR spectra of CTPO, CoTPO, and StTPO	92

5.5	GC-HRMS spectra of CTPO, CoTPO, and StTPO	95
5.6	Types of compounds in CTPO, CoTPO, and StTPO	96
5.7	TGA of CTPO, CoTPO, and StTPO	97
5.8	Gummy deposits formed during the storage of CTPO.	98
5.9	Morphology of silica gel and methanol washed silica gel	98
5.10	Process flow diagram of batch scale upgradation strategy	99
5.11	Silica gel deposits collected in a membrane-based disc filter.	102
5.12	1D GC-MS of silica gel washed by methanol	102
5.13	The surface tension of diesel, StTPO <sub>xx</sub> , and CTPO	105
5.14	The density of diesel, StTPO <sub>xx</sub> , and CTPO	105
5.15	The calorific value of diesel, StTPO <sub>xx</sub> , and CTPO	106
5.16	Flashpoint of diesel, StTPO <sub>xx</sub> , and CTPO	106
5.17	Kinematic viscosity of diesel, StTPO <sub>xx</sub> , and CTPO	107
5.18	Cetane index of diesel, StTPO <sub>xx</sub> , and CTPO	107
5.19	Phase stability examination of upgraded tire pyrolysis oils	109
5.20	Cleanliness and compatibility studies of StTPO-DF blends	109
5.21	Contour plot obtained from GC×GC TOF-MS (apolar×polar) during the analysis of CTPO, StTPO, and diesel	112
5.22	Contour plot of sulfur compounds in CTPO, StTPO, and diesel detected by GC×GC TOF-MS	114
5.23	Surface plot of value-added compounds in CTPO, StTPO, and diesel.	116
5.24	Mechanism of formation of aromatic hydrocarbons during depolymerisation of scrap tire	117
5.25	Schematic representation of elution pattern obtained for various classes of compounds in CTPO, StTPO, and diesel	119
5.26	Value-added compounds in StTPO.	119
5.27	Differential scanning calorimetry of CTPO and StTPO	122
5.28	UV-Visible spectra of CTPO and StTPO	122
5.29	Fluorescence of CTPO and StTPO	123
5.30	Scale up of CTPO in a continuous regime	124
6.1	Variation of BTE of CTPO <sub>xx</sub> and StTPO <sub>xx</sub> with load	129
6.2	Variation of BSEC of CTPO <sub>xx</sub> and StTPO <sub>xx</sub> with load	130
6.3	Variation of maximum in-cylinder pressure of CTPO <sub>xx</sub> and StTPO <sub>xx</sub> with load	132
6.4	Variation of net heat release of CTPO <sub>xx</sub> with load	133
6.5	Variation of net heat release of StTPO <sub>xx</sub> with load	133
6.6	Selective benzene derivatives identified in CTPO	135
6.7	Variation of the rate of pressure rise of CTPO <sub>xx</sub> blends with diesel	136
6.8	Variation of the rate of pressure rise of StTPO <sub>xx</sub> blends with diesel	136
6.9	Variation of NO <sub>x</sub> emission from CTPO <sub>xx</sub> and StTPO <sub>xx</sub> with load	139

6.10	Variation of EGT from CTPOxx and StTPOxx with load	140
6.11	Variation of CO emission from CTPOxx and StTPOxx with load	141
6.12	Variation of CO <sub>2</sub> emission from CTPOxx and StTPOxx with load	142
6.13	Variation of unburned hydrocarbons from CTPOxx and StTPOxx with load	143
7.1	Cleanliness and compatibility studies of StTPOxxEL10 ternary blends	146
7.2	Variation of BTE of StTPOxxEL10 blends with load	148
7.3	Variation of BSEC of StTPOxxEL10 with load	148
7.4	Variation of maximum in-cylinder pressure of StTPOxxEL10 with load	149
7.5	Variation of net heat release of StTPOxxEL10 with load	150
7.6	Variation of the rate of pressure rise of StTPOxxEL10 with load	151
7.7	Variation of nitrous oxide emission from StTPOxxEL10 with load	152
7.8	Variation of exhaust gas temperature from StTPOxxEL10 with load	152
7.9	Variation of carbon monoxide emission from StTPOxxEL10 with load	154
7.10	Variation of carbon dioxide emission from StTPOxxEL10 with load	154
7.11	Variation of hydrocarbon emission from StTPOxxEL10 with load	155
7.12	Proposed pathway of auto oxidation mechanism of EL	158

<b>Table No.</b>	<b>LIST OF TABLES</b>	<b>Page No.</b>
1.1	Typical components in a scrap tire	3
1.2	Overview of selective pyrolysis plant in various countries	7
2.1	Various types of reactors for pyrolysis of scrap tires and comparison with the present study	19
2.2	Various analytical techniques used to characterize CTPO	23
2.3	Summary of studies on the utilization of CTPO in diesel engine	35
2.4	Classification of diesel spray break up regimes	39
3.1	Physical properties of silica gel	48
3.2	Physical properties of petroleum ether	48
3.3	Fuel properties of ethyl levulinate	48
3.4	Specification of 10-ton Tire pyrolysis plant	49
3.5	Physical properties and methods used for the analysis of liquid samples	53
3.6	Parameters for fluorescence analysis	60
3.7	Specifications of the various equipment used for batch scale upgradation experiments	64
3.8	Specifications of single cylinder diesel engine	65
3.9	Various instrumentation used in engine experiments	66
3.10	Research strategy for engine experiments	67
3.11	Specifications of AVL digas 444 gas analyzer	67
4.1	Details of samples and analysis carried out during present study	73
4.2	Typical elemental composition of CTPO	75
4.3	Physicochemical properties of CTPO	77
5.1	ICP-AES analysis of CTPO, CoTPO, and StTPO	85
5.2	Comparative study on fuel properties of CTPO, CoTPO, and StTPO with industrial standards	87
5.3	<sup>1</sup> H NMR results of CTPO, CoTPO, and StTPO	93
5.4	Comparative study of laboratory-scale strategy with batch scale process	100
5.5	Hedonic scale for odour measurements	100
5.6	Rating scale and description for a spot test	110
5.7	Comparison of various classes of compounds in CTPO, CoTPO, and diesel	121
6.1	Additives and their functions during tire production	139
7.1	Physical properties of StTPOxxEL10 ternary fuel blends	146
7.2	Carbon content in EL, StTPO, CTPO, and diesel	153
7.3	Summary of the performance, combustion and emission characteristics of various fuel blends with diesel	156

## NOMENCLATURE

ASTM	American society for testing and materials
a.m.u	Atomic mass unit
BSEC	Brake specific energy consumption
BTE	Brake thermal efficiency
BSFC	Brake specific fuel consumption
BS	Bharat stage
BDL	Below detectable limit
CCD	Charge coupled device
CuO	Copper oxide
CTPO	Crude tire pyrolysis oil
CTPO <sub>xx</sub>	Blend of crude tire pyrolysis oil with xx% of diesel; where xx denotes the percentage of upgraded tire pyrolysis oil and remaining amount of diesel
CTPO DF	Crude tire pyrolysis oil blended with diesel
cSt	Centistokes
CRDI	Common rail direct injection
CoTPO	CTPO passed through a column of silica gel
CO <sub>2</sub>	Carbon dioxide
CO	Carbon monoxide
CCI	Calculated cetane index
CaO	Calcium oxide
CP	Mean in-cylinder pressure
DSC	Differential scanning calorimetry
DI	Direct-injected
DEE	Diethyl ether
DTPO	Distilled tire pyrolysis oil
EPA	Environmental protection agency
ETRMA	European tire rubber manufacturers association
EL	Ethyl levulinate



EGT	Exhaust gas temperature
FTIR	Fourier transform infrared spectroscopy
FCC	Face centered cubic
GCV	Gross calorific value
GC-MS	Gas chromatography-mass spectrometry
GC×GCTOF-MS	Two-dimensional gas chromatography with time-of-flight mass spectrometry
HC	Hydrocarbon
H/C <sub>eff</sub>	The effective ratio of hydrogen to carbon
IS	Indian standard
ISO	International organization for standardization
I.D	Internal diameter
ICP-AES	Inductively coupled plasma atomic emission spectroscopy
JME	Jatropha methyl ester
LPH	Liter per hour
LHE	Latent heat of evaporation
MS	Mild steel
NO <sub>x</sub>	Nitrous oxide
NMR	Nuclear Magnetic Resonance Spectroscopy
NIST	National Institute of Standards and Technology
NHR	Net heat release
ppm	Parts per million
PAH	Polyaromatic hydrocarbons
RPR	Rate of pressure rise
rpm	Revolutions per minute
RT	Room temperature
SS	Stainless steel
SEM	Scanning electron microscopy
StTPO <sub>xx</sub> EL10	Blend of upgraded tire pyrolysis oil with xx% of diesel and 10%EL; where xx denotes the percentage of upgraded tire pyrolysis oil and remaining amount of diesel
StTPO <sub>xx</sub>	Blends of upgraded tire pyrolysis oil with xx% of diesel; where xx denotes the percentage of upgraded tire pyrolysis oil and remaining amount of diesel
StTPO-EL-DF	Upgraded tire pyrolysis oil blended with diesel and ethyl levulinate

StTPO DF	Upgraded tire pyrolysis oil blended with diesel
SO <sub>2</sub>	Sulfur dioxide
TiO	Titanium oxide
TGA	Thermo gravimetric analysis
UV-Vis	UV-Visible spectroscopy
UBHC	Unburnt hydrocarbons
ZnO	Zinc oxide

# CHAPTER 1

## INTRODUCTION

### 1.1 Background

The global scrap tire production is estimated to be 15 million annually, out of which, 1 million ton is contributed by India (Sharma et al. 2021). The current estimate suggests that India has a 125% increase in annual vehicle registration, and projected vehicle growth by 2035 showed 80.1 million passenger vehicles and 236.4 million two-wheelers. Also, the ban on old vehicles accelerates the increase in end-of-life tires (Chaturvedi 2017).

As per statistical data from European Tire and Rubber Manufacturers Association (ETRMA), the worldwide number of passengers and commercial vehicles will exceed 1.6 billion by 2024 (Czajczynska et al. 2020). Tire companies in India are highly competitive, with over 40 manufacturers (URL 01). The key players in the Indian tire market are MRF (27%), APOLLO (19%), JK (16%), CEAT Ltd. (12%), Birla (11%), and others (15%). Bridgestone and Michelin are the other tire production industries. As per statistical data from the Ministry of Petroleum and Natural Gas, India, production of petroleum products increased from 203.20 to 254.40 Million Metric Tons (MMT), whereas the consumption escalates from 148.13 to 204.92 MMT from 2011 to 2018. Further, with the increase in oil price, there is a growing demand in search of alternate fuel sources to substitute for petroleum reserves. Many researchers and scientists are exploring innovative technologies to produce fuels and value-added chemicals from waste-based feedstocks such as tires, plastic, sewage sludge, etc. (Agbulut et al. 2021, Hariadi et al. 2021, and Wang et al. 2021).

The management of scrap tires or any other waste is intended to follow a hierarchical approach such as waste minimization, reuse, recycling, energy recovery, and landfilling. The life of a standard tire depends on road conditions, manufacturer, driver's habits, maintenance, design parameters, and climate of a particular region. The life span of car tires, truck tires, and bicycle tires is estimated to be 40,000-80,000 km, 10,000 km, and 40,000 km, respectively (Jain 2016). More than 50% of scrap tires are discarded to dump yards after the end of life without any further processing (Junquing et al. 2020). The approximate lifetime of end-of-life tires in landfills is 80-100 years (Sharma et al. 2021).

## **1.2 Problems with scrap tires**

Illegally dumped scrap tires often provide habitat for breeding mosquitoes, vermin, snakes due to doughnut shape, which spread malaria, dengue fever, yellow fever, encephalitis, West Nile virus (Jain 2016). Stockpiles of scrap tires in landfills gradually release toxic contaminants that adversely affect the soil and water bodies. Stockpiles can also lead to "tire fire". Tire fire is a thick cloud of black smoke that contains hazardous solid and gaseous pollutants, which pose a threat to the ecosystem and public health. Sometimes, the cooling of tire fire emits poisonous substances such as benzene. Open burning of scrap tires releases criteria pollutants such as particulates, carbon monoxide, sulfur oxides, oxides of nitrogen and volatile organic compounds, and non-criteria pollutants include the polynuclear aromatic hydrocarbons, dioxins, furans, hydrochloric acid, benzene, polychlorinated biphenyls, and metals such as chromium, zinc, mercury, arsenic, and vanadium. Both the criteria and non-criteria pollutants inducing short-term and long-term health hazards to nearby residents were reported (Reisman et al. 1997). The continuous exposure to these emissions causes asthma and respiratory complications, cough and chest pain, depression in the nervous system, high blood pressure, heart disease, inflammation in mucous membrane, cancer, dizziness, euphoria, headache, nausea, weakness, drowsiness, pulmonary edema, pneumonia, skin, and eyes irritation (Chaturvedi 2017, Aya et al. 2016).

## **1.3 Typical composition in a scrap tire**

Tires are mainly made up of natural rubber, synthetic polymer, carbon black, stearic acid, additives, accelerators, steel wires, textile chord, and aromatic oils (Ware, 2015). Fig. 1.1 shows the transverse section of a typical radial tire. Table 1.1 shows typical components in a scrap tire. The major component in a scrap tire is a mixture of natural rubber and synthetic rubber. Carbon black and silica are the second-largest components. Metals, vulcanization agents, and additives are the other components. Additives such as antioxidants, antiozonants, extender oil, and waxes are usually added into tire polymer to enhance the tire performance. Vulcanization is a chemical process by which rubber is heated along with sulfur (1.5 wt.%), activators (zinc oxide or stearic acid) to alter the chemical structure at 140 °C to 160 °C to form cross-linked sulfur bridges with a polymer chain to improve the hardness, durability, and mechanical properties (Mastral et al. 2000). The cross-linked elastomers with a three-dimensional structure impart high strength and resilience, causing difficulty in decomposing the tire. During tire production, aromatic compounds like benzopyrene, chrysene, benzo anthracene, benzo fluoranthene, and dibenzo anthracene are also added to soften the rubber and

to improve workability (Petchkaew, 2015). Fig. 1.2 describes the life of a standard tire from the origin to the end of service life.

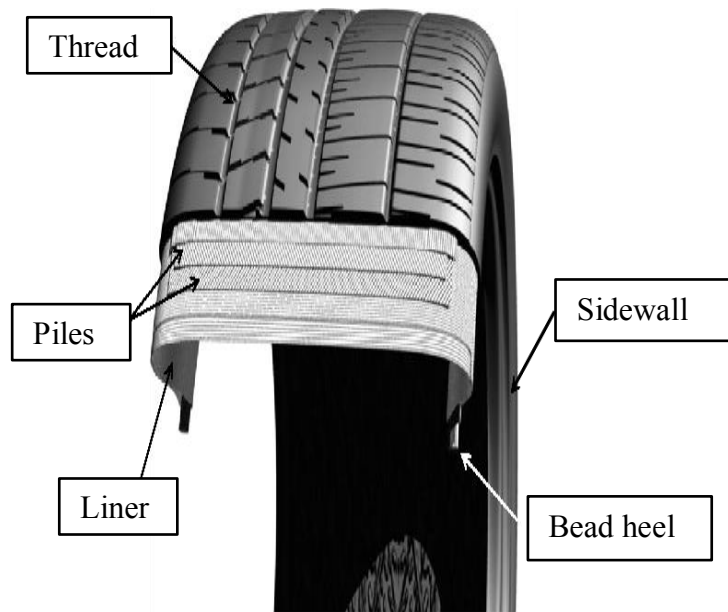


**Fig. 1.1 Section of a radial tire and the essential parts**  
(Source: Hita et al. 2016)

**Table 1.1 Typical components in scrap tire**  
(Source: Seinkiewicz et al. 2012)

S. No.	Composition	Car tire (%)	Truck tire (%)
1.	Natural rubber	28	20
2.	Synthetic rubber	22	30
3.	Carbon black	23	15
4.	Steel	13	25
5.	Fabric, filler, accelerator, antiozonants, etc.	14	10

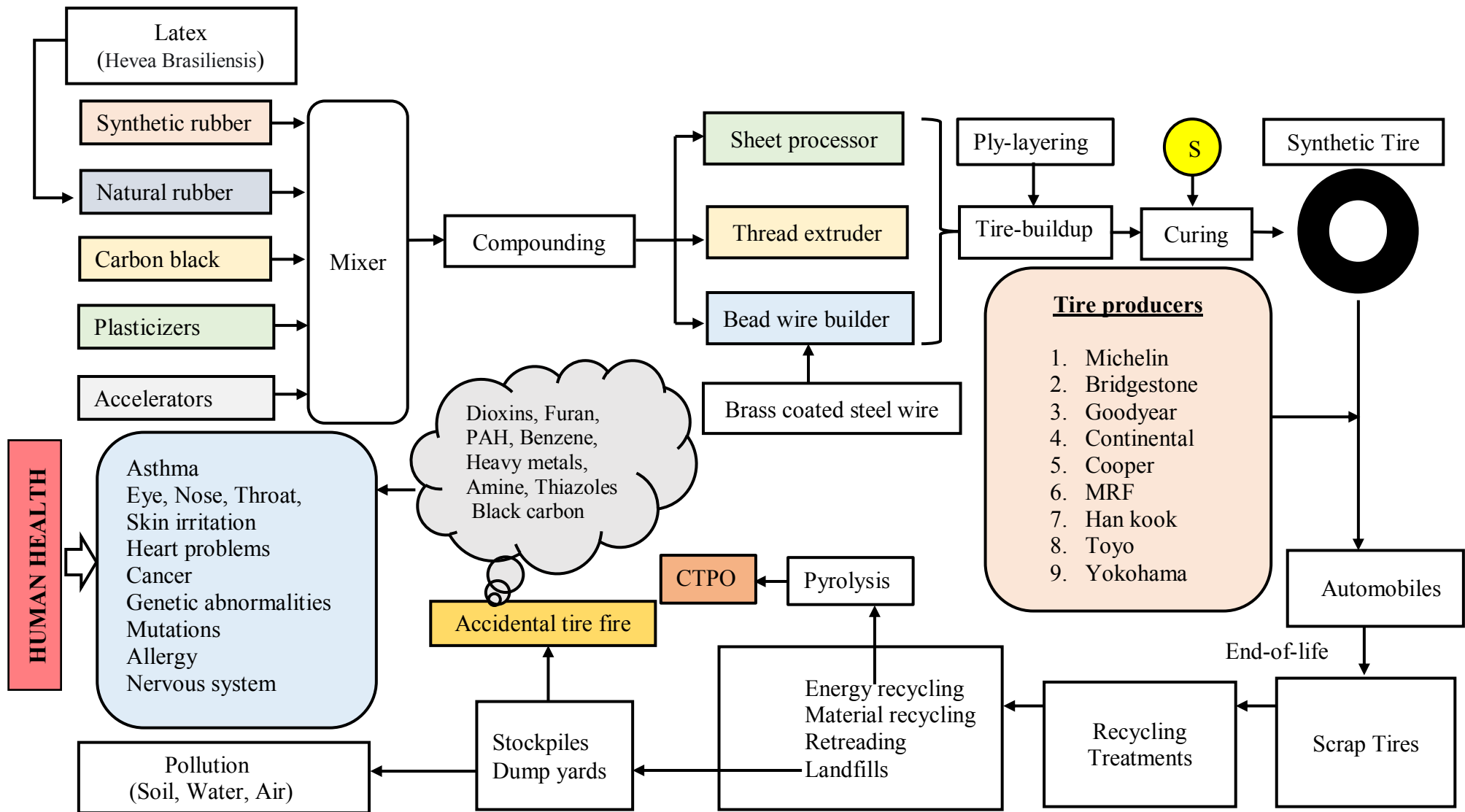
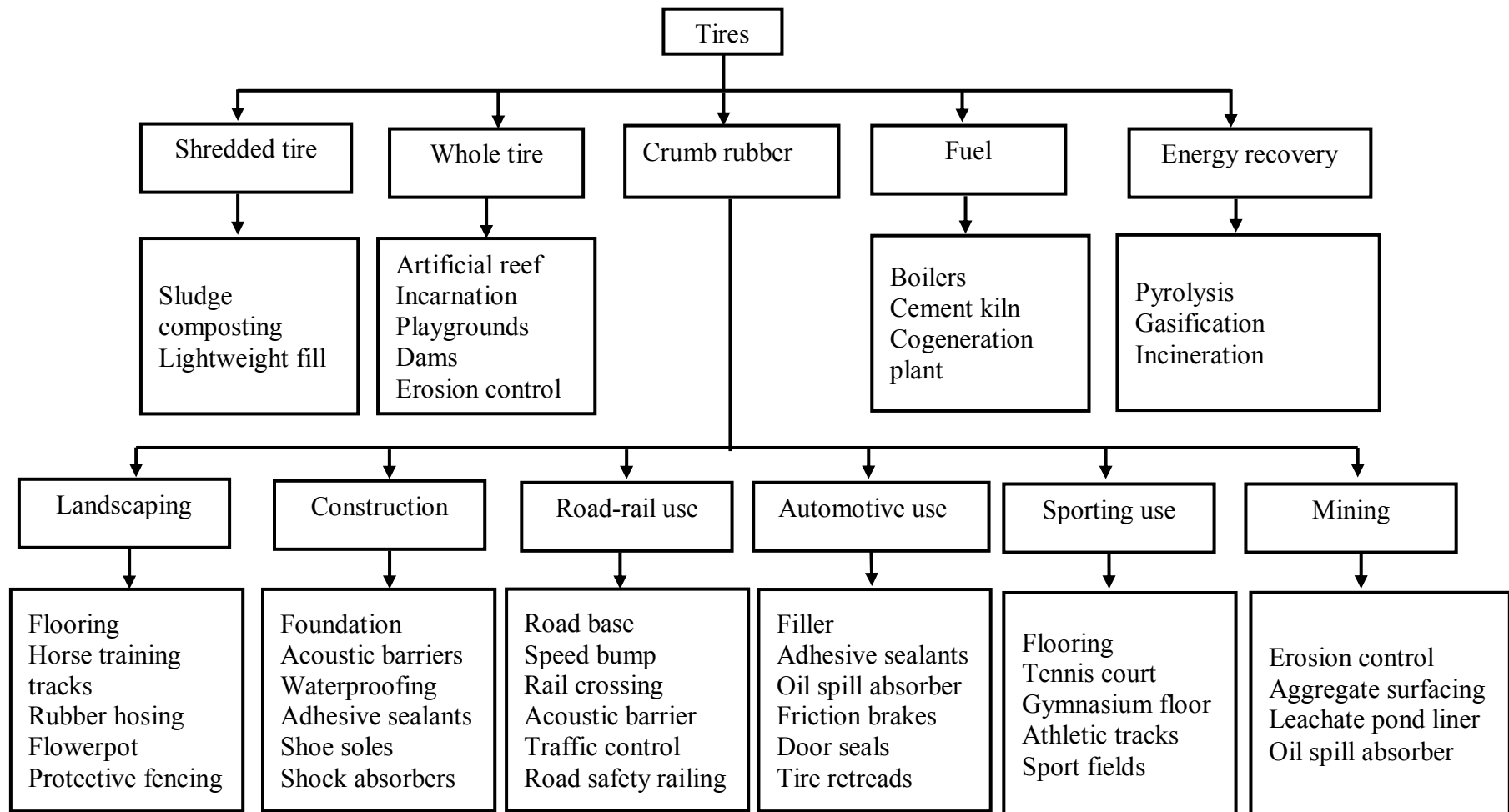


Fig. 1.2 Life of Tire from production to end of service life

#### **1.4 Recycling methods for scrap tire**

Scrap tires are used in asphalt manufacture, aggregate production, boat, dock fenders, road pavement, playgrounds, roofing applications, noise control systems, artificial reef, protection to young plants and coastal defences, etc. (Siddique 2004, Benazzouk 2007, Arabani 2010, Navarro 2010). Further, waste tires are also used for various applications such as cooking food, tire manufacturing facilities, power plants, cement kilns, pulp, paper manufacturing units, etc. (Barlaz et al. 1993). Traditionally, butchers used to scorch meat using scrap tires in West African countries. The usage of these tires causes the discharge of various heavy metals such as mercury, chromium, copper, iron, cadmium, lead, and zinc into the meat. Besides, scrap tires to singe flesh release the polyaromatic hydrocarbons and volatile organic compounds into the environment, which adversely affects human health (Amfo et al., 2014). The commonly used energy recovery options are incineration, gasification, and pyrolysis. Incineration is an environmentally acceptable method to combust the tire in a controlled high-temperature atmosphere. However, high capital investment and availability of skilled labour forces are the obstacles for the widespread deployment on a pilot scale (Muzenda 2014). Gasification is another method, which is generally carried out in a sub-stoichiometric oxidation atmosphere at a temperature of 700 °C and 800 °C. Low liquid yield and high capital cost are the limitations of scrap tire gasification (Muzenda 2014). Out of various recycling options, pyrolysis is one of the environmentally attractive thermo-chemical technologies carried out in an oxygen-deprived atmosphere at a temperature of 400-600 °C to produce liquid fuel and recover the value-added compounds (Banar et al. 2015). Fig. 1.3 shows the various application of waste tires (Schwarzenegger 2006).



**Fig. 1.3 Various application of tires**



## 1.5 Thermal pyrolysis of scrap tires

Pyrolysis is an attractive thermochemical pathway to produce value-added fuel and chemicals from scrap tires. Pyrolysis can be classified based on the environment, such as oxidative pyrolysis, hydro-pyrolysis, steam pyrolysis, catalytic pyrolysis, vacuum pyrolysis, microwave pyrolysis, radiofrequency pyrolysis, and plasma pyrolysis (Martinez et al. 2013). Out of these, thermal pyrolysis is a widely adopted thermochemical technology in tire pyrolysis industries. There are various types of reactors such as fixed bed, rotating autoclave, fluidized bed, screw conveyers, fixed, spouted, entrained and fluidized beds, rotating cone, vortex reactor, melting vessels, plasma reactors, free-fall, tubing bomb reactor used to depolymerize the worn tire to fuels and chemicals are reported by various authors (Martinez et al. 2013, Arabiourrutia et al. 2020). During pyrolysis, the scission of tire fragments leads to the formation of ethane, propane, and 1, 3-butadiene, which reacts to form cyclic olefins. Table 1.2 shows an overview of the selective list of commercial and semi-commercial tire pyrolysis plants in various countries. The unique advantages of a rotary kiln over other reactors, such as the slow mixing of feedstock in a rotary kiln, favours uniformity in the pyrolysis products, and residence time, can be adjusted to obtain optimum conditions for the pyrolysis reaction. The solid waste of various shapes, sizes, and calorific values can be fed into the rotary kiln in a batch or continuous operation (Spitz 2010).

**Table 1.2 Overview of selective pyrolysis plants in various countries**  
(Source: Williams, 2013)

S. No.	Company	Location	Type of reactor	Capacity (Tons/day)
1.	Splainex Limited	Hague, Netherland	Rotary kiln	~20
2.	Xinxiang Doing Renewable Energy Equipment Ltd.	Xinxiang, China	Rotary kiln	6-10
3.	Resem	Shani, China	Rotary kiln	8-20
4.	Kouei Industries	Vancouver, Canada	Fixed bed, batch	16
5.	DG Engineering	Gummers Bach, Germany	Rotary kiln	~10
6.	FAB India Limited	Ahmedabad, India	Rotary kiln	5-12
7.	Octagon consolidated	Selangor, Malaysia	Rotary kiln	2.4-120
8.	No waste technology	Reinach, Germany	Fixed bed/batch	4
9.	Pyreco	Teeside, United Kingdom	Rotary kiln	200

Thermal depolymerization of styrene-butadiene rubber in the absence of oxygen at a temperature of 400 to 600 °C produces a dark brown syrupy liquid called crude tire pyrolysis oil (CTPO) that consists of various classes of compounds such as aliphatic, aromatics, heteroatoms, and polar fractions. This can be used as a fuel or blended with petroleum refinery feedstocks (Frigo et al. 2014). The oil obtained from the rotating autoclave reactor is unsuitable for engine applications due to its inferior fuel properties such as high viscosity, low flash point, low calorific value, high acidity, low cetane index, low thermal stability, and low storage stability.

Another challenge to work with CTPO is its unpleasant odour due to the presence of sulfur-containing compounds. CTPO also consists of valuable chemicals like dL-limonene, benzene, toluene, xylene, and styrene. The by-products of pyrolysis reaction include non-condensable volatiles, carbon black and steel wires. The non-condensable gases released from the pyrolysis reactor, called syngas, contain significant amounts of carbon monoxide, hydrocarbons, and hydrogen (Cunliffe and Williams, 1998). Pyro char includes a high amount of carbon and can be used for the adsorption of harmful pollutants.

### **1.6 Upgradation of CTPO**

Crude tire pyrolysis oil can be used as fuel in boilers. However, for the application of CTPO in engines further refining processes such as sulfur reduction, moisture removal, and distillation are the widely used methods (Satish Kumar et al. 2019). Oxidative desulfurization, hydrotreating, hydrocracking, treatment with hydrochloric acid, photocatalytic oxidation, vacuum distillation, ultrasound-assisted oxidation, methanol extraction, adsorption, and supercritical processes are the commonly used methods for upgrading CTPO (Somsri et al. 2018). Distillation is a widely used upgradation method adopted in most tire pyrolysis industries to refine CTPO and extract value-added chemicals and fuels. These methods are highly energy-intensive and need huge capital investment for deployment on a larger scale (Agarwal et al. 2020).

### **1.7 Fuel additives**

The main impediment to utilize CTPO and upgraded tire pyrolysis oils in diesel engines are the high amount of unburned carbon emissions, unburned hydrocarbons, and oxides of nitrogen and subsidiary cold flow properties. To reduce the oxides of carbon, hydrogen, and nitrogen

from diesel engines to the maximum possible extent, there is a need to select a suitable bio-based diluent as a fuel additive. The various kinds of additives such as oxygen-based additives (diethyl ether), alcohol-based additives (methanol), multiple types of biodiesel (Jatropha, green-seaweed), lubricant based (motor silk diesel additive), nano-additives are used along with CTPO to improve the performance, combustion, and emission from single-cylinder diesel engines (Hariharan et al. 2013, Karagoz et al. 2020, Sharma et al. 2015, Simsek et al. 2020, and Kumaravel et al. 2019).

In the present study, the mixture of end-of-life tires has been pyrolyzed in a rotating autoclave reactor in optimum reaction conditions (400 °C, 0.2 bar, 10°C/min, and 4 rpm) and upgraded the obtained oil by various refining strategies. The characterization of CTPO and upgraded oil was carried out using different analytical techniques to comprehend the detailed physical, chemical, thermal, and stability characteristics to utilize as a fuel in diesel engines. The refined oil was then tested in a single-cylinder diesel engine to study the performance, combustion, and emission characteristics and compared with CTPO and diesel. Ethyl levulinate is selected as a fuel additive in upgraded tire pyrolysis oil due to the presence of high oxygen content (33 wt.%), bio-based origin, low sulfur content, high latent heat of evaporation, low ignition delay, higher solubility, low viscosity, high fire reliability, cleanliness, low acidity and improved cold flow properties.

### **1.8 The organization of the report**

A literature review on the thermal depolymerization of scrap tires using various types of reactor, reaction conditions with product yield, different up-gradation strategies to refine CTPO and utilization of CTPO-diesel blends as a fuel in single-cylinder diesel engines and the effect of ethyl levulinate as a bio additive in diesel engines are detailed in chapter 2.

The materials and methods used for the present study are presented in chapter 3. These comprise pilot field studies on a 10-ton rotating autoclave reactor at Mandakan Energy Products, Oyalapathy, Palakkad, Kerala. The instrumentation and various analytical methods employed to characterize the CTPO, specifications of engine experiments, and scheme of experimental approach for refining CTPO.

Extensive characterization of CTPO samples is discussed in the first part of chapter 4. The discussion on various upgradation strategies for refining CTPO for application in the single-cylinder diesel engine is detailed in chapters 5 and 6. Studies on the effect of ethyl levulinate

as bio-diluent in upgraded tire pyrolysis oil to predict the performance, combustion, and emissions from a single-cylinder diesel engine are described in chapter 7.

Conclusions and the scope of future work are presented in chapter 8. A consolidated list of references is included at the end of chapter 8.

There are five appendices at the end of the report. The identified compounds and their peak area of compounds in CTPO, StTPO, and diesel, are summarised in Appendix A. The chromatogram of saturates in CTPO, StTPO, and diesel are included in Appendix B. The upgradation facility photographs, the engine test rig are presented in Appendix C. List of equations used, and a list of web references are given in Appendix D and Appendix E.

The road map of the present study is given in Fig. 1.4., which includes the previous literature works on CTPO, pyrolysis of CTPO in a rotating autoclave reactor, various upgradation strategies to refine CTPO, extensive characterization of CTPO and StTPO using multiple analytical techniques, and the utilization of CTPO and StTPO as partial and full fuel substitute in a single-cylinder diesel engine.

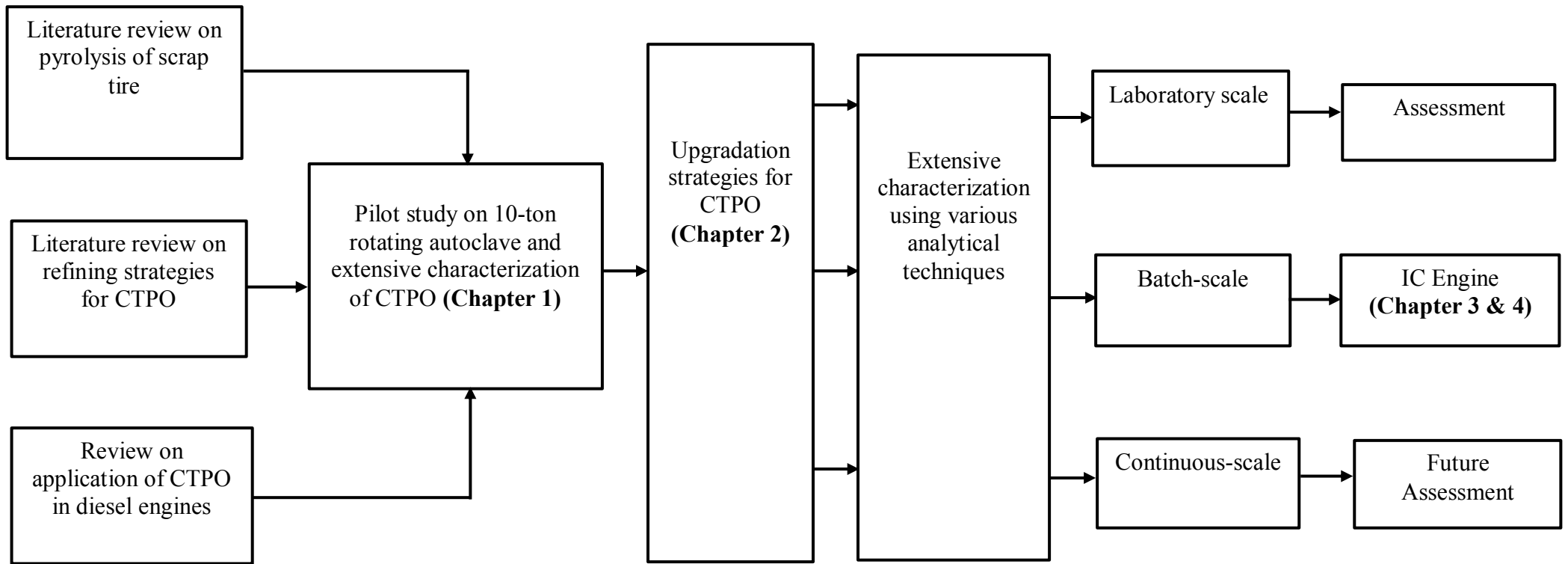


**Fig. 1.4 Road map of research work in the present study**

## CHAPTER 2

### LITERATURE REVIEW

An extensive review of crude tire pyrolysis oil from various reactor configurations, upgradation strategies for refining crude tire pyrolysis oil, performance, emission, and combustion characteristics of a single-cylinder diesel engine fuelled with upgraded tire pyrolysis oil (StTPO) blended with diesel is presented in this chapter. The review also scrutinises the influence of ethyl levulinate as a bio-diluent on the performance, emission, and combustion characteristics of a single-cylinder diesel engine fuelled with StTPO<sub>xx</sub>DF blends.

#### 2.1 Thermal depolymerisation of scrap tires

Pyrolysis is a thermochemical conversion of solid waste like tires and plastics in an oxygen-starved atmosphere. The significant factors that affect the pyrolysis operation are pressure, temperature, feed size, heating rate, retention time, the configuration of the reactor, etc. Several researchers have used various reactors for thermochemical conversion of tire waste like the fixed bed, auger, rotary, fluidised bed, continuous, vortex, externally retort type, plasma, vacuum, microwave, radiofrequency (Arabiourrutia et al. 2020). The selection of reactors is based on a variety of raw materials used in pyrolysis reaction (granules, powder, pieces, and shredded, whole tires), the heat of combustion of feedstock. Mode of operation (periodic or fixed), method of supplying thermal energy, reaction conditions (under atmospheric pressure, overpressure of inert gas or presence or absence of catalyst), range of heating rate (slow, intermediate, or fast). However, the present study uses the pilot-scale rotating autoclave reactor for the pyrolysis of scrap tires.

Fig. 2.1 and Fig. 2.2 describes various types of slow and fast pyrolysis reactors commonly used for pyrolysis of scrap tires. There are several factors to classify pyrolysis reactors. In this section, the reactors are classified as slow, intermediate and fast pyrolysis based on the heating rate, temperature, retention time of solid and vapour residence time. Conventionally, slow pyrolysis is commonly operated in a batch regime. In slow pyrolysis reactors, the reaction is carried out at a low heating rate, low temperature, longer solid and vapour residence time whereas in intermediate pyrolysis reactors is characterised by its moderate heating rate, moderate temperature and moderate solid and vapour residence time. In fast pyrolysis reactors,

the reaction is achieved by higher heating rate, high temperature, shorter solid and vapour residence time.

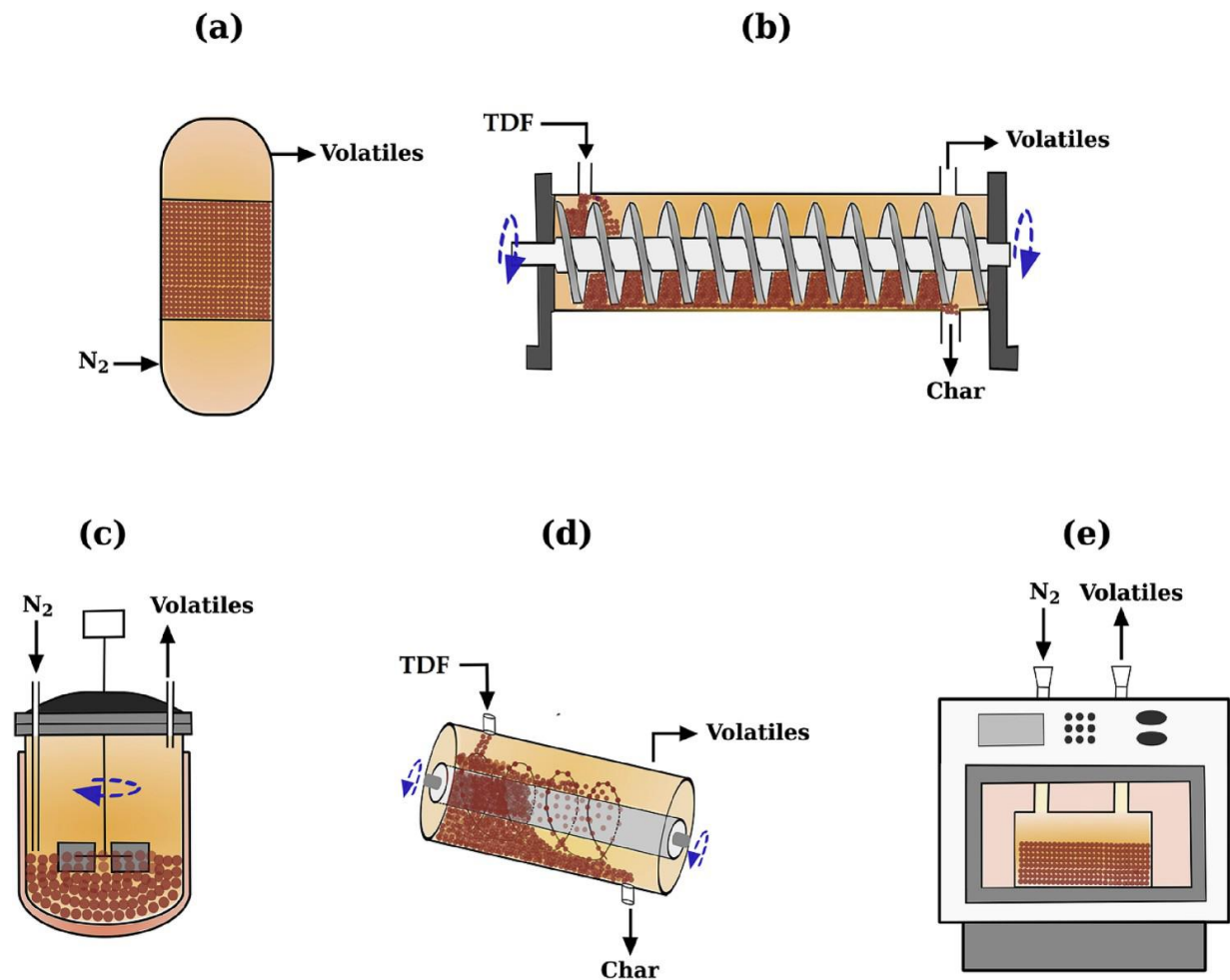


**Fig. 2.1 Various types of slow pyrolysis reactors used for production of tire derived fuels (TDF)**

**((a) fixed bed (b) auger reactor (c) stirred reactor (d) rotary oven (e) microwave reactor)**  
(Source: Adapted with permission, copyright 2020, Elsevier)

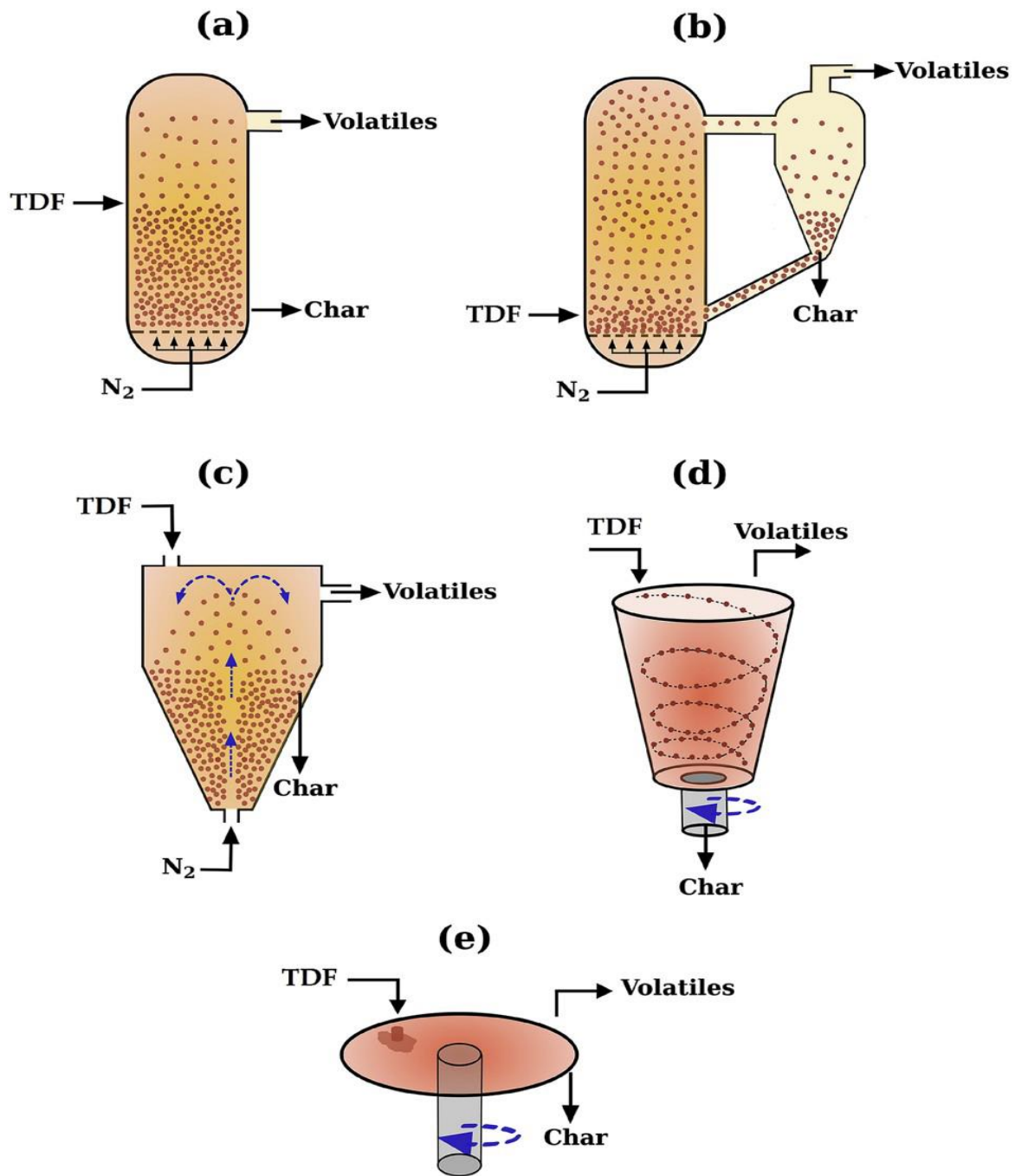


**Fig. 2.2** Various types of fast pyrolysis reactors ((a) bubbling fluidised bed (b) circulating fluidised bed (c) spouted bed (d) rotating cone (e) ablative reactor) (Source: Adapted with permission, copyright 2020, Elsevier).



Ablative pyrolysis technology is a novel fast pyrolysis method to depolymerise scrap tires. In ablative pyrolysis, heat is transferred by the direct contact between rotating heated disc or cone and particles of the feedstocks. The attractive feature of the ablative pyrolysis reactors are high heat transfer, low conductivity of feed materials, no contamination with heat transfer media, metallic or non-combustible materials can be processed along with organics. A simplified continuous ablative reactor is developed for the fast pyrolysis of scrap tire in a constant mode (Black et al. 1992). Pyrolytic liquefaction of scrap tires at 570 °C, the residence time of 960 s, produces a liquid yield of 49.8 wt. %.

Vacuum pyrolysis of scrap tires was investigated by Roy et al. (1999). Experiments were performed using passenger car tire in continuous mode at 550 °C, passenger car tire at 520 °C in batch mode, passenger car tire with silica filler in batch mode at 500 °C and truck tires in batch mode at 485 °C. In this process, shredded tires are conveyed over two horizontal plates using a mechanical system. The plates are heated internally by a mixture of molten salt maintained at a different temperature, which decomposes rubber molecules with a maximum yield of 47 wt. % was reported by using passenger car tires in batch scale mode of operation at 500 °C. Compared with conventional pyrolysis, the residence time of gaseous pyrolysis products is short in vacuum pyrolysis, which can suppress the secondary reaction such as aromatisation and condensation.

The fluidised bed is another type of reactor used for pyrolysis of scrap tires. Wey et al. (1995) studied the effect of operating temperature on the yield of liquid oil composition and quality of liquid and solid fractions during auto thermal pyrolysis of scrap tire in a fluidized bed reactor. The composition of liquid hydrocarbon is affected by air factor, high operating temperature, increased gasoline and diesel. The addition of zeolite promoted gasoline from 24% to 31% at the same operating temperature.

Dai et al. (2001) carried out studies on the continuous pyrolysis of scrap tires in a fluidised bed using quartz sand as a circulating fluidisation agent. The main objective of this study was to predict the influence of temperature and gas residence time on pyrolysis reactions. The tire powder undergoes the fast pyrolysis and instantly removed from the continuous fluidised bed reactor. Simultaneously, quartz sand and char are separated by cyclones and produce vapours sent to the condensation system. They reported that maximum oil yield of 52 wt. % at 450 °C, decreased to 30 wt. % at 810 °C. Further, the particle's influence showed that higher yield (50

wt. %) of oil was obtained with tire particles with the smaller size (0.32 mm) at the same pyrolysis temperature of 500 °C.

Galvagno et al. (2002) reported that rotating autoclave operations between 550 °C and 680 °C improved the gaseous composition (hydrogen, carbon monoxide, methane, ethane, ethene, and higher hydrocarbons). The rotating autoclave reactor is widely used for pyrolytic liquefaction of scrap tire in the industry in comparison with other reactors are due to the better mixing of feedstocks, enhanced the heat transfer due to slow rotation, can regulate the residence time of feedstock inside the reactor and continuous operation (Lewandowski et al. 2019).

A drop tube pyrolysis reactor for the pyrolysis of waste tire particles (4 mm) was investigated by Conesa and co-authors (2004). The tire particles were fed into a hot reactor (450, 750 and 1000 °C) of 65.4 cm. The increase in pyrolysis temperature showed reduction of oil yield from 37.8 wt. %, decreasing to 10.9 wt. % at 750 °C and to less than 0.0112 wt. % at 1000 °C.

Spouted bed reactors are similar to fluidised reactors in terms of the isothermal condition of bed, high heat and mass transfer, good solid mixing with gas-solid contact. The main difference between the fluidised bed and spouted bed is fluidised bed ability to entrain the whole, coarse and irregular tire particles. Also, the gas residence time in the spouted bed is shorter than a fluidised bed, which improves the heat transfer rate by suppressing secondary reactions. Olazar et al. (2004) used a conical spouted bed reactor to depolymerise scrap tires. The spouted bed is a fluidised bed reactor, enhancing the heat transfer rate and reducing gas residence time (minimises the secondary reactions).

Aylon et al. (2011) investigated various parameters such as temperature (600-800 °C), the mass flow rate of the tire during scrap tire pyrolysis, yield and product composition. The reactor was a continuous screw kiln reactor, externally heated by electric furnace. The reactor is fed by screw feeder from a hopper containing shredded tires from 3.5 to 8.0 kg/h. They have reported a yield of 48.4 wt. % at a temperature of 600 °C and tire mass flow rate of 8 kg/h.

Fixed bed reactors are widely used technology for pyrolysis of scrap tire in academic institutions and research and development organisation due to the simplicity in construction compared to others. The pyrolysis of 10 g tires in a nitrogen-purged fixed bed reactor at a heating rate of 10 °C/min. The maximum oil yield of 60 wt.% is obtained at 425 °C was obtained during the pyrolysis process (Kar et al. 2011). The significant limitation of fixed reactors is low heat transfer, intricacy in operating conditions, and difficulties in working in continuous mode (Arabiourrutia et al. 2020).

Passenger car tires were pyrolyzed in a fixed bed reactor at a temperature of 500 °C, the heating rate of 10 °C/min for 1h. The condensable gas evolved from the first reactor is then passed through the second reactor (a catalyst is placed by a perforated support plate). The study aims to predict the influence of various catalyst temperature (430-600 °C) on product yield and chemical composition during catalytic pyrolysis. ZSM-5 and Y-zeolite are selected as a catalyst, and the tire to catalyst ratio is maintained as 1:1 for the entire reaction. The maximum yield of 55.80 wt. % was obtained at optimum reaction conditions. The results showed that the catalytic pyrolysis reduced the yield with increased gas and coke formation on the catalyst. Also, the Y-zeolite produces a higher amount of benzene, toluene, xylene, naphthalene and alkylated naphthalene due to higher surface acidity and larger pore size than ZSM-5 catalyst.

Auger reactor is promising thermochemical technology to vaporise scrap tires that allow the operation from fast to slow pyrolysis. The main features of the auger reactor are a simple design, ease of operation, low energy input, no requirement of carrier gas for its operation, operating conditions can be regulated easily to obtain desired products. Martinez et al. (2013) present the pyrolysis of scrap tires using a continuous scale auger reactor at a reaction temperature of 500 °C, the pressure of 1 bar and 100 h of operation. The maximum yield of 42.6 wt.% of liquid was obtained. The fuel properties of obtained oil such as density, acidity, water content, and viscosity were matched with marine fuel standards.

Li et al. (2016) investigated the catalytic (ZSM-5, USY, SAPO-11 and ZSM-22) and thermal pyrolysis of scrap tire in a stirred type batch reactor at various temperature. The addition of catalyst increased the gas yield, decreases the char yield. The product yield is found be same after catalytic pyrolysis. The highest yield of oil is observed with ZSM-5 catalyst with a gas yield of 6.49 wt. % due to inherent surface area and firm acidity of ZSM-5, which speed up the conversion of scrap tire into low molecular hydrocarbons.

There is a growing interest in the scientific community towards the pyrolysis of scrap tires using microwave reactors due to enhanced heat transfer, and its operation under isothermal conditions. Song et al. (2018) conducted experiments to study the effect of various factors such as weight hourly space velocity, micropower, size of tire particle, and steel wire on limonene yield from the waste tire. The outcome of limonene depends upon the cleavage of  $\beta$  bonds between the double bonds in the polyisoprene chain and cyclisation of two isoprene monomers. Low micropower (15w/g), high weight hourly space velocity (3.15/ h), small tire size (0.6 mm) and absence of steel wire favours the maximum limonene yield (23.4 wt.%).

Rotating autoclave is a cylindrical type, slow rotating refractory-lined steel cylinder, widely used as incineration of municipal solid waste, medical waste, contaminated soil, waste sludge and hazardous waste. End seals, drive assembly, refractory, control system are the major parts of a typical rotary kiln reactor. Most commercial and semi-commercial pyrolysis plant across the world utilises rotary kiln for pyrolysis of feedstocks due to high production volume of 100 tons per day (Williams, 2013). Compared with other types of reactors for pyrolytic liquefaction of scrap tires, rotary kiln differs in terms of better heat transfer due to slow rotation and slight inclination from the feed end to the outlet during its design. The rotary kiln also finds application in the waste lime recovery, recycling scrap tire and plastics, recovery of activated carbon, thermal desorption of organic waste, and mineral roasting. The present study utilises a rotating autoclave reactor for the pyrolytic liquefaction of scrap tires. Table 2.1 summarizes various types of reactors for pyrolysis of CTPO.

**Table 2.1 Various types of reactors for pyrolysis of scrap tires and comparison with the present study**

<b>Reactor Configuration</b>	<b>Type (Slow/Fast)</b>	<b>Reaction conditions (Temp, Heating rate, Feed, RT)</b>	<b>Temperature (°C)</b>	<b>Optimum yield (wt.%)</b>	<b>Scale up</b>	<b>References</b>
Ablative reactor	Fast	570 °C, -, 5-20 kg/h, 960 s	570	49.8	Simple	Black et al. 1992
Bubbling fluidised bed	Fast	370-570 °C, -, 5-30 g/30 s	-	-	Difficult	Wey et al. 1995
Vacuum	Slow	480-520 °C, 10 °C/min, 80 kg, -	500	47	Easy	Roy et al. 1999
Circulating fluidised bed	Fast	360-810 °C, 10 <sup>3</sup> °C/min, 5 kg/h, 1-5 s	450	52	Easy	Dai et al. 2001
Rotary kiln	Slow	550-680 °C, -, 4.8 kg/h, -	550	38.12	Easy	Galvagno et al. 2002
Fixed bed	Slow	500 °C, 10 °C/min, 200 g, 1h	500	55.8	Difficult	Williams et al. 2002
Drop tube reactor	Fast	450-1000 °C, -, 30 g/h, -	450	37.8	-	Conesa et al. 2004
Conical spouted bed	Fast	425 °C and 500 °C	500	62	Medium	Olazar et al. 2008
Moving screw bed	Fast	600-800 °C, -, 3.5-8.0 kg/h,	600	48.4	Easy	Aylon et al. 2011
Fixed bed	Slow	375-500 °C, 10 °C/min, 10 g, 60 min	425	60	Difficult	Kar et al. 2011
Auger	Intermediate	550 °C, -, 6.7 kg/h, -, 100 h	550	42.6	Medium	Martinez et al., 2013
Stirred reactor	Slow	420-510 °C, 15 °C/min, 150 g, 30 min	500	55.65	Batch scale	Li et al. 2016
Microwave	Intermediate	270 w, 450 w, and 720 w, -, 30g, 30 min	-	23.4*	Difficult	Song et al. 2018
Rotating autoclave	Slow	400 °C, 10 °C/min, 8 tonnes, 10 h	400	44	Easy	Present study

\* yield of limonene

## 2.2 Characterisation of CTPO using various analytical techniques

There are numerous analytical techniques reported in the scientific literature to comprehend the detailed physical, chemical, thermal and stability properties of CTPO. Pyrolysis of scrap tires is conducted at a temperature of 350-600 °C in a fixed-bed batch type reactor with a heating rate of 5 and 35 °C/min to produce crude tire pyrolysis oil—the maximum yield of 38.8 wt. % is obtained at a temperature of 400 °C at 5 °C/min. The obtained oil was characterised using various fuel property testing methods such as ultimate analysis, proximate analysis, chemical composition using different spectrometric techniques such as GC-MS, NMR, FT-IR. The study showed that the fuel properties are comparable with diesel and gasoline from higher heating value, viscosity and density. Functional analysis affirms that the pyrolysis oil from scrap tire is partially similar to diesel and petrol with a significant amount of aliphatic and aromatic hydrocarbons.

One-dimensional gas chromatography-mass spectrometry (1D GC-MS) is conventionally adopted analysis method to find the chemical composition in an oil sample. The major hindrance of 1D GC-MS is the co-elution of peaks at the same retention time during analysis of CTPO. To rectify these problems, Ngxangxa (2016) developed a method to quantify the compounds in tire-derived oils using two-dimensional gas chromatography time of flight mass spectrometry (2D GC×GC TOFMS). DI-limonene, p-cymene, benzothiazole, ethylbenzene, toluene, p-xylene, 3-ethyl toluene,  $\alpha$ -terpinolene are the dominant compounds found in CTPO. Various classes of compounds such as aliphatic, aromatics, terpene, polyaromatic hydrocarbons, oxygen, sulfur and nitrogen-containing compounds are identified in CTPO using 1D GC-MS and 2D GC×GC TOFMS. Another study on pyrolysis of scrap tires was carried out in batch reactor for 30 minutes at 400 °C. The physical properties of CTPO and diesel blends were investigated by Umeki et al. (2016). The compositional analysis by 1D GC-MS revealed that aromatic compounds and olefins are significant compounds in CTPO. Cetane index of CTPO (49.8) is calculated by ASTM methods and similar to diesel. The heating value of CTPO is found to matches with other pyrolysis oil reported in the literature but slightly lower than diesel. CTPO was observed to be miscible with diesel in all concentration. Thus, CTPO cannot be directly utilised in the engine without any further processing.

Pyrolysis of car tires was conducted at a temperature of 500 °C for 10 h. The distillation of collected oil at various temperatures (160 °C, 204 °C and 350 °C) was carried out to study the fluorescence emission from the CTPO using a spectrofluorometer. The whole distilled samples

showed fluorescence emission in the ultraviolet range. They have also concluded that fluorescence emission from tire oil is mainly due to polycyclic aromatic hydrocarbons.

Studies were then conducted on the thermal pyrolysis of bicycle tires in an externally heated fixed-bed pyrolysis reactor at 375 °C by Khan et al. 2016. The CTPO collected from the reactor consists of sediments, char and alkali metals. Thus, distillation was carried out to refine the CTPO and characterised using various analytical techniques. It can be seen that the physicochemical properties such as viscosity, density, calorific value, carbon residue, pour point, ash content and water content of 50 % distilled tire pyrolysis oil (DTPO 50) was found to be similar to diesel. Carbon residue was found to be lower than diesel due to processing of CTPO by distillation. The low pour point of distilled tire pyrolysis oil (less than -16 °C) makes unfit for utilising cold weather conditions.

The CTPO was distilled in batch type distillation apparatus by Obadiah et al. (2017) for 4.5 h. The condensed liquid was then characterised using various analytical techniques such as sulfur content, copper strip corrosion, water content, total contamination, sulphated ash, viscosity, density, heating value, and flashpoint. They concluded that viscosity, density and copper strip corrosion of DTPO were found to be within acceptable limits. The sulfur content of CTPO reduced by 22% due to distillation. However, the major limitation of DTPO in engine study is high amount of sulfur. Sulfur content is relatively higher in comparison with diesel. Sulfur is generated from feedstock during the hardening of raw rubbers.

Chumpitaz et al. (2019) conducted studies on various physicochemical analysis to investigate the atomisation property of CTPO in a Y-jet injector and compared with standard fuel samples. Surface tension is a fundamental parameter to study the atomisation property of any fuel samples. The surface tension of CTPO was found as 0.028 N/m and whereas the surface tension of diesel is reported as 0.026 N/m. Thus, the surface tension of CTPO is found to be higher than diesel due to high density than diesel.

Mohan et al. conducted experiments on scrap tire pyrolysis using a rotating autoclave reactor and presented various upgradation strategies to refine CTPO. Then the obtained oil was extensively characterised using different analytical instruments and compared with diesel. The studies revealed that the inferior properties of CTPO are due to the presence of oxygenates, nitrogen and sulfur-containing compounds. CTPO was then upgraded into diesel range fuels using various cost-effective refining strategies to modify the fuel properties. The stability test was performed before and upgradation to confirm the thermal stability of CTPO using the spot

test and oxidation stability experiments. Studies have shown that the upgraded tire pyrolysis oil was better in physical, chemical, thermal and stability analysis than CTPO due to the adsorption of oxygenates, sulfur, and nitrogen containing compounds silica gel.

Pyrolysis of 5 tons of scrap tires using horizontal axis cylindrical reactor at a temperature of 420-500 °C, 0.8 bar with a rotation speed of 0.4 rpm was investigated by Abdallah et al. (2020). The yield of the reaction was observed to be 45 wt. %. Then, the oil was characterised using various analytical techniques. The density of CTPO is higher than diesel due to the heaviness of the sample. The viscosity of CTPO is observed to be higher than diesel due to the high amount of char particles in CTPO. The flashpoint of CTPO is lower than diesel because the CTPO composes the unrefined fraction with a wide distillation range. Pour point of CTPO is found to relatively lower than diesel. The weak acidity of CTPO may not cause any problems during storage and transportation of pyrolysis oil in polyethene terephthalate bottles. Table 2.2 describes the various analytical techniques used for characterization of CTPO.



**Table 2.2 Various analytical techniques used to characterise CTPO**

S. No.	Author	Analytical techniques	Measurements	Major findings/outcome
1.	Banar et al. 2012	CHNS-O analyser	Elemental composition	The higher amount of nitrogen comes from scrap tire.
2.	Banar et al. 2012	Bomb calorimeter	Calorific value	Matches with diesel
3.	Banar et al. 2012	TGA analyser	Thermal stability	Inferior thermal stability
4.	Banar et al. 2012	<sup>1</sup> H-NMR Spectrometer	Chemical composition	Aromatic fraction increased with increment in heating rate.
5.	Banar et al. 2012	ASTM D-1298	Density	Matches with diesel
6.	Banar et al. 2012	ASTM D-88	Viscosity	Matches with diesel
7.	Banar et al. 2012	ASTM D-93	Flashpoint	Lower due to wide range of compounds with a various distillation range
8.	Banar et al. 2012	ASTM D-86	Distillation	Lighter than diesel fuel
9.	Banar et al. 2012	GC-MS	Chemical composition	Aliphatic compounds are predominant in CTPO.
10.	Banar et al. 2012	ICP-AES (EPA 200.7)	Elemental composition	Heavy metals, chloride, halogen is under the limit of category I waste oil (South African standards)
11.	Ngxangxa 2016	GC×GC TOF-MS	Chemical composition	Developed methods to detect compounds in CTPO
12.	Umeki et al. 2016	Cetane analyser	Cetane index	CTPO of CTPO matches nearly with diesel
13.	Walacik et al. 2016	Spectrofluorometer	Fluorescence	Fluorescence emissions due to polycyclic aromatic hydrocarbons
14.	Khan et al. 2016	ASTM D 97-57	Pour point	Unsuitable to utilise in cold climate conditions
15.	Khan et al. 2016	ASTM D 189-65	Carbon residue	Low for distilled pyrolytic oil
16.	Obadiah et al. 2017	ASTM D5773	Cloud point	Inferior cold flow property than diesel
17.	Obadiah et al. 2017	X-ray fluorescence	Sulfur content	Sulfur is mainly due to the vulcanisation process during manufacturing.

18.	Obadiah et al. 2017	ISO 2160	Copper strip corrosion	No tendency to corrode the metallic parts as per standards
19.	Obadiah et al. 2017	Karl Fischer Titration	Water content	Found to higher than diesel due to high moisture upon storage
20.	Obadiah et al. 2017	EN 12662	Total contamination	Higher than diesel due to the presence of deposits and sediments
21.	Obadiah et al. 2017	ISO 3987	Sulfated ash content	Lower than diesel
22.	Chumpitaz et al. 2019	Du Nouy tension meter	Surface tension	Matches with diesel fuel
23.	Mohan et al. 2019	Spot test	Stability	CTPO has inferior stability
24.	Mohan et al. 2019	Oxidation stability	Thermal stability	CTPO has inferior thermal stability due to polymerisation of olefins
24.	Abdallah et al. 2020	ASTM D 7946-19	Acidic content	Higher storage stability due to weak acidic nature of CTPO

### **2.3 Various refining strategies for upgradation of crude tire pyrolysis oils**

CTPO is a complex liquid mixture from thermal pyrolysis of scrap tire consists of aliphatic, aromatics, hetero-atoms and polar oxygenates. CTPO cannot be directly utilised in single-cylinder diesel engines due to the subsidiary fuel properties. Hydrotreatment, co-pyrolysis, fractionation, sulfur reduction methods, hydrogenation, various catalyst, steam distillation, and different catalyst are the multiple methods for upgrading CTPO in literature. Distillation is a widely implemented upgradation method in semi-commercial and commercial tire oil upgradation units.

Ucar et al. (2007) upgraded crude tire pyrolysis oil at a temperature of 300 °C, 350 °C, and 400 °C in an initial hydrogen atmosphere of 4 and 7 MPa using a different carbon-supported metal catalyst (Co-Ni, Co-Mo, Ni-Mo). The upgraded oil obtained after hydrotreatment using Ni-Mo impregnated in activated carbon showed superior catalytic activity to reduce sulfur content and improve naphtha content.

Islam et al. (2008) conducted experiments on pyrolysis of scrap tires in a fixed bed fire tube heating reactor system to study the effect of feed size, temperature, and residence time on product yield and chemical composition. The maximum liquid output of 49 wt.% was obtained at 475 °C, feed size of 4 cm<sup>3</sup> with a residence time of 5s. Fuel properties such as density, viscosity, gross calorific value, carbon, and hydrogen content are comparable with conventional diesel. There is a significant divergence in the sulfur content and flash point of pyrolysis oil compared to commercial diesel. Sulfur content is higher in CTPO due to addition of sulfur during the vulcanisation process. In contrast, the flashpoint is relatively lower for tire-derived oil due to various chemical compounds with a wide distillation range. Further, they noted that low temperature and large feed size lead to lower liquid and gas yield. The higher temperatures and residence time favour secondary reactions, resulting in the higher liquid yield.

Martinez et al. (2014) conducted the experiments on pyrolysis using forestry biomass and waste tires in a fixed bed reactor (final pyrolysis temperature was 500 °C at 80 °C/min for 15 min. retention time) and continuously auger reactor (final pyrolysis temperature of 500 °C at a final temperature of 500 °C by using nitrogen gas at 5L/min and mass flow rate of 5 kg/h). The experimental results revealed that the addition of a waste tire significantly reduces the amount of aldehyde, phenolic compounds, improve the bio-oil properties and stability. Besides, the addition of scrap tires into biomass significantly lowers the acid content, moisture, oxygenates. However, there is an improvement in the calorific value and acidity of obtained pyrolytic oil.

Ucar et al. (2014) conducted the experiments on co-pyrolysis of pine nut shells and scrap tires in various blend ratio (1:1, 2:1, 4:1, 1:2, 1:4) at 500 °C under an inert atmosphere of nitrogen in a stainless-steel reactor with a diameter of 6 cm and height of 21 cm. The highest bio-oil yield of 47 wt.% was obtained at 1:4 (pine nutshell to scrap tire). They have also pointed out that the addition of scrap tires into pine nut shells decreased the number of aldehydes, ketones, and phenolic compounds in bio-oil with significant improvements in the heating value of gaseous products evolved during the co-pyrolysis reaction.

Undri et al. (2014) conducted the experiments in a batch-type laboratory oven (system A), operating at 2.45 GHz, with an energy output of 6 kW. The pyrolysis setup was then modified by inserting a fractionating system between the pyrolysis reactor and condenser (system B). System B gave more efficient pyrolysis, resulting in a liquid with superior fuel properties matching diesel due to the fractionating system. Due to a fractionating system, the higher boiling compounds may condense inside the reactor and return to the pyrolysis reactor and help retain the unsaturated compounds for a longer duration. The fractionating column lowers density and viscosity with many aromatics and olefins compared to liquid fraction from system A.

Yuwapornpanit et al. (2015) investigated the impact of copper on various types of zeolites (HBETA, HY, and HMOR) in a bench reactor at a temperature of 500 °C with a ramp rate of 10 °C/min and a holding time of 90 min. After reaching the final temperature, they observed that the Cu-promoted catalyst plays a significant role in sulfur reduction from CTPO due to the self-adsorption property.

Debek et al. (2015) investigated the hydro-refining of crude tire pyrolysis oil in the presence of a commercial catalyst such as CoMo-SiO<sub>2</sub>-Al<sub>2</sub>O<sub>3</sub> and NiMo-Al<sub>2</sub>O<sub>3</sub> in a hydro-refining apparatus at 360 °C and a hydrogen pressure of 5 kPa with a retention time of 3h. Hydro-refining of pyrolysis oil in the presence of a catalyst mainly results in the hydrogenation of unsaturated hydrocarbons to saturated hydrocarbons and hydrogenolysis of organic sulfur compounds. They have noted that the CoMo-SiO<sub>2</sub>-Al<sub>2</sub>O<sub>3</sub> catalyst reduces the sulfur from 1.1% to 0.2, and NiMo-Al<sub>2</sub>O<sub>3</sub> decreased the sulfur content to 0.1%. The boiling point of hydro-refined oils (an initial boiling pint is found to be less than 180 °C whereas the final boiling point is reported as below 400 °C) was found to be in the range of gasoline/diesel/fuel oil.

Hita et al. (2015) studied the effect of three Ni-Mo catalysts supported on activated porous materials ( $\gamma$ -Al<sub>2</sub>O<sub>3</sub>, SiO<sub>2</sub>-Al<sub>2</sub>O<sub>3</sub>, SBA-15, MCM-41, equilibrated FCC catalyst) on refining crude tire pyrolysis oil in a fixed-bed reactor working in trickle bed regime at 275-375 °C at a pressure of 65 bar and a space-time of 0.16 h. The study reports that the hydro-treatment of CTPO using Ni-Mo catalyst supported in various porous materials caused 99.99% removal of sulfur and improved the cetane number by five units.

Li et al. (2016) pyrolysed scrap tires in a continuously stirred batch reactor in the presence and absence of catalysts. The maximum yield of derived oil was 55.65 wt.% at the optimum temperature of 500 °C. The catalytic pyrolysis was performed using 1.0 wt.% of catalysts based on ZSM- 5, USY  $\beta$ , SAPO- 11, and ZSM- 22. Catalytic pyrolysis gave better- quality derived oils with higher light oil yields (70–75 wt.%), H/C ratios (1.55–1.65), and lower content of sulfur (0.3–0.58 wt.%) and nitrogen (0.78–1.0 wt.%). Compared with thermal pyrolysis, catalyst increased reaction rate, shortened reaction time, increased conversion efficiency, reduction in char yield, increased gas yield, and yield of derived oil were unchanged. Due to the higher acidity and appropriate pore size of ZSM- 5, USY  $\beta$ , SAPO- 11, and ZSM- 22 catalysts significantly increased single ring aromatics to 45 wt.%.

Dai et al. (2017) conducted experiments on the microwave-assisted co-pyrolysis of soapstock and waste tire using HZSM-5. The highest bio-oil yield was obtained at a temperature of 550 °C. The usage of catalyst significantly enhanced the aromatic composition at the expense of oil reduction. The addition of a waste tire induces a significant synergistic effect in improving the yield of aromatics. It was also found that the addition of the tire reduced the proportion of oxygenates significantly, which was also attributed to the low oxygen content in the tire.

Han et al. (2017) studied the co-pyrolysis of the waste tire and vegetable oil in the presence of CoMo/Al<sub>2</sub>O<sub>3</sub> as a catalyst for the production of transportation fuels. The central focus on the upgradation of bio-oils using co-hydrotreatment is to produce alternative fuels with aliphatic and aromatic hydrocarbons. Aliphatic hydrocarbons ranging from C<sub>7</sub> to C<sub>20</sub> derived from vegetable oils and aromatics from C<sub>6</sub> to C<sub>16</sub> derived from the tire oil were identified as products. Naphtha, diesel, and kerosene fractions were isolated from hydrotreated oils by simple distillation. The properties such as hydrogen to carbon ratio, flash point, and kinematic viscosity were comparable with petroleum fuel.

Obadiah et al. (2017) distilled tire pyrolysis oil at 150-360 °C in a batch scale reactor, and the collected oil was extensively characterised for utilising as an engine fuel application. The study was carried out using a batch apparatus (500 mL round bottom flask condenser packed with steel wool). The steel wool acts as a medium for fractionating CTPO. They have concluded that the fuel properties such as flash point, calorific value, viscosity, and acid value are improved after the distillation of CTPO. Further, the sulfur content in CTPO was reduced by 22.70% after the distillation process.

Miandad et al. (2018) studied the effects of various catalysts such as activated alumina, calcium hydroxide, natural zeolite, and synthetic zeolite on tire pyrolysis oil. The oil yield for activated alumina is found to be maximum due to mild acidity. The use of catalysts decreased the concentration of aromatic compounds in liquid oil down to 60.9% with activated calcium hydroxide, 71.0% with natural zeolite, 84.6% with activated alumina, except for synthetic zeolite producing 93.7% aromatic compounds. Catalytic pyrolysis lowers product yield with an increase in gas and char yield. The fuel properties such as viscosity, density, higher heating value, pour point, and flash point are close to conventional diesel. FT-IR data, coupled with GC-MS analysis, showed that aliphatic and aromatics compounds are found in produced oil samples.

Wang et al. (2018) investigated the synergistic effects of scrap tires and biomass on product distribution and reaction kinetics. Two biomasses were separately mixed based on  $H/C_{\text{eff}}$ , and co-pyrolysis of mixtures was performed using Pyro-GC MS. The percentage of hydrocarbons was found to be increased when increasing  $H/C_{\text{eff}}$  ( $\frac{H-2O-3N-2S}{C}$ ), and the optimal  $H/C_{\text{eff}}$  was determined considering the correspondingly higher yield of polycyclic aromatic hydrocarbons and char residuals at a higher percentage of scrap tire. The experimental derivative thermo gravimetric curves of mixtures at the optimal  $H/C_{\text{eff}}$  were compared with the calculated results based on kinetic analysis of three individual components using the distributed activation energy model. Significant synergetic effects were observed at the initial and final stages of the pyrolysis process. The radical theory showed that biomass could act as an activator for waste tire decomposition. The waste tire could be a hydrogen donor to upgrade the volatile products evolved during co-pyrolysis.

Chen et al. (2019) studied kitchen waste and tire waste's co-pyrolysis using analytical instruments such as TGA-FTIR and pyro GC-MS. The results obtained from TGA-FTIR showed that CO<sub>2</sub>, CO, NO, NH<sub>3</sub>, SO<sub>2</sub>, CeH, and C=C groups were found in the vapours released during co-pyrolysis kitchen waste and scrap tire. Co-pyrolysis reactions showed a positive synergy in pyrolysis kinetics in the ratio of 5:5. Copyrolysis could increase the number of hydrocarbons (13.25 to 37.42% of olefins) and inhibits non-hydrocarbon compounds (63% of volatile products).

Costa et al. (2019) fractionated crude tire pyrolysis oil by steam distillation to produce light fuel fractions. The light fuel oil fraction (mainly consists of volatile organic compounds) was yellow, translucent liquid with a specific gravity of 0.76 g/cm<sup>3</sup>. Light fuel fraction mainly composed of main benzene substituted compounds (62.06 %) with a viscosity of 0.25 mPaS. GC-MS analysis found that light fraction contains benzene substituted compounds, branched-chain alkanes, olefins. In short, the properties of light fuel fraction are found to be matches with petroleum-derived gasoline properties.

Liu et al. (2019) studied hydrothermal liquefaction of scrap tires with waste engine oil for liquid fuel production. They had investigated various activated carbon-supported noble catalysts like Pd/C, Pt/C, Ru/C, Ir/C, and Rh/C to study the effect on product yield. The Rh/C and Pd/C displayed better performance for removing sulfur-containing compounds. Upgraded pyrolysis oils exhibited increased carbon and hydrogen contents but significantly decreased nitrogen, oxygen, and sulfur contents. The upgraded pyrolysis oil mainly consists of saturated and unsaturated hydrocarbons, aromatics, and found to be matched with jet fuel and diesel composition.

Shah et al. (2019) investigated the effect of waste tires on the cotton stalk's thermal pyrolysis in a fixed bed reactor, focusing on liquid quantity and quality. The various blend of the cotton stalk with a waste tire (CS/WT) has experimented in a fixed bed reactor at 20 °C/min with an optimum heating temperature of 550 °C. The blend ratio CS/WT (2:3) showed maximum oil yield (48 wt.%) with organic phase above 78 wt. % of the total liquid yield. A significant increase in carbon and decreased oxygen content of the CS/WT (2:3) pyrolysis oil was observed, which improved its calorific value to 41 MJ/kg. The CS/WT (2:3) oil showed a significant presence of alkanes in GC-MS results, which is associated with the synergistic effect of the co-pyrolysis process. The addition of waste tire to cotton stalk during thermal

pyrolysis improved liquid yield and its quality. The primary limitation of the study is excessive sulfur content in CS/ST (2:3), which can be utilised for road and non-road applications after refining procedures.

Chen et al. (2020) conducted a study on the co-pyrolysis of scrap tire and water hyacinth with a specific motive of improving monocyclic aromatic hydrocarbons. Co-feeding of scrap tire and water hyacinth at a ratio of 1:1 showed significant synergy in product yield and composition. Thermal pyrolysis of water hyacinth at a reaction temperature of 600 °C with a heating rate of 20 °C/ms results in 5.31% monocyclic aromatics, which was significantly increased with co-pyrolysis of scrap tire (13.11%). Further, they have also investigated a comparative study on zeolite and multilamellar MFI nanosheets to study these catalysts' effect on the yield of aromatic hydrocarbons. The higher surface area and accessibility of acid sites favour a higher proportion of monoaromatic hydrocarbons (37.35% - 69.18%) than conventional zeolite.

#### **2.4 Crude tire pyrolysis oil and upgraded tire pyrolysis oil as an alternate fuel in diesel engine**

Studies on CTPO revealed that crude tire pyrolysis oil (CTPO) could be effectively utilised as an alternative fuel for internal combustion engines due to its similarities in alkane fractions and high heat content in comparison with diesel. Murugan et al. (2008) reported that using 10 to 50% of CTPO with diesel fuel in a diesel engine without any modifications results in an increase in brake thermal efficiency (BTE) at constant engine speed. Still, there is a significant increase in the smoke and particulates in the environment due to long ignition delay and high aromatic composition of CTPO compared to diesel.

Another study was conducted to test the performance, emission, and combustion of distilled tire pyrolysis oil in a single-cylinder diesel engine reported by Murugan et al. (2014). The engine was successfully run at 80 to 90% of distilled tire pyrolysis oil (DTPO). NO<sub>x</sub> was lowered by 21% in the case of DTPO80 and an 18% decrease in DTPO90. NO<sub>x</sub> reduction is attributed to the lower viscosity of DTPO80 and DTPO90 compared to other blends, leading to the formation of a proper combustible mixture inside the combustion chamber. The unsaturated compounds like olefins, polyaromatics in crude tire pyrolysis oil produce a higher number of unburned hydrocarbons than diesel.

Studies have been conducted using CTPO in a direct-injected diesel engine produced from pyrolysis of scrap tire using Ca(OH)<sub>2</sub> as a catalyst reported by Ilkiliç & Aydin (2011). They



have concluded that the utilisation of tire fuel blended with diesel increased the emissions (CO, HC, and SO<sub>2</sub>) and smoke opacity. The authors attributed the significant rise in emission from CTPO due to poor atomisation in the combustion chamber and low cetane number. The high density of CTPO caused rich combustion plumes inside the combustion chamber, resulting in higher smoke opacity of tire fuel blends than diesel fuel. They also optimised that the utilisation of 5% of Ca (OH)<sub>2</sub> reduces sulfur content by 35%. They pointed out that 5-35% of tire oil with diesel fuel can be utilised as an alternative fuel for a direct-injected diesel engine without any further modifications.

In another study, Frigo et al. (2014) studied the performance, combustion, emissions, and genotoxicity studies of CTPO from an innovative pilot-scale pyrolyzer with a twin-screw extruder with decreasing section facilitates mechanical compression of materials. The performance studies such as torque, mechanical efficiency, and power revealed no significant variation up to 20% volume of TPO with diesel. The usage of a higher TPO ratio worsens the engine performance and a drastic increment in the emission due to the high sulfur content and low cetane value of CTPO. They also pointed out no mechanical inconvenience during engine operation and no significant carbon deposits found in the piston or cylinder surface. Similarly, Tudu et al. (2014) observed that the utilisation of 10 to 40% of light fraction pyrolysis oil caused higher emissions (HC, NO, CO) and smoke than diesel fuel viscosity, high density, low volatility, and low heating value.

According to Vihar et al. (2015), the study was conducted in a non-inter-cooled turbocharged compression ignition multi-cylinder engine using 100% TPO as a fuel source. They observed that CTPO can be fully utilised in an internal combustion engine and found that diesel-like stable combustion was observed without any external modifications. However, nitrogen and sulfur oxides are increased with rising in load due to the high amount of nitrogen and sulfur in the crude tire pyrolysis oil compared to diesel.

Kumaravel et al. (2016) discussed an overview of the literature that explains an exhaustive idea about the pyrolysis mechanism for designing various types of reactor, performance, combustion, and emission analysis of CTPO in the diesel engine. The review suggests that the CTPO blend up to 35% with diesel can be utilised directly in the diesel engine without any modification. Still, 50-100% of CTPO blend with diesel decreases the engine performance and increases the emission due to the high aromatic content of CTPO. In short, CTPO can be

utilised entirely in an internal combustion engine with a reduction in aromatic compounds and viscosity.

CTPO was being used in a modern turbocharged inter-cooled diesel engine by Žvar Baškovič et al. (2017). The widely used approaches for utilising CTPO in diesel engines are blending with cetane improvers, improving inlet air temperature, and increasing the compression ratio. The proposed study used a pilot-scale tailored injection strategy to utilise 100% CTPO in the engine without any hardware modifications. The results showed that emissions are comparable to diesel. However, there was a slight elevation in releasing unburnt hydrocarbons due to variation in the cetane number and ignition delay of CTPO.

Verma et al. (2018) investigated the potential of oil derived from scrap tire pyrolysis as a fuel for internal combustion engines. The majority of studies concluded that emissions such as CO, CO<sub>2</sub>, and NO<sub>x</sub> are increased with an increase in the composition of CTPO. This is mainly ascribed due to the high density and aromatic content of oil derived from scrap tires. Uyumaz et al. (2019) studied pyrolysed scrap tires in a fixed bed reactor at 400-500 °C at a heating rate of 20 °C/min in the presence of N<sub>2</sub> as a sweeping gas. They have found that 400 °C showed more liquid yield than other temperature profiles. The test results showed an increase in the detonation tendency with a rise in engine load. Further, the emission studies displayed a 13.7% reduction in CO and a 7.62% increase in nitrous oxide emission.

Shahir et al. (2020) investigated the performance and emission characteristics of tire pyrolysis oil using a standard common rail direct injection diesel engine (CRDI) by varying the CTPO blend with diesel in the ratio of 0 to 50%. They found that the brake thermal efficiency increases with an improved blend ratio of tire pyrolysis oil with diesel. They also optimised that CTPO30 exhibits better emission and performance than diesel fuel due to higher oxygen content, which causes lower specific fuel consumption. In another study by Bodisco et al. (2019), the analysis was conducted in a modern commercial light-duty diesel vehicle to measure nitrous oxide emission using tire oil and diesel blends. They found that the utilisation of tire oil blended diesel fuel does not significantly increase the nitrous oxide emission than neat diesel.

Recently a novel approach using destructive distillation techniques developed by Green distillation technologies, up-gradation plants in Australia reduced the NO<sub>x</sub> and particulate matter emissions by 30 and 35-60%. They argued that the fuel has superior performance and emission due to the higher fuel quality produced by Hossain et al. (2020). Table 2.2 summarises

various studies on utilising crude tire pyrolytic oil as a fuel blend to study the performance, combustion, and emission characteristics in a single-cylinder diesel engine.

## **2.5 Use of ethyl levulinate as a bio-fuel additive**

Fuel additives are natural substances added to fuel to improve the combustion quality and reduces the emissions from diesel engines. Conventionally, fuel additives are added in terms of ppm levels. Ethyl levulinate is a biomass-derived bio-diluent produced by esterification of levulinic acid and ethanol. Levulinic acid is obtained from wheat straw, cane sugar, grain, sorghum and agricultural wastes (Wang et al. 2012). Alkyl levulinates have many applications as a fuel oxygenate, diesel additive, green solvent, surfactant, plasticisers and renewable intermediate in value addition pathway. The specific reasons for the consideration of ethyl levulinate in upgraded tire-derived oil are high miscibility, high oxygen content, high latent heat of evaporation, low ignition delay, low viscosity, high fire reliability, improved cold flow properties, cleanliness, non-toxic, low acidity and biomass-derived (Imdadul et al. 2015).

Experiments were conducted to investigate the effect of ethyl levulinate as an additive in a single-cylinder diesel engine to measure the performance, combustion, and emissions. The authors proposed a relationship between emission and combustion using grey relational analysis by Lei et al. (2013). They suggested that oxygen content in fuel blends play an inevitable role in performance and combustion from diesel engines. Lei et al. (2016) conducted experiments to test the influence of ethyl levulinate as a fuel additive on the performance and emission from single-cylinder diesel engines. They have tried various fuel blends like B1E4, B3E4, B2E3, and B2.5E2.5, where B and E represent the percentage of biodiesel and diesel in respective fuel samples. The remaining portion in each fuel sample has neat diesel fuel. The engine tests corroborate that the torque and power of the engine are found similar to diesel. The fuel consumption of the tested blends was drastically reduced due to decreased density and viscosity of ethyl levulinate, resulting in lower fuel consumption than diesel. Interestingly, the emission data from the emission analyser shows a significant reduction in the release of unburnt hydrocarbons, carbon monoxide, and smoke content but the nitrous oxide content and carbon dioxide emission were found to be in a higher percentage than diesel. The reduction in smoke and unburned hydrocarbons is due to complete combustion inside the cylinder due to abundant oxygen from ethyl levulinate during combustion.

Wang et al. (2012) studied the effect of 5%, 10%, and 15% (with 20% n-butanol) and 20% (with 5% n-butanol) with ethyl levulinate and diesel to study the performance and emission

characteristics in a single-cylinder diesel engine. Studies revealed that smoke emissions are drastically reduced with the usage of EL as an additive. Further,  $\text{NO}_x$  is found to be reduced by 5% and 10% EL with diesel.

The studies by Ahmad et al. (2016) reported the catalytic and mechanistic insights into the production of ethyl levulinate from bio-renewable feedstocks. A search on Scopus suggests that EL studies as a fuel additive have gained significant momentum over the past few years. EL has a high solubility in aromatics. Ethyl levulinate showed merits over other additives by reducing harmful emissions, miscibility, and shorter degradation time. Another study to test ethyl levulinate's antiknock quality on a gasoline-based engine was documented by Tian et al. (2017). Due to ketone and ester groups in a carbon chain of ethyl levulinate, it boosts the chemical reaction during the auto-oxidation process inside the engine cylinder, which lowers the reaction rate forming a stable intermediate (based on derived cetane index data). In short, it can be concluded that the ethyl levulinate is regarded as a good additive for biofuel combustion due to superior fuel properties.

Further, the studies on the effect of n-butanol in tire pyrolysis oil-diesel blend were conducted by Karagoz et al. (2020) to study a single-cylinder diesel engine's performance and emission characteristics. Test results have shown that the performance parameters like brake thermal efficiency and brake specific fuel consumption are significantly improved due to higher amounts of oxygenates, calorific value, and lower density. The emission component such as nitrous oxide, carbon monoxide, and hydrocarbon emissions was found to be lowered than tire-derived oil-diesel binary blends by adding n-butanol as an oxygenated additive. Table 2.3 summarizes the various studies on the utilization of CTPO in diesel engine.

**Table 2.3 Summary of some studies on the utilisation of tire pyrolysis oil in diesel engine**

Literature	(Murugan et al., 2008)	(Murugan et al., 2008)	(Tudu et al., 2014)	(Sharma & Murugan, 2015)	(Uyumaz et al., 2019)	(Hossain et al., 2020)	Present study (StTPO)	Present study (EL as an additive)
Blend composition	10%,30%,50 %CTPO+90 %,70%,50% diesel	80%,90% DTPO+20%, 10% diesel	20%,40%,60 % LFPO and 80%,60%,40 % diesel and 40% LFPO+10% DEE	80% JME and 20% diesel	10% tire oil and 90% diesel	10% tire oil+90% diesel, 20% tire oil+80% diesel	20,40,60,80, 100% of StTPO with 80,60,40,20, 100% of diesel	20, 40, 60, 80, 100% of StTPO with 80,60,40,20 and 10% EL
Form of blend	Binary	Binary	Ternary	Binary	Binary	Binary	Binary	Ternary
Fraction	Tire oil+diesel	Tire oil +diesel	LFPO+DEE+ diesel	Tire oil+ JME+diesel	Tire oil+diesel	Tire oil+diesel	Tire oil+diesel	Tire oil+EL+diesel
Fuel production method	Pyrolysis	Pyrolysis	Pyrolysis	Pyrolysis and trans-esterification	Pyrolysis	Pyrolysis	Pyrolysis	Pyrolysis
Refining/ up-gradation technology	Direct application	Distillation	Addition of DEE	Adding biodiesel	Direct application	Destructive distillation	Preferential adsorption by the adsorbent	Preferential adsorption by the adsorbent
Reference fuel	Diesel	Diesel	Diesel	Diesel	Diesel	Diesel	Diesel	Diesel
BTE	Lower	Lower	n.r	n.r	Lesser	Lesser	Lower	Lower
BSFC	Higher	Higher	Lower	n.r	Higher	Higher	Lower	Lower
CO	Higher	Higher	Higher	Higher	Lower	Higher	Higher	Lower
CO <sub>2</sub>	n.r	n.r	Lower	n.r	Higher	n.r	Higher	Lower
HC	Higher	Higher	Higher	Higher	n.r	n.r	Higher	Lower

NO <sub>x</sub>	Higher	Lower	Lower	Higher	Higher	Lower	Higher	Lower
Smoke/particulates	Higher	Higher	Lower	Lower	Lower	Lesser	n.r	n.r
Cylinder pressure	Higher	Higher	Higher	Decrease	Higher	Lower	Higher	Higher
Heat release rate	Higher	Higher	Higher	Decrease	n.r	Lower	Higher	Higher
Rate of pressure rise	Higher	Higher	Higher	n.r	n.r	Lower	Higher	Higher

\*n. r (not reported)

## 2.6 Mechanism of diesel spray development in diesel engines

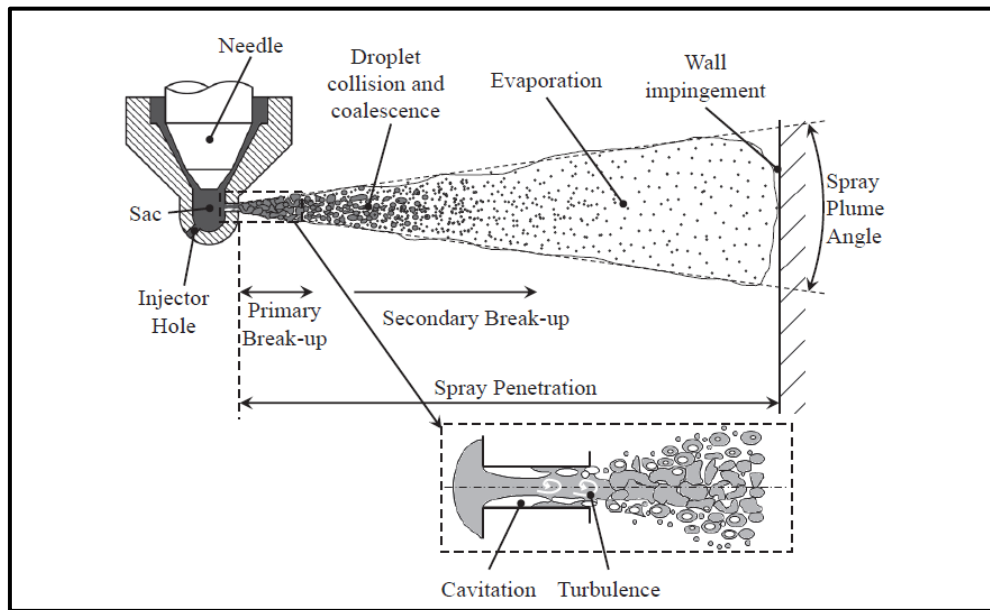


**Fig. 2.3 Mechanism of diesel spray development and break up.**  
(Source: Adapted from Boggavarapu et al. 2013)

Liquid spray should rapidly be atomized into a spray. Short breakup length and wide spray angle are the favourable factors to promote well-distributed spray. The second process in diesel spray combustion is the mixing of fuel and air in the combustion chamber. Swirl flow induced by the intake air has significant effects on the bulk movement of spray and air in the combustion chamber. Squish flow generated by the piston triggers the mixing at the lip of the cavity. Turbulent flow caused by swirl and squish motion accelerates the local mixing inside the spray. Fuel atomization is determined by various factors such as physical properties, surrounding gas conditions, and type of atomizer (Tonini et al. 2009, Ejim et al. 2007). When the fuel is introduced into the diesel engine's combustion chamber, the liquid column leaving the nozzle disintegrates within the cylinder over a finite length called breakup length (Lindstrom 2009). As the spray moves away from the nozzle, the mass of air within the spray increases diverges, and the velocity of the spray is reduced. As the low jet velocity in the Rayleigh regime, break up is progressed due to the unstable growth of surface waves caused by surface tension, which results in larger droplets than the jet diameter (Heywood 1988). As the velocity increases, the force due to the relative motion of the jet and the surrounding air elevates the surface tension force leads to drop sizes in the order of the jet diameter is called the first wind-induced breakup regime. In the second wind-induced breakup regime, the unstable growth of short wavelength waves induced by the relative motion between liquid and air produces droplets whose average size is less than nozzle diameter.

Further, an increase in the jet velocity leads to catastrophic breakup in the atomization regime, which results in droplets whose average diameter is much smaller than nozzle diameter. Aerodynamic interactions at the liquid-gas interface play a prominent role in the atomization regime of diesel spray. Reynolds number and Weber number are two-dimensional terms to predict the atomization of diesel sprays. The fragmentation of diesel spray can be classified into various modes such as vibrational, bag, chaotic, sheet stripping, wave crest stripping, and catastrophic breakup methods based on weber number (Tretel 2020).

If the turbulent intensity of the nozzle flow is high, it induces the liquid breakup and nozzle exit rapidly. Cavitation occurs when the local pressure of liquid decreases to saturation pressure. The cavitation reduces the effective flow area in the nozzle and enhances the liquid breakup when the low-pressure bubbles collapse within the flow. The liquid is fragmented aerodynamically by the velocity difference between the liquid core and surrounding air outside the nozzle. Turbulence, cavitation, and aerodynamic shear are the prominent driving forces of spray breakup near the nozzle (Kawaharada et al. 2020).

$$Re = \frac{\rho v d}{\mu}$$

$$We = \frac{\rho v^2 d}{\mu}$$

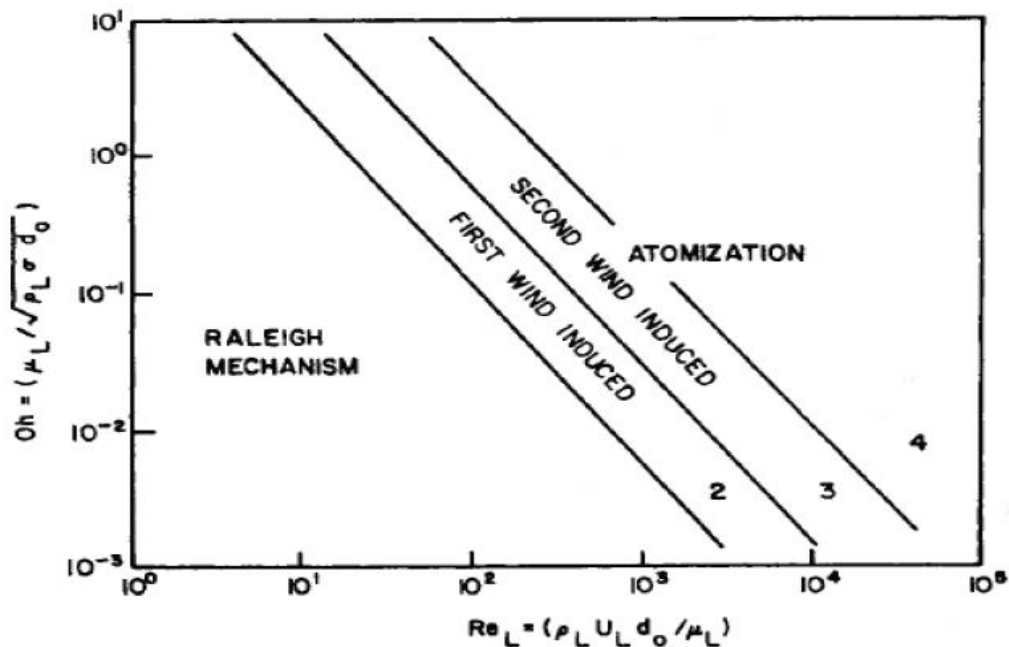


**Fig. 2.4 Various modes of liquid disintegration**  
(Source: Lindstrom et al. 2009)



**Table 2.4 Classification of diesel spray breakup regimes**

<b>Regimes</b>	<b>The mechanism involved in various regimes</b>
Rayleigh breakup	Surface tension
First wind-induced breakup	Surface tension, dynamic pressure, air
Second wind-induced breakup	The dynamic pressure of air opposed by surface tension
Atomization	Unknown

Spray angle, breakup length, the core of the spray, spray penetration, the size distribution of the spray, mean diameter of the spray, the spatial distribution of the spray, turbulence, cavitation phenomena are the various terminologies to designate the characteristics of a typical diesel spray (Arai et al. 2012, Xin et al. 2014, Tziourtzioumis et al. 2017, Dizay 2016). Generally, high viscosity fuels provide more considerable penetration length and slight cone angle, causing poor atomization and the formation of large fuel droplets (Hoang et al. 2019, Lefebvre et al. 2017, and Verduzco et al. 2012). Thus, cone angle and penetration length are considered two essential parameters characterizing the diesel spray, which impact the air-fuel mixture formation in the combustion chamber. The detailed mechanism of spray characteristics of CTPO and StTPO blends will be studied as a future course of present investigations.

## **2.7 Combustion in diesel engines**

The major combustion phase in diesel engines comprises premixed combustion, mixed-phase combustion and late phase combustion (Ashok et al. 2019). The heat release from the diesel engine depends on the viscosity, heating value, duration of ignition delay, volatility and lower heating value of fuel (Babu et al. 2019). The heat release rate is a crucial combustion parameter obtained by applying the first law of thermodynamics on the in-cylinder gas pressure variable. It plays a significant influence on combustion noise, rate of pressure rise and nitrous oxide emissions. Heywood's traditional single zone first law heat release model was given by the following equation (Rao et al. 2018).

$$\frac{dQ}{d\theta} = \frac{\gamma}{\gamma - 1} \times P \frac{dv}{d\theta} + \frac{\gamma}{\gamma - 1} V \times \frac{dP}{d\theta}$$

Where  $\frac{dQ}{d\theta}$  (J/deg.) and rare heat release and the ratio of specific heat, respectively.

The cylinder pressure and crank angle signals were obtained from the data logger for the defined engine load. The data was stored in a computer-based data acquisition system for 100 cycles. Using the data obtained from the combustion cycle, the net heat release was calculated based on the first law of thermodynamics by considering the average pressure and crank angle

data. The in-cylinder pressure reflects the combustion process, which involves the piston work done on gas, heat transfer to combustion chamber walls, and the mass of the flow inlet and outlet of the crevice regions between the piston, piston rings and cylinder liner. The combustion process propagates through the combustion chamber, and each of the processes must be related to cylinder pressure. A single-zone model is used to find heat release from a single-cylinder diesel engine based on the first law of thermodynamics, where  $du$  is the change of internal energy of mass in the system,  $dQ$  is the heat transfer to the system, and  $dw$  is the work produced by the system (Rao et al. 2018).

$$dU = dQ - dW + \sum hi dmi$$

Heat transfer in the cylinder occurs by convection and radiation, where the forced convection constitutes a prominent role in applications. Heat transfer by convection is the transfer of energy within the fluid due to the movement from the solid surface.  $Q_{ht}$  gives the magnitude and rate of energy transfer. This occurred in the direction perpendicular to the fluid surface and was obtained by the newton law of cooling as follows (Rao et al. 2018).

$$Q_{ht} = h A \Delta T = h A (T - T_w)$$

During the combustion process, the chemical energy released from a typical fuel is given as follows, where  $dQ_{ch}$  is the heat energy released due to chemical energy,  $dQ_{ht}$  is the heat transfer due to convection,  $V_{cr}$  is crevice volume,  $T_w$  is the wall temperature, and  $T$  is the temperature of gas flow out of the crevice volume (Rao et al. 2018).

$$\begin{aligned} dQ_{ch} &= \frac{1}{\gamma-1} V dp + \frac{\gamma}{\gamma-1} p dV + dQ_{ht} + (c_v T + RT \left(1 + \frac{1}{\gamma-1}\right)) \frac{V_{cr}}{RT_w} dp \\ &= \frac{1}{\gamma-1} V dp + \frac{\gamma}{\gamma-1} p dV + dQ_{ht} + \left(\frac{1}{\gamma-1} T + T \left(1 + \frac{1}{\gamma-1}\right)\right) \frac{V_{cr}}{T_w} dp \end{aligned}$$

## 2.8 Mechanism of NO<sub>x</sub> Formation in diesel engines

There are mainly three mechanisms that govern NO<sub>x</sub> formation in diesel engines (Stone 2012, Kim et al. 2020, Mahallawy et al. 2002, Ma et al. 2015, Sindhu et al. 2018, Timpanaro 2019) are Thermal NO<sub>x</sub>, Prompt NO<sub>x</sub> and Fuel bound NO<sub>x</sub> (Fig. 2).

### 1. Thermal NO<sub>x</sub>

The primary mechanism of NO<sub>x</sub> formation in the combustion process occurs from burning fuel at high temperatures in a process known as thermal NO<sub>x</sub>. In this high temperature (above

1873K), the strong triple bond in nitrogen is broken to react with oxygen to form  $\text{NO}_x$ . The primary reaction of nitrous oxide formation by zeldovich is shown in the following figure.

## 2. Prompt $\text{NO}_x$

Fennimore discovered the mechanism of prompt nitrous oxide formation in 1971. When  $\text{N}_2$  rapidly react in first stages of combustion with oxygen and radical, typically carbon, methylidyne radicals and methylene to form  $\text{NO}$ ,  $\text{NO}_2$ ,  $\text{CO}$  and  $\text{H}_2\text{O}$ . Various intermediate radicals such as imidogen and hydrogen cyanide form and continue to form  $\text{NO}_x$  through numerous and complex chemical reactions. This process typically takes place in the initial stages of fuel combustion in fuel-rich regions near the flame front.

## 3. Fuel bound $\text{NO}_x$

When bound nitrogen in certain fuels like coal and petroleum are directly oxidized during combustion,  $\text{NO}_x$  is formed. This mechanism occurs due to the formation of  $\text{HCN}$  and  $\text{NH}_3$  from the fuel bound nitrogen. These intermediate compounds are then oxidized in the early stages of combustion through multiple reactions. These newly formed compounds complete hundreds of various reactions that lead to the formation of  $\text{NO}_x$ .

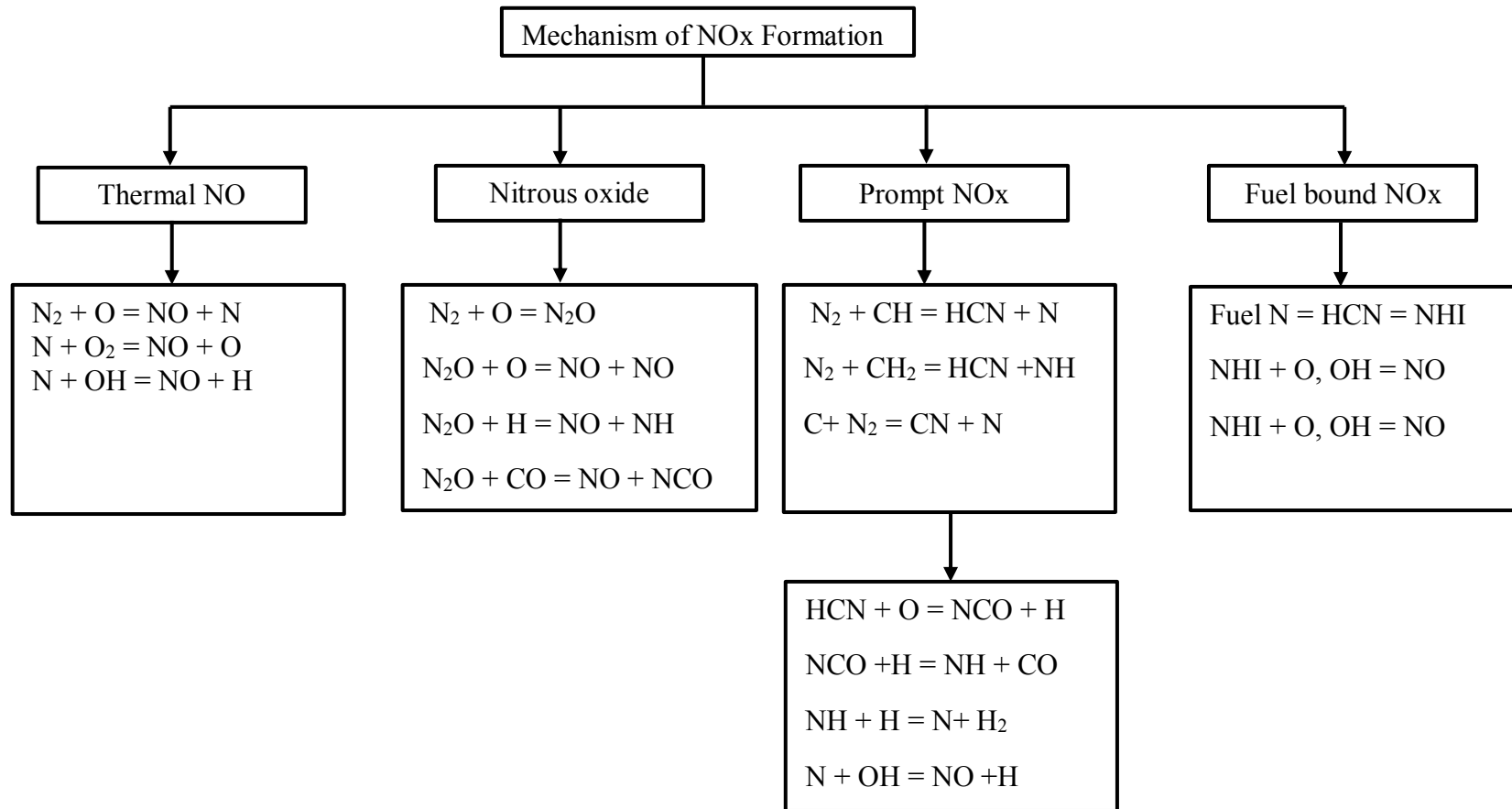


**Fig. 2.5 Various mechanisms of NO<sub>x</sub> formation**  
 (Source: Adapted from El-Mahallawy et al. 2002)

## 2.9 Summary of literature review

Pyrolysis is an attractive thermochemical conversion technology to depolymerise scrap tires into liquid oil, char and steel wires in an inert atmosphere at a temperature of 400-600 °C. The significant factors that affect the pyrolysis reaction are the configuration of the reactor, the particle size of the feedstock, temperature, pressure, and heating rate. Several types of reactors such as fixed bed, auger reactor, stirred reactor, microwave reactor, rotary oven, bubbling fluidised bed, circulating fluidised bed, spouted bed, rotating cone, ablative reactors are reported in the scientific literature for pyrolysis of scrap tires. Pyrolysis reactors are classified as slow or fast, depending on the heating rate of reaction and residence time. Slow pyrolysis is characterised by low heating rate, longer vapour residence time and carried out at a low temperature and fast pyrolysis is characterised by high heating rate, shorter residence time and take place at a higher temperature. Among these reactors, fixed bed reactors are commonly used in the academic community due to simplicity in construction. The major technical constraint is the loading and unloading of samples in the fixed bed reactor. Very few studies were reported on the pyrolytic liquefaction of scrap tire into fuel using a rotating autoclave reactor. However, the present research focuses on the pyrolysis of scrap tires using a rotating autoclave reactor due to better mixing, improved heat transfer, the residence time of feedstocks can be easily adjusted and uniformity in the liquid product.

The major obstacles to direct utilisation of CTPO in a single-cylinder diesel engine are low flash point, low calorific value, high viscosity, high acidity, low cetane index, subsidiary cold flow properties, presence of sulfur, oxygen and nitrogen-containing compounds and unpleasant odour. The unpleasant odour from CTPO is due to sulfur and nitrogen-containing compounds such as mercaptans, thiols, benzothiazoles, sulfides and disulfides. To understand the detailed properties of pyrolysis oil, the extensive characterisation needs to be performed using various analytical techniques.

CTPO obtained from pyrolysis reactors was analysed using various analytical instruments. Most of the studies are reported on the ultimate analysis, proximate analysis, physical property analysis, compositional analysis (GC-MS, GC×GC TOF-MS, NMR, FT-IR), thermal analysis (DSC). There are no studies reported on the prediction of the stability of tire-derived oils. Besides, very few studies are reported on the extensive characterisation using GC×GC TOF-MS.

CTPO cannot be directly used in single-cylinder diesel engines for a long-term run due to the high amount of sulfur, nitrogen, and inferior oil properties. Thus, CTPO needs to be further processed using various methods of refining techniques. Distillation, hydroprocessing, esterification, hydrodesulphurization, oxidation desulfurization, multiple adsorbents, hydrotreating, hydrocracking, and photocatalytic oxidation, vacuum distillation and catalytic upgrading. Among these, thermal distillation is a widely employed refining method in most tire processing plants. Distillation is an energy-intensive process and high capital investment for the deployment at a larger scale. Hence, a cost-effective refining strategy for CTPO needs to be formulated using cost-effective adsorbents and solvents.

To predict the performance, combustion and emission of CTPO from a single-cylinder diesel engine, most of the researchers blended CTPO with diesel. Higher brake specific energy consumption, inferior combustion properties (longer ignition delay, high heat release rate, increased cylinder pressure), a higher amount of nitrous oxides formation, high amount of carbon oxides, increased quantity of unburned hydrocarbons, more amount of particulates are the detrimental issues with CTPO. There is scarce literature that focuses on the performance, combustion and emission analysis using upgraded tire pyrolysis oil refined using cost-effective adsorbents and solvents.

Researchers have used various additives such as oxygen-based (diethyl ether), alcohol-based (methanol, butanol), different biodiesel (seaweed, jatropha), lubricant based additive (motor silk lubricant oil), nano-based additives (cerium oxides) to improve the combustion quality of CTPO. Out of which, oxygenated based additives are widely explored in the case of engine study using CTPO in comparison with others due to the high amount of oxygenates. Oxygenated additives have the inherent capability to decrease cylinder temperature due to higher latent heat of evaporation (lower nitrous oxide formation). Very few literature reported applying ethyl levulinate (EL) as a bio-diluent upgraded tire-derived oil in single-cylinder diesel engines to study the performance, combustion and emissions. The significant constraints to utilise EL in diesel is its low miscibility. Compared with other oxygenated additives for blending with CTPO such as diethyl ether, methanol and butanol, EL differs from others in terms of inherent features such as non-toxic, biomass-derived and sustainable. Based on the literature review, significant points are summarised as follows.

1. Very few literature are available on the detailed characterisation of CTPO using different analytical instruments.
2. Stability studies of tire-derived oil are found to be very scarce in the literature.
3. No studies are available on the refining of CTPO using cost-effective adsorbents and solvents.
4. EL as a diluent in StTPO to study the performance, combustion and emission from the single-cylinder diesel engine is reported for the first time.

### **2.10 Research gap**

The following research gap is found in the open literature survey.

1. The upgraded tire pyrolysis oil obtained from novel scalable refining technology using silica as adsorbent and petroleum ether as diluent are very scant in the open literature.
2. It can be noticed that the comprehensive fuel characterisation of CTPO using various analytical techniques is scarce in the open literature.
3. There is no literature reported on the effect of upgraded oil from the proposed up-gradation strategy (preferential adsorption using silica gel as adsorbent and petroleum ether as diluent) on performance, combustion, and emission characteristics in a single-cylinder diesel engine.
4. No studies were found in the open scientific literature to inspect the effect of an ethyl levulinate as a bio-fuel additive on performance, combustion, and emissions from a single-cylinder diesel engine.

### **2.11 Objectives of the present investigation**

The present study examines the extensive characterisation of fuel produced from the novel up-gradation technology. It investigates the effect of obtained oil on the performance, combustion, and emission characteristics of a single-cylinder, direct-injected diesel engine. The detailed objectives of the present research work are summarised as follows.

1. To carry out pyrolytic liquefaction of scrap tires in a 10-ton rotating autoclave reactor in optimum reaction conditions and the extensive characterisation of CTPO using various analytical techniques.

2. Designing various cost-effective upgradation strategies for refining CTPO into diesel range fuel and extensive characterisation of refined oils compared with CTPO and diesel.
3. To study the performance, combustion, and emission studies of upgraded tire pyrolysis oil in a single-cylinder diesel engine and compare CTPO and diesel as a reference fuel.
4. Scrutinise ethyl levulinate as a bio-diluent on performance, combustion, and emission from the single-cylinder diesel engine and comparative study with upgraded oil, CTPO diesel as a reference fuel.

### **2.12 Scope of the work or results expected**

- a. Setup of an upgradation test rig for refining polymer derived oils from tires, plastics.
- b. Many of the inferior properties of CTPO like a low flash point, high acid value, low calorific value, low oxidation stability, the pungent smell may revamp after up-gradation strategy.
- c. The engine may run successfully with 100% upgraded oil without any seizing or blocking in the engine parts.
- d. The use of ethyl levulinate as a bio-diluent may curb the soot content and lowers the ignition delay in diesel engines.



## CHAPTER 3

### EXPERIMENTAL METHODOLOGY

This chapter discusses the various analytical techniques and instrumentation employed for fulfilling the framed objectives in the present study. Furthermore, the study delineates various components, measurement techniques, instrumentation in single-cylinder diesel engine test-rig at the Internal Combustion Engines Research Laboratory, National Institute of Technology Karnataka, Surathkal.

#### 3.1 Materials

Diesel was procured from an Indian oil corporation. Silica gel (CAS No. 112926-00-8) and petroleum ether (CAS No. 8032-32-4) was purchased from Loba Chemie Private Limited. Ethyl levulinate with (CAS No. 539-88-8) ( $\geq 98\%$  purity) was procured from Sigma Aldrich. The fabrication of laboratory stirrer, microfiltration assembly, and rotary evaporator were fabricated by Amit and Abhishek Scientific Enterprises, Mumbai. The specifications of silica gel and petroleum ether are detailed in Table 3.1, Table 3.2 and Table 3.3.

**Table 3.1 Physical properties of silica gel** (Source: URL 02)

S. No.	Parameters	Silica gel (SiO <sub>2</sub> )
1.	Boiling point	2230 °C
2.	Melting point	> 16 °C
3.	pH	7
4.	Pore diameter	40-60 Å
5.	Surface area	350-450 m <sup>2</sup> /gm
6.	Colour	White solid
7.	Particle size	60-120 mesh (250-125 µm)
8.	Solubility in water	Insoluble
9.	Odour	Odourless
10.	Bulk density	500-650 kg/L
11.	Physical state	Crystalline

**Tale 3.2 Physical properties of petroleum ether** (Source: URL 03)

S. No.	Parameters	Petroleum ether
1.	Boiling point	60-80 °C
2.	Vapour pressure at 20 °C	200 hPa
3.	Auto-ignition temperature	240 °C
4.	Density	0.66-0.68 g/cm <sup>3</sup>
5.	Flash point	-26 °C
6.	Physical state	Liquid
7.	Colour	Clear, colourless
8.	Solubility in water	Insoluble
9.	Odour	Gasoline or kerosene
10.	Flammability in solid, gas	Flammable

**Table 3.3 Fuel properties of ethyl levulinate** (Source: Windom et al. 2011)

Property	Ethyl levulinate
Appearance	Yellow
Chemical formulae	C <sub>7</sub> H <sub>12</sub> O <sub>3</sub>
Molecular weight	144.17 gm/mol
Boiling point	205.8 °C
Melting point	- 32.8 °C
Density at 25 °C	1.00831 g/mL
Flash point	90.6 °C
Refractive index at 20 °C	1.4225
Enthalpy of combustion	-3523 kJ/mol

### 3.2 Thermal depolymerisation of scrap tire into CTPO

Pyrolysis oil was prepared by conducting experiments in a rotating autoclave pilot-scale facility at Mandakan Energy Products, Palakkad, India, at a 400 °C, 0.2 bar, 4 rpm at a heating rate of 10 °C/min. Thermal pyrolysis of scrap tire to crude tire pyrolysis oil in a 10-ton industrial scale tire pyrolysis facility. The process scheme for the production of CTPO from worn tires and whole process equipment for oil production is also detailed in Fig. 3.1. Rotating autoclave reactor, primary pressure vessel, condenser for condensation of gas, wet scrubber, oil collection

drums, forced-draft air cooler, etc., are main parts of pyrolysis system. The attractive feature is gas storage balloons set-up for collecting non-condensable volatiles during the depolymerisation of scrap tires. The compressed gas stored in the balloons is feedback in the rotating autoclave, which acts as a heating source for further pyrolysis reactions. The detailed specifications of 10-ton pyrolysis plant with technical specifications are detailed in Table 3.4 and Fig. 3.2. The photographs of 10-ton rotating autoclave reactor is shown in Appendix (Fig. I-1) and Fig. I-2)

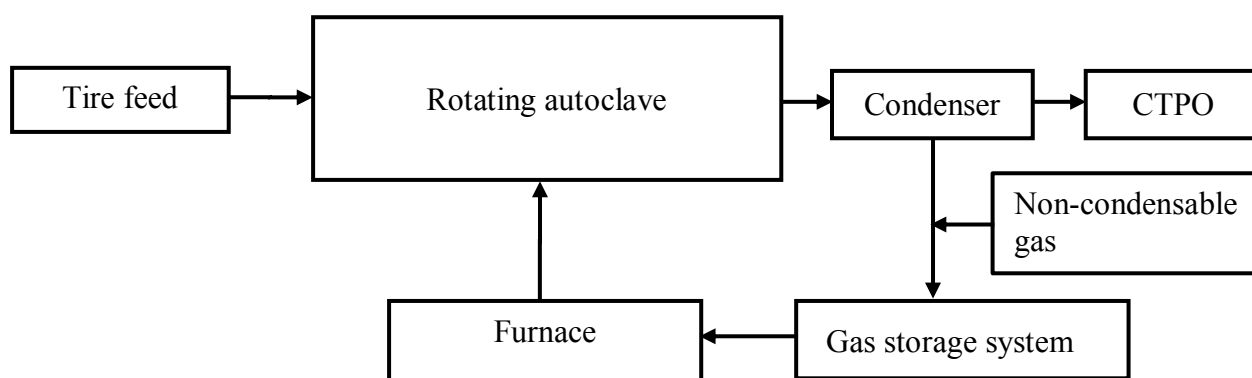


**Fig. 3.1 Basic layout of pyrolysis of scrap tires**

**Table 3.4 Specification of 10-ton Tire pyrolysis plant**

S. No.	Item	Description
1.	Main reactor	14 mm BQ Plate (6600 mm length×2800 mm width×0.014m thick), 4 rpm (horizontal rotation)
2.	Pipe Condenser	C Class Pipe- 5mm MS
3.	Insulation tank	5 mm MS Plate
4.	Water seal tank	5 mm MS Plate
5.	Gas tank	5 mm MS Plate
6.	Oil tank	5 mm MS Plate
7.	Water coolant pipe	C Class Pipe – 5 mm MS
8.	Chimney	C Class Pipe – 5mm MS
9.	Gas blower	0.5 hp
10.	Gas burner	100×450 mm
11.	Cooling tower	Capacity 70 TR 5.25×5.25 feet
12.	Reactor Cover	Cera wool, Temp- 1260 °C, Thickness – 14 mm

13.	Transmission system	Dual speed motor
14.	Reactor Gear box	Shricon brand 10 hp Helical gear
15.	Noise	Less than or equal to 85 dB
16.	Cooling area of condenser	5100 mm <sup>2</sup>
17.	Total power	25 kW
18.	Auxiliary equipment's	Tire side wall cutting equipment, Hydrocarbon gas storage system, Carbon briquetting machine

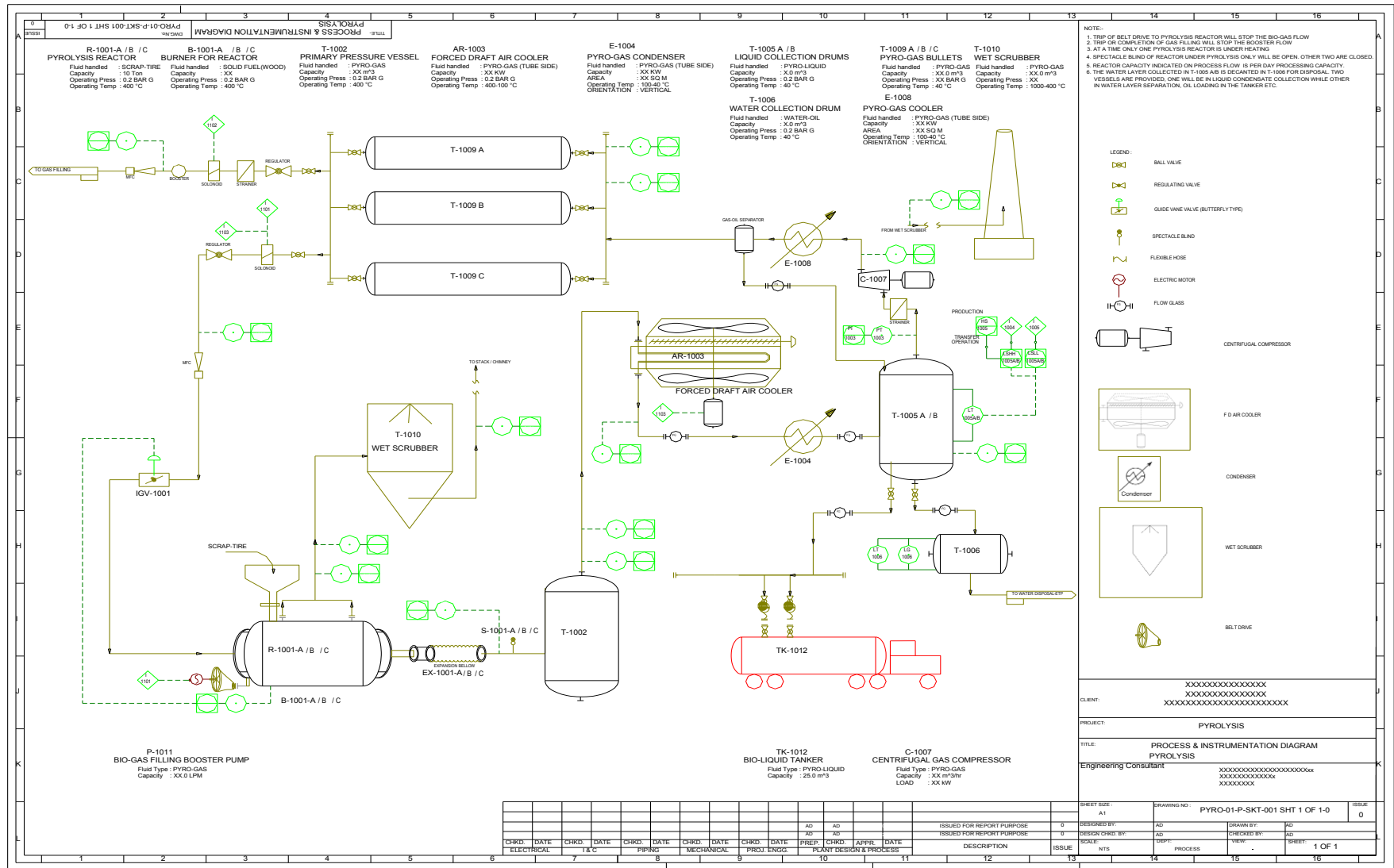
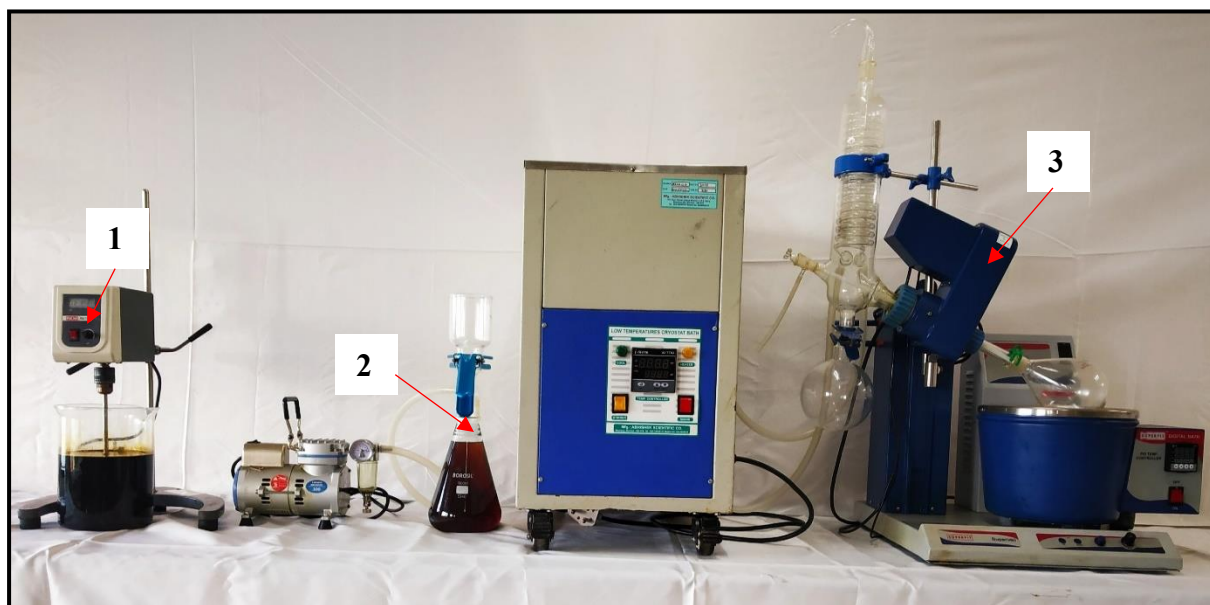


Fig. 3.2 Process scheme of 10-ton tire pyrolysis layout

### 3.3 Batch-scale upgrading experiments

CTPO (1 L) was diluted with 3 L petroleum ether and the solution was decanted into a 6 L beaker. To the solution, 1 kg silica gel was added carefully and the suspension was stirred at 500 rpm by an overhead stirrer for 1 h at RT. After 1 h, the supernatant was decanted filtered under vacuum through a microfiltration system (pore size 0.2  $\mu\text{m}$ , thickness 140-178  $\mu\text{m}$ , and nylon 6, 6). Petroleum ether was evaporated using a rotary evaporator at 45 °C under reduced pressure. The used silica gel was washed with methanol to remove the polar deposits and the methanol was recycled by distillation under reduced pressure. Fig. 3.3 shows the experimental facility for batch scale upgradation strategy to upgrade CTPO (URL 05).



**Fig. 3.3 Batch scale upgradation strategy**

(1- Blending of CTPO, silica gel, and petroleum ether using a lab stirrer in 6L glass beaker, 2- Millipore filtration system, 3- Evaporation system coupled with low temperature cryostat bath and vacuum pump)

### 3.4 Physicochemical characteristics of CTPO, StTPO

The physicochemical properties such as density, flash and fire point, surface tension, kinematic viscosity, cetane index, atmospheric distillation, spot test was conducted as per ASTM or IS standards are shown in Table 3.5.

**Table 3.5 Physical properties and methods used for the analysis of liquid samples**

Property	Method used	Instrument	Accuracy
Density at 30 °C (gm/cc)	IS 1448 P:32	Standard method	± 0.0005g/cc
Flashpoint (°C)	IS 1448 P:21	Pensky martens closed cup test	± 0.2 °C
Surface tension (mN/m)	Pendant drop method	Drop shape analyser	0.1mN/m
Kinematic viscosity (cSt)	ASTM D 445	Redwood viscometer	± 0.01 cSt
Calculated cetane index	ASTM D 4737	Empirical relation	-
Atmospheric distillation	ASTM D 86-19	Distillation apparatus	±2 °C
Spot test	ASTM D 4740-02	Standard method	-
Calorific value (kJ/kg)	ASTM 4809-18	Computerized bomb calorimeter	±1 kJ/kg.

### 3.5 Surface tension measurements

Surface tension plays a vital role in fuel atomization in engines and burners. Surface tension was measured based on the principle by which drop hangings from a syringe needle, which is in hydro chemical equilibrium. The liquid-air interface can be located from digital image of pendant drop. The Young Laplace equation is used to derive surface tension for pendant drop in an equilibrium state. When the Laplacian curve is fitted into the liquid-air interface, surface tension can be determined. Pendant drop was formed in a stainless-steel droplet needle attached to the glass made syringe fitted with a stepper motor. Fine-tuning of droplets can be achieved with the help of inbuilt software built by KRUSS Germany. The software requires the density of samples and gas before sample analysis. The density of the gas is calculated using the ideal gas equation. Each drop is allowed to reach equilibrium for 10 minutes, at which the image is captured using a high-quality CCD camera and a light source. Then the fresh sample is loaded for subsequent analysis.

$$\Delta P = \sigma \times \left[ \frac{1}{R_1} + \frac{1}{R_2} \right] \text{ (Young Laplace equation)}$$

$$\Delta P = \sigma \times C$$

Where  $\sigma$  is the surface tension of drop and air interface is,  $\Delta P$  is the pressure difference between inside and outside the bubble, and  $R_1$  and  $R_2$  are the radii of curvature at any point of a pendant drop. Fig. 3.4 shows the schematic representation of the drop shape analyser.

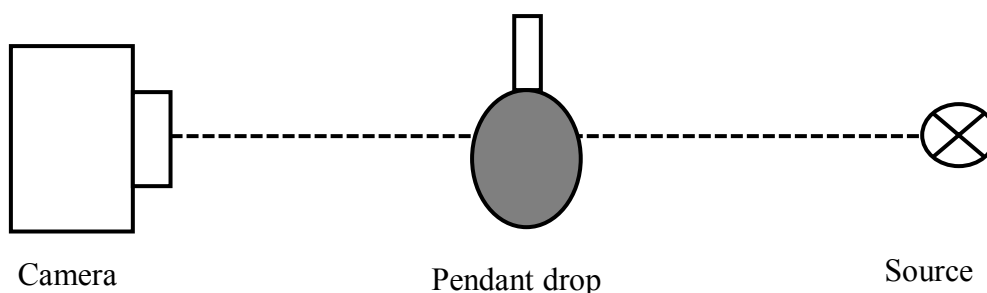


**Fig. 3.4 Schematic representation of axisymmetric drop shape analyser**

### 3.6 Calculated cetane index (CCI)

The diesel cetane index signifies the ignition delay in diesel engines. It also determines the quality of fuel in diesel engines. As per ASTM standards, the cetane index is measured using a correlation as follows (Umeki et al. 2016).

$$\text{CCI} = 45.2 + (0.0892 (T_{10} - 215) + [(0.131 + 0.901B) (T_{50} - 260)] + [(0.0523 - 0.420B) (T_{90} - 310)] + 0.00049[(T_{10} - 215)^2 - (T_{90} - 310)^2] + 107B + 60B^2$$

$B = [e^{(-3.5) \times (D)} - 1]$ ; where  $D = \text{Density at } 10^\circ\text{C} - 0.8 \times \text{Density at } 15^\circ\text{C}$ ,  $T_{10}$ ,  $T_{50}$ , and  $T_{90}$  are the temperature at which 10%, 50%, and 90% by the volume of the sample are distilled and  $D$  is the density at  $15^\circ\text{C}$  as per ASTM D4737. (Aleme et al. 2012, Umeki et al. 2016, and Fidayuningrum et al. 2020).

### 3.7 Elemental analysis

Elemental analysis gives an idea about the various types of elements present in tire derived oil. The various elements present in crude and upgraded oil samples was analysed by CHNS/O analyser and Inductively coupled plasma atomic emission spectroscopy (ICP-AES).

#### 3.7.1 CHNS/O analyser

The various elements such as carbon, hydrogen, nitrogen, sulfur, and oxygen (calculated by difference) were detected by CHNS/O analyser (make: Thermo Finnigan, Italy, model: FLASH EA 112 series) based on Dumas method. The method involves the complete and instantaneous oxidation of the sample by flash combustion. The combusted products are then separated by a chromatographic column and detected by a thermal conductivity detector (TCD). The output



of thermal conductivity detector is proportional to the concentration of individual components in a particular sample. The instrumentation consists of an auto sampler, combustion reactors, chromatographic column, and TCD detector. Fig. 3.5 illustrates the working principle of the CHNS/O analyser.

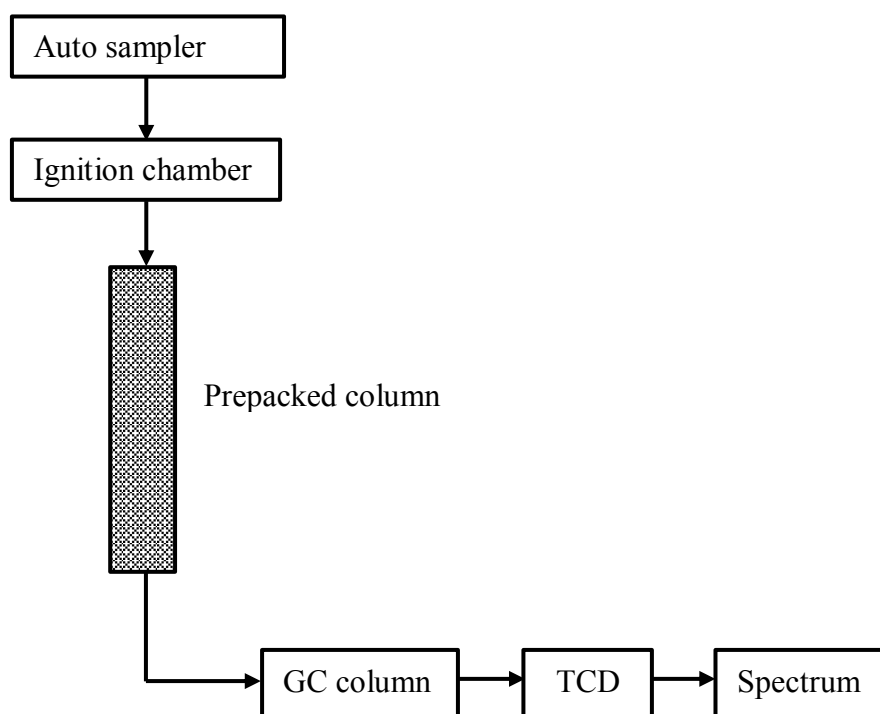


**Fig. 3.5 Basic working principle of CHNS/O analyser** (Source: SAIF, IIT Bombay)

### 3.7.2 Inductively Coupled Plasma Atomic Emission Spectroscopy (ICP-AES)

ICP-AES is a spectrophotometric technique (SPECTRO Analytical Instruments, Germany, Model: ARCOS, Simultaneous ICP Spectrometer). Excited electrons in the sample emit energy at a particular wavelength as it bounces back to the ground state after excitation by a high-temperature argon plasma source. The instrumentation's fundamental characteristics are that the sample elements emit energy at a particular wavelength peculiar to their atomic character. Energy transfer from the sample is inversely proportional to its wavelength. The intensity of energy emitted by a sample is proportional to the percentage of elements in the sample. The basic principle of inductively coupled plasma atomic emission spectrometry is shown in Fig. 3.6.

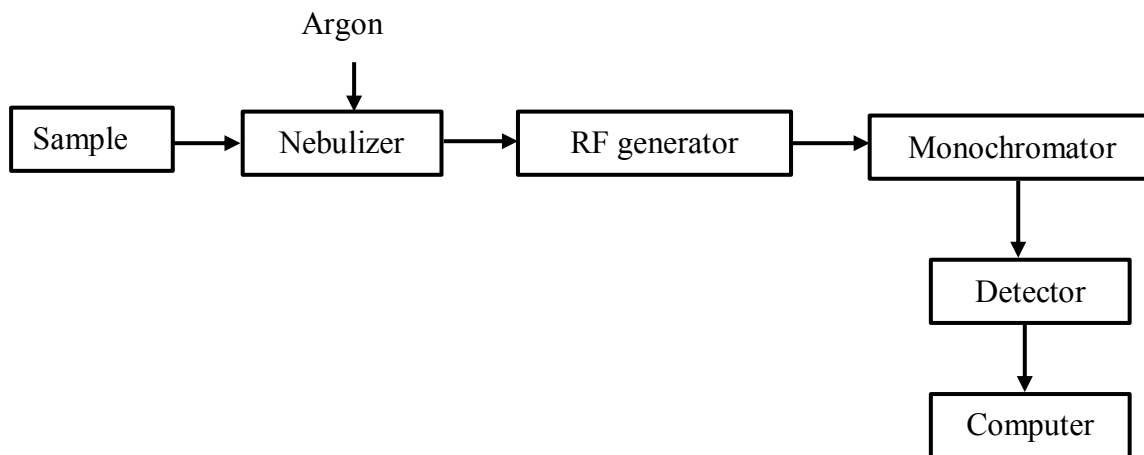


**Fig. 3.6 Basic working principle of ICP-AES Spectroscopy** (Source: SAIF, IIT Bombay)

### 3.8 Fourier Transform Infrared Spectroscopy (FT-IR)

FT-IR with attenuated reflectance device (ATR) gives information about the type of chemical functionalities such as aliphatic, aromatic, ketone, aldehyde, carboxylic acid, etc., present in a particular liquid sample based on the transmittance and wavenumber. The basic principle of FT-IR is shown in Fig. 3.7. Source, collimator, fixed and moving mirror, beam splitter, sample compartment, and detector, which are significant parts of an FT-IR spectrometer. When the source generates radiation, it passes through the liquid sample through the interferometer and reaches the sensor. The signal is amplified in the amplifier and converted to digital form by analog to digital converter. Similar analysis for CTPO were reported by Pakdel et al. 1994, Sharma, 2017.

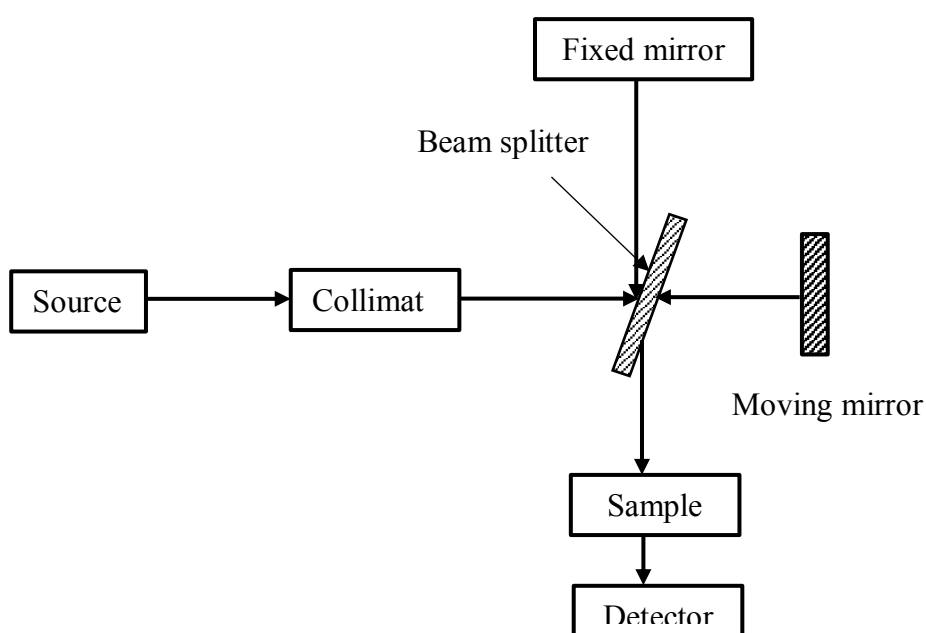


**Fig. 3.7 Working principle of FT-IR Spectroscopy** (Source: SAIF IIT Bombay)

### 3.9 Gas Chromatography High-Resolution Mass Spectrometry (GC-HRMS)

GC-HRMS analysis was performed to determine the compounds in crude and upgraded oil samples by Accu-TOF GCV 7890, Joel, GC-MS spectrometer (DB-Petro column, cross-linked 5% methyl phenyl silicone, 50m × 0.25mm internal diameter, 0.5µm film thickness was used). Helium gas with a purity of 99.99% was used as carrier gas at a constant rate of 1mL/min. The oven temperature of GC was programmed from 50 °C to 270 °C at a ramping rate of 10 °C/min and held for 2min. The total run time of the GC run was 45 min. The mass spectra of compounds were identified from respective GC chromatograms using the National Institute of Standards and Technology library (NIST). Fig. 3.8 shows the basic principle of gas chromatography high resolution mass spectrometry.

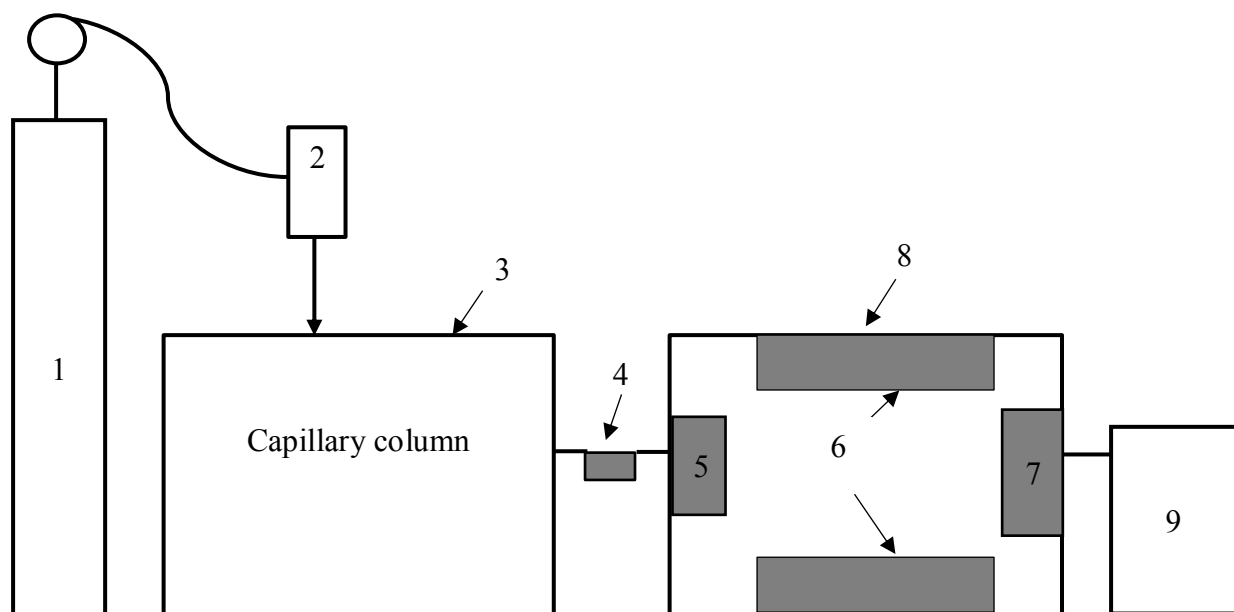


**Fig. 3.8 Basic principle of gas chromatography high resolution mass spectrometry**  
(Source: SAIF, IIT Bombay)

(1- carrier gas, 2- injection port, 3- temperature regulated oven, 4-transfer line, 5- ion source, 6- in trap mass analyser, 7- electron multiplier, 8- mass spectrometer, 9- detector)

### 3.10 Two-dimensional gas chromatography time of flight mass spectrometry (GC×GC TOF MS)

Qualitative estimation of various chemical compounds in CTPO, StTPO, and diesel are identified using comprehensive two-dimensional gas chromatography equipped with the time-of-flight mass spectrometer (Pegasus GC×GC TOF-MS, LECO Corporation, St-Joseph, MI, USA). The basic instrumentation of GC×GC TOF-MS is displayed in Fig. 3.7. The system

houses an Agilent 6890 gas chromatograph, a LECO GC×GC module, and a time-of-flight mass spectrometer (TOF-MS). The central principle behind the separation of compounds in two columns (non-polar and polar) is based on primary attributes like molecular weight and polarity of compounds.

The non-polar column with (Rtx-5ms,5%diphenyl,95%diphenyl polysiloxane, low bleed, Restek, USA) having dimensions 30m (L)×0.25mm (I.D) and 0.25µm film thickness and the polar column with dimensions of 1m (L)×0.1mm (I.D) and 0.10µm thickness with the stationary phase of 50% diphenyl,50% dimethyl polysiloxane (Rxi-17, Restek, USA) was used. The secondary column is equipped inside its own oven inside the main GC-oven. The inlet temperature was set at 270 °C. Helium was used as a carrier gas at a constant flow rate of 1.3 mL/min. The temperature program used for analyzing pyrolytic oil obtained from scrap tires is as follows: Hold at 70 °C for 0.40 min., ramp from 70 °C to 250 °C at 5 °C/min. The secondary column was offset at 10 °C from the primary column. The sample was injected at a split ratio of 1:100.

The modulator temperature was offset at 25 °C relative to secondary column temperature. The modulation period was recorded as 4 seconds. Modulation was carried out using two-stage modulators cooled by a consumable free cryogenic system. Hot pulse and cold pulse were set as 0.6 and 1.4 seconds. The chiller was maintained at a constant temperature of -80 °C. The source temperature of TOF-MS is maintained at 250 °C, and transfer lines were maintained at 280 °C. The TOF detector signal was received at an acquisition rate of 200 spectra per second and ten spectra seconds for 2D and 1D analysis. The mass spectrometer employed 70 eV ionization and scanned over 40 to 500 a.m.u. Data processing was done using LECO Chroma Software. The compounds are identified based on extracted ion-chromatogram and matching with retention time peak of the standard compounds and matching the mass spectra of the peak with the National Institute of Standards and Technology library (NIST).

### **3.10.1 GC×GC TOF-MS optimization**

Several quality features like adjustment of acquisition system, ion source lens focusing, mass calibration, leak check, and tune check need to be done before sample analysis to improve the accuracy and reliability of obtained data. Perfluoro tributylamine is used for tuning mass selective detectors in electron ionization mode. During optimization, the report generated gives valuable information regarding the condition of GC×GC TOF-MS. Leak check need to be carried out to avoid the leakages from injection port septum, injection port column nut, or

fractured capillary columns. Optimization can avoid common issues during two-dimensional analyses like the high background, peak width, and incorrect alignment of mass fragments. Fig. 3.9 shows a schematic representation of GC×GC TOF-MS analysis.

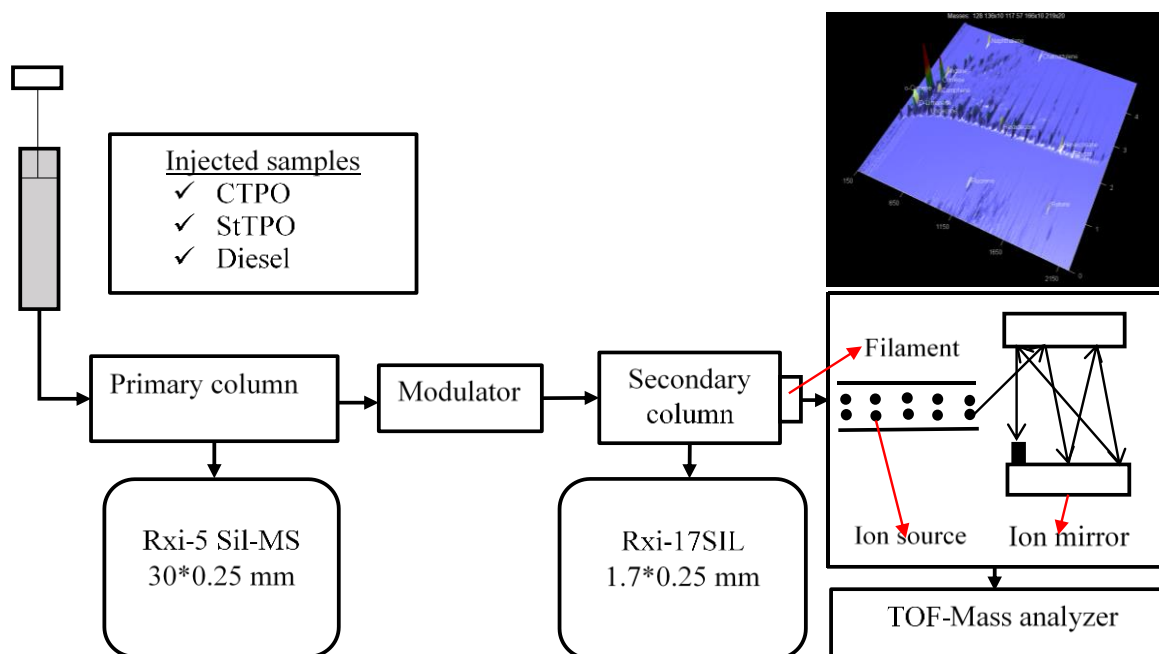


**Fig. 3.9 Schematic instrumentation of GC×GC TOF-MS analysis** (Source: Ngxangxa, 2016)

### 3.11 Thermal analysis by DSC Spectrometer

Differential Scanning Calorimetry (DSC) measures the difference in heat flow rate between sample and reference as a function of temperature. 2 mg of samples were loaded in alumina crucible in the DSC analyser (Model: DSCQ200) to quantify the heat release rate from the samples. The loaded samples were heated from 30-500 °C at a heating rate of 10 °C/min in liquid nitrogen (30 mL/min).

### 3.12 Fluorescence property analysis

Samples were diluted in n-hexane of 99.99% purity (4 ppm). Fluorescence of samples were analysed by Spectrofluorometer (Model: Fluoromax-4, Horiba scientific instruments). The excitation wavelength for each sample was determined from a UV-visible spectrometer (UV-NIR-3000, Agilent Technologies). UV-Visible spectrometer works on the principle of absorption of UV light by chemical compounds in the sample, which results in characteristic spectra. A 150 W xenon lamp illuminated the diluted samples with continuous output. The monochromatic excitation source has an optical range of 200-600 nm blazed at 330 nm. The

emission monochromatic source has an optical range of 290-850 nm, blazed at 500 nm. The slit width is adjusted through 0-30 nm band pass filters.

The present analysis was performed using parameters documented in the following Table 3.6. Fig. 3.10 represents the instrumentation of fluorescence spectrometer used in the present study.

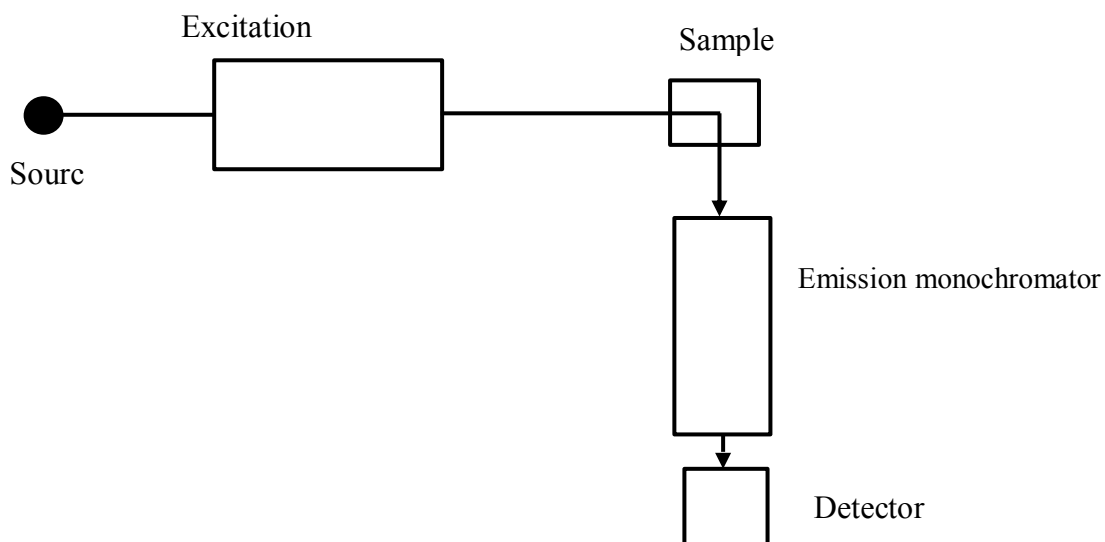


**Fig. 3.10 Instrumentation of fluorescence spectrometry** (Source: SAIF, IIT Bombay)

**Table 3.6 Parameters for fluorescence analysis** (Source: SAIF, IIT Bombay)

Parameters	Range
Scan range	200-480 nm
Excitation start	200 nm
Excitation end	480 nm
Excitation sampling interval	5 nm
Emission start	260 nm
Emission end	700 nm
Emission sampling interval	5 nm
Scan speed	1200 nm/mm
Excitation slit	10 nm
Emission slit	10 nm
Photomultiplier voltage	400 v

Fig. 3.9 describes the products obtained from thermal pyrolysis of scrap tires such as pyrolysis oil, carbon black and the steel wires. The CTPO obtained from pyrolysis of scrap tires is refined by batch scale refining strategy using silica as adsorbent and petroleum ether as diluent. The characterization of crude and upgraded oil was performed using various analytical instruments to understand the detailed chemistry, physical, thermal properties. Then the refined oil is blended with diesel to study the performance, combustion and emission from single cylinder diesel engines. The detailed specifications of equipment used in upgradation experiments are listed in Table 3.7.

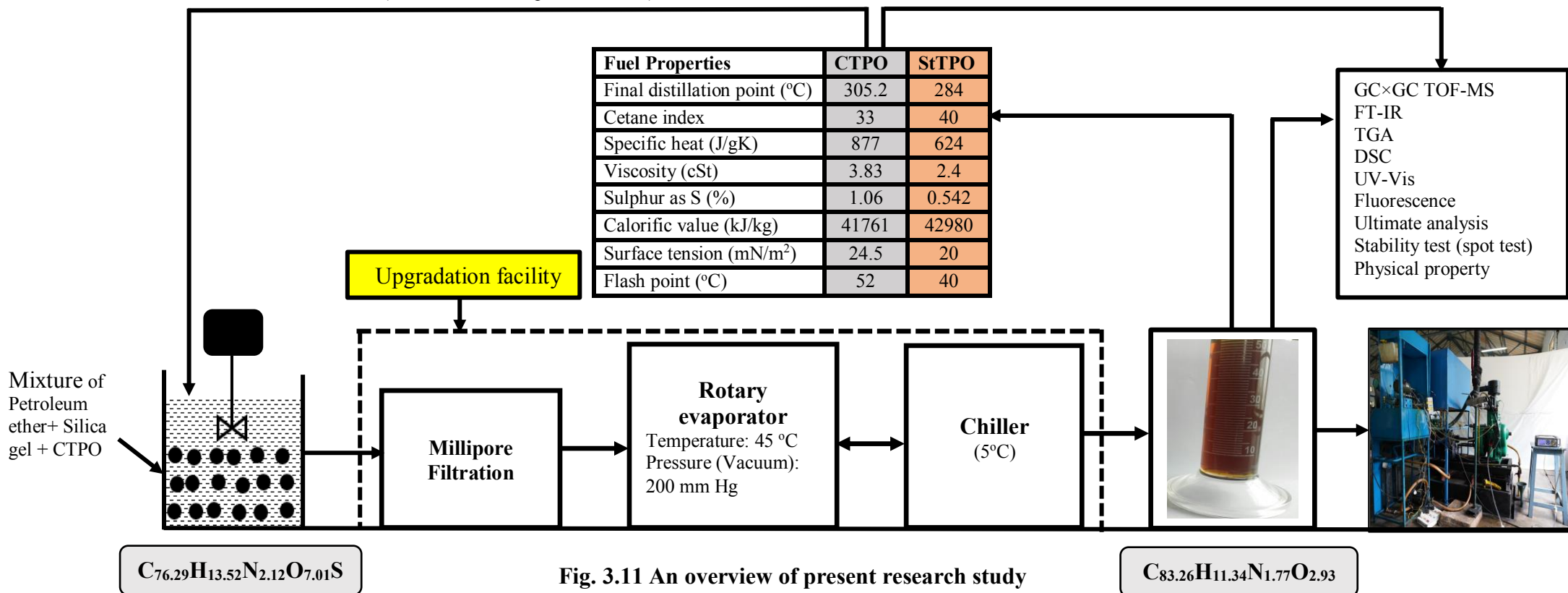
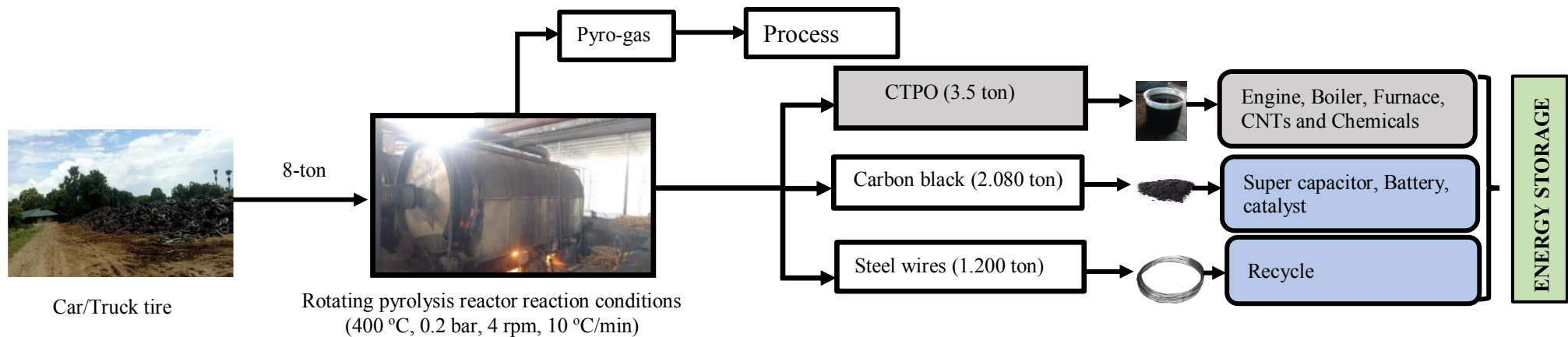


Fig. 3.11 An overview of present research study



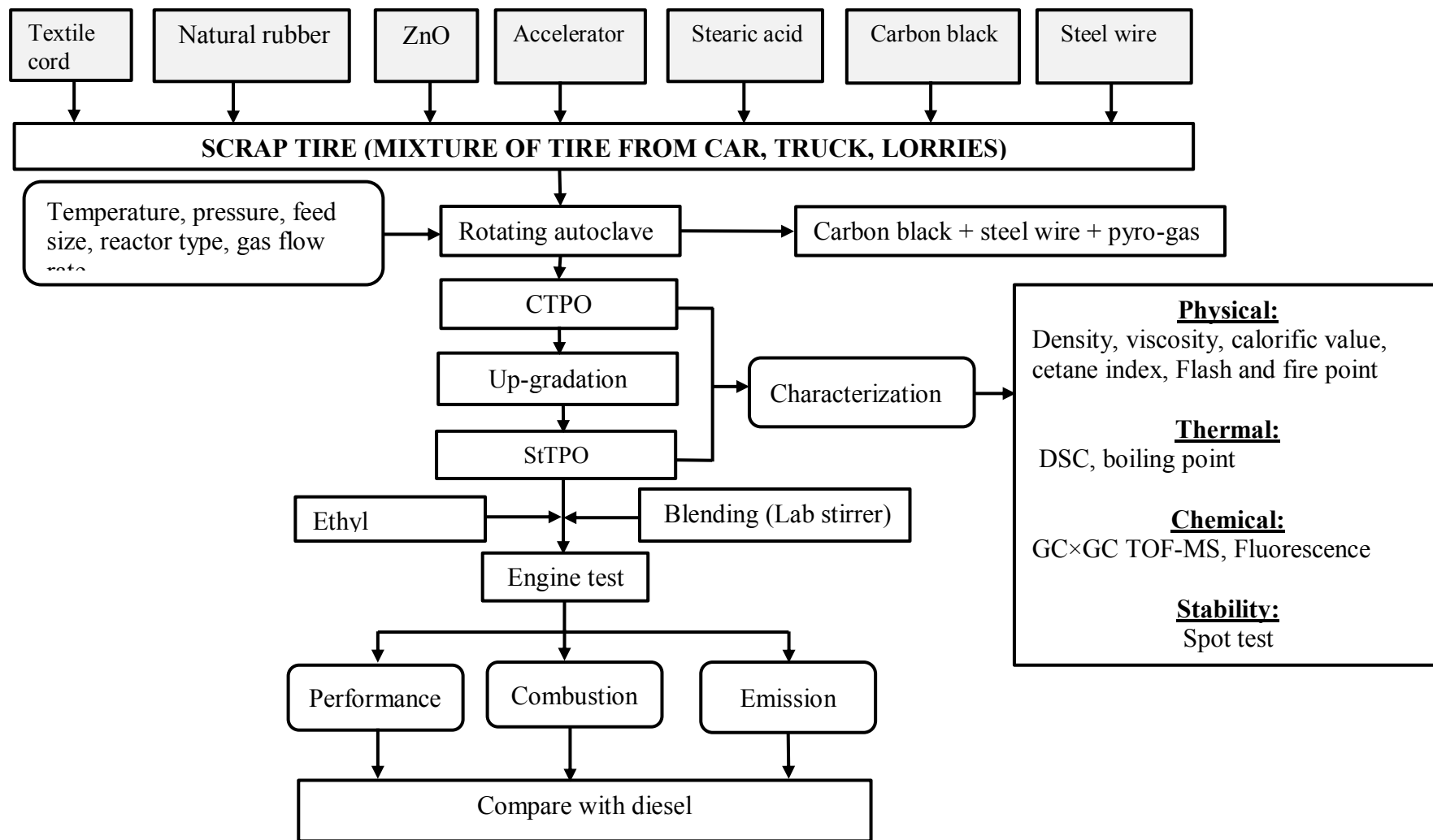


Fig. 3.12 Methodology proposed in the present study

**Table 3.7 Specifications of the various equipment used for batch scale upgradation experiments**

S. No.	Sub system	Make/Model	Specifications
1.	Magnetic stirrer	REMI Electrotechnik Ltd., 1MLH	Max. speed – 1200 rpm Max. volume – 1L Heating capacity – 150 w
2.	Laboratory stirrer	REMI Electrotechnik Ltd., RQ-121/D	Min. speed – 200 rpm Max. speed – 2000 rpm Max. volume – 10 L Fluid type – Water or light oil
3.	Millipore filtration assembly	Fabricated	Filtration capacity – 2L
4.	Ultipor N66 Membrane Disc Filter	Pall India Private Ltd., NR047100	Pore size – 0.2 $\mu$ m Diameter – 47 mm Thickness – 140-178 $\mu$ m
5.	Rotary evaporator	SUPERFIT	Speed – 20 to 200 rpm Double walled water bath (SS 304) Temperature – 5 to 180 °C
6.	Low temperature cryostat bath	Amit & Abhishek Enterprises Mumbai, India	Temperature range (-20 to 50 °C) Capacity – 15 L Water circulation – 15 L/min Power – 3 kW Cool down time – 45 min
7.	Vacuum Pump	ROCKYVAC	Pressure range – 760 mm Hg - 0 mmHg
8.	Measuring balance	Aczet Private Ltd.	Rang - 1 g to 2000 g

### 3.13 Engine testing set-up and instrumentation

The whole fuel samples were blended using a laboratory stirrer at 2500 rpm in a 5L beaker before testing in a single-cylinder diesel engine (make: Kirloskar, model: TV1) to ensure the homogeneity and stability of the samples. The engine set-up houses a naturally aspirated, direct injection air cooled diesel engine system with a rated power of 3.5 kW at 1500 rpm, coupled with an eddy current dynamometer for loading. The detailed specifications of the single-cylinder diesel engine and the schematic are presented in Table 3.8. and Table 3.9. The schematic layout of single cylinder engine test-rig is shown in Fig. 3.13. The research strategy for engine experiments is described in Table 3.10. The single-cylinder diesel engines are used as prime movers for irrigation applications and electricity generation. Also, this type of engine has been extensively used to carry out real research work in most of the academic institutions on alternate fuels. The fuel consumption is measured by using a burette and stopwatch arrangement. A pressure sensor made of Kistler is mounted on the top of the cylinder to retrieve

combustion data through the data acquisition system. The lubrication oil and exhaust gas temperature were recorded using a K-type (Cr-Al) thermocouple with a temperature indicator. The tailpipe emission from all fuel samples is measured using a sample probe connected with five gas portable emission analyser (model: AVL Digas 444). The retrieved combustion data is fed into combustion analysis software (Engine soft, Version 9.0) by using a data acquisition system. The combustion characteristics like in-cylinder pressure, net heat release, and rate of pressure data is obtained and presented in the following sections. The specification of exhaust gas analyser used in present research study is shown in Table 3.11. The photographs of engine set-up are displayed in Appendix (Fig. I-3). For each experiment, the engine is allowed to run for 30 minutes to reach steady-state conditions. In order to check repeatability, each test was repeated thrice, and average data is reported in the present study. Uncertainty analysis is carried out to study the accuracy of measuring instruments used during experiments. The uncertainty analysis is carried out using the square root method (Stephanie, 1999).

**Table 3.8 Specifications of single cylinder diesel engine**

Model	Kirloskar TV1
Ignition type	Compression ignition
No. of cylinder	1
No. of strokes	4
Fuel	Diesel
Rated power	3.5 Kw
Speed	1500 rpm
Cylinder diameter	87.5 mm
Stroke length	110 mm
Connecting rod length	234 mm
Orifice diameter	20 mm
Dynamometer arm length	185 mm
Displacement volume	661.45 cc
Fuel pipe diameter	12.40 mm
Pulse per revolution	360°
Compression ratio	17.5:1
Fuel ignition timing	23° before TDC
Fuel injection pressure	180 bar

Cooling	water cooled
Lubricant	20W40

**Table 3.9 Various instrumentation used in the engine experiments**

Instrument	Parameter measured	Specifications
Temperature indicator (°C)	Temperature	K type (Cr-Al)
Load indicator (W)	Engine load	Model AX-409
Speed sensor (rpm)	Engine speed	0-9999
Pressure transducer (bar)	In-cylinder pressure	0-345
Crank angle encoder (deg.)	Crank position	0-360
Exhaust analyser	HC (Flame ionization)	0-20,000 ppm
Emission components with detectors	NO <sub>x</sub> (Chemiluminescence)	0-5000 ppm
	CO (Non-dispersive infrared)	0-10% vol.
	CO <sub>2</sub> (Non-dispersive infrared)	0-20% vol.
Data acquisition system (bit)	Convert signal to digital value	USB-6210,16 bit
Combustion analysis software	Engine soft	Version 9.0

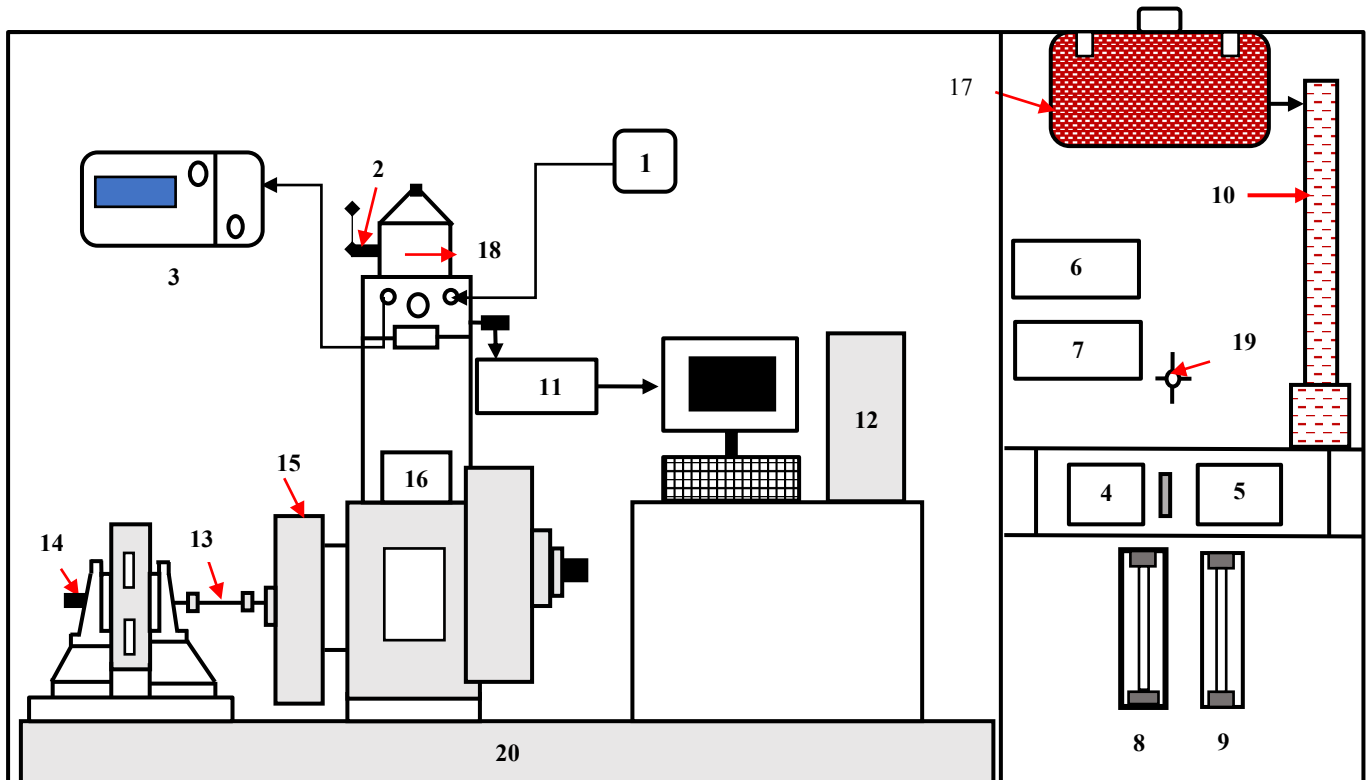


**Fig. 3.13 Schematic layout of single cylinder engine test-rig**

[1-Air filter, 2- Decompression lever, 3-Exhaust gas analyser, 4,5-Loading unit (voltmeter, ammeter), 6-Temperature indicator, 7-Speed indicator, 8- Rotameter for engine cooling (0-100 LPH), 9- Rotameter for dynamometer cooling (0-100 LPH) 10- Measuring burette, 11- Data acquisition system, 12 – Computer, 13- Universal coupling, 14- Crank angle sensor and rotational speed indicator, 15- flywheel), 16-Fuel pump, 17- Fuel tank, 18- Overhead valve mechanism 19- Fuel valve, 20- Engine test bed]

**Table 3.10 Research strategy for engine experiments**

<b>Fuel blends</b>	<b>CTPO-DF<sup>a</sup></b>	<b>StTPO-DF<sup>b</sup></b>	<b>StTPO-EL-DF<sup>c</sup></b>
Blend percentage (%)	0-100	0-100	20-10-70
	20-80	20-80	40-10-50
	40-60	40-60	60-10-30
	60-80	60-80	80-10-10
	100-0	100-0	90-10-0
Blending procedure	Lab stirrer	Lab stirrer	Lab stirrer
Performance analysis	BTE, BSFC, BP	BTE, BSFC, BP	BTE, BSFC, BP
Combustion analysis	NHR, RPR, CP	NHR, RPR, CP	NHR, RPR, CP
Emission analysis	CO, CO <sub>2</sub> , NO <sub>x</sub> , HC	CO, CO <sub>2</sub> , NO <sub>x</sub> , HC	CO, CO <sub>2</sub> , NO <sub>x</sub> , HC

<sup>1</sup>CTPO blended with various fraction of diesel, <sup>2</sup>StTPO blended with various fraction of diesel, <sup>3</sup>StTPO blended with various fraction of diesel and ethyl levulinate

**Table 3.11 Specifications of AVL'S digas 444 exhaust gas analyser**

<b>Parameters</b>	<b>Measurement range</b>	<b>Resolution</b>
CO	0-10% vol.	0.01% vol.
HC	0-2000 ppm vol.	10 ppm
CO <sub>2</sub>	0-20% vol.	0.1% vol.
NO	0-5000 ppm vol.	1 ppm

The overall uncertainty of experiments is given by the following equation:

Overall uncertainty = square root of [(uncertainty in crank angle encoder)<sup>2</sup> + (uncertainty in in-cylinder pressure)<sup>2</sup> + (uncertainty in temperature)<sup>2</sup> + (uncertainty in load)<sup>2</sup> + (uncertainty in

$\text{HC})^2 + (\text{uncertainty in NO}_x) + (\text{uncertainty in CO})^2 + (\text{uncertainty in CO}_2)^2 + (\text{uncertainty in time})^2 + (\text{uncertainty in speed})^2]$

Overall uncertainty = square root of  $[(0.6324)^2 + (0.1111)^2 + (0.7432)^2 + (0.0096)^2 + (0.86)^2 + (0.6546)^2 + (0.084)^2 + (0.2923)^2 + (0.44)^2 + (0.2746)]^2$

Thus, the overall uncertainty is given by  $\pm 1.5793\%$

## CHAPTER 4

### CHARACTERIZATION AND PYROLYTIC LIQUEFACTION OF SCRAP TIRE IN A 10-TON PILOT SCALE ROTATING AUTOCLAVE REACTOR

#### 4.1 Introduction

This chapter describes the process of depolymerization of worn tires in a rotating autoclave reactor at Mandakan Energy products, pilot-scale tire pyrolysis facility at Palakkad, Kerala, India at optimum reactor conditions. The obtained oil was extensively analyzed using various analytical techniques to understand the detailed physical, chemical, and thermal properties. This chapter also discusses the identification of existing problems in the tire pyrolysis industries and the inferior properties of CTPO.

#### 4.2 Thermal pyrolysis of worn tires into CTPO

Pyrolysis is a thermochemical conversion of any biomass in an oxygen-deprived atmosphere at 400-600 °C. The significant factors that influence the pyrolysis operation are pressure, temperature, feed size, retention time, reactor configuration, etc. A mixture of end-of-life automotive tires was used as a feed for thermal pyrolysis. The experimental study was carried out at 400 °C (heating rate 10 °C/min) in a rotating autoclave reactor with ten tons capacity. The optimized residence time was 5 h for the best yield of CTPO. Since the tires are sliced and fed directly into the reactor without further size reduction, a longer residence time is required for pyrolysis. The residence time can be shortened significantly by using smaller and uniform particle sizes of the tire feed.

The system has several components like a reactor, primary pressure reactor, electronic control panel, non-condensable gas tank, scrubber with blowers and pumps, condenser, water spray tower, and gas storing balloons. The cylindrical shape reactor is the central part of the system. The reactor used in the study is 6.6 m in length and 2.8 m in diameter and has a 10-ton capacity. The reactor is rotated with the help of a motor attached with gear and pulley arrangement. Initially, the reactor is fired with wood. In the later stage of pyrolysis experiments, the non-condensable gases stored in the gas storage system act as the heating source for three furnaces attached to the rotating autoclave reactor's bottom. A mixture of car tire and truck tire is fed in the reactor through the front door,

opened or closed with the aid of fasteners in the plant. The other end of the reactor is connected to a condenser through a flexible and sealing element. The volatile vapour is then passed through the condenser, inserted in the base of the water bath, and the non-condensable gases are stored in a gas holding balloons. The cooling tower helps to bring the temperature of the coolant in the condenser to the atmospheric temperature. A control panel controls the whole setup and accessories. Thus, the pyrolysis of 8-ton of tire yields 3.5 tons of oil, 1200 kg of steel wire (SS410), and 2080 kg of carbon black (Fig. 4.1). The flowchart of analytical techniques used for the characterization of CTPO is shown in Fig. 4.2. Fig. 4.3 shows the industrial pyrolysis parameters, product distribution, problems of CTPO, existing upgradation methods, novel upgradation strategy, issues of existing upgradation strategy, and characterization technique involved in the present study. Table 4.1 presents the details of samples and analysis carried out during the present study on thermal depolymerisation of scrap tires and refining methods for application as a fuel for single cylinder diesel engine.

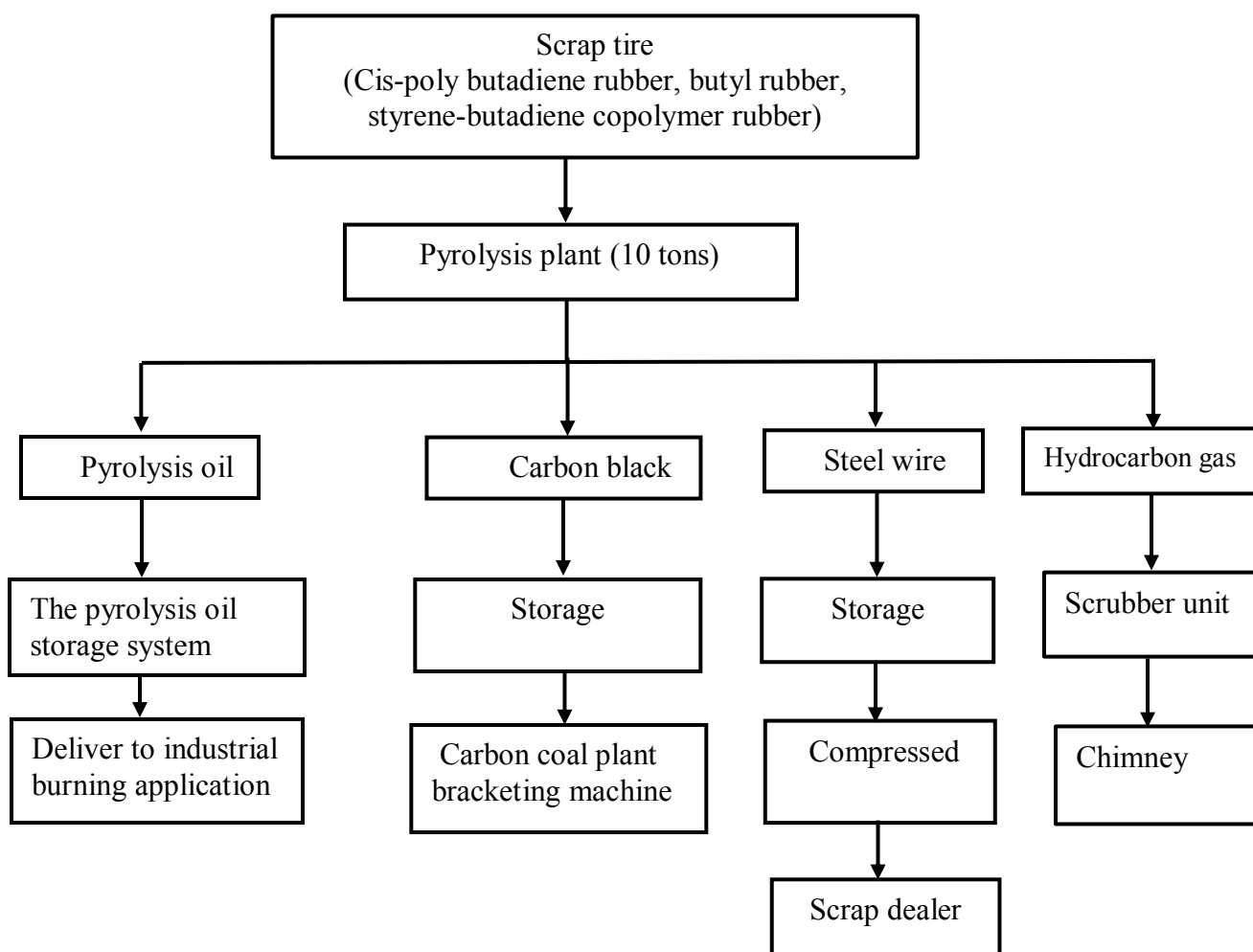


**Fig. 4.1 Products from pyrolysis of scrap tires**



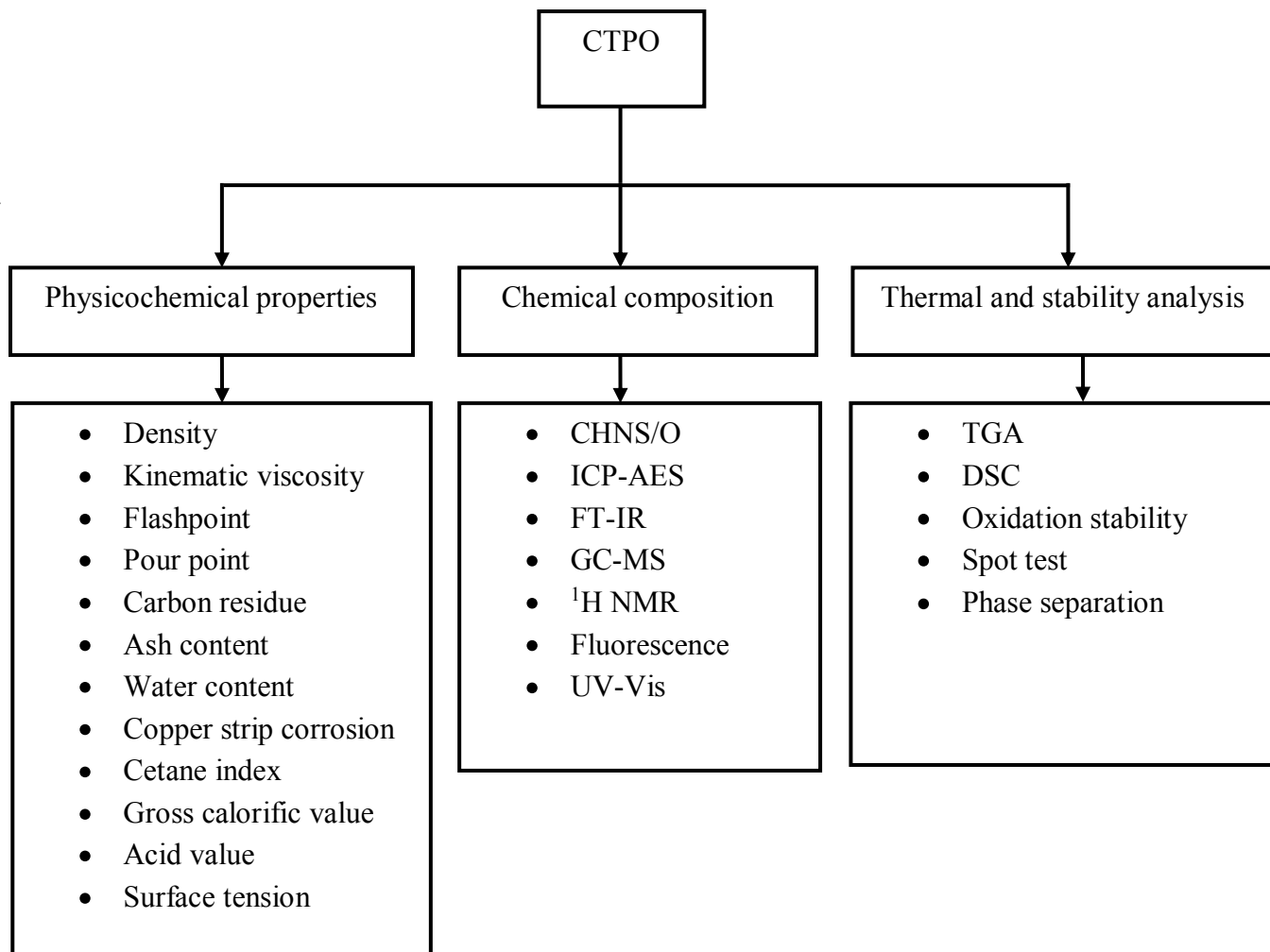


**Fig. 4.2 Characterization techniques used in the analysis of CTPO**

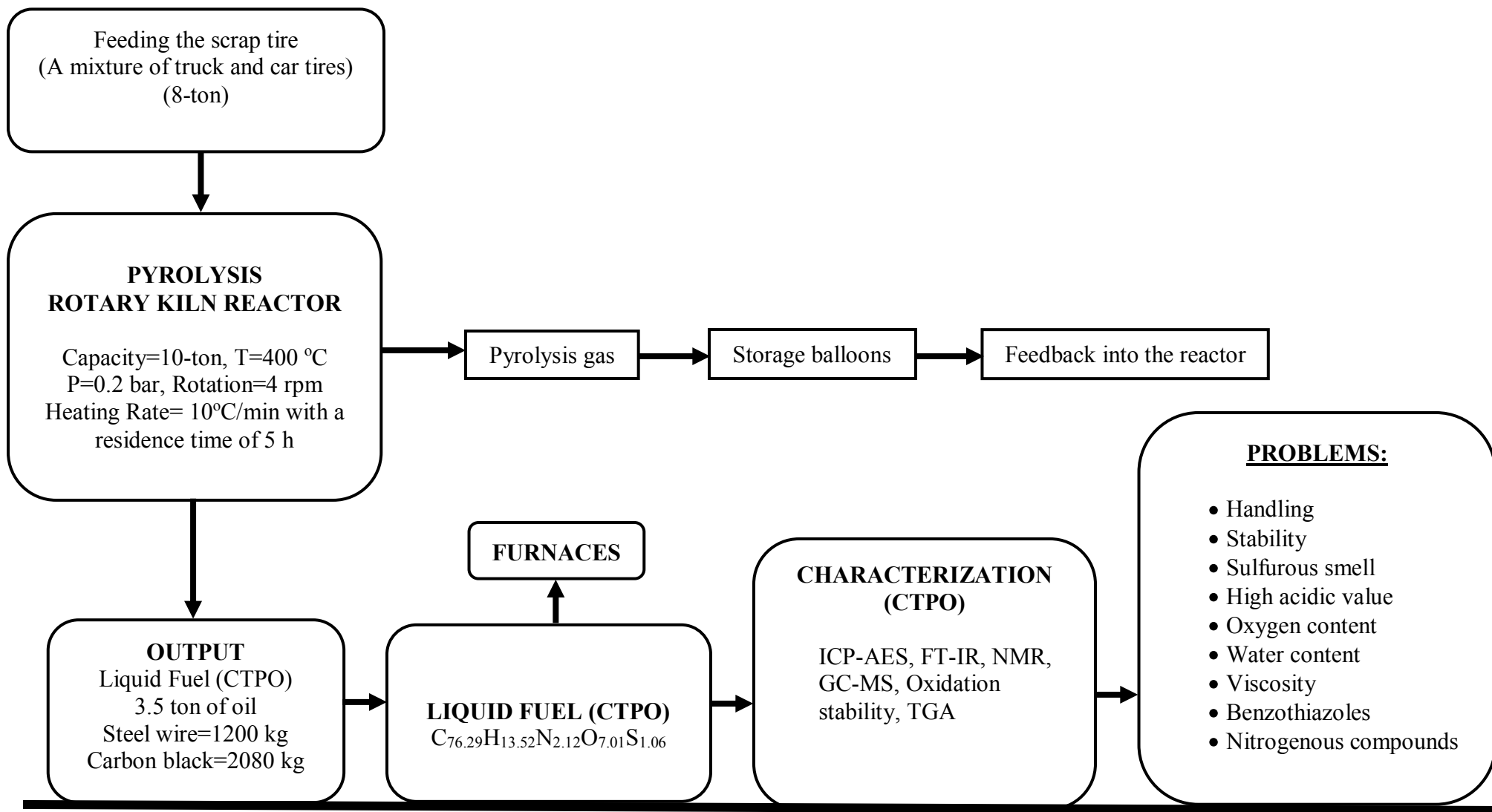


Fig. 4.3 Schematic of methodologies used in the preliminary investigations on CTPO

**Table 4.1 Details of samples and analysis carried out during present study**

Sections	Liquid stream analysis	What	Where	Methods	No. of samples	Analysis
1.	Field study on 10-ton rotating autoclave	CTPO	Condenser outlet	ASTM/IS	1	GC-MS GC×GC TOF-MS NMR FT-IR Elemental analysis Stability tests TGA Physical properties Fluorescence UV-Visible
2.	Column based upgradation	CoTPO	Refined product after column based upgradation	ASTM/IS	1	GC-MS NMR FT-IR Elemental analysis TGA Physical properties
3.	Mechanically stirring based upgradation	StTPO	Refined product after mechanically stirring based approach	ASTM/IS	1	GC-MS GC×GC TOF-MS NMR FT-IR Elemental analysis TGA Physical properties Fluorescence UV-Visible
4.	IC Engine studies (CTPOxx)	CTPO20 CTPO40 CTPO60 CTPO80 CTPO100	Blends are prepared using laboratory stirrer	ASTM/IS	6	Physical properties (Flash and fire point, calorific value, viscosity, density, cetane index)

		Diesel				Stability tests
5.	IC Engine studies (StTPOxx)	StTPO20 StTPO40 StTPO60 StTPO80 StTPO100	Blends are prepared using laboratory stirrer	ASTM/IS	6	Physical properties (Flash and fire point, calorific value, viscosity, density, cetane index) Stability tests
6.	IC Engine studies (StTPOxxEL10)	StTPO20EL10 StTPO40EL10 StTPO60EL10 StTPO80EL10 StTPO90EL10	Blends are prepared using laboratory stirrer	ASTM/IS	6	Physical properties (Flash and fire point, calorific value, viscosity, density, cetane index) Stability tests
<b>Solid stream analysis (Recovery of used silica gel and petroleum ether)</b>						
7.	Recovery of used silica gel	Used silica gel	Methanol washing	ASTM/IS	1	SEM, GC-MS
8.	Recovery of used silica gel	Pure silica gel	-	ASTM/IS	1	SEM, GC-MS

### 4.3 Physicochemical properties of CTPO

Tire derived oils contain complex mixtures of C<sub>6</sub>-C<sub>24</sub> organic compounds of various classes such as paraffin, olefins, terpenes, aromatics, oxygenates, nitrogen and sulfur-containing compounds (Quek et al. 2013). Elemental analysis of CTPO was carried out using inductively coupled plasma atomic emission spectroscopy (ICP-AES) is shown in Table 4.2.

**Table 4.2 Typical elemental composition of CTPO**

S. No.	Element	Composition
1.	Carbon	76.29 %
2.	Hydrogen	13.52 %
3.	Nitrogen	2.12 %
4.	Sulfur	1.06 %
5.	Oxygen	7.01 %
6.	Vanadium	BDL
7.	Zinc	BDL
8.	Phosphorous	BDL
9.	Calcium	BDL
10.	Alumina	BDL
11.	Silica	BDL

BDL- Below detectable limits

Boron, calcium, iron, magnesium, manganese, sodium, sulfur, silicon, strontium, titanium, and zinc are the primary elements found in CTPO. Fuels with higher density are likely to produce more power than with low-density alternate fuels. However, this induces the generation of rich air-fuel mixture, causing a significant rise in carbon monoxide, unburnt hydrocarbons, and nitrogen oxides in the exhaust gases. The density of tire pyrolysis oil is slightly higher than conventional transportation fuels, which indicates that CTPO consists of a more significant number of fuel molecules. Flashpoint is a parameter that gives the idea about the storage of fuel at room temperature. The flashpoint of CTPO is lower than the diesel; the chances of getting fire are more in the case of CTPO. The intense flashpoint of CTPO can be attributed to various classes of compounds with a wide distillation range.

Copper strip corrosion is a term widely used to investigate the potential of a fuel to corrode the metal parts. Copper strip corrosion is found to be below detectable limits for CTPO. The acid value of CTPO was found to be higher than diesel. Calorific value is a parameter used to assess the amount of energy released per unit mass of fuel burned. The calorific value of CTPO is slightly lower than diesel. The pour point is the lowest temperature at which the liquids can no longer flow. The pour point is a temperature at which the gelling of fuel occurs and resulting in injection pump failures. The pour point of the CTPO is found to be lower than diesel fuel. The cetane number of the fuel can be defined as the percentage of volume by cetane (hexadecane) and isocetane (hepta methyl nonane) with the same ignition quality or delay period as that of the test fuel. Cetane number measures the ability of a fuel to ignite promptly after ignition and ensure smooth burning and combustion. The cetane number of CTPO is lower than diesel, which ensures low combustion and burning stability. Table 4.3 shows the physicochemical properties of pyrolytic oil and its comparison them with diesel. Viscosity measures the resistance of the oil to shear and plays significant role in fuel atomization. The viscosity of CTPO was found to be very close to the viscosity of diesel. The effect of temperature on viscosity is a significant factor for utilizing oil as a fuel source. The viscosity of CTPO was measured by using the Redwood viscometer. The results revealed that the kinematic viscosity and absolute viscosity of crude CTPO decreases with an increase in temperature. The kinematic and absolute viscosity is found to be closer to the conventional diesel. The surface tension of CTPO is found to be higher than diesel due to interfacial tension between the aqueous and bulkier tar phase in crude tire pyrolysis oil. The accelerators such as N, N-diisopropyl-2-benzothiazole-sulfenamide, 2-(4-morpholinylthio)-benzothiazole, N, N-caprolactumdisulfide, and 2-mercaptobenzothiazole are added to accelerate the vulcanization. The thermal degradation of such accelerators leads to excessive oxygenates and nitrogen-containing compounds in CTPO. The major challenge in the utilization of CTPO in furnace and engine is high sulfur content. During tire production, sulfur is usually added to make a crosslink between rubber molecules to improve the hardness (Obadiah et al. 2017). During pyrolysis, 77% of sulfur remains in carbon black and 23% in pyrolysis oil, as per literature (Frigo et al. 2014).

**Table 4.3 Physicochemical properties of CTPO**

S. No	Parameters	Test method	Tire oil (Present Study)
1.	Density at 30 °C (g/cc)	IS;1448 P:32	0.907
2.	Kinematic viscosity at 40 °C (cSt)	ASTM D445	3.83
3.	Kinematic viscosity at 100 °C (cSt)	ASTM D445	1.85
4.	Flashpoint by Pensky Marten closed cup test (°C)	ASTM D 93	52
5.	Pour point (°C)	IS;1448 P:10	Below -15
6.	The carbon residue (%)	IS;1448 P:8	0.21
7.	Ash content (%)	IS;1448 P:4	0.02
8.	Water content (%)	IS;1448 P:40	0.05
9.	Total sediments in toluene (%)	IS;1448 P:41	0.05
10.	Copper strip corrosion	IS;1448 P:15	Not worse than 1
11.	Cetane index (By calculation)	IS;1448 P:9	33
12.	Gross calorific value (kJ/kg)	Bomb calorimeter	41761
13.	Acid value (%)	IS;1448 P:1	12.21
14.	Surface tension (mN/m)	Pendant drop	24.5

#### 4.4 FT-IR analysis

The FT-IR spectra of CTPO are shown in Fig. 4.4. The C-H stretching vibrations (symmetric and antisymmetric in -CH<sub>2</sub> and -CH<sub>3</sub>) appeared at 2951-2855 cm<sup>-1</sup>, and C-H bending vibrations between 966.12-698.86 cm<sup>-1</sup> indicate the presence of alkanes. The C-H bending vibrations between 1454-1375 cm<sup>-1</sup> indicate the presence of alkanes. Absorbance between 1650 and 1750 cm<sup>-1</sup> represents the presence of carbonyl functionality such as ketone or aldehydes. The absorbance of C-H stretch above 3000 cm<sup>-1</sup> shows the presence of aromatic hydrocarbons and or alkenes.

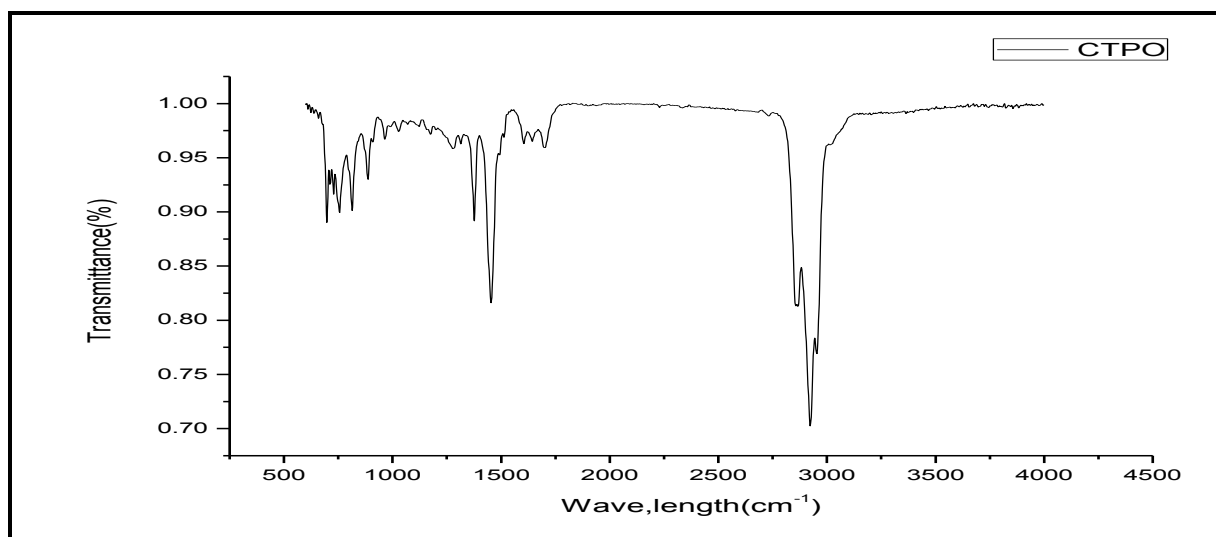


**Fig. 4.4 FT-IR spectra of CTPO**

#### 4.5 Nuclear Magnetic Resonance spectroscopy

NMR studies of CTPO was carried out using Bruker Advance III 500 MHz spectrometer, and samples were dissolved in deuterated methanol. Fig. 4.5 showed the  $^1\text{H}$  NMR spectrum of crude tire pyrolysis oil obtained from a rotating autoclave reactor. The presence of limonene in refined oil was found at 4.7 ppm and 5.4 ppm. NMR study revealed that the aliphatic compounds are pre-dominant than aromatics, oxygenates, aldehydes, and ketones in CTPO (71.1%), CoTPO (86.98%), and StTPO (89.71%). The same results were reported in literature (Islam et al. 2011).

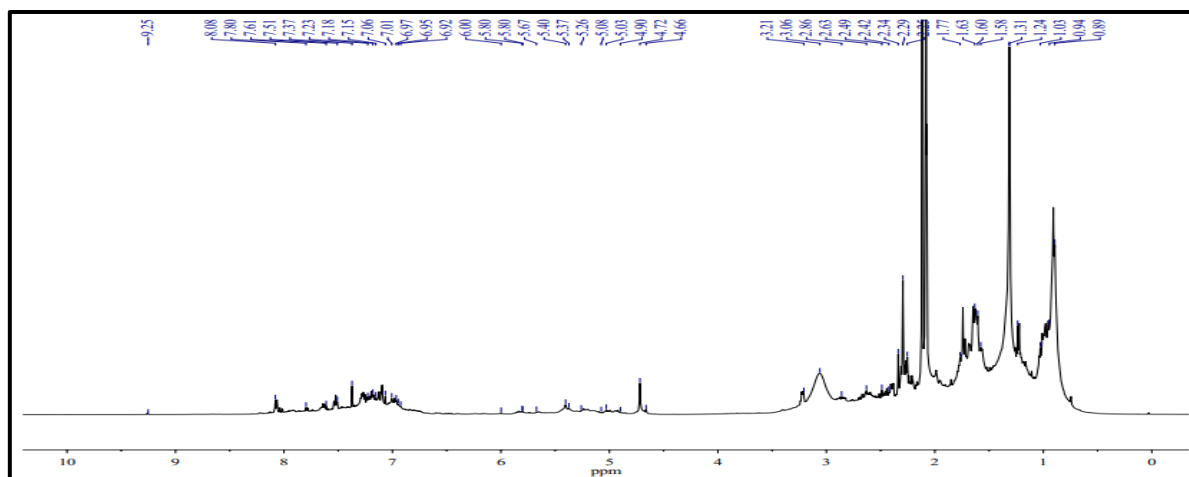


**Fig. 4.5 Nuclear magnetic resonance spectra of CTPO**

#### 4.6 Gas chromatography-mass spectrometry analysis

GC-MS analysis of CTPO was carried out to identify the compounds present in the respective samples. The chromatogram of CTPO is shown in Fig. 4.6. The compounds were identified with NIST-08 (National Institute of Standards and Technology-08) library and were compared



with the data reported in the literature (Hita et al. 2015, Banar et al. 2012, and Laresgoiti et al. 2004). The identified compounds and relative peak area percentages are listed in Appendix II (1), Appendix II (2) and Appendix II (3). These compounds are grouped as aliphatic, aromatics, poly-aromatic hydrocarbons, and other compounds. These compounds are classified on related chemical structure properties and molecular weight (Ayanoglu et al. 2016). The analysis showed that compounds present in CTPO were similar to the literature (Hita et al. 2015, Banar et al. 2012). GC-MS study of CTPO is reported in cited literatures (Hita et al. 2015, Banar et al. 2012, and Laresgoiti et al. 2004). GC-MS analysis supported with FT-IR analysis of CTPO revealed the composition of aliphatic (47.69%), aromatics (2.99%), and other compounds (7.60%). In CTPO, the composition of aliphatic and aromatics were found to be similar to the literature. However, the other compounds are found to be lesser in the present study. The major limitation of GC-MS analysis is the difficulty of developing the calibration curve to predict the exact concentration of compounds in the CTPO, CoTPO, and StTPO. Another difficulty to separate the compounds in CTPO based on their boiling point in the GC column is the overcrowding of a wide range of compounds and can be practicable using 2D GC TOF-MS.

The major application of 2D GC TOF-MS is to improve the resolution power to separate complex mixture in CTPO by increasing the peak capacity with better separation. Due to better resolving power, the co-elution of compounds having similar boiling points during 1D GC-MS of CTPO can be easily eliminated.

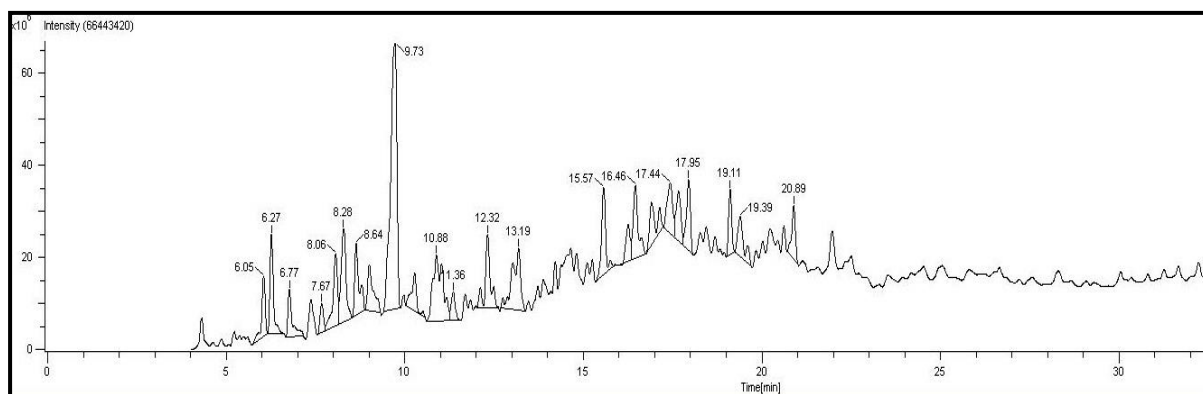


**Fig. 4.6 One dimensional gas chromatography-mass spectrometry of CTPO**

#### **4.7 Thermo gravimetric analysis (TGA)**

Fig. 4.7 shows the thermo gravimetric analysis of CTPO. Thermo gravimetric analysis shows the decomposition behavior of crude when the sample is heated from room temperature to 350 °C. The study showed that there are mainly three stages in TGA curves, which includes drying and two decomposition zones. The initial stages of decomposition of CTPO start at 30-75 °C,

but the variation is steeper in CoTPO. This is mainly due to the loss of moisture, loss of oils, etc. This is followed by thermal decomposition at 250 °C. Williams et al. (1995) also observed that the decomposition of CTPO starts at 250 °C. The second stage of decomposition is kept in the region of 200-275 °C due to the destruction of intermolecular bonds. The weaker chemical bonds are destroyed resulting in the production of the gaseous phase. The loss of weight percentage in CTPO is more significant compared to CoTPO. The data obtained from the present studies revealed that the decomposition temperature of CTPO, CoTPO, and StTPO is 270 °C, 320 °C, and 330 °C, respectively. Fig. 4.8 shows the thermo gravimetric analysis of CTPO. TGA analysis of CTPO seems an extreme variation in comparison with CoTPO and StTPO. The primary reason is attributed to the decomposition of crude oil triggered by the polar and acidic compounds.

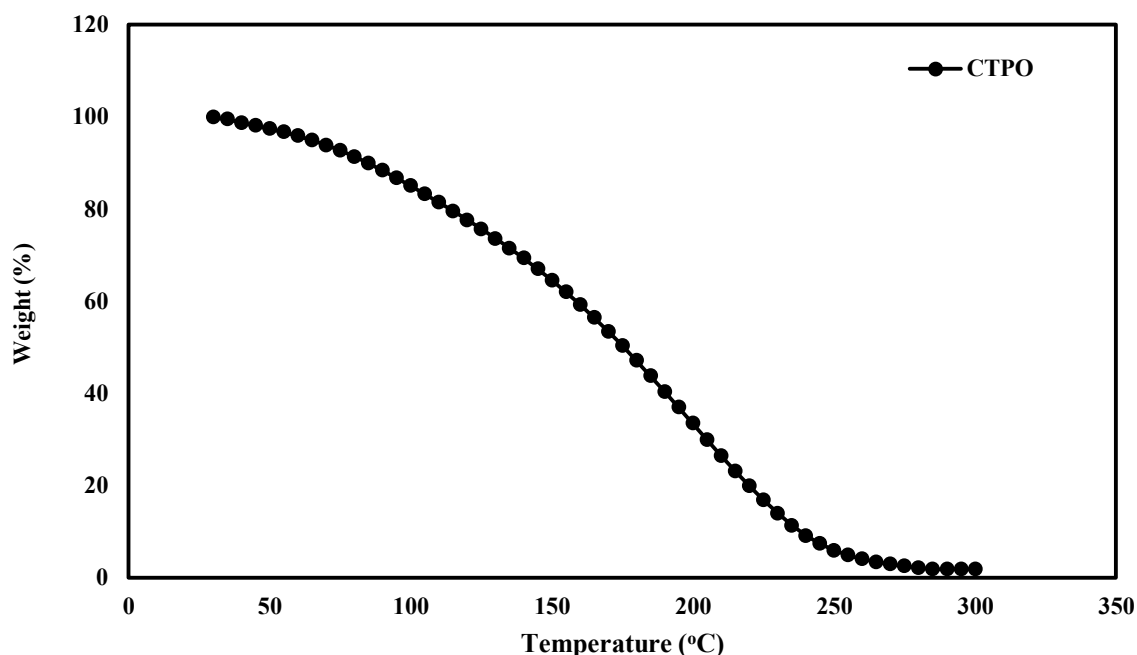


**Fig. 4.7 Thermo gravimetric analysis of CTPO**

#### **4.8 Oxidation stability**

The oxidation stability studies were carried out by keeping the crude and upgraded tire pyrolysis oil in a hot air oven at 120 °C for 20h. The gummy deposits were found in CTPO due to the polymerization of olefins upon long term storage. Fig. 4.8 (a) shows the oxidation stability studies of CTPO, and Fig. 4.8 (b) shows the photograph of CTPO before and after heating during oxidation stability tests. The study depicts the existing problems in the industry for the long-term storage of oil. Besides, this will cause corrosion and deteriorate the storage

walls and pipelines in the industry. The storage and handling of CTPO are problematic due to the pungent odor and cause phase separation and olefin deposits during long term storage.

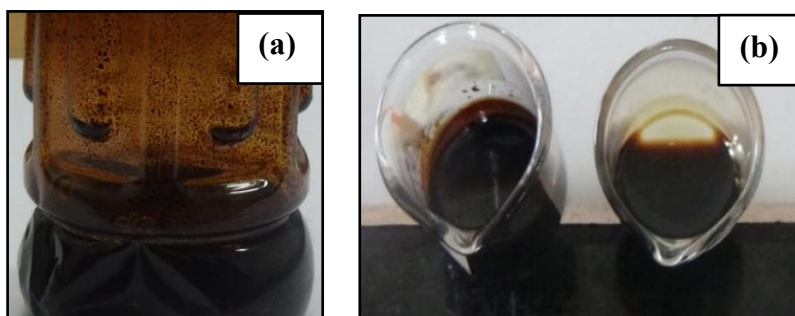


**Fig. 4.8 Gummy deposits formed during storage of (a) CTPO (b) CTPO before and after heating**

#### **4.9 Conclusions**

A mixture of end-of-life automotive tires has been thermally pyrolyzed in a rotating autoclave reactor, and the obtained oil was extensively characterized for physical, chemical and thermal analysis using analytical techniques such as Fourier transform infrared spectroscopy (FT-IR), one-dimensional gas chromatography-mass spectrometry (1D GC-MS), thermogravimetric analysis (TGA), thermal stability, inductively coupled plasma atomic emission spectroscopy (ICP-AES). The important conclusions obtained from the present chapter is given as follows.

1. Pyrolysis of 8-ton of scrap tire yields 3.5 ton of crude tire pyrolysis oil, 1200 kg of steel wire, and 2080 kg of carbon black at optimum reactor conditions.
2. Low calorific value, low flash point, high acidity, high viscosity, low cetane index, sulfurous smell are the significant issues with the tire pyrolysis industry.
3. Obtained CTPO was extensively characterized the CTPO using various analytical techniques to comprehend the detailed physical, chemical, and thermal properties.
4. GC-MS studies revealed that pungent odor in CTPO is mainly due to sulfur-containing compounds like mercaptans, thiols, sulfides, and disulfide.
5. Storage stability of CTPO was found to be inferior with significant gum formation due to a high amount of oxygenates.

In order to improve the fuel quality of CTPO, various cost-effective refining strategies need to be formulated to utilize partially/fully in single cylinder diesel engine. In the next chapter, various upgradation strategies, extensive characterization of upgraded oil and comparative study with crude and diesel are summarized.

## CHAPTER 5

### VARIOUS UPGRADATION STRATEGIES FOR REFINING CTPO

#### 5.1 Introduction

This chapter mainly explores the various upgradation strategies (i.e., laboratory and batch scale) for refining crude tire pyrolysis oils. The upgraded tire pyrolysis oils were extensively characterized by multiple analytical techniques to understand the detailed chemistry, physical, chemical, thermal properties, and stability of the oil.

#### 5.2 Upgradation of CTPO using column chromatography

Crude tire pyrolysis oil was refined based on the principle of selective adsorption and preferential solubility. 150 mL of CTPO was diluted with 450 mL of petroleum ether. The obtained slurry was passed through a column of 2.5 cm diameter and 50 cm bed height. Generally, tire pyrolysis oil is a multicomponent mixture with various compounds such as aliphatic, aromatics, aldehyde, ketone, nitrogen, and sulfurous compounds. These compounds have a different interaction with silica gel (stationary phase) and petroleum ether (mobile phase). The obtained fraction was collected in an Erlenmeyer flask and termed as CoTPO. The petroleum ether was regenerated using a rotary evaporator under 3-in. Hg and 60 °C to get refined CTPO. The obtained oil looked like a golden yellowish color and showed better thermal stability upon storage. The used silica gel was recovered using methanol washing. Fig. 5.1 shows the column-based up-gradation strategy using silica and petroleum ether

#### 5.3 Upgradation of CTPO using a magnetic stirrer

100 mL of CTPO was added to 300 mL petroleum ether in a beaker and magnetically stirred for 15 minutes under room temperature. The supernatant was decanted to a conical flask of 500 mL containing 100g silica (60-120 mesh). Then the suspension was stirred for 1h. The solution is filtered under a vacuum, and the filtered solution was evaporated using a rotary evaporator at 60°C under reduced pressure (3-in. Hg). The yield of reddish-brown coloured liquid was estimated to be 85 mL. Fig. 5.2. shows the stirring strategy used for the upgradation of CTPO.

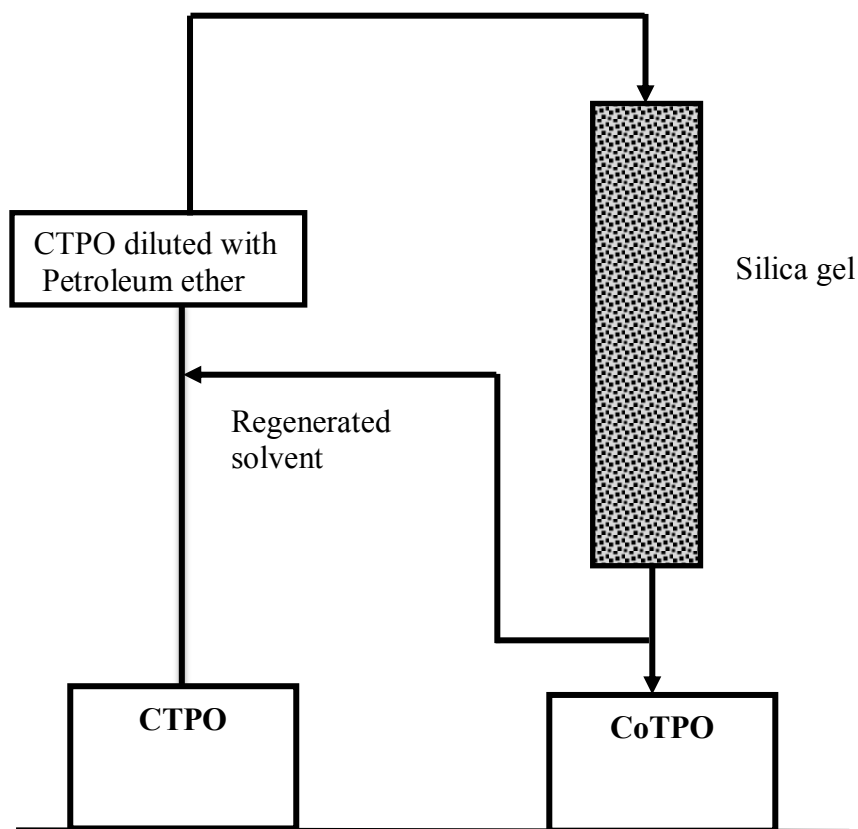


**Fig. 5.1 Up-gradation of CTPO using a bed of silica in a column**



**Fig. 5.2 Upgradation of CTPO using a magnetic stirrer**

#### **5.4 Effect of upgrading on the physicochemical and thermal properties of upgraded TPO**

Tires are made up of rubber (60-65 wt.%), carbon black (25-35 wt.%), and the rest consists of accelerators and fillers (Martinez et al. 2013). Vehicle tires are mainly composed of natural rubber and synthetic rubber, such as butyl rubber and styrene-butadiene rubber. An accelerator, an organo-sulfur compound, is added together with zinc oxide and stearic acid as a catalyst to control

vulcanization and improve the physical properties of tires (Mastral et al. 1999; Williams et al. 1999, Kyari et al. 2005). The data obtained from GC-MS, NMR, and FT-IR spectra revealed that nitrogen, sulfur, and oxygen-containing compounds are abundant in CTPO than upgraded oils. The inferior properties of CTPO are due to the presence of a high amount of oxygenates. The present study focuses on devising a scalable upgradation strategy to remove the polar compounds using cost-effective adsorbent like silica gel and solvent as petroleum ether. Fractional distillation is a widely employed strategy in most tire pyrolysis plants to distill the CTPO based on their relative boiling points. However, the process requires enormous capital investment and maintenance to run the distillation equipment for the long-term (Kiss, 2014). We have argued that polar compounds in CTPO are preferentially adsorbed using silica gel as an adsorbent due to its characteristic pore size (40-60 Å) and surface area (350-450 m<sup>2</sup>/gm). The polar compounds have more affinity towards silica gel and get adsorbed into its pores. Petroleum ether is chosen as a solvent to minimize the physical holdup of CTPO in silica gel. CTPO was diluted using petroleum ether as the solvent, and the diluted CTPO was passed through a column of silica gel or mechanically stirred with silica gel. Then, the suspension was filtered, and the solvent was evaporated under reduced pressure to get refined TPO. The used silica gel can be quickly recover by methanol washing, and simple distillation techniques can regenerate petroleum ether. The fuel properties of upgraded oils were compared against CTPO. The fuel properties of upgraded oils are drastically improved over CTPO and compatible with diesel. As per data obtained from GC-MS, <sup>1</sup>H-NMR, and elemental analysis, CoTPO and StTPO have significantly fewer polar compounds than CTPO. The storage and thermal stability of CoTPO and StTPO are improved considerably, as confirmed by TGA data. This improvement can be explained by the removal of unstable polar compounds like aldehyde and carboxylic acid that catalyze polymerization of olefins present in CTPO. The percentage of nitrogen, oxygen, sulfur in CoTPO and StTPO decreased significantly, and the hydrogen to carbon molar ratio closely matches diesel. StTPO showed superior fuel properties than CoTPO since the contact time with silica gel is longer for removing polar fractions (contact time in stirring based refining strategy is higher than column-based refining strategy)

## **5.5 Elemental analysis and chemical composition**

During the production of scrap tires, numerous metallic elements are added to improve the physical properties. Boron, calcium, iron, magnesium, manganese, sodium, sulfur, silicon, strontium, titanium, and zinc are the elements in CTPO whereas, StTPO contains elements such as boron,

calcium, iron, magnesium, sodium, sulfur, silicon, strontium, titanium, zinc and zirconium. The carbon and hydrogen content in CTPO showed similar values to the same in the reported literature (Quek et al. 2013). The nitrogen content is higher in CTPO due to accelerators, which is very less in Aylon et al. (2011). The nitrogen content in StTPO (1.77%) is very lower than CoTPO and CTPO due to the higher contact area of CTPO and silica gel in a stirring-based upgradation strategy. Sulfur compounds are released as oxides of sulfur during pyrolysis reaction. The pungent smell can be sensed in the entire course of the pyrolysis study in a rotating autoclave reactor due to the release of sulfur-containing compounds. As per data obtained from Inductively Coupled Plasma Atomic Emission Spectrometry, the sulfur content in CTPO, CoTPO, and StTPO is noted as 1.06%, 0.86%, 0.70%, respectively. The carbon content in CTPO (76.29%) is slightly lower than CoTPO (84.74%) and StTPO (83.26%). A high amount of carbon content in CoTPO than StTPO attributes to the higher calorific value of CoTPO. Table 5.1 shows the elemental composition of CTPO, CoTPO, and StTPO and compared it with diesel. The oxygen content in upgraded oil from the stirring strategy is estimated to be lower (2.93%) than CTPO due to the adsorption of all polar compounds by silica gel due to its characteristic pore size and surface area.

**Table 5.1 ICP-AES analysis of CTPO, CoTPO, and StTPO**

<b>Element (wt. %)</b>	<b>CTPO</b>	<b>CoTPO</b>	<b>StTPO</b>	<b>Raw Diesel (Hughey et al. 2001)</b>
Carbon (C)	76.29	84.74	83.26	87.4
Hydrogen (H)	13.52	8.74	11.34	12.1
Nitrogen (N)	2.12	2.08	1.77	0.039
Sulfur (S)	1.06	0.86	0.70	1.39
Oxygen (O)*	7.01	3.58	2.93	-
Vanadium	BDL	BDL	BDL	BDL
Zinc	BDL	BDL	BDL	BDL
Phosphorous	BDL	BDL	BDL	BDL
H/C <sup>#</sup>	2.11	1.23	1.62	1.65

## **5.6 Comparative study on fuel properties of CTPO, CoTPO, and StTPO with diesel**

This section mainly describes the physicochemical properties of CTPO before and after upgradation and compare it to the properties reported in the literature. The pyrolysis oil obtained from scrap tires has a strong irritating odor due to the enormous number of organic components, and it looks like a blackish syrupy liquid. Still, the oil obtained after upgrading has no peculiar smell. It has turned from black color to pale yellow due to the adsorption of polar compounds by silica gel. Sulfur analysis plays an inevitable role in identifying irritating odors due to sulfur-containing compounds in CTPO. The sulfur content in CTPO is 1.06% due to sulfur-containing compounds such as mercaptans, benzothiazoles, dibenzothiophenes, and thiols. CoTPO and StTPO in this study showed that elemental sulfur in CoTPO and StTPO decreased rapidly by 18.86% and 33.96%, respectively. However, the elemental sulfur content of CTPO, CoTPO, and StTPO is slightly higher than diesel fuel (Mufide et al. 2012), and the sulfur content of CoTPO and StTPO is much lower than petroleum fuel. The acid values of CTPO, CoTPO, and StTPO are 11.54, 0.8, and 0.6. The significant decrease in acid number is due to the adsorption of polar compounds of CTPO adsorbed on silica gel, identified using the NMR and GC-MS spectra of CTPO, CoTPO, and StTPO. Table 5.2 summarizes the comparison of CTPO and upgraded oils with industry standards.



**Table 5.2 Comparative study on fuel property of CTPO, CoTPO, and StTPO with industrial standards**

Properties	ASTM D975	ARAI <sup>#</sup>	(BS-VI)	(BS-IV)	(BS III)	(BS-II)	CTPO	CoTPO	StTPO
Density (g/m <sup>3</sup> )	0.7994	-	0.810-0.845	0.80-0.845	0.80-0.845	0.80-0.860	0.907	0.8926	0.8682
Kinematic viscosity (cSt)	1.9	2.5- 4	2 - 4.5	2-4.5	2-4.5	2 to 5	3.83	3.74	2.54
Flashpoint (°C)	52	32 min*	35 min*	35 min*	35 min*	35 min*	52	46	40
Carbon (%)	-	-	-	-	-	-	76.29	84.74	83.259
Hydrogen (%)	-	-	-	-	-	-	13.52	8.74	11.343
Nitrogen (%)	-	-	-	-	-	-	2.12	2.081	1.766
Oxygen (%)	-	-	-	-	0.6	-	7.01	3.58	2.93
Sulfur as S (%)	0.05	-	0.001	-	-	-	1.06	0.86	0.7
The carbon residue (%)	0.35	-	0.30 max	0.30 max	0.3	0.30 max	0.2	0.21	0.2
Ash content (%)	0.01	0.20 max	0.01 max	0.01 max	-	0.01 max	0.02	0.02	0.01
Cetane index	40	45 min	46 min	46 min	46 min	46 min	33	35	40
Gross calorific value (kJ/kg)	45814	-		-	-	45814	41761	42221	42980
Acid value (KOH/g)	-	0.5	Nil	Not worse than No.1 <sup>@</sup>	0.05	-	12.21	0.8	0.6
Copper corrosion (3 h at 50°C)	-	1 max	Not worse than No. 1		-	Not worse than No.1	Not worse than No.1	Not worse than No.1	Not worse than No.1
Pour point (°C)	-	-	max 3 (winter)	max 6 (winter)	max 6 (winter)	max 6 (winter)	< -15	< -15	< -15

<sup>#</sup>ARAI - Automobile research association of India, min-minimum, max-maximum

\*Flashpoint is calculated by Abel method, <sup>@</sup>No.1 indicates the standard used for copper corrosion test

Ash denotes the suspended solids, soluble organometallic compounds in pyrolysis oil. The StTPO in this study has similar ash content (0.01) comparable to the diesel standard. The ash content in CTPO and CoTPO is slightly higher due to suspended solids during the pyrolysis in the rotating autoclave reactor (0.02). The direct usage of CTPO100 may cause severe deterioration of the fuel injection system due to excessive accumulation of airborne solids and organometallic compounds, which can interfere with the diesel engine's smooth operation. However, the ash content of StTPO is low and can be used directly in diesel engines. The calorific value of CTPO (41761 kJ/kg) found from the bomb calorimeter in this study is similar to that reported in literature (Kumaravel et al. 2016). However, the calorific value of upgraded oils (CoTPO and StTPO) was increased by 540 kJ/kg and 1219 kJ/kg, respectively. The sharp increase in the heat content of StTPO is ascribed due to the function of the stirring based strategy (complete mixing with a magnetic stirrer) compared to the column-based refining strategy (no mixing or rotation). Thus, StTPO has a much higher heat content than CTPO and CoTPO. However, the heating value of StTPO is slightly lower than the standard diesel fuel (Umeki et al. 2016). Residual carbon is another parameter that indicates a fuel's tendency to form carbonaceous deposits in an engine. CTPO, CoTPO, and StTPO in this study have very low carbon residues (0.02, 0.02, and 0.01) compared to diesel (0.35) and petroleum fuels. The cetane index indicates the ignition quality and ignition delay (ignition and start of combustion). The higher the cetane number, the shorter the ignition delay and the smoother the combustion. The cetane index approximates the cetane number based on the empirical relationship between density and volatility (Umeki et al. 2016). CTPO, CoTPO, and StTPO in this study showed cetane indices of 33, 35, and 40. Therefore, StTPO showed the same value of cetane index compared to the diesel standards.

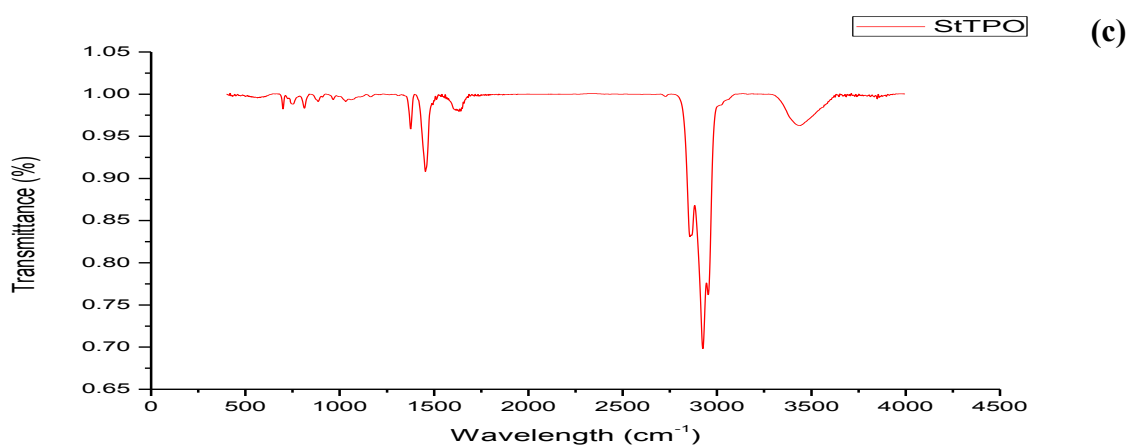
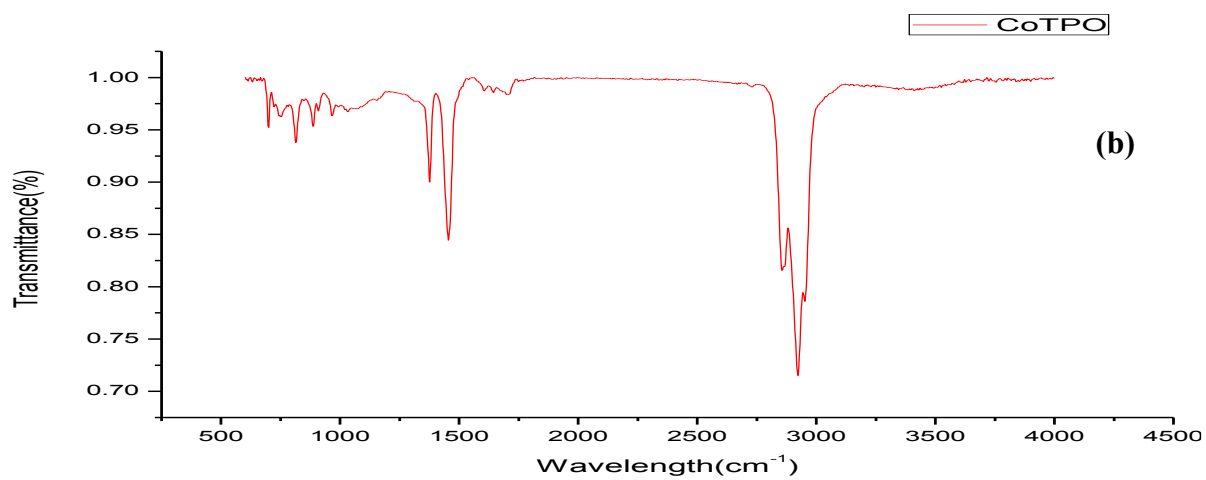
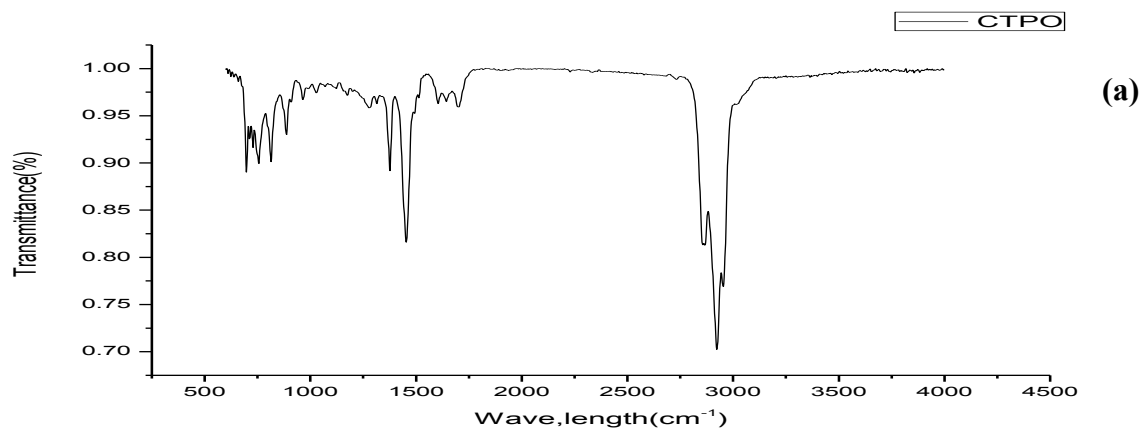
CTPO, CoTPO, and StTPO have a higher density than diesel and petroleum fuels. Regarding specification criteria, the diesel fuel and petroleum fuel density are in the range of 0.799 Kg/m<sup>3</sup> and 0.78 Kg/m<sup>3</sup>, respectively. The density of CTPO in this study is very similar to other tire pyrolysis oils in the reported literature (Kumaravel et al. 2016). The high density of CTPO in this study means that the amount of fuel injected into the engine per unit volume may increase. The flashpoint expresses the lowest temperature at which oil vapor ignites under a lower flame. The flashpoints of CTPO, CoTPO, and StTPO showed flash point values of 52 °C, 46 °C, and 40 °C. There are vast differences in the flashpoint studies of liquids from scrap tires compared to current studies (Williams et al. 2013). The flashpoint may change depending on the storage conditions and

the condensation reaction during long term storage. However, the CTPO (52 °C) in this study has a similar flashpoint to diesel fuel (52 °C).

Furthermore, the flashpoint of StTPO was about 40 °C due to the condensation reaction (presence of petroleum ether) that occurred during the storage period before analysis. The flashpoint of pyrolysis oil from tires is lower than diesel and petroleum fuels due to high amounts of volatile organic compounds, aromatics, and olefins in the product liquid a wide distillation range. Similar results were reported by Williams et al. 2013. However, the viscosity value of StTPO is lower than that of petroleum fuel. The literature reports a wide range of viscosity values for oils derived from worn tires (Kumaravel et al., 2016). The main reason for reducing the viscosity after upgradation is the adsorption of high molecular weight compounds by silica gel due to the large pore volume between the crystal lattices. Suppose CTPO is directly injected into a diesel engine. In that case, CTPO viscosity should be a limiting parameter. Still, after upgradation, the viscosity is matched with diesel (Martinez et al. 2013) and petroleum fuels (Kumaravel et al. 2016).

### **5.7 Fourier transform infrared resonance spectroscopy (FTIR)**

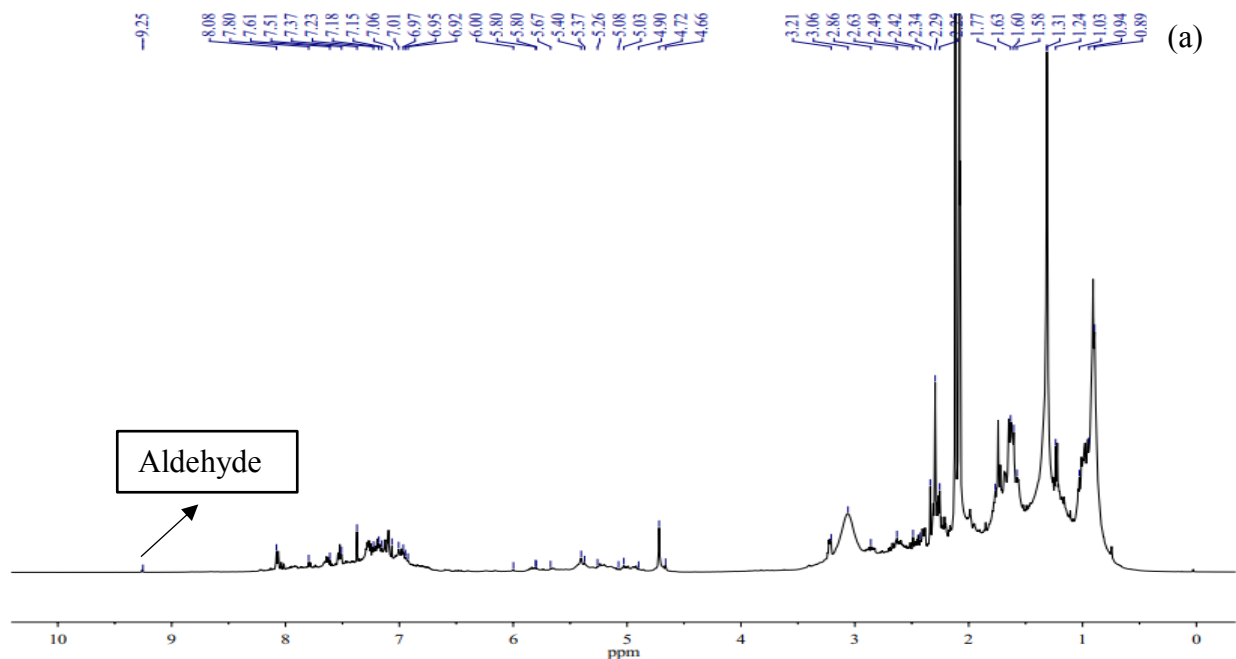
FT-IR gives information about the functional groups in an oil sample. The C-H stretching vibrations (symmetrical and asymmetrical at  $-\text{CH}_2$  and  $-\text{CH}_3$ ) appear at  $2951\text{-}2855\text{ cm}^{-1}$ , and C-H bending vibrations between  $966.12\text{-}698.86\text{ cm}^{-1}$  indicate the presence of alkanes. C-H bending vibrations between  $1454\text{-}1375\text{ cm}^{-1}$  indicate the presence of alkanes. Absorbance between  $1650$  and  $1750\text{ cm}^{-1}$  indicate the presence of carbonyl functional groups such as ketones and aldehydes. The absorbance of C-H stretches above  $3000\text{ cm}^{-1}$  indicates the presence of aromatic hydrocarbons and alkenes. The low-intensity peak between  $1600$  and  $1700\text{ cm}^{-1}$  indicates the low number of oxygenated compounds in CoTPO. StTPO mainly contains aliphatic, aromatic, and aromatic hydrocarbons, and the FT-IR spectrum looks much more straightforward. Fig. 5.3 shows the FT-IR spectra of CTPO and the upgraded oil.



**Fig. 5.3 FT-IR spectra of (a) CTPO (b) CoTPO (c) StTPO**

## 5.8 Nuclear magnetic resonance spectroscopy (NMR)

NMR studies were performed using a Bruker Advance III 500 MHz spectrometer, and samples were dissolved in deuterated methanol. Fig. 5.4 (a), (b), and (c) show  $^1\text{H}$  NMR spectra of crude tire pyrolysis oils obtained from rotating autoclave reactor and upgraded pyrolysis oils, respectively. Nuclear magnetic resonance spectra of CoTPO and StTPO showed that troublesome compounds were removed during purification. For example, peaks above 8 ppm responsible for heteroaromatics such as pyridine, benzothiophenes, and benzothiazole were removed. CoTPO and StTPO have a minimum of about 3.5–4.5 ppm oxygenates. In the CoTPO and StTPO NMR spectra, the aldehyde peak at 9.6 ppm was removed. Removal of aldehydes and carboxylic acids means that the acid number and oxidative stability of the purified TPO are greatly improved significantly. The presence of limonene in refined oils was found at 4.7 ppm and 5.4 ppm. NMR studies revealed that aliphatic compounds dominate aromatics, oxygenates, aldehydes, and ketones in CTPO (71.1%), CoTPO (86.98%), and StTPO (89.71%). The same result was reported by Islam et al. (2011). Table 5.3 shows the percentage of hydrogen distribution in CTPO, CoTPO, and StTPO.



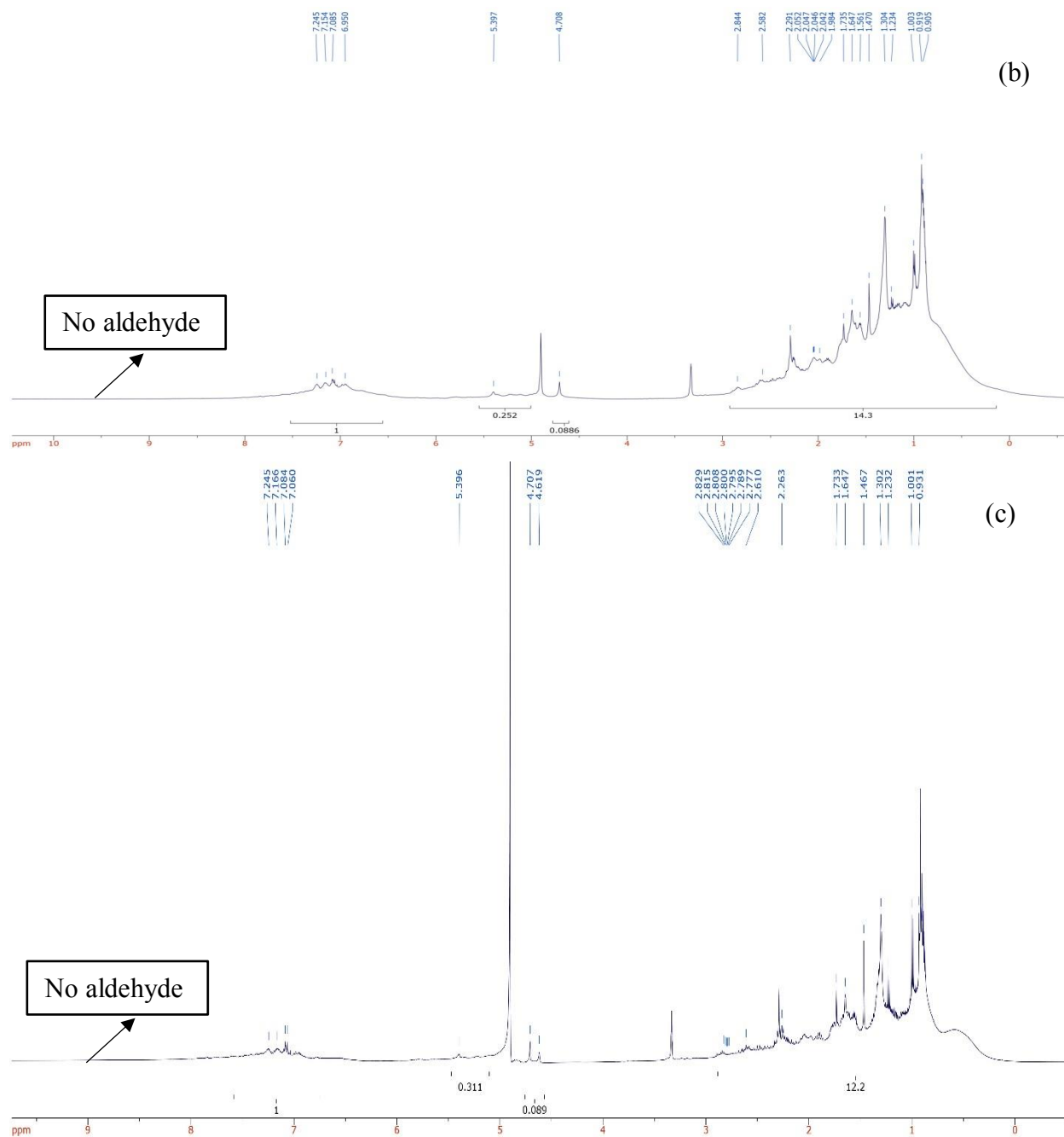


**Fig. 5.4 NMR spectra of (a) CTPO and (b) CoTPO (c) StTPO in deuterated methanol**

**Table 5.3 <sup>1</sup>H NMR results of CTPO, CoTPO, and StTPO**

<b>Chemical shift (ppm)</b>	<b>Components</b>	<b>Percentage of total hydrogen in CTPO (mol %)</b>	<b>Percentage of total hydrogen in CoTPO (mol %)</b>	<b>Percentage of total hydrogen in StTPO (mol %)</b>
3.2 - 0.9	Alkane or aliphatic	71.1	86.98	89.71
3-2	Aliphatic connected to aromatics.	12.7	4.87	4
6.6 - 4.6	Olefins or Oxygenates	4.1	2.07	2.94
8.3 - 6.8	Aromatics	12.1	6.08	3.35
9.3	Aldehydes	0.1	-	-

### **5.9 One dimensional gas chromatography-mass spectrometry (1D GC-MS)**

GC-MS analysis of CTPO, CoTPO, and StTPO was performed to identify the various compounds present in each oil sample. Fig. 5.5 displays the GC-MS chromatograms of CTPO, CoTPO, and StTPO. Compounds were identified using the NIST-08 (National Institute of Standards and Technology-08) library and compared to data reported in the literature (Hita et al. 2015, Banar et al. 2012, and Laresgoiti et al. 2004). The percentages of peak areas relative to the identified compounds are shown in Appendix (Table II-1, Table II-2, and Table II-3). These compounds are grouped as aliphatic, aromatic, polyaromatic hydrocarbons, and other compounds. The analysis shows that compounds present in CTPO were similar to the results found in the literature (Hita et al. 2015, Banar et al. 2012). GC-MS analysis of CoTPO using the current upgradation strategy with silica and petroleum ether was not found in the published literature. GC-MS analysis of CTPO has been reported in published literature (Hita et al. 2015, Banar et al. 2012, Laresgoiti et al. 2004, and Abdulkhadir et al. 2016). GC-MS analysis corroborate with FT-IR analysis of CTPO revealed that the composition of aliphatics (47.69%) is found to be dominant than aromatics (2.99%), and other compounds (7.60%). In CTPO, the composition of aliphatic and aromatics was found to be

similar to the literature. Current research has shown that other compounds are less abundant in CTPO. In CoTPO, aliphatic and aromatic compounds are 24.65% and 11.92%, while StTPO contains 53.25% and 23.341%, respectively. In this study, there was a reduction in aliphatic (23%) and increased aromatics (8.93%). In contrast, after stirring based strategy, aliphatic (5.56%) and aromatic composition (20.35%) showed a drastic rise as per GC-MS data. For CoTPO, the increase in aliphatic and aromatics in the stirring based upgradation strategy is due to the higher contact area between the pyrolysis oil and the silica surface, facilitating complete adsorption. The main reason for the decrease in polyaromatics in CoTPO and StTPO is due to larger pore size (40-60 Å) and large surface area (350-450 m<sup>2</sup>/gm) that make the silica retained in the column and magnetic stirrer adsorbs most of the polyaromatic compounds. The major limitation of GC-MS analysis is the difficulty in creating a calibration curve to predict the exact concentration of compounds in CTPO, CoTPO, and StTPO. Column chromatography is planned for future research to address the overcrowding of peaks in the GC-MS spectra of CTPO. Fig. 5.6 represents the type of compounds identified in CTPO, CoTPO, and StTPO.



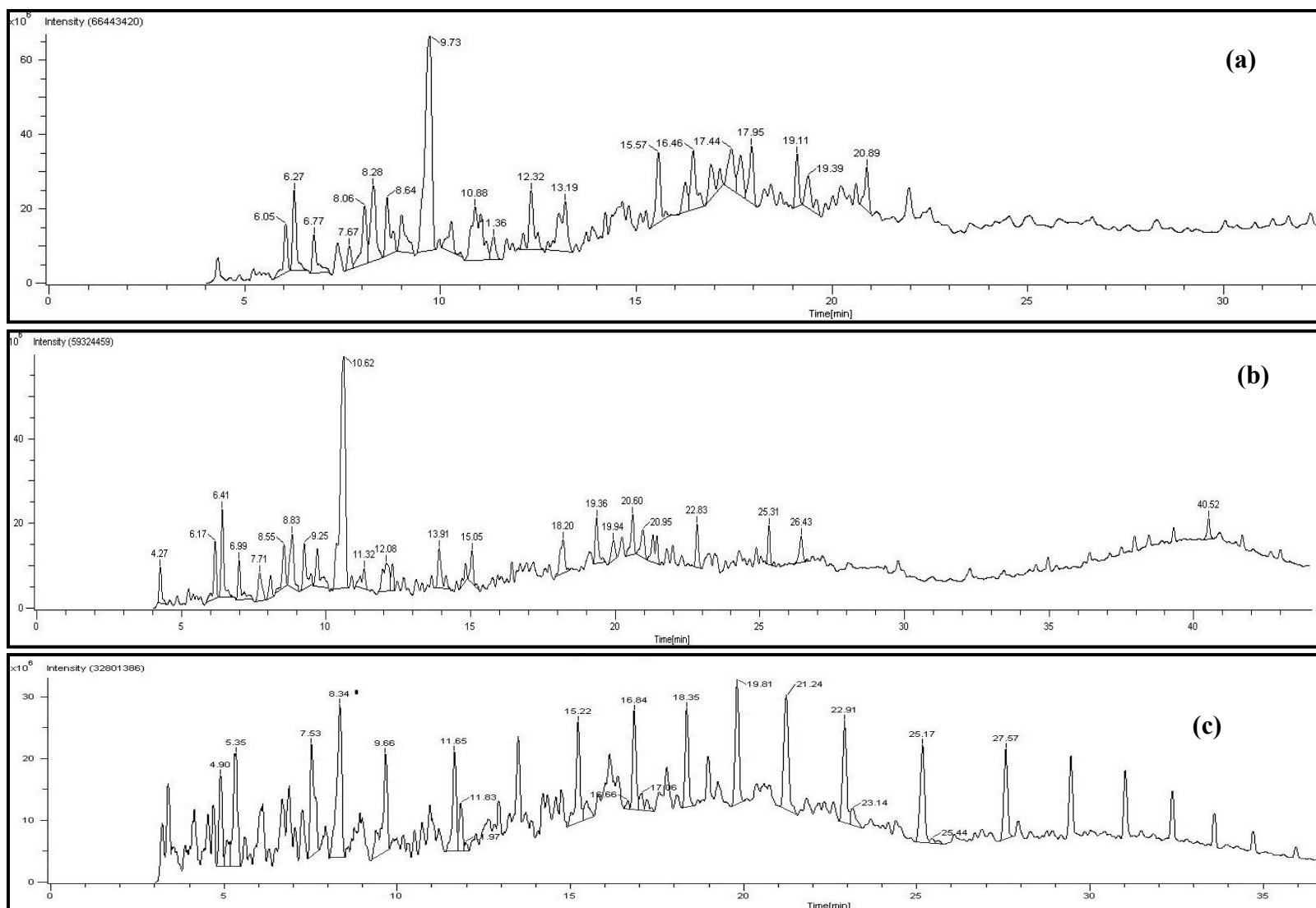


**Fig. 5.5 GC-HRMS spectra of (a) CTPO and (b) CoTPO (c) StTPO**

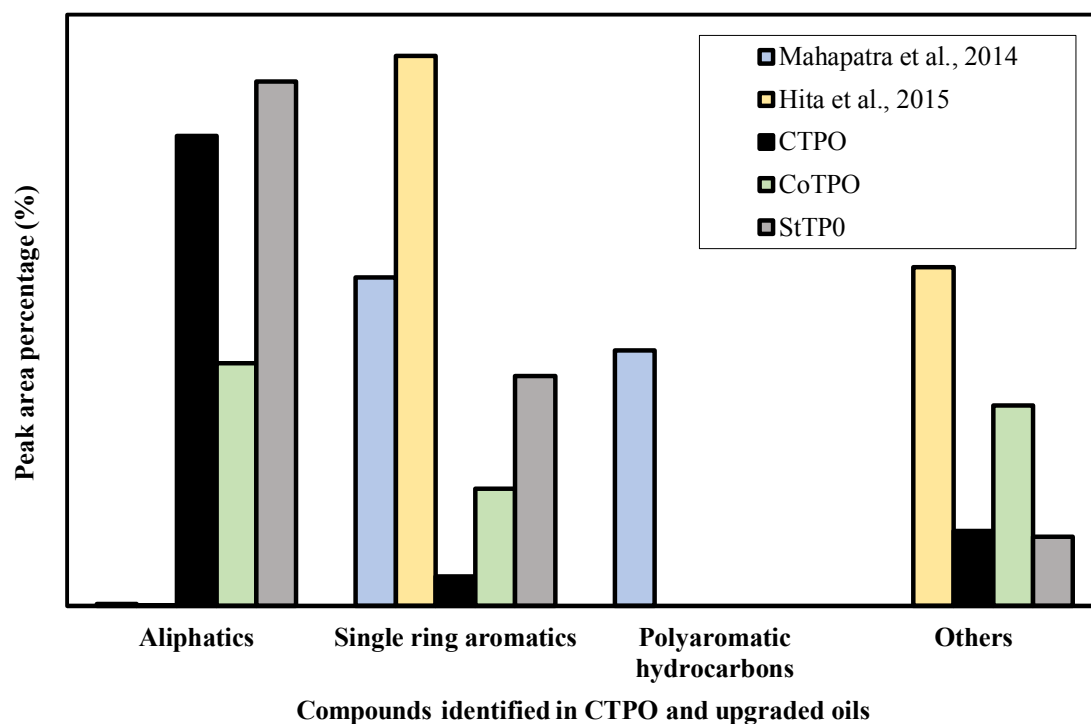


**Fig. 5.6 Types of compounds in CTPO, CoTPO, and StTPO**

### 5.10 Thermo gravimetric analysis (TGA)

TGA analysis shows the cracking behavior of crude oil and refined oil samples. Fig. 5.7 showed that there are mainly three stages, like drying and two decomposition zones of CTPO, CoTPO, and StTPO. The initial stages of degradation of CTPO begin at 30-75 °C. Still, for CoTPO, the changes are more drastic, mainly due to water loss, loss of oil, etc., followed by pyrolysis at 250 °C. Williams et al. (1995) also observed that the decomposition of CTPO started at 250 °C. The second stage of degradation is kept in the 200-275 °C region. This is mainly due to the breaking of intermolecular bonds, which break the weak chemical bonds and produce the gaseous phase. The weight percent loss in CTPO is found to be higher compared to CoTPO and StTPO. In the current study, the decomposition temperatures of CTPO, CoTPO, and StTPO are reported to be 270 °C, 320 °C, and 330 °C, respectively. This study revealed that CoTPO and StTPO exhibit much higher thermal stability than CTPO. TGA analysis of CTPO appears to have significant variability compared to CoTPO and StTPO. The main reason is the breakdown of crude oil caused by polar and acidic compounds. However, the upgraded oils (CoTPO and StTPO) showed much better thermal stability than CTPO.

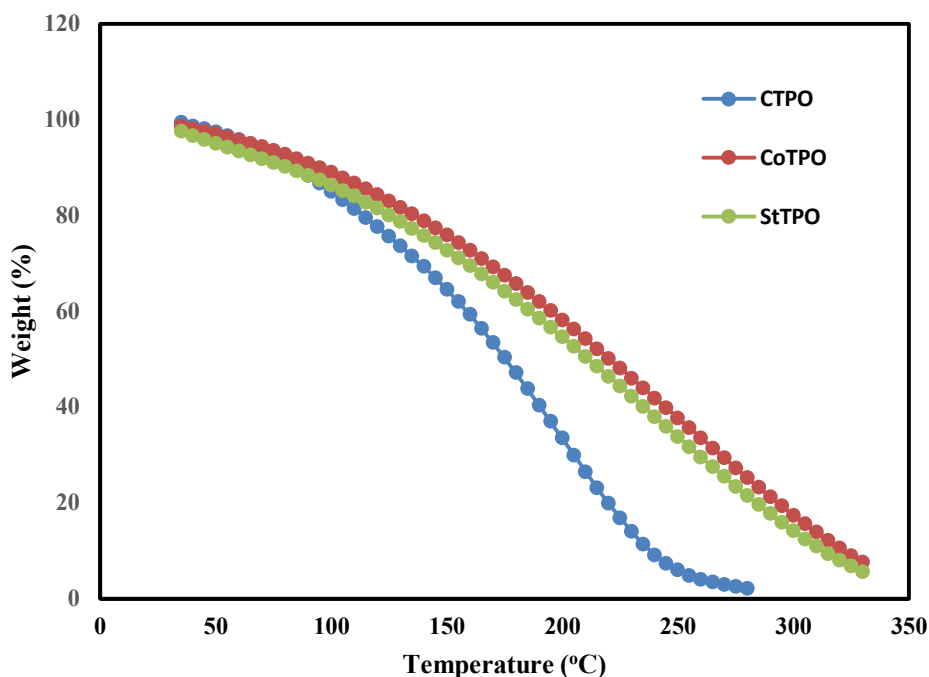


**Fig. 5.7 TGA of CTPO, CoTPO, and StTPO**

### 5.11 Oxidation stability

Oxidative stability studies are conducted by keeping crude tire pyrolysis oil and upgraded oil in a hot air oven at 120 °C for 20 h. Sticky deposits were found in CTPO due to olefin polymerization, but CoTPO appeared unchanged and did not change during long term storage. Fig. 5.8 shows an oxidative stability study of CTPO and CoTPO. This study demonstrates the existing problems in the pyrolysis industry with the long-term storage of oil. Besides, it may cause corrosion and degrade the pipelines. The upgraded oils (CoTPO and StTPO) have a diesel-like odor compared to CTPO (sulfurous odor which was due to excessive acid and sulfur compounds after the upgradation strategy). Also, the storage and handling of CTPO are problematic due to pungent odor and phase separation, and olefin deposition during long term storage. In contrast, CoTPO and StTPO have not shown significant improvement in thermal stability. There is no published scientific literature on the oxidative stability of CTPO from pilot-scale rotating autoclave reactor and upgraded oils using the present upgradation strategy.



**Fig. 5.8 Gummy deposits formed during storage of CTPO**

### **5.12 Recovery and regeneration of used adsorbent and solvent**

The silica used during the upgradation process can be recovered by methanol washing. The calcination study was conducted in a muffle furnace maintained at a temperature of 800 °C. Fig. 5.9 (a) and (b) shows scanning electron microscopy (SEM) images of pure silica and silica washed with methanol as solvent using a Jeol JSM-6380LA scanning electron microscope. In Fig. 5.9 (a), particles are dominant, and after calcination, white crystals are significantly reduced, as shown in Fig. 5.9 (b). The morphological studies on pure silica and recycled silica by methanol washing showed no significant crystal structure changes and can be used further upgradation process. The petroleum ether used during the refining strategy can be recovered from the rotary evaporator.

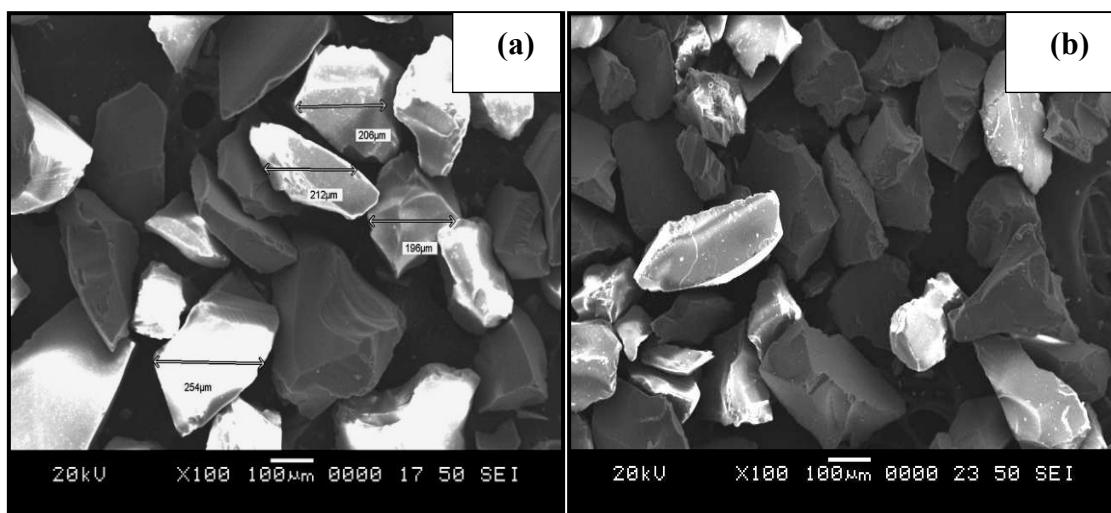


**Fig. 5.9 Morphology of (a) silica gel and (b) methanol washed silica**

### 5.13 Overhead stirring upgradation process

The laboratory-scale upgradation strategy is upscaled with micro-filtration apparatus, laboratory stirrer, and low temperature cryostat bath. CTPO (1L) was stirred using a laboratory stirrer rotating at a speed of 500 rpm for 1h. Then silica gel (60-120 mesh size) and petroleum ether (60-80 °C) were added in the ratio of 1:3. The supernatant was then transferred through the microfiltration system under a vacuum. The petroleum ether was evaporated using a rotary evaporator at 45 °C under vacuum. The yield from overhead stirring upgradation process is found to be 95% compared to the lab-scale upgradation strategy (85%). Thus, the outcome of the batch scale upgradation process improved by 15% in comparison with the laboratory scale upgradation strategy. The refined oil appears to be a reddish-brown colored transparent liquid. Fig. 5.10 shows the process flow diagram of a scalable upgradation strategy. Table 5.4 describes the comparative study on the lab scale and overhead stirring upgradation process.

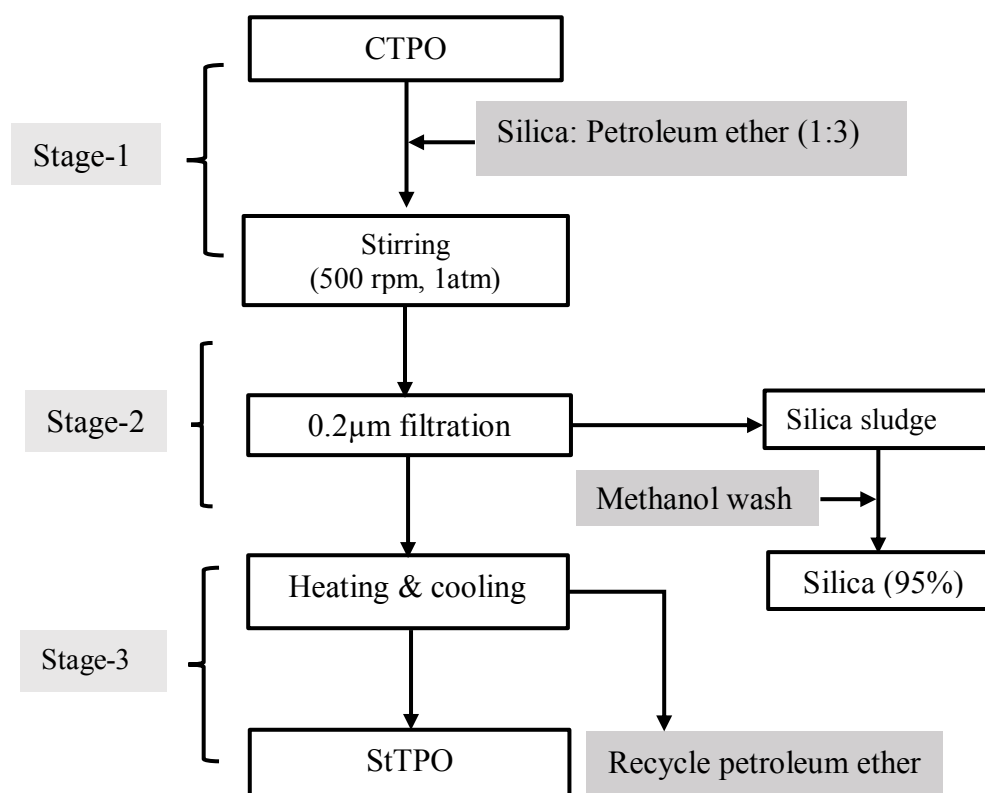


**Fig. 5.10 Process flow-diagram of overhead stirring upgradation strategy**

**Table 5.4 Comparative study of laboratory-scale strategy with overhead stirring process**

S. No.	Parameters	Laboratory scale process	Overhead stirring process
1.	Mixing equipment	Magnetic stirrer	Laboratory stirrer
2.	The rotational speed of the stirrer	Fixed	Adjustable
3.	Evaporation of solvent	Non-uniform cooling	Uniform cooling
4.	Oil loss	15%	5%
5.	Color	Reddish-brown	Red
6.	Odor	Improved	Improved significantly
7.	Sulfur content (%)	0.70	0.54

#### 5.14 Effect of batch scale upgradation on oil quality and yield

The oil yield from overhead stirring upgradation strategy is significantly improved by 15% compared to the laboratory-scale approach. The overhead stirring upgradation strategy creates a sufficient vacuum inside the condenser chamber during evaporation, and mixing effectiveness can be improved with the aid of a laboratory stirrer. The oil obtained from both the process is reddish-brown colored oily liquid and miscible with diesel at the entire concentration range. The odor of the upgraded oil is significantly improved in comparison with CTPO. The hedonic scale is used to compare the odour of crude and upgraded oil samples based on pleasant and unpleasant sensations. The hedonic scale for odor measurements is shown below (Lin et al. 2011) Based on the consensus of the occupants of the laboratory where the oil samples were prepared and studied, CTPO was rated as 8 (dislike very much). On the other hand, StTPO was rated as 5 (neither like nor dislike) due to the faint smell of aromatic hydrocarbons. The reduction of polar fractions including sulphur-containing compounds in StTPO by selective adsorption on silica gel was responsible for the improvement of odour. Table 5.5 represents the hedonic scale for odour measurements.

**Table 5.5 Hedonic scale for odour measurements**

Rating Scale	Explanation
1	Like extremely
2	Like very much
3	Like moderately
4	Like slightly

5	Neither like nor dislike
6	Dislike slightly
7	Dislike moderately
8	Dislike very much
9	Dislike extremely

The fuel properties and chemical composition of the laboratory scale and modified upgradation strategy appeared to be similar. However, there is a significant improvement in the odor and yield from the proposed batch scale upgradation strategy. We have suggested that the scalable, straightforward upgradation strategy using cost-effective adsorbent and solvent is necessary to address the above challenge. Upgradation of CTPO by silica gel as adsorbent and petroleum ether as solvent yield diesel range fractions with carbon atom ranges from C<sub>9</sub> to C<sub>27</sub>.

The upgraded oil obtained from the overhead stirring upgradation strategy looks better in terms of odor and yield. Compared with the laboratory scale upgradation strategy, the stirring propeller fitted inside the 6L beaker provides more surface area for mixing the supernatant (a mixture of CTPO + silica gel + petroleum ether), thus enhances the capture of more polar compounds into the silica gel from CTPO. The Millipore filtration system consists of three regions: the first region holds the supernatant (a mixture of CTPO + silica gel and petroleum ether), the second region has the filtration system, which contains a Nylon 6, 6 membrane disc filter has a diameter of 47 mm with a pore size of 0.2µm (ultipor®), the thickness of 140-178µm allows only the oil molecules under gravity separation. The refined oil molecules with solvent (petroleum ether) can be collected in the third region. Then the solvent is recovered with the help of a rotary evaporator connected with a low temperature cryostat bath.

Rotary evaporation is a conventionally used approach to separate the solvent at room temperature and pressure. In the laboratory scale upgradation method, we have used ice as a cooling medium during evaporation. Insufficient cooling in the condenser required heating of StTPO-petroleum ether mixture for faster evaporation, lead to evaporative loss of the solvent, and led to possibility of trace solvent remaining in StTPO. The low temperature cryostat provides uniform cooling during evaporation of solvent under vacuum (200 mm Hg) and did not require heating the solution. Finally, the refined oil was collected at the evaporating flask, and the solvent is collected at the receiving flask. We have argued that the yield from the

overhead stirring upgradation is significantly improved compared to laboratory scale upgradation by 15%.

The oil quality and odor were removed considerably due to reduced nitrogen-containing fractions, polar compounds, and acidic fractions. This reduction is due to the longer contact time of silica gel with the CTPO in overhead stirring upgradation strategy, facilitating better adsorption of polar compounds by silica gel. The silica gel particles collected in the disc filter are shown in Fig. 5.11. GC-MS identified sticky compounds like caprolactam, toluene, p-xylene, cyclohexene, 1-methyl-4-(1-methyl ethynyls), dodecane nitrile, heptadecane nitrile, which were adsorbed inside the silica gel. Methanol washing also regenerates the used silica gel in its original size for further upgradation of CTPO as shown through GC-MS spectra (Fig. 5.12).

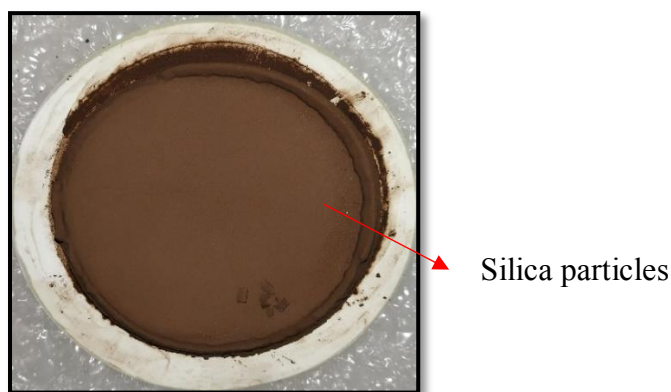


**Fig. 5.11 Silica gel deposits collected in membrane-based disc filter**

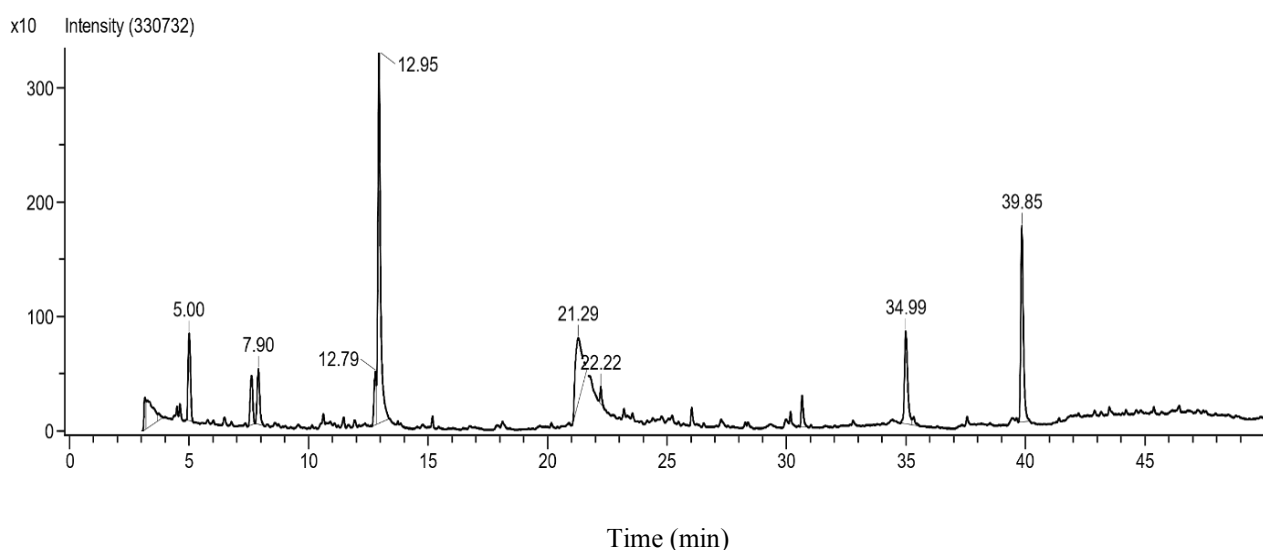


**Fig. 5.12 1D GC-MS Chromatogram of used silica gel washed by methanol**



### 5.15 Fuel property analysis

Surface tension studies reveals that the surface tension of upgraded oil is nearly matched with diesel due to the same chemical composition in both samples. Fig. 5.13 represents the surface tension of CTPO, StTPO, and diesel. Surface tension of diesel is very close to the studies reported in literature (Chhetri et al. 2013). However, there is a significant variation in the surface tension of CTPO due to a higher number of polar compounds compared to upgraded tire pyrolysis oil. Similar results were reported in literatures (Chumpitaz et al. 2019, Lehto et al. 2013, Tzanetakis et al. 2008, Wang et al. 2019).

During pendant drop formation in CTPO, there appears a phase separation between the bulkier tar phase and aqueous liquid phase exerts a high interfacial tension compared to StTPO. Tests were carried out to study surface tension's effect by increasing the percentage of StTPO with diesel. The blending of StTPO with various diesel fraction (say 20-80%) causes not much variation in surface tension due to the hydrophilic nature of upgraded tire oil compared with diesel molecules (more miscibility). The surface tension of StTPO corroborates that the StTPO diesel blends have good atomization and spray behaviour properties compared to diesel. Still, CTPO has higher surface tension due to more amount of carbonaceous deposits than StTPO. The density of StTPO blended diesel fuels looks similar due to the high miscibility of StTPO blends with diesel (Fig. 5.14). The density of CTPO and StTPO blends are found to be higher than diesel due to more carbon content.

During blend preparation, StTPO is mixed with diesel with various proportions using a laboratory stirrer at 500 rpm before calorific value analysis to ensure homogeneous mixing of the samples. The heating value of crude tire pyrolysis oil is 42-44 MJ/kg (Khaleque et al. 2015). Calorific value was determined using a digital bomb calorimeter (semi-automated bomb calorimeter with PC based software). The calorific value analysis reveals that the StTPO has a higher heating value (GCV) of 42.54 MJ/kg compared with diesel (46.18 MJ/kg). Wongkhorsub et al. (2013) reported the same calorific value for CTPO. The calorific value of StTPO increased by 0.78 MJ/kg after upgradation due to the removal of moisture, sediments, sulfur, and low energy polar compounds, which again confirmed the high carbon content in StTPO (83.26%) than CTPO (76.29%). Fig. 5.15 shows that the variation of calorific value by increasing the StTPO percentage concerning diesel. As the percentage of StTPO increases, the calorific value decreases gradually and then declined up to StTPO 100. It was noticeable that the calorific value of StTPO 20 is found comparable to diesel. The study also confirms the

suitability of using upgraded oil as a fuel for diesel engines without any further modifications. There is literature reported on the calorific value of CTPO for application in engines. However, there are no studies found on the calorific value analysis of StTPO.

Flashpoint of StTPO diesel blends was found using Pensky-Martens closed cup tester (ASTM D93). The flashpoint is defined as the lowest possible temperature at which the test flame ignites the fuel. Fig. 5.16 displays the flashpoint of various StTPO diesel blends and comparison with conventional diesel. The flashpoint of StTPO 20 is found to be comparable with diesel. The flashpoint of StTPO was found to be lower when compared to the diesel due to the presence of a wide range of boiling point compounds in StTPO compared with diesel. The flashpoint of StTPO diesel blends was reduced with an increase in the percentage of StTPO.

The viscosity of fuel mainly affects injector, lubrication, and fuel atomization. The viscosity of StTPO was found to be 2.54 cSt, 2.20 cSt, 2.07 cSt and 1.96 cSt at 40 °C, 50 °C, 60 °C and 70 °C. The viscosity of upgraded oil was reduced after the upgradation by silica gel (60-120 mesh size) and petroleum ether due to the removal of gummy like deposits by silica gel, dilution caused by petroleum ether (solvent). Murugan et al. (2008) conducted experiments in the internal combustion engine using CTPO as fuel and reported that the viscosity of CTPO was 1.5 times greater than diesel. Fig. 5.17 shows the kinematic viscosity of StTPO diesel blends at various temperatures of 40-70°C. The study revealed that the variation of viscosity with temperature showed a similar trend at various temperatures. The viscosity of StTPO-diesel blends appear to reduce by rise in temperature due to less intermolecular interaction between fuel molecules in StTPO-diesel blends.

Generally, the CTPO has a lower cetane index than diesel due to high aromatic content and higher cycloalkanes as per fuel property analysis (Martinez et al. 2013). The cetane index is indirectly proportional to aromatic composition in fuel. The cetane index is significantly improved after upgradation due to the adsorption of most aromatic compounds by silica gel. As the upgraded tire pyrolysis oil increases with the diesel, the aromatic content increases drastically, and the cetane index reduces, as shown in Fig. 5.18. StTPO shows a cetane index of 40 in comparison with diesel fuel. Aromatic content is found to be higher in StTPO than diesel.

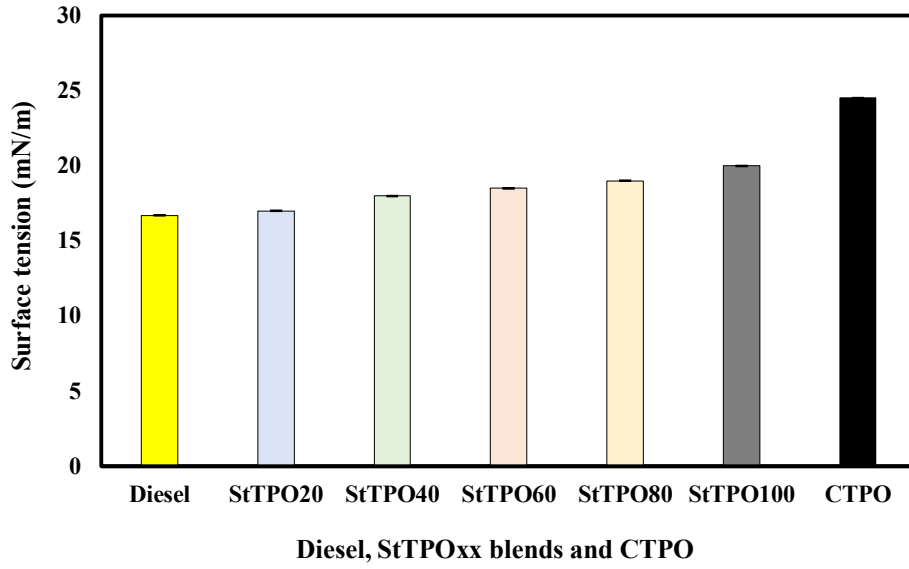


**Fig. 5.13** Surface tension of diesel, StTPOxx, and CTPO

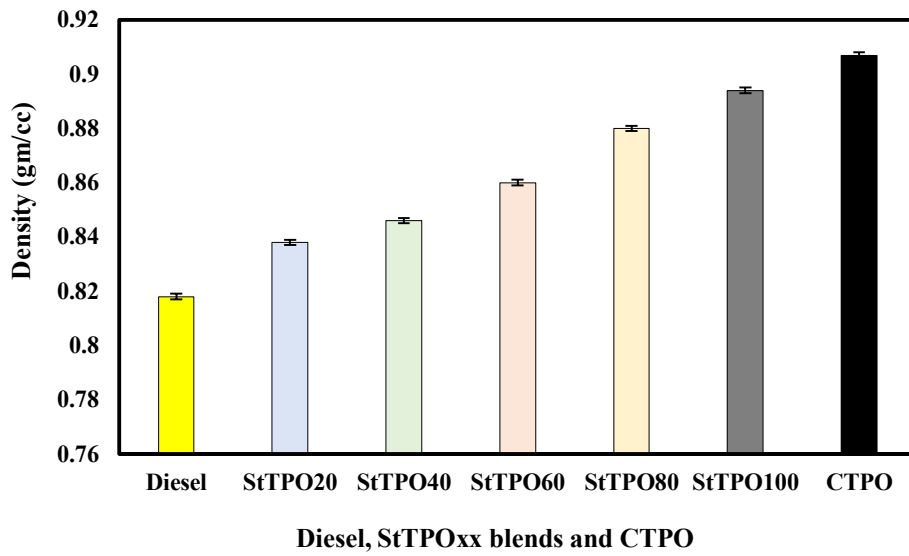


**Fig. 5.14** Density of diesel, StTPOxx, and CTPO

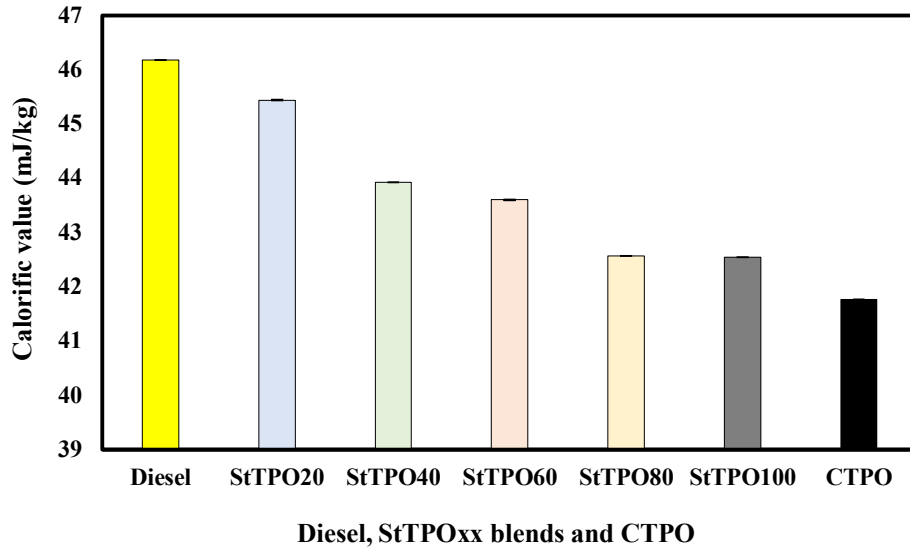


**Fig. 5.15** Calorific value of diesel, StTPOxx, and CTPO

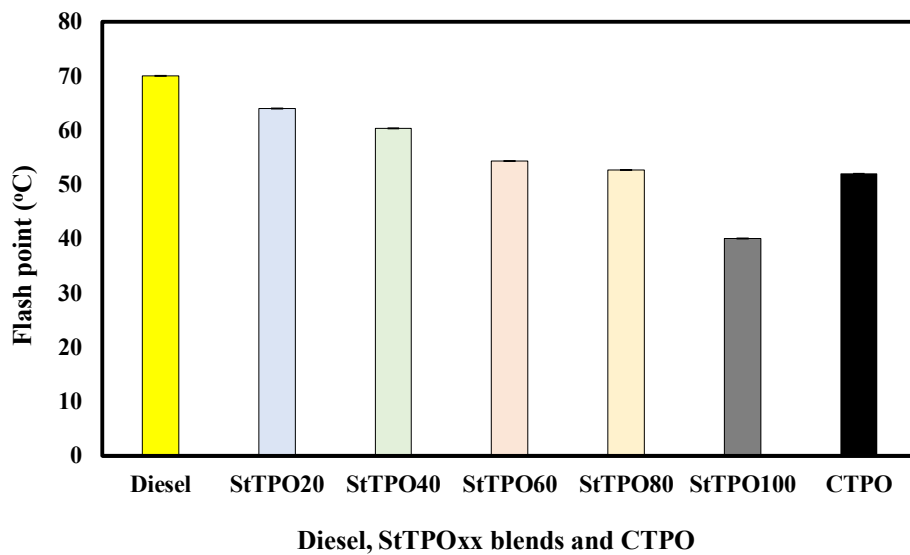


**Fig. 5.16** Flashpoint of diesel, StTPOxx, and CTPO

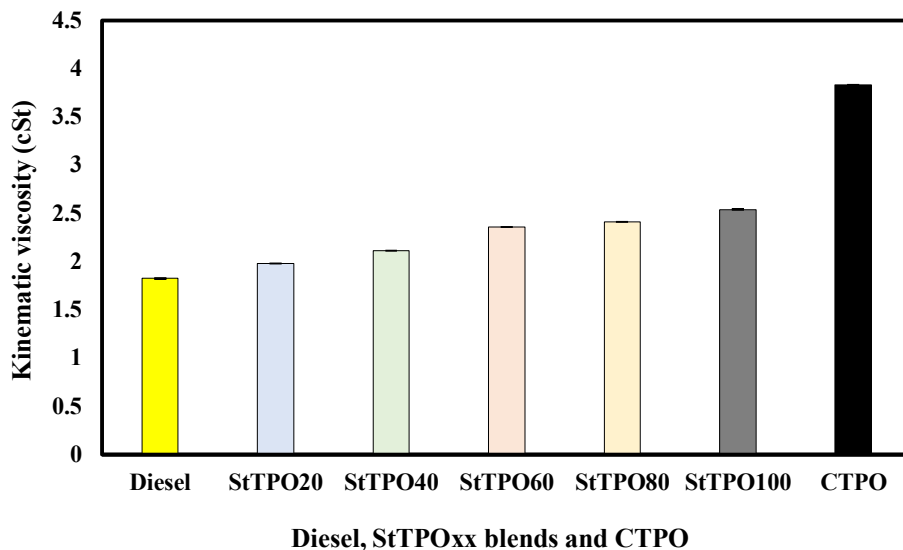


**Fig. 5.17 Kinematic viscosity of diesel, StTPOxx, and CTPO**

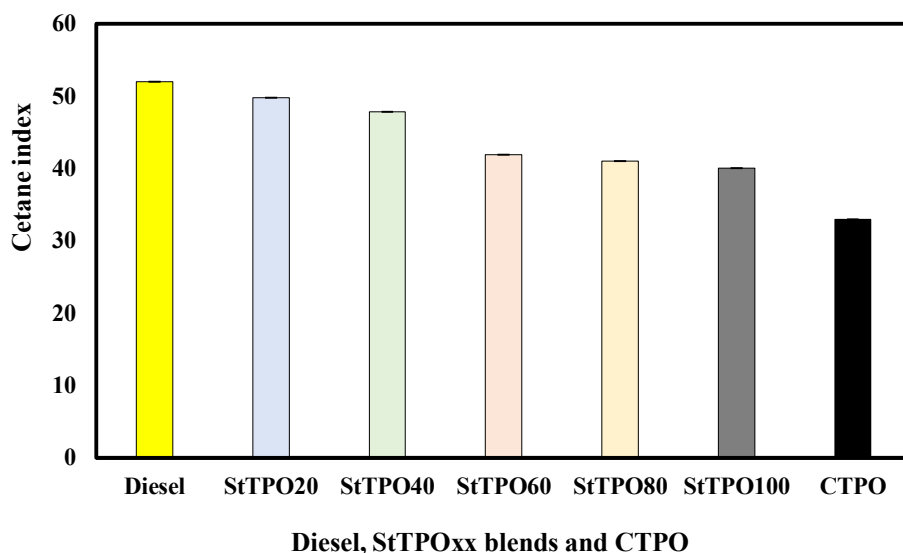


**Fig. 5.18 Cetane index of diesel, StTPOxx, and CTPO**

### 5.16 Boiling point determination

The boiling point compares the volatility of liquid samples, defined by (Godlewska et al. 2016, Chhetri et al. 2013). Distillation is a widely used separation technique in most petroleum refineries to separate compounds based on their boiling point. The sample was added to a quartz round bottom flask and gradually heated with the aid of a heating mantle. Then the distillates were collected, and the initial and final boiling point of samples was recorded in literatures (Godlewska et al. 2016, Elkasabi et al. 2019). The present study attempts to check the boiling point of StTPO and diesel. The crude form of pyrolysis oil is a multicomponent black colored

liquid comprised of a wide range of compounds with various distillation range. Martinez et al. (2013) reported that the tire pyrolysis liquid has an initial boiling point of 82.2 °C and a final boiling point of 305.2 °C. It was observed that the initial boiling point of StTPO and diesel are 120 °C, 145 °C, respectively, and the final boiling point of StTPO and diesel are 284 °C and 286 °C, respectively. It can also be observed that the StTPO is lighter than CTPO and diesel. Flashpoint studies supported with distillation behaviour revealed that tire oil samples are complex multicomponent fractions with various boiling range compounds, reported by Godlewska et al. (2016). Similar results were reported for CTPO in literature (Martínez et al. 2013). The boiling point of StTPO is in close range with diesel due to similarities in chemical composition. Thus, it can be concluded that StTPO can be directly used in a diesel engine without modification in the ignition timing. In contrast, the CTPO needs further improvement in ignition timing due to its high volatility.

### **5.17 Stability analysis**

A stability study was conducted to evaluate any change in the StTPO upon long term storage in the industry. The storage of upgraded oil in our laboratory for a six-month duration showed no phase separation on the wall of storage containers due to its stability which prevents the polymerization reactions. It can be further explained that most reactive functionalities like olefins, aldehydes, ketones, and carboxylic acid are removed after upgradation. The pungent smell of CTPO is significantly improved after a scalable upgradation strategy due to the adsorption of sulfides, mercaptans, and odorants by silica gel. Miscibility studies were conducted to check the solubility of StTPO with diesel. It was also observed that StTPO-diesel blends were found to be miscible at the entire concentration range. The GC-MS chromatogram of methanol washed silica gel supported with viscosity studies confirmed that the high viscosity of CTPO was due to the presence of gummy like deposits. The viscosity was drastically improved after upgradation using a modified strategy. It was also noticed that StTPO-diesel blends were miscible at the entire concentration range. Stability and spot tests give insights into the long-term storage stability of fuel and formulation of stable mixture for engine testing. The spot test is widely used to predict the possibility of fuel injector blockage, precipitate formation in fuel tank of marine engines as per ASTM D4740. A spot test is characterized by the formation of a distinctive circular ring after heating the fuel at 100°C and refers to the instability or incompatibility of fuels. The significant factors affecting the fuel stability are formulation, thermal and mechanical stresses upon storage and duration. It can be seen that there is no distinctive spot in StTPO-diesel blends compared with CTPO. The formulation of

the specific circular ring at the filter paper centre suggests the phase separation in CTPO. The main reason for no particular circular ring in StTPO is better miscibility during blending and greater affinity of StTPO with diesel. Fig. 5.20 describes the cleanliness and compatibility of various fuels by spot test. As per comparison with ASTM D4740 Adjunct reference spot, it can be observed that all the tested fuel samples are found to be stable and compatible except CTPO. The aging studies for six months showed the same results, confirming the stability of blends without any degradation or creaming effects. However, the major limitations of spot test are (1) waxy fuel (more paraffin content) may leads to false interpretation in the results (b) care need to be taken for analysing indistinctive spots during visual inspection. Table 5.6 describes the rating scale and description of the standard spot test. It was also noticed that StTPO-diesel blends were miscible at the entire concentration range (Fig. 5.19).



**Fig. 5.19 Phase stability examination of upgraded tire pyrolysis oil**

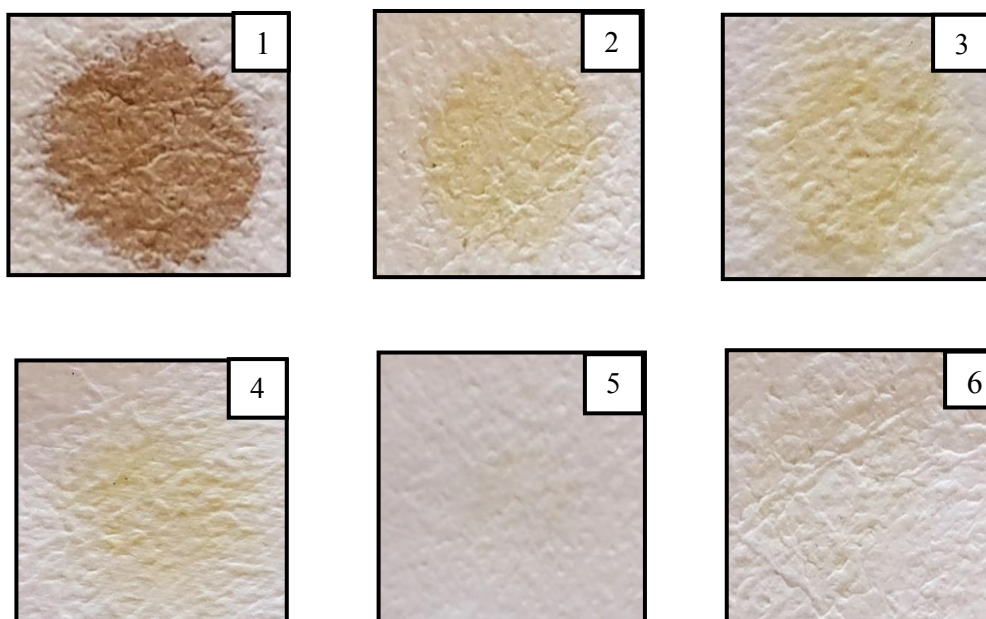


**Fig. 5.20 Cleanliness and compatibility of StTPO-diesel fuel blends by spot test**  
(1-CTPO100, 2- StTPO20, 3-StTPO40, 4-StTPO60, 5-StTPO80, 6-StTPO100)

**Table 5.6 Rating scale and description for a spot test**

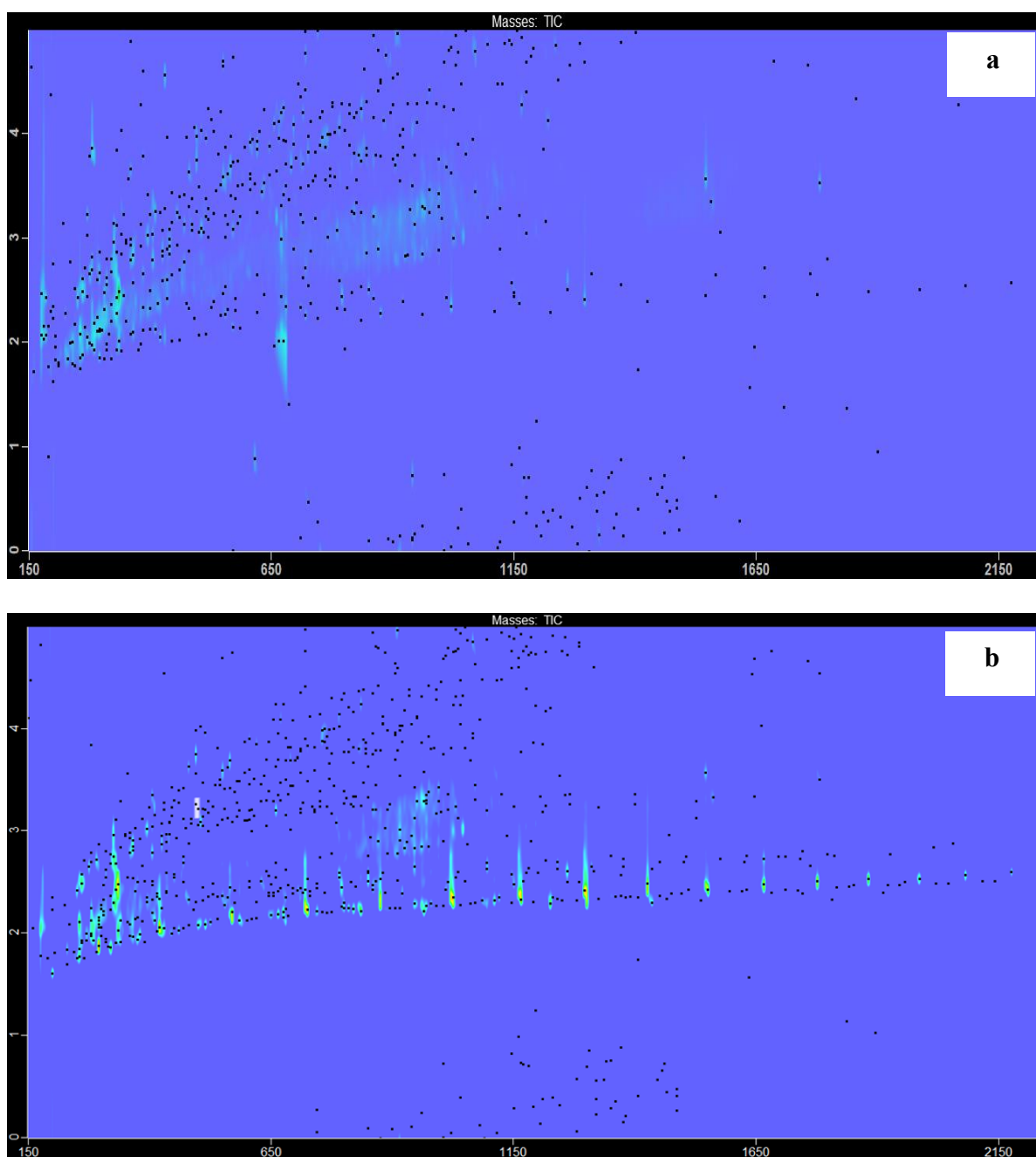
Rating factor	Description
1	Homogeneous spot with no inner ring
2	The faint or low inner ring
3	The well-defined inner circle, slightly darker than the background
4	Well defined inner ring, darker than the background
5	Very dark solid at the centre, darker than the background

### 5.18 Two dimensional gas chromatography time of flight mass spectrometry

Comprehensive two-dimensional GC×GC TOF-MS is one of the powerful analytical tools to analyze the pyrolysis oil from waste-derived feedstocks like tires, plastics, etc. (Vozka and Vrtis 2019). One of the existing challenges with traditional one-dimensional gas chromatography-mass spectrometry is the overcrowding of peaks or unresolved peaks, i.e., co-elution of the same boiling compounds in CTPO as reported by our previous research studies (Ngxangxa 2016). In addition to the low resolution, low peak capacity, exploration of few compounds, non-specific dispersion interaction of compounds by apolar column are some of the other issues with one dimensional GC-MS analysis (Ngxangxa 2016). One dimensional GC-MS problem can be overcome by transferring the samples into two separate columns separated with a modulator by spreading compounds in a two-dimensional space based on the orthogonal separation. The exciting principle behind two-dimensional GC×GC TOFMS is the separation of mixtures by the polarity of species compared to one-dimensional GC-MS separation based on the boiling point of compounds. Similar principles were reported in literatures (Muzyka et al. 2019, Onorevoli et al. 2017, Ware et al. 2017, and Ware et al. 2018). There are very few studies in the open literature regarding the analysis of tire oil fractions using this advanced chromatographic technique. Studies by Ngxangxa (2016) reported that tire oil contains a complex mixture of 6 carbon atoms to 24 carbon atoms supported by various compound classes like paraffins, olefins, terpenes aromatics, polyaromatic hydrocarbons, nitrogen and sulfur-containing compounds. Due to the complexity in the chemical structure and composition, the CTPO cannot be directly utilized in internal combustion engines or burners. Upgradation of crude tire pyrolysis oil is necessary to make it an attractive fuel for the future. Tire pyrolysis oil also offers an opportunity to excel in terms of the value-added compounds. Ngxangxa pointed out that dl-limonene, 4-vinyl cyclohexane, toluene, ethylbenzene, xylene, styrene, and benzothiazole are the significant value-added compounds



present in tire oil. Xylene is used for the production of industrial fibers. Benzothiazole is a commonly used accelerator during tire production. DL-Limonene offers attractive application as resin, fragrant, an industrial solvent, adhesives, dispersing agent for pigments, cleaning products, etc. DL-Limonene is formed by a series of mechanisms like the thermal decomposition of rubber to intermediate isoprene radicals. Then the isoprene radicals are transferred through a de-propagation reaction to gaseous phase products. Finally, the dimerization of isoprene yields dipentene as an end product. Fig. 5.21 represents the two-dimensional GC×GC TOF-MS chromatogram of CTPO, StTPO, and diesel.



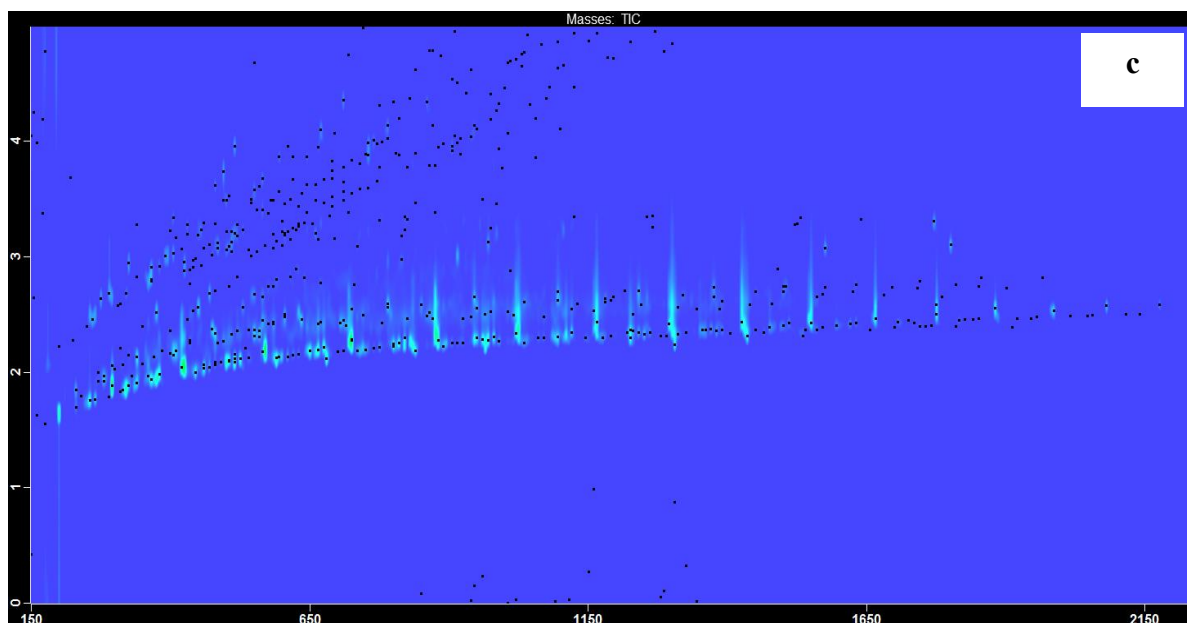
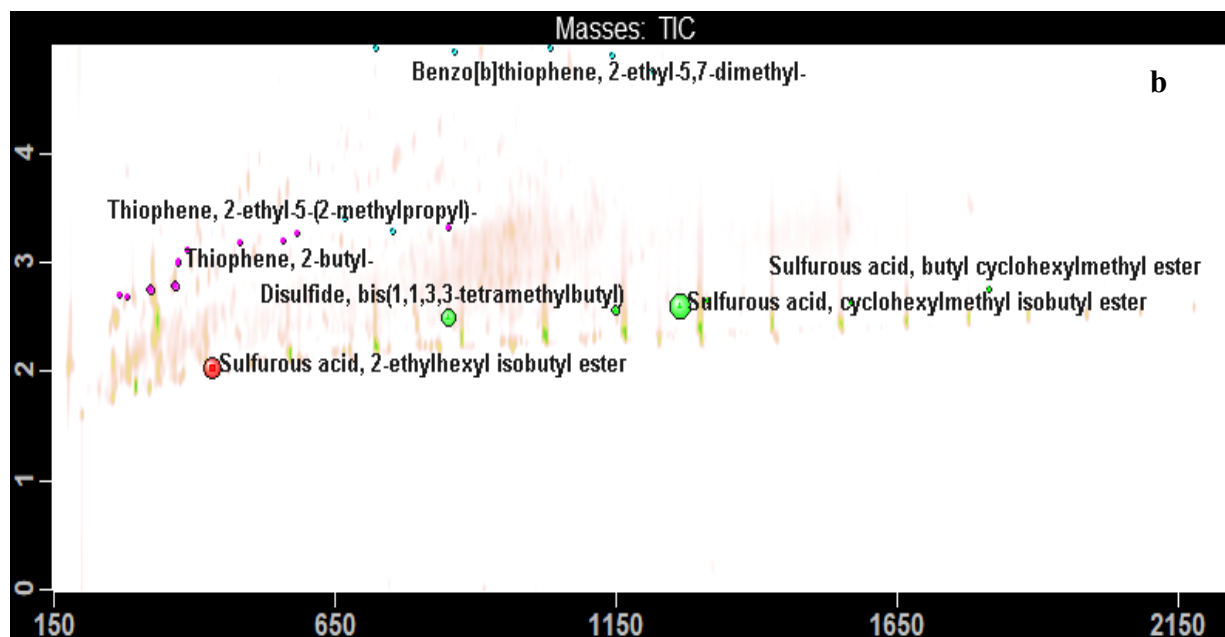
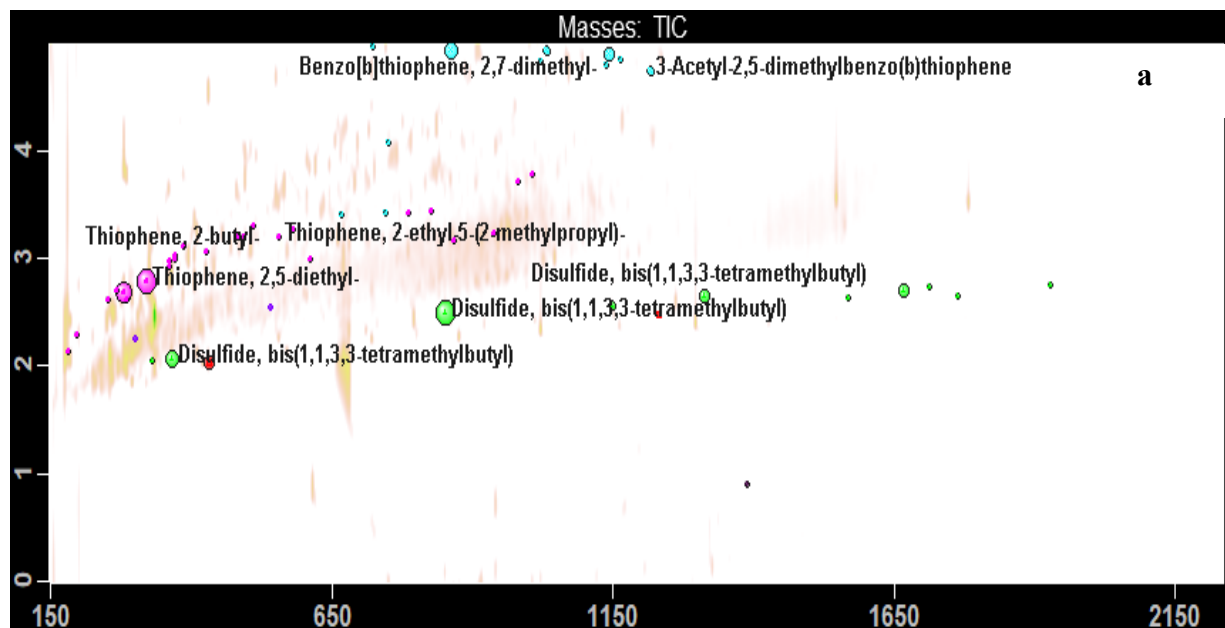


**Fig. 5.21 Contour plot obtained from GC×GC TOF-MS (apolar×polar column combination) during the analysis of CTPO, StTPO, and diesel**

The present study focuses on applying the two-dimensional GC×GC TOF-MS technique to analyze the CTPO, StTPO, and diesel with unique insights to the convergence to diesel range compounds. Further, reasons for the pungent odor during long term storage of CTPO and the market value of products from CTPO and StTPO. Aldehydamines, guanidines, thiazoles, sulfenamides, thiurams, dithiocarbamates, xanthates are the curing agents added during tire vulcanization. Out of these, thiazoles are widely used in most of the industries (Joseph et al. 2015). During the thermal depolymerization of tires, the polymer chains sulfur bridges were broken due to thermal softening. They resulted in a liquid fraction at 400 °C, at a heating rate of 10 °C/min, 0.2 atm, 4 rpm. The blackish colored liquid from the pyrolysis process emits a foul smell to the environment due to sulfur compounds such as thiazoles, sulfides, and disulfides. Fig. 5.22 (a), (b), and (c) represent the contour plot of sulfur compounds detected by GC×GC TOF-MS in CTPO, StTPO, and comparison with diesel. The GC×GC TOF-MS data supported with ICP-AES data suggests that the sulfur compounds from batch scale processes are reduced by 48.86% compared to laboratory-scale strategy. As we have expected, the sulfur content is very low in diesel than CTPO and StTPO.

The high sulfur content in CTPO is due to compounds like Diallyl sulfide, 2-mercaptobenzothiazole, Thiobisphenols, Tetramethylthiuram disulfide, 2-mercaptobenzothiazole disulfide, Alkylphenol polysulphide, 2-2'-dibenzamidodiphenyl disulfide, Thiosalicylic acid, N-cyclohexyl-2-benzothiasulfenamide are the compounds added during vulcanization

(Bockstal et al. 2019). This study can also positively impact the existing tire pyrolysis industries to modify their target goals and open a new way for biorefineries.



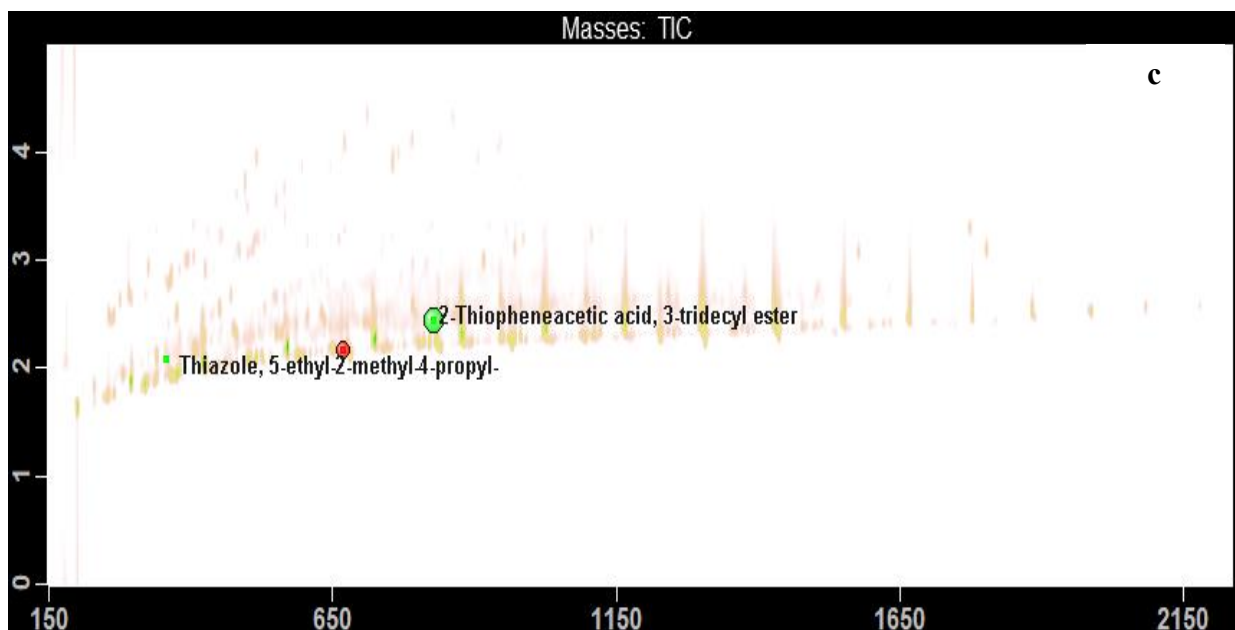


**Fig. 5.22 Contour plot of sulfur compounds in CTPO, StTPO, and diesel detected by GC×GC TOF-MS**

The typical surface plot of interesting compounds identified by GC×GC TOF-MS in CTPO, StTPO, and diesel are shown in Fig. 5.23 (a), (b), and (c). From our preliminary observation in the GC×GC surface plot, the separation space (peak capacity) is expanded compared to one-dimensional GC-MS. In the non-polar column, the analytes are separated based on the boiling point as in one dimensional GC-MS. However, the polar column separates the analytes based on their polarity (enhances the peak capacity) in CTPO, StTPO, and diesel. Equation 5.2 and 5.3 signifies the spatial allocation of compounds by apolar and polar columns in two-dimensional spaces by orthogonal separation. The following equations were proposed by (Toraman et al. 2014 and Dutriez et al. 2009).

$$RS_{2D} = \text{Square root of } (RS_1^2 + RS_2^2) \quad (5.2)$$

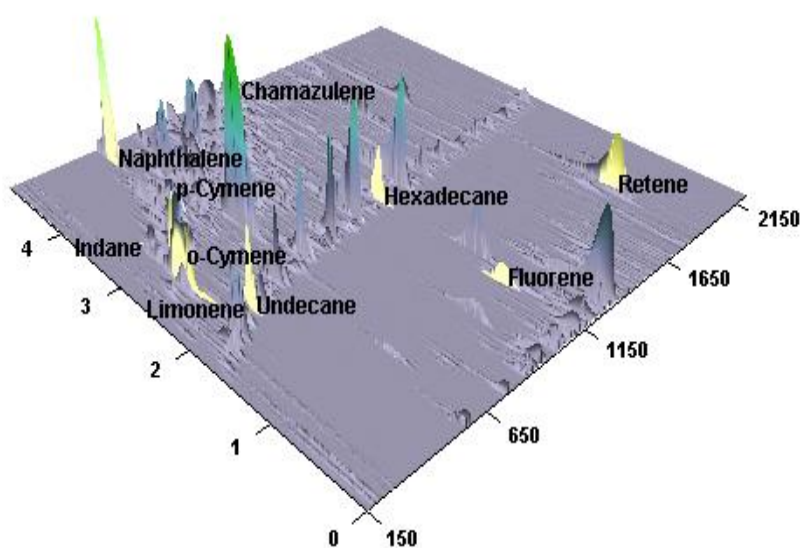
$$RS_{2D} = 2 \times \sqrt{\left(\frac{(\Delta tr_1)^2}{(WA_1+WB_1)^2}\right) + \frac{(\Delta tr_2)^2}{(WA_2+WB_2)^2}} \quad (5.3)$$

Where  $RS_1$  and  $RS_2$  correspond to first and second-dimensional resolution,  $\Delta tr_1$  and  $\Delta tr_2$  represent the difference in the retention time of compound A and B,  $WA_1$  and  $WA_2$  indicate the peak width of compound A and B in first and second dimensions, respectively. During analysis, the value of two-dimensional resolution was found to be 1.5. The resolution can be acceptable if the resolution is above 1 (Dutriez et al. 2009). Interestingly, column bleeding phenomena (thermal break down of the stationary phase at a temperature close to the upper-temperature limit of the column) and wrap around was not observed (elution period exceeds

modulation period) during GC×GC TOF-MS analysis of CTPO, StTPO, and diesel in comparison with the studies on bio-oil obtained from pyrolysis of coconut fibers (Almeida et al. 2013). Upgraded tire pyrolysis oil is a multicomponent mixture containing various compounds like aliphatic, aromatics, naphthalene's and benzene derivatives, etc. Camphene, chamazulene, cumene, n-hexadecane, and dl-limonene are some of the value-added compounds in StTPO and CTPO identified by two-dimensional GC×GC TOF-MS.

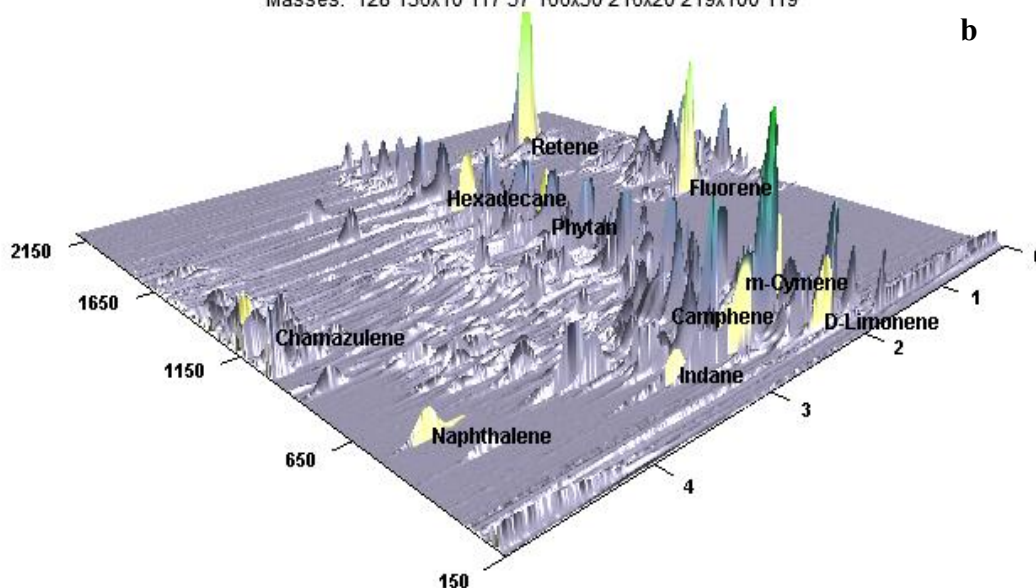
Masses: 166 71 128 219x5 169 134

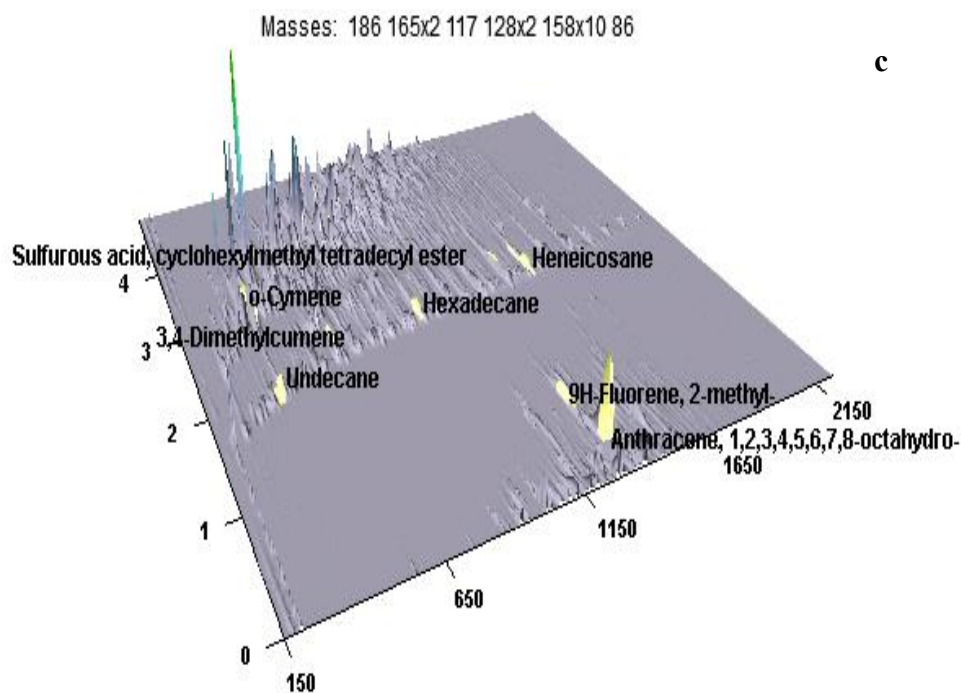
**a**



Masses: 128 136x10 117 57 166x50 216x20 219x100 119

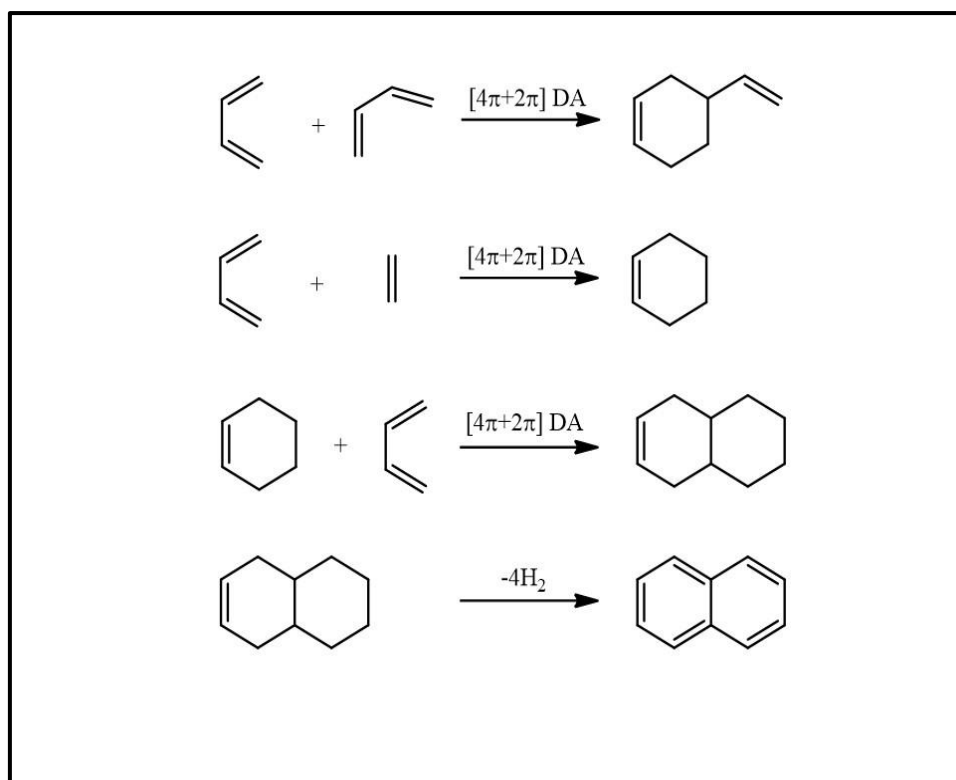
**b**





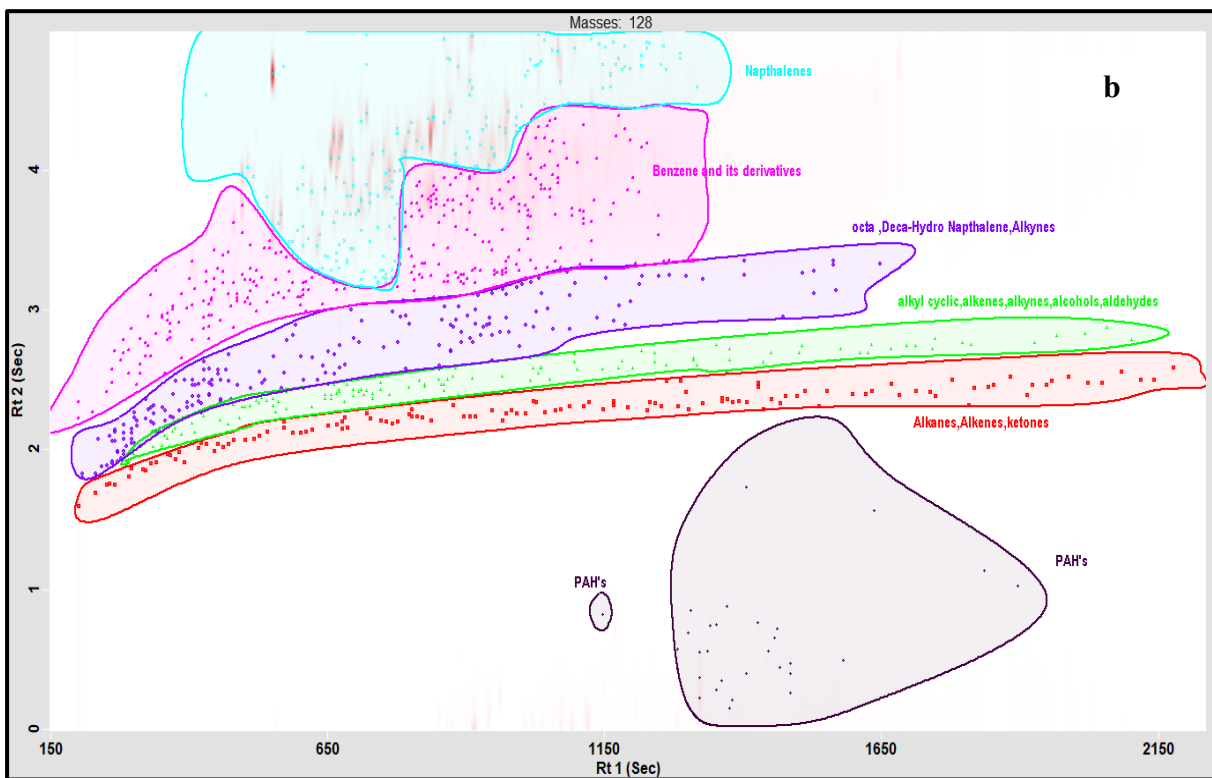
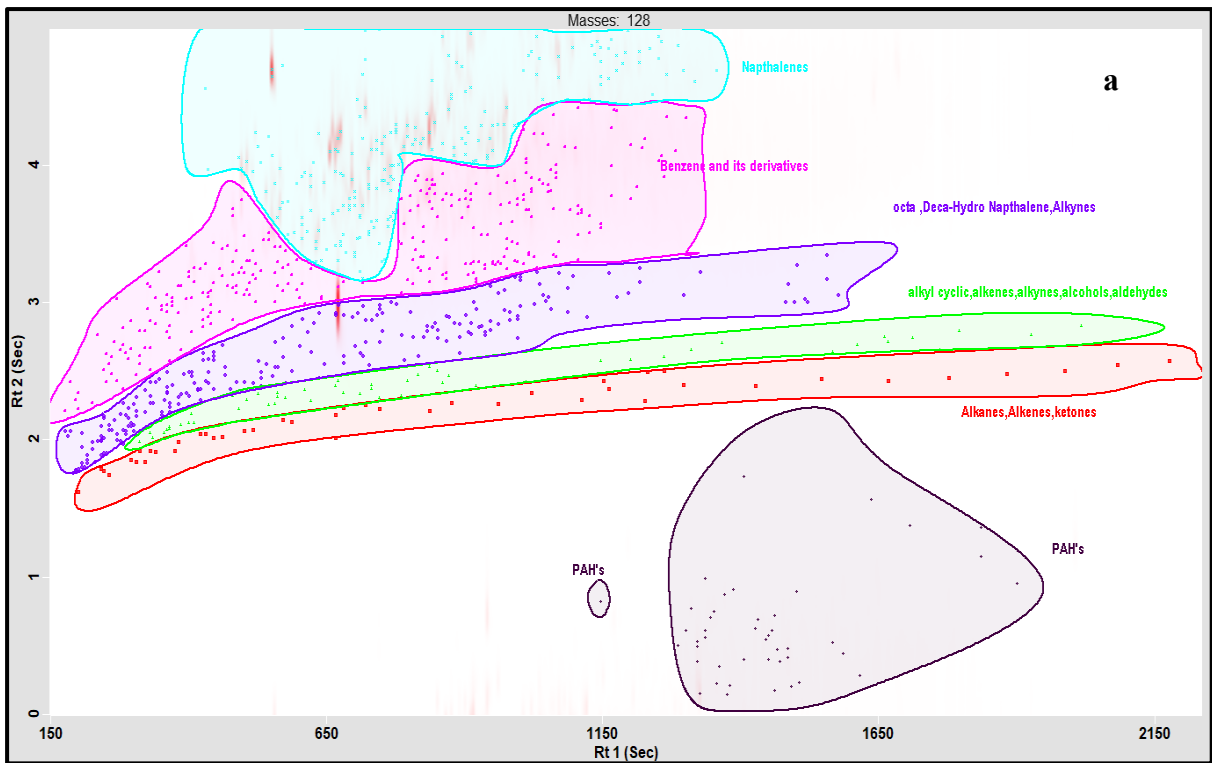
**Fig. 5.23 Surface plot of value-added compounds in CTPO, StTPO, and diesel**

It can be seen that StTPO contains a more significant number of value-added compounds in comparison with diesel. Williams et al. (1993) reported that the primary mechanism in polyaromatic formation in rotating autoclave is cyclization, aromatization, and Diels-alder reactions. During the pyrolysis of scrap tire, the depolymerisation reactions triggered inside the rotating autoclave due to  $\beta$ -scission reaction at double bond of styrene-butadiene rubber results in the formation of ethane, propane, and 1, 3-butadiene, which then reacts to form cyclic olefins. The same concepts were reported in literature (Williams 2013). The mechanism for polyaromatics formation during the depolymerisation of scrap tires inside the rotating autoclave is included in Fig. 5.24. They found that the polyaromatic compounds like benzopyrene, chrysene, and fluoranthene increase with the secondary reaction temperature of pyrolysis reactor.



**Fig. 5.24 Mechanism of aromatic hydrocarbon during depolymerisation of scrap tire in rotating autoclave reactor**

DL-Limonene, undecane, fluorene, phytan, indane, camphene, retene, hexadecane, cumene, o-cymene, chamazulene, naphthalene are the major compounds identified in StTPO. Hexadecane, one of the most valuable hydrocarbons and regarded as the diesel surrogate is found in tire pyrolysis oil. Limonene is another interesting chemical widely found in CTPO, which is conventionally used to produce solvents, surfactants, pigments, etc. The quantification of value-added compounds will be planned as a future course of study, which can also provide an opportunity to create a new bio refinery for tire waste. The various classes of compounds identified in CTPO, StTPO, and diesel are displayed in Fig. 5.26 (a), (b), and (c). Fig. 5.27 displays the contour plot of value-added compounds identified in StTPO by 2D GC×GC TOFMS.





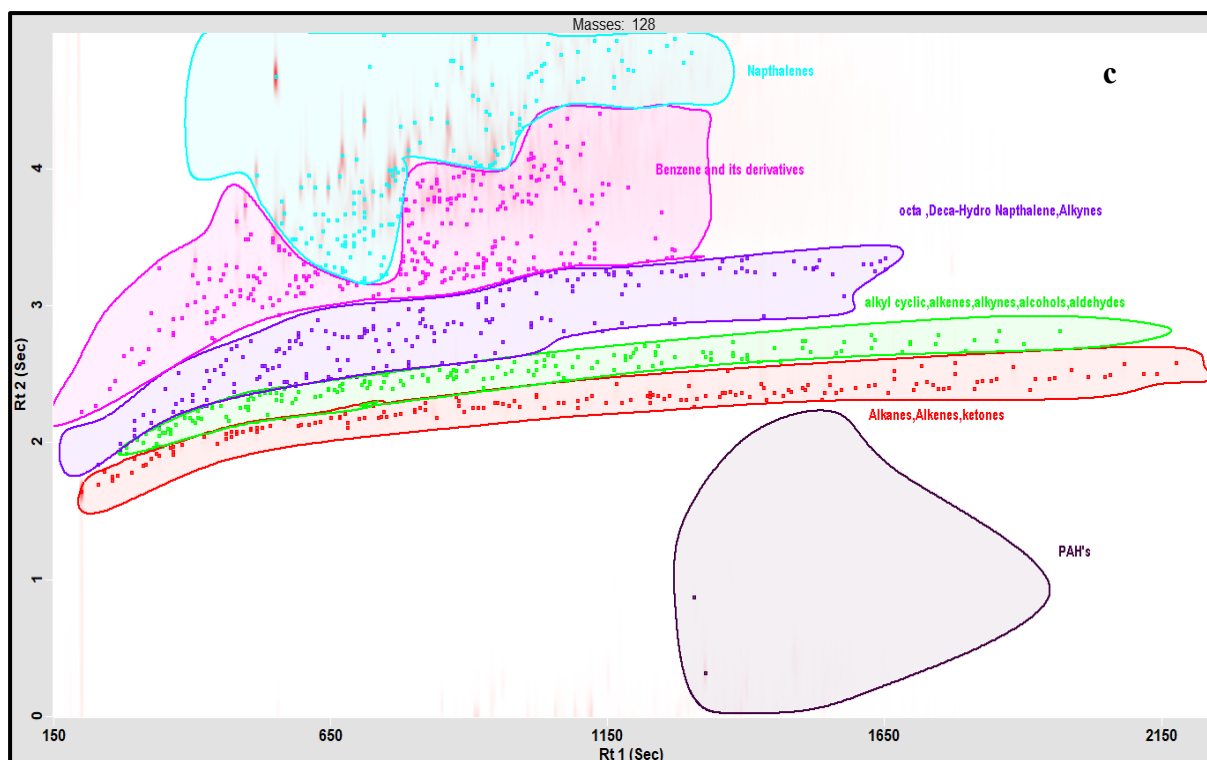


**Fig. 5.25** Schematic representation of elution pattern obtained for various class of compounds in CTPO, StTPO, and diesel by GC×GC TOF-MS

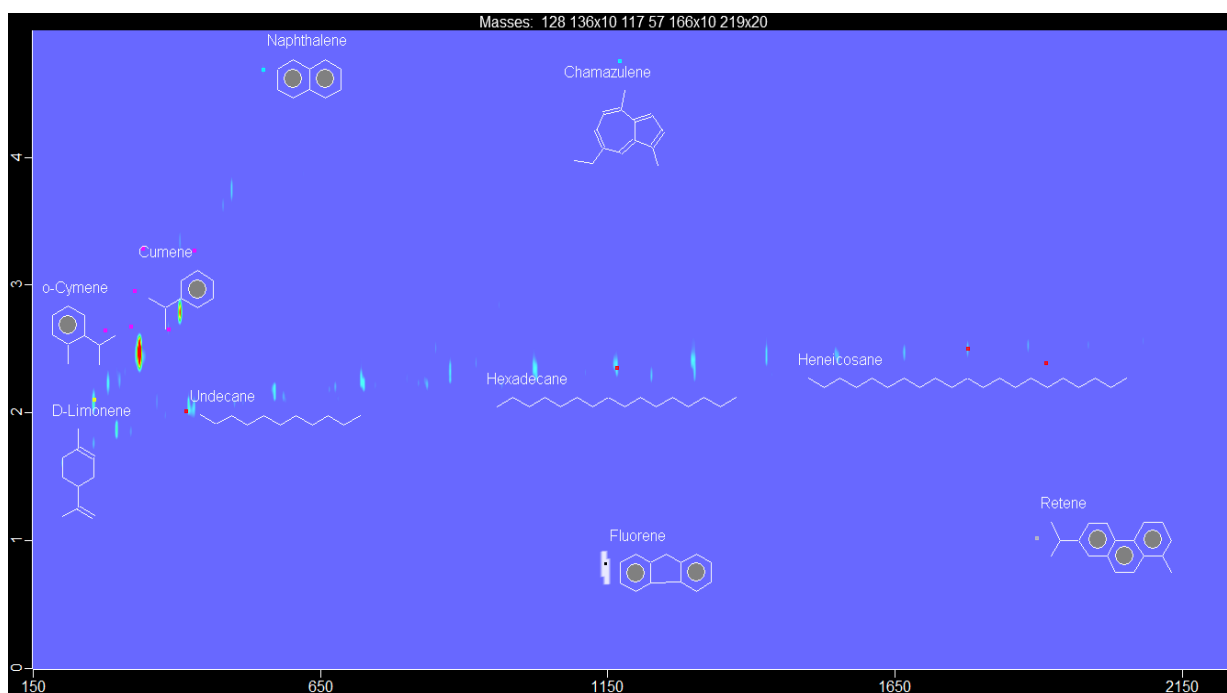


**Fig. 5.26** Value-added compounds in StTPO

The chromatogram of n-alkanes in CTPO, StTPO and diesel are shown in Appendix (Fig III-1). The saturated hydrocarbons (straight-chain alkanes) in StTPO are comparatively more by 9.60% compared to diesel. It can also be noted that the n-alkanes in StTPO is found to be predominantly higher than diesel (20.22% increase). Table 5.7 shows the percentage of various classes of compounds in CTPO, StTPO, and diesel. A higher amount of aliphatic composition in StTPO can be explained due to the higher surface area due to the adequate mixing of CTPO with petroleum ether in a stirring-based approach. The same reason was reported in our previous studies. The naphthalene in StTPO (8.88%) and diesel (5.96%) show almost a similar range due to the same chemical composition in both samples.

Fig. III-3 represents the peak area percentage of carbon atoms in StTPO and diesel. It is seen that the alkanes are dominant in StTPO in comparison with diesel, which is corroborated to stirring based up-gradation strategy, which aids in better mixing due to more surface contact between CTPO and silica in stirring based upgradation. Interestingly, compounds like dodecane, tetradecane, and pentacosane are similar in both samples. Paraffin is one of the significant components in diesel, which enhances the combustion properties. The cetane number of diesel depends on the presence of n-, iso-, and cycloparaffins. The relative solubility of paraffin's and iso-paraffin signifies the cold flow properties of diesel. Naphthalenes are other essential components in petroleum refinery products (Toraman et al. 2014).

The aromatics are another exciting fraction in tire oil (Muzyka et al. 1998), which boils at a higher temperature. Aromatics are classified into monocyclic and polycyclic aromatics. These mainly constitute the benzene fractions and naphthalenes. As far as we know, there are no studies reported in the open scientific literature regarding the exploration of upgraded tire oil analysis using GC×GC TOF-MS. The present study reveals that the benzene and its derivatives are more in CTPO than StTPO and diesel. The naphthalenes are lowered by 43.69% after upgradation, whereas the polyaromatic hydrocarbons are scaled-down by 27.79% compared to CTPO. Benzene fractions have a significant role in combustion chemistry to accelerate the in-cylinder pressure and temperature. The benzene and its derivatives are truncated by 25.68%. The primary reason for reducing benzene fraction in StTPO is the escape of benzene fractions due to a series of heating and cooling operations during the modified up-gradation strategy in the rotary evaporator. Mohan et al. (2019) reported that the reduction in polyaromatics in StTPO compared to CTPO is due to the adsorption of polyaromatics by silica gel. The same results were obtained for diesel sample analysis by Chakravarthy et al. (2018). The ignition delay in the engine mainly due to higher aromatic content. The higher aromatic content in

StTPO causes a longer ignition delay than diesel fuel. However, the ignition delay of StTPO is lower than CTPO due to removing a high polar fraction and oxygenates during upgradation. The scalable upgradation strategy reduced most of the nitrogen and sulfur-containing compounds in the CTPO using silica gel as adsorbent and petroleum ether as a diluent. Silica gel adsorbed most of the polyaromatic hydrocarbons due to its characteristic pore size and surface area of 40-60 Å and 350-450 m<sup>2</sup>/g.

**Table 5.7 Comparison of various class of compounds in CTPO, StTPO, and diesel**

<b>Class of compounds</b>	<b>CTPO (%)</b>	<b>StTPO (%)</b>	<b>Diesel (%)</b>
Alkane, Alkene, Ketones	3.709	15.38	26.171
Alkyl cyclic, alkenes, alkyne, alcohol, aldehyde	6.22	13.94	22.16
Octa, Deca-Hydro Naphthalene, Alkynes	34.534	32.32	27.38
Benzene and derivatives	36.372	27.03	17.49
Naphthalene's	15.772	8.88	5.96
Polyaromatic hydrocarbons (PAH)	3.393	2.45	0.839
Total identified (%)	100	100	100

### 5.19 Differential scanning calorimetry (DSC)

Differential scanning calorimetry (DSC) supported with thermo gravimetric data gives insights about heat flow from the sample and reference (Indium nitrate) as a linear function of temperature (Sathiskumar et al. 2019). Fig. 5.27 shows the DSC curve of crude and upgraded tire pyrolysis oil. This study also investigates whether the reaction nature is either endothermic or exothermic. The exothermic reaction is characterized by scission reactions, depolymerisation, and endothermic reactions due to crosslinking and poly-condensation reactions (Policella et al. 2019). It can be seen that endothermic peaks between 50-100 °C are due to the softening of molecular bonds in CTPO and StTPO. This softening mainly occurs due to the release of moisture, low boiling compounds from both samples. Glass transition starts at 200 °C due to phase change of both samples due to linear heating from 30-500 °C at a constant heating rate of 10 °C/minutes. The region in between 400-500 °C shows a frequent fluctuation in thermal behaviour of crude and upgraded oil samples. This fluctuation is caused due to rupture of bonds in samples due to decomposition reactions, which results in an exothermic peak. The drastic rise in the thermal behaviour of StTPO at 500 °C is due to

complex degradation reaction due to a wide range of boiling compounds in the crude compared to upgraded tire pyrolysis oil. Thus, the study revealed that the StTPO is much stable at higher temperatures than CTPO. DSC studies showed the specific heat of CTPO and StTPO is 877 J/g K and 624 J/g K. It can be concluded that the StTPO required less energy to vaporize than CTPO, which is attributed to less amount of polar fraction in StTPO.

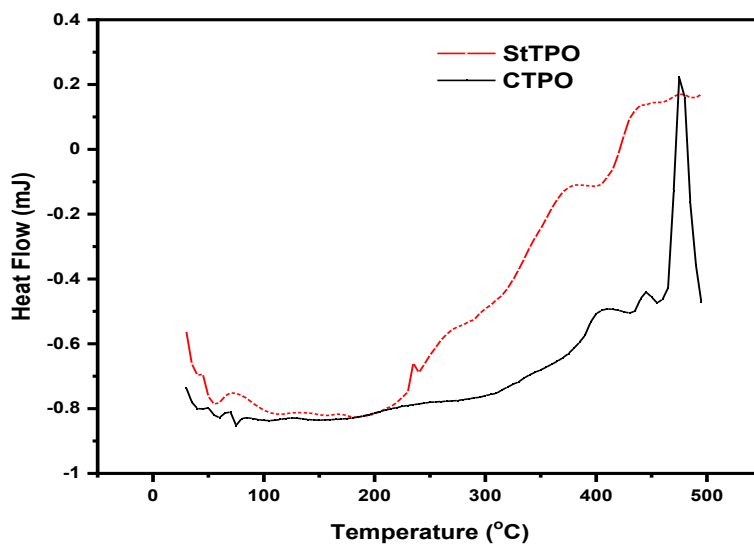


Fig. 5.27 Differential scanning calorimetry of crude and upgraded tire pyrolysis oils

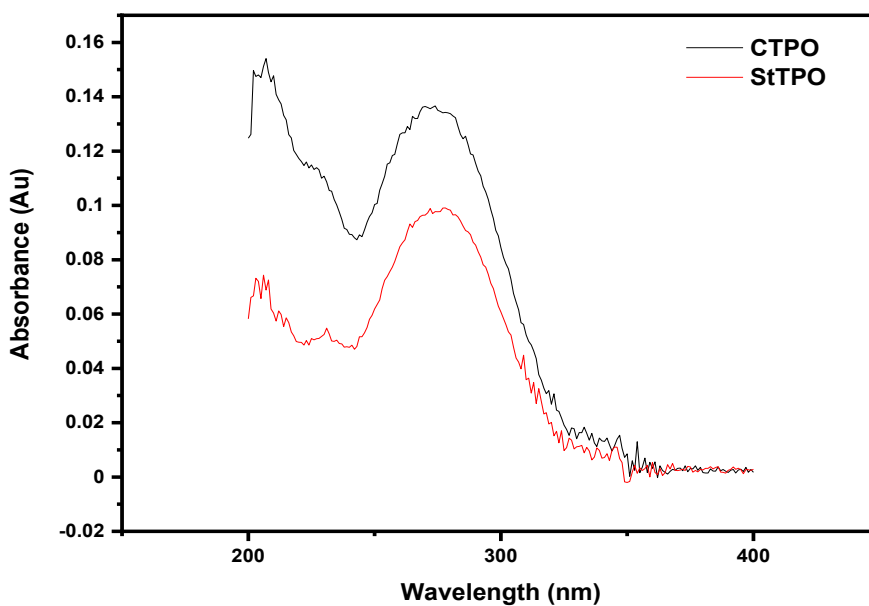
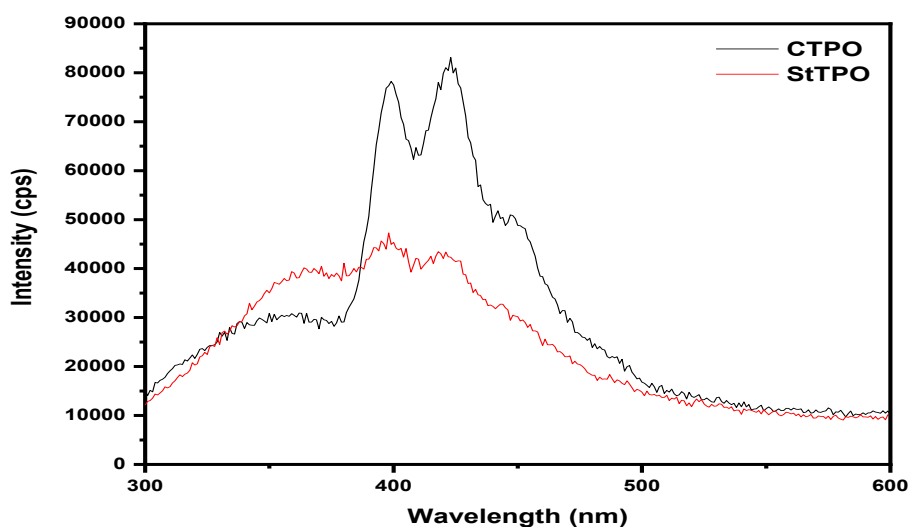


Fig. 5.28 UV-visible spectra of crude and upgraded tire pyrolysis oil

Fluorescence studies give information about the presence of polyaromatic fractions in pyrolysis oil. The shape and position of peaks in fluorescence spectra mainly affect the chemical composition, stability, etc. Ambrosewicz-Walacik et al. (2016) studied the fluorescence spectra of distilled tire pyrolysis oil and concluded that presence of polycyclic hydrocarbons is the primary reason for fluorescence. There are very few kinds of literature about the fluorescence studies of crude tire pyrolysis oil to the best of our knowledge. UV-visible spectroscopy is used to find out the excitation wavelength of whole samples (Fig. 5.28). Fig. 5.29 shows the fluorescence spectra of CTPO and StTPO. The UV-visible spectra supported with fluorescence data showed that the high fluorescence property of CTPO is due to the presence of extender oil, stearic acid, and polyaromatic hydrocarbons like anthracene, benzopyrene, benzo fluoranthene, perylene, and anthanthrene (Lloyd 1975). The fluorescence emission from StTPO is significantly reduced due to the adsorption of polyaromatics by silica gel during stirring based upgradation strategy.

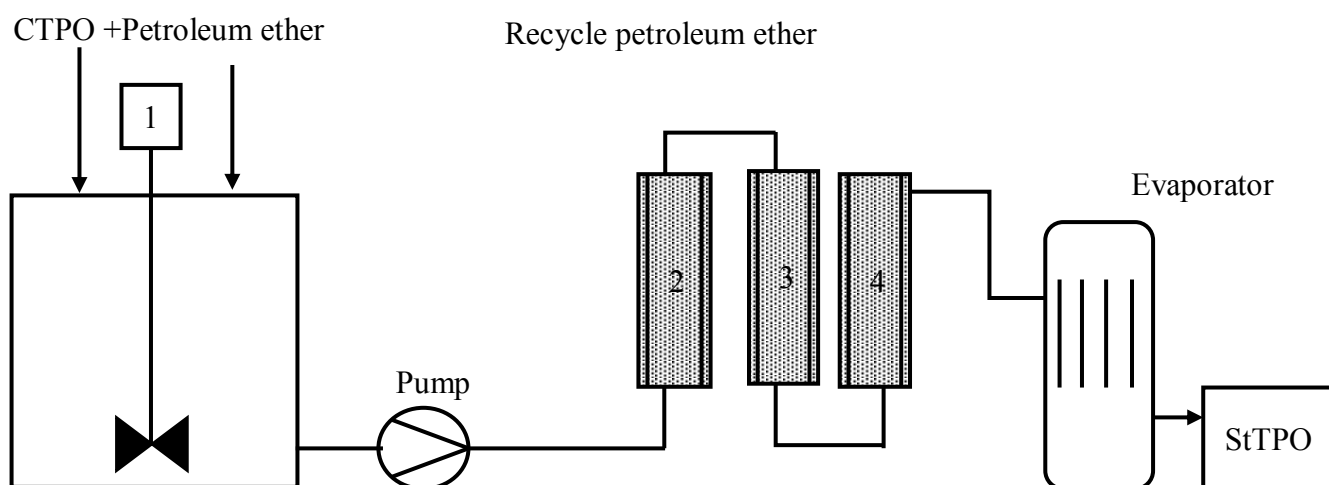


**Fig. 5.29 Fluorescence of crude and upgraded tire pyrolysis oil**

### **5.20 Scale-up strategy of upgraded TPO in a continuous regime**

The scale-up of the batch scale upgradation strategy will be planned as a continuation of present study. The solution of CTPO and petroleum ether can be passed through columns packed with silica gel connected in a continuous regime. The contact time of silica gel with CTPO can be monitor by the flow rate or the number of columns used in the experiments. The silica gel can be either washed using methanol or can be recovered by calcination. The petroleum ether can

be recycled by atmospheric distillation. Fig. 5.30 shows the scale-up of CTPO in a continuous regime.



1. Overhead stirrer fitted in an autoclave reactor, 2, 3, 4- Removable and recycle silica gel

**Fig. 5.30 Scale-up of CTPO in a continuous regime**

## 5.21 Conclusions

The present chapter focused on the various refining strategies, i.e., (laboratory and batch scale), for refining crude tire pyrolysis oils. The most significant conclusions obtained from the research study is presented as follows:

1. A mechanically stirring based strategy is found to be more effective in removing polar compounds than compared with passing CTPO through a column packed with silica gel.
2. Batch scale upgradation reduced the oil loss by 5% compared to laboratory-scale strategy, i.e., improvement of oil yield by 15%.
3. Silica gel efficiently removes the polar fractions, oxygenates, nitrogen, and sulfur-containing compounds responsible for the inferior properties of CTPO.
4. Sulfur content in the batch scale upgradation strategy is reduced by 48.86% compared to CTPO.
5. Experimental data obtained from GC×GCTOFMS revealed that polyaromatic hydrocarbons and naphthalene in CTPO are significantly reduced after upgradation by 27.79% and 43.69%, respectively.
6. GC×GCTOF-MS revealed that the linear alkanes in StTPO are higher than CTPO and diesel (increase by 20.22%).

7. Phase stability studies supported with spot tests confirm the stability of all fuel samples in comparison with diesel.
8. No phase separation or creaming is observed when the oil sample is stored in a container for six months.

CTPO obtained from a 10-ton rotating autoclave reactor was processed using various cost-effective refining methods such as column-based and stirring based upgradation. Stirring based upgradation is very effective in removing polar oxygenates (agents that causes inferior properties of CTPO) than column-based upgradation strategy. The improvement is due to the large surface area of the stirring based method, which helps to adsorb polar oxygenates into the silica gel. A comparative study was then conducted to analyse the fuel properties of crude and upgraded oil using various analytical techniques. The studies showed that upgraded tire oil properties were found to be similar to diesel range hydrocarbons. Thus, the next step is to blend the upgraded oil with various diesel fractions to test in a single-cylinder diesel engine to study the performance, combustion and emission characteristics.

## CHAPTER 6

### EXPERIMENTAL STUDIES ON PERFORMANCE, COMBUSTION, AND EMISSION OF A SINGLE CYLINDER DIESEL ENGINE FUELLED WITH UPGRADED TIRE PYROLYSIS OIL AND ITS BLENDS WITH DIESEL

#### 6.1 Introduction

This chapter presents the effect of upgraded tire pyrolysis oil in a single-cylinder diesel engine to study the performance, combustion, and emission characteristics and compared with diesel fuel. The fuel blends were prepared on a volumetric basis by blending different percentages of StTPO and diesel and named as StTPO<sub>xx</sub>, where the xx indicates the volumetric percentage of upgraded tire pyrolysis oil in sample and remaining is diesel. The prepared fuel blends were named as diesel, StTPO20, StTPO40, StTPO60, StTPO80, StTPO100 and CTPO100.

#### 6.2 Performance characteristics

Brake thermal efficiency and brake specific energy consumption are the critical parameters used to ascertain the performance characteristics of a compression ignition engine operated with fuel samples. These parameters are explained in subsequent sections:

##### 6.2.1 Brake Thermal Efficiency (BTE)

BTE indicates the usable power delivered from the chemical energy stored in the fuel (Ashok et al. 2019). Therefore, it gives an idea of fuel conversion efficiency. It depends upon the aromatic content, viscosity, density, calorific value, and fuel consumption (Dogan et al. 2012, Verma et al. 2018). Fig. 6.1 delineates the brake thermal efficiency of CTPO<sub>xx</sub>, StTPO<sub>xx</sub> and diesel. It can be noticed that the BTE increases with a rise in load due to an increase in brake power of the engine for all the tested fuel samples. The BTE of CTPO20, CTPO40, CTPO60, CTPO80, CTPO100 at full load are recorded as 31.85%, 31%, 30.56%, 30% and 29% whereas the BTE of StTPO20, StTPO40, StTPO60, StTPO80 and StTPO100 at full load was 30.12%, 29.95%, 28.65%, 27.50% and 27% respectively.

The study conducted by Hariharan et al. (2013) concluded that the lower brake thermal efficiency of CTPO-diesel blends is due to lower heating value than diesel. The heat release from diesel engines mainly depends on the viscosity, heating value, ignition delay, volatility and latent heat of evaporation of testing fuels (Babu et al. 2019). The brake thermal efficiency of StTPO<sub>xx</sub> is lower than CTPO<sub>xx</sub> due to the lower density of the former than the latter. Engine experiments using CTPO<sub>xx</sub> and StTPO<sub>xx</sub> were conducted based on constant fuel injection



pressure (120 bar). Higher density of CTPOxx compared with StTPOxx may result in poor atomization and spray characteristics resulting in incomplete combustion of fuel (Verma et al. 2018). Thus, the poor atomization causes lower brake thermal efficiency of fuel blends. However, heat release is the other factor that determines brake thermal efficiency. The heat release rate is used to identify the start of combustion, the fraction of fuel burned in premixed mode and the difference in combustion rate of fuels (Leyan et al. 2009). The Brake thermal efficiency of StTPOxx is lower than CTPOxx due to its lower heat release from StTPOxx than CTPOxx. Thus, the predominant factor in the present study is heat release in comparison with density (Verma et al. 2018).

Another factor is lower heat release during the premixed combustion phase from the combustion data. Another study by (Murugan et al. 2008) discussed the effect of distillation on CTPO for utilization as a fuel in diesel engines. It was noted that a 30% blend of CTPO and distilled CTPO had lower brake thermal efficiency than diesel. The reduction in brake power is due to the decrease in viscosity. Thus, fuel spray did not propagate deeply into the combustion chamber and some of the fuel droplets remain unburnt inside the combustion chamber.

Fuel atomization mainly depends on the injection pressure, viscosity and density of fuel samples (Develop et al. 2019; Shin et al. 2020). The viscosity of fuel is one of the reasons for the reduction in brake power (Verma et al. 2018). Reduction in brake thermal efficiency by about 2% is noticed at full load in the cases of DTPO90 (90% distilled tire oil and 10% diesel) compared to diesel. The viscosity of DTPO90 is found to be lower, and the fuel spray does not propagate deeper into the combustion chamber and is left unburned. As per the reasons stated by Murugan et al. (2008)<sup>a,b</sup>, the droplets of fuels with low viscosity cannot go deeper into the combustion chamber because they tend to generate smaller droplets that will have lower momentum than high viscous fuels. Unlike the diesel fractions, the tire-derived fuels are multi-component liquid fraction contains volatile and non-volatile fractions with wide distillation range. This may restrict the deeper penetration of fuel droplets into the combustion chamber, and non-volatile fraction may leave unburned inside the combustion chamber. This causes a reduction in the brake power of diesel engines.

A study conducted by Tudu et al. (2016)<sup>a</sup> found that aromatic content with high boiling range compounds of light fraction tire pyrolysis oil increases the brake thermal efficiency compared

with diesel. Another study by Tudu et al. (2016)<sup>b</sup> revealed that a higher density of CTPO (910 kg/m<sup>3</sup>) compared to diesel (830 kg/m<sup>3</sup>) causes poor atomization and spray formation inside the engine cylinder. From this, it can be concluded that the BTE of StTPO<sub>xx</sub> was slightly lower than CTPO<sub>xx</sub>, which is attributed to the lower heat release of StTPO than CTPO (Hariharan et al. 2013).

GC×GC TOF-MS data supported with combustion analysis corroborates that presence of high amount of polyaromatics, naphthalene's, benzene, and its derivatives in CTPO results in an abrupt rise in the heat release rate during premixed combustion and causes higher BTE in CTPO than StTPO. The diesel showed higher thermal efficiency of 32.50% among the fuel tested due to a higher calorific value than other tested fuel samples. Interestingly, the heat release rate is a predominant factor in the present study due to diversity in the chemical composition in CTPO and StTPO. Similar results of CTPO were found in literatures ( Murugan et al. 2008, Hariharan et al. 2013). BTE of CTPO<sub>xx</sub> blends is relatively higher than StTPO<sub>xx</sub> blends due to the higher carbon residues, moisture, and sulfur content.

In the present study, higher heat release rate of CTPO in the premixed combustion is the reason for increased thermal efficiency compared to StTPO. In CTPO, the presence of various classes of compounds such as aliphatic hydrocarbons, benzene derivatives (25.68%), polyaromatic hydrocarbon (27.79%), naphthalene (43.69%) scaled down after upgradation, which resulted in lower heat release after upgradation. Another reason is a reduction in the viscosity of upgraded tire pyrolysis oil (2.54 cSt) compared to CTPO (3.83 cSt), which exhibits an increase in the frictional power and reduces the brake power of the engine.

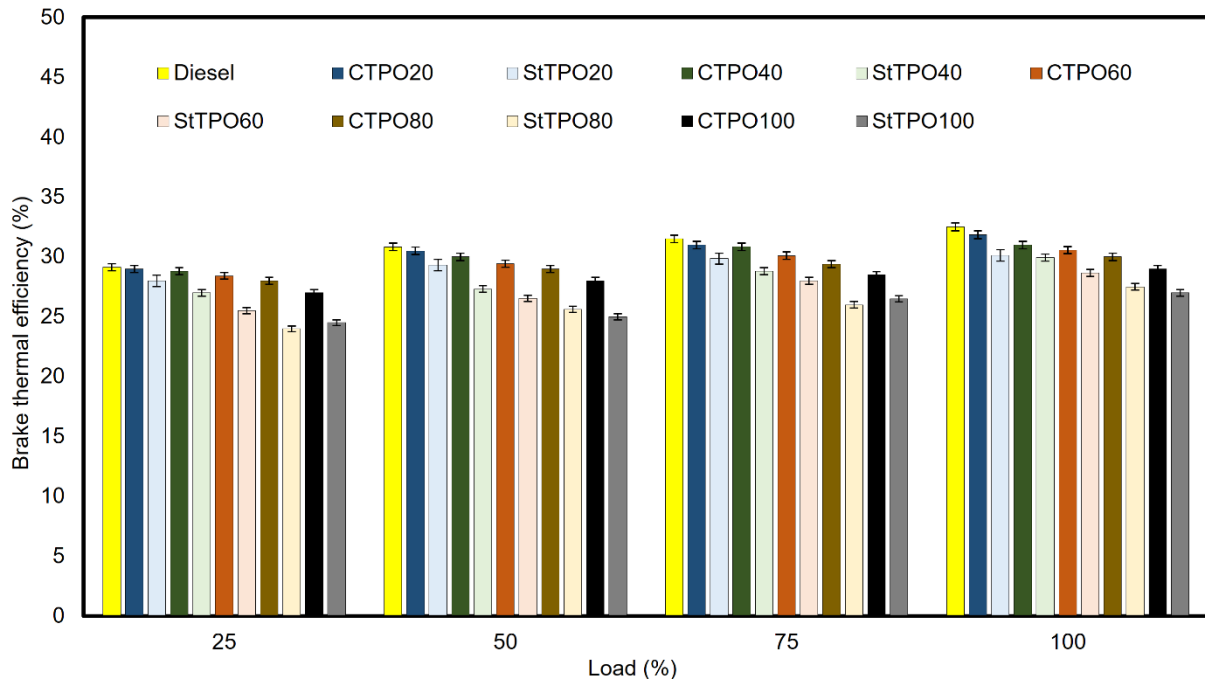


**Fig. 6.1 Variation of brake thermal efficiency of CTPOxx and StTPOxx with load**

### 6.2.2 Brake Specific Energy Consumption (BSEC)

BSEC is an important parameter used to find the amount of energy spent to produce unit power. BSEC is a reliable factor in accessing fuel consumption when fuels of different densities and calorific values are blended. BSEC is a product of brake specific fuel consumption and calorific value. Thus, a lower BSEC of fuel is better to maximize engine performance. The BSEC of CTPOxx and StTPOxx blends are portrayed in Fig. 6.2. BSEC decreases with an increase in load for all fuel samples. It can be seen that the BSEC of CTPOxx and StTPOxx are relatively higher than diesel due to the high density of tire oil samples. The BSEC of CTPOxx and StTPOxx are relatively higher than diesel due to higher density. The higher density of fuel blends form non-homogeneous mixture in the combustion chamber resulting in lower brake thermal efficiency and vice-versa. BSEC of CTPOxx and StTPOxx are relatively higher than diesel due to lower heat release from CTPOxx and StTPOxx (low calorific value) than diesel. In the present study, the dominating factor attributed to the variation in BSEC is the calorific value of the fuel blends.

Diesel shows lower energy consumption among the fuel tested due to its higher energy content with lower aromatics compared to CTPOxx and StTPOxx. Generally, crude oil extracted from scrap tire consume less fuel than diesel. The type and configuration of diesel engine played a significant role in reaching a common variation in BSEC with respect to load. The amount of

fuel needed to produce the same power output is higher, with an increase in the percentage of CTPO as per the conclusion of the study of CTPO (Murugan et al. 2008).

In the present investigation, the primary factor affecting BSEC is the calorific value of the fuel. Fuel with a higher energy density has the lowest brake-specific energy consumption. Verma and co-authors reviewed various factors such as production condition and reactor configuration that significantly affects engine performance and emissions of tire-derived fuels (Verma et al. 2018). BSEC mainly signifies the energy content of a typical fuel, which relates to the density and calorific value.

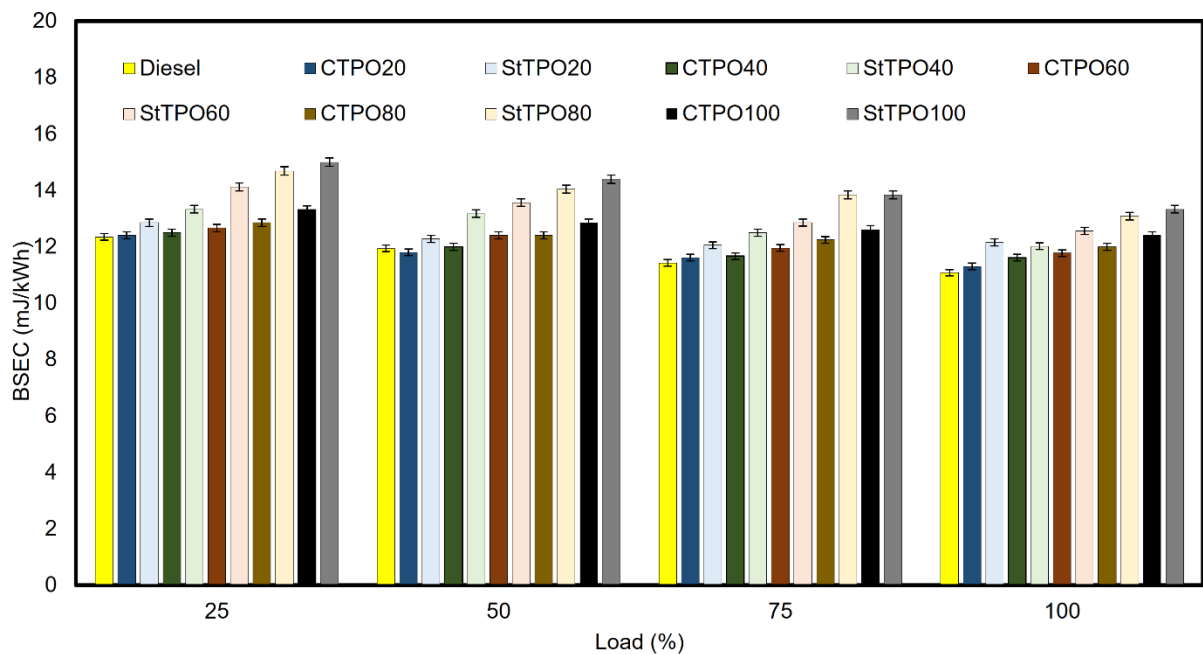


**Fig. 6.2 Variation of brake specific energy consumption of CTPOxx and StTPOxx with load**

### 6.3 Combustion analysis

#### 6.3.1 In-cylinder pressure

The in-cylinder pressure, mean gas temperature, net heat release, and pressure rise rate are the important parameters to characterize the combustion process of CTPO and StTPO in diesel engines. The variation of maximum cylinder pressure for CTPO, StTPO, is shown in Fig. 6.3. It can be observed that the peak pressure increases with an increase in load for all fuel blends. The maximum in-cylinder pressure of CTPO20, CTPO40, CTPO60, CTPO80 and CTPO100 are 43.19, 43.89, 45.48, 46.40, 47.4 bar respectively whereas the StTPO20, StTPO40, StTPO60, StTPO80 and StTPO100 are 42.5, 43.2, 44.50, 45.09, 46.38 bar respectively.

The cylinder pressure is increased from 32.17 bar to 47.14 bar in the case of CTPO100, 27.4 bar to 42.5 bar in the case of StTPO100, and 27 bar to 40.48 cases diesel, respectively. There is no significant variation in-cylinder pressure of CTPO and StTPO blends at lower loads than peak loads. However, the variation in the cylinder pressure is more pronounced at peak load. It can also evidence that the cylinder pressure of CTPO blends is much higher than StTPO and diesel due to more aromatic hydrocarbons. However, there is a significant reduction in the polyaromatics by silica gel used in the upgradation strategy. The significant factors affecting the peak pressure are ignition delay, amount of fuel combusted during the premixed combustion phase as per the study of CTPO in a single-cylinder diesel engine as per literature data (Murugan et al. 2008).

Crude tire pyrolysis oil (CTPO) consists of a multi-component mixture with a wide range of boiling compounds like an alkane, alkenes, aldehydes, ketones, carboxylic acids, etc. The high temperature inside the cylinder causes a sudden breakdown of unsaturated compounds with a higher molecular weight in CTPO compounds with lower molecular weight. These complex reactions induce a dense inner core with higher molecular weight and a gaseous phase formation on the periphery. Rapid gasification of volatile compounds in the periphery may ignite rapidly and cause a sudden rise in the cylinder pressure. Similar results were reported in the literature (Murugan et al. 2008).

The peak pressure is higher in CTPO than StTPO due to a wide range of boiling compounds in CTPO than StTPO. The silica gel used in the upgradation strategy adsorbs most of the high molecular weight compounds in CTPO resulted in lower cylinder pressure during engine operation. Another reason may be longer ignition delay, higher viscosity, and low cetane index of CTPO<sub>xx</sub> and StTPO<sub>xx</sub> than diesel. The fuel deposited on the cylinder walls during premixed combustion can also result in a steep rise in pressure and temperature during the premixed combustion phase.

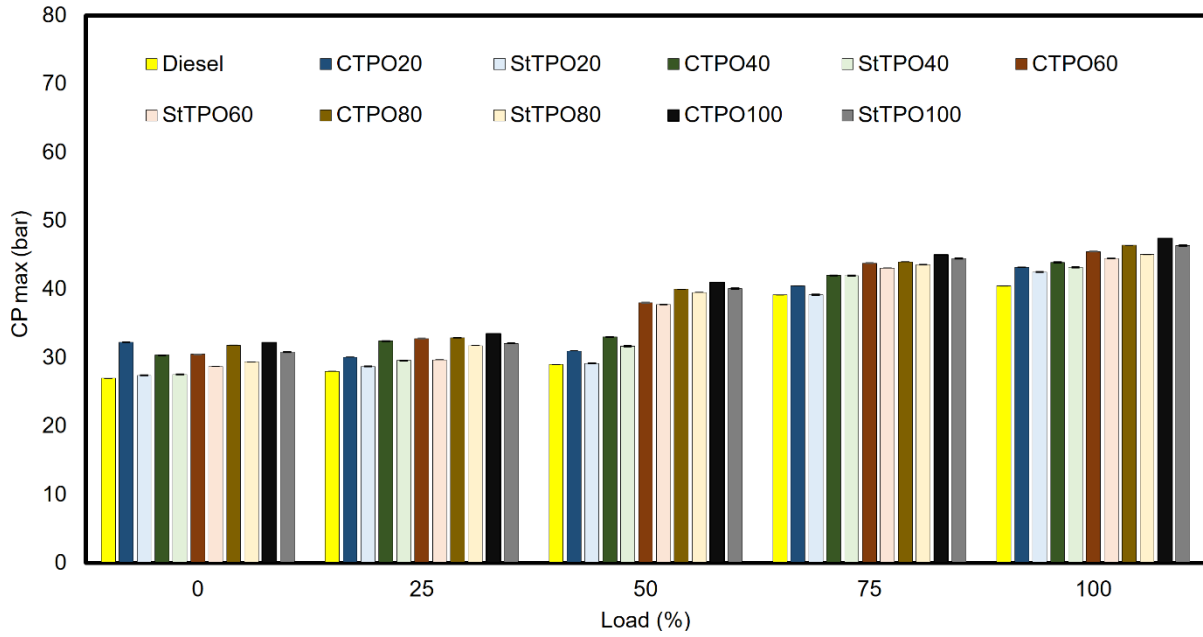


**Fig. 6.3 Variation of maximum in-cylinder pressure with load**

### 6.3.2 Net heat release rate

Net Heat Release rate (NHR) gives information about the premixed, controlled, and late combustion phases during combustion in the diesel engine. The net heat release function in-cylinder gas pressure can be derived using the first law of thermodynamics. The cylinder pressure data and crank angle value can be used to determine the NHR using the first law of thermodynamics as given in Eq. 6.1 and Eq. 6.2, where  $P$  is the in-cylinder gas pressure,  $V$  is instantaneous gas volume,  $\gamma$  is the specific heat of ideal gas, and is taken as 1.35 for the diesel engine.

$$\frac{dQ}{d\theta} = \text{Gross heat release} - \text{heat transfer to the walls} \quad (6.1)$$

$$\frac{dQ}{d\theta} = \frac{\gamma}{\gamma-1} P \times \frac{dV}{d\theta} + \frac{\gamma}{\gamma-1} V \times \frac{dP}{d\theta} \quad (\text{Krieger and Boreman single-zone model}) \quad (6.2)$$

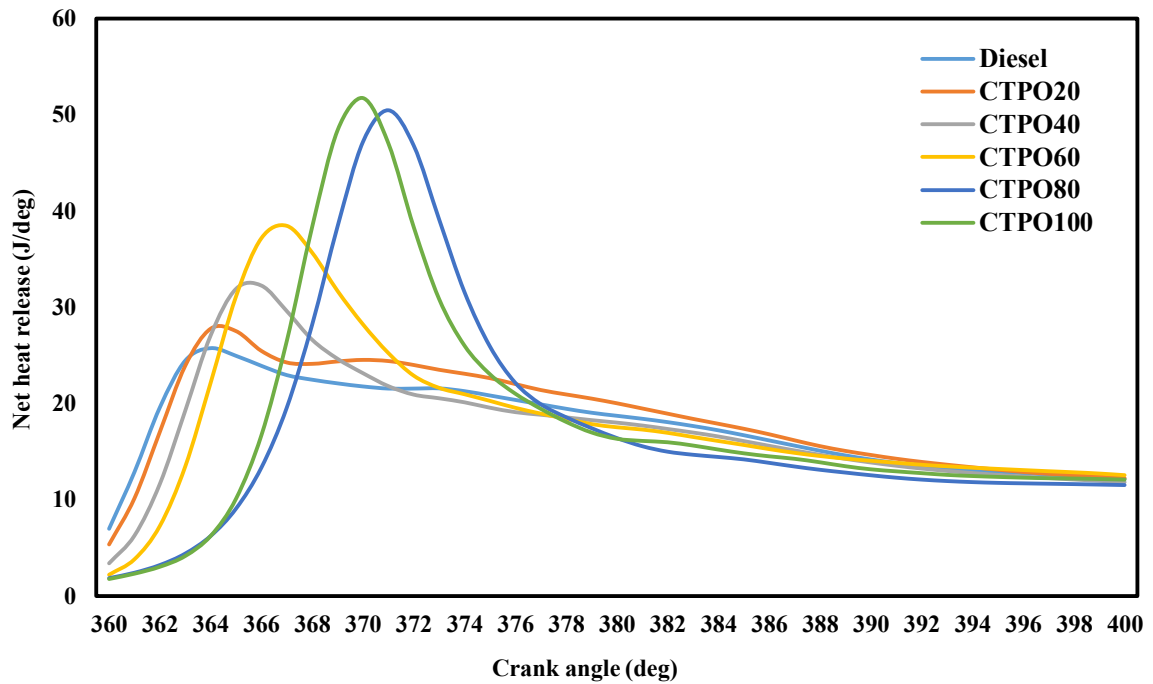


**Fig. 6.4 Variation of net heat release of CTPOxx blends with load**

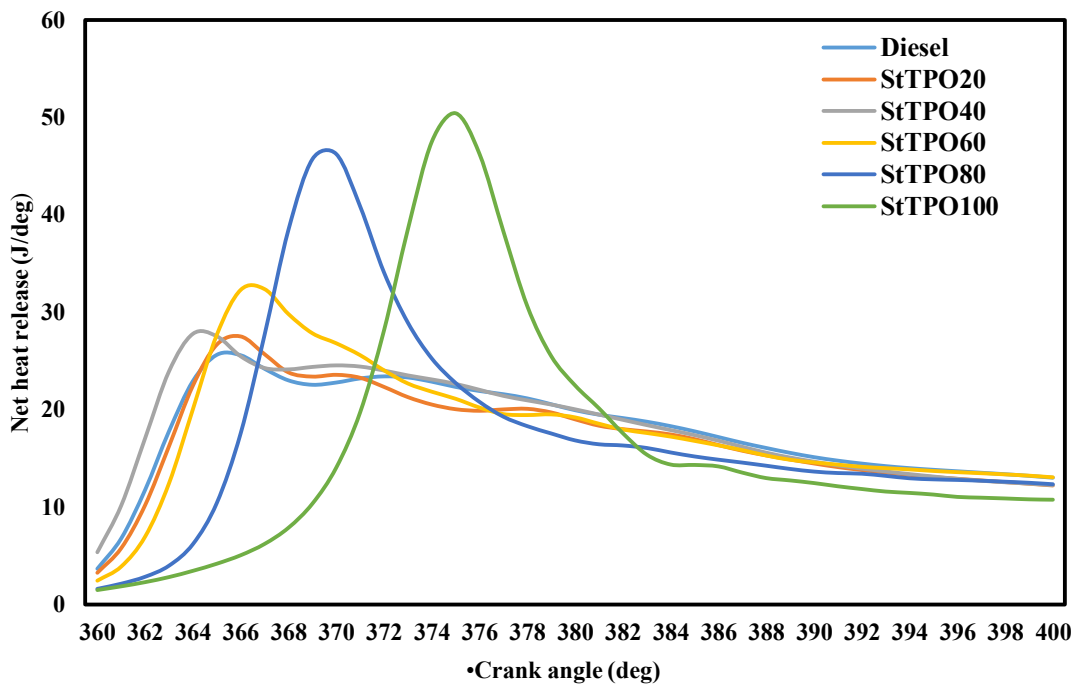


**Fig. 6.5 Variation of net heat release of StTPOxx blends with load**

The net heat release of diesel, CTPO20, CTPO40, CTPO60, CTPO80 and CTPO100 are 25.77 J/°CA, 27.79 J/°CA, 32.27 J/°CA, 38.48 J/°CA, 50.49 J/°CA and 51.76 J/°CA respectively are displayed in Fig. 6.4. Furthermore, the heat release of diesel, StTPO20, StTPO40, StTPO60, StTPO80 and StTPO100 are 25.77 J/°CA, 27.52 J/°CA, 27.79 J/°CA, 32.38 J/°CA, 46.25 J/°CA

and 50.43 J/°CA respectively are showed in Fig. 6.5. It can be inferred that the net heat release is found to be increased with higher blend ratio of StTPO and CTPO. The peak pressure data supported with the NHR curve corroborates that the higher ignition delay of CTPO and StTPO blends is due to aromatic hydrocarbons in CTPO and StTPO, which is supported with studies investigated by (Lheywood 2010, Kidoguchi et al. 2000).

The aromatic hydrocarbons in CTPO are responsible for higher heat release during combustion of fuels in the engine cylinder (Verma et al. 2018, Murugan et al. 2008, Pilusa et al. 2013). The aromatic compounds in higher blends of CTPO<sub>xx</sub> and StTPO<sub>xx</sub> are relatively higher than lower blends of CTPO<sub>xx</sub> and StTPO<sub>xx</sub> (Kidoguchi et al. 2000, Verma et al. 2008, Murugan et al. 2018). The bond dissociation energies of aromatic rings are relatively higher than straight-chain alkanes, which results in increased heat release in the case of higher blends of CTPO<sub>xx</sub> and StTPO<sub>xx</sub> (McMurry 2015). The aromatic hydrocarbons are relatively higher in the higher blend ratio (say CTPO100 and StTPO100) in comparison with (CTPO20 and StTPO20), which leads to the increased ignition delay and consequent higher premixed or uncontrolled combustion. Figure 6.4 and 6.5 show that the CTPO80, CTPO100, StTPO80 and StTPO100 have a very strong premixed mode of heat release compared to other blends.

Ring structured compounds in pyrolysis oil increase the adiabatic flame temperature and heat release rate in the cylinder chamber (Fig. 6.6). The longer delay period is the primary reason for the higher heat release rate and cylinder pressure (Kalargaris et al. 2017). The NHR curve for CTPO20, StTPO20, and diesel showed a similar trend because a large amount of diesel in StTPO20 dominates the combustion processes in cylinder. Another reason for the increase in NHR of pyrolysis oil blend are inherent oxygen coming during tire processing. Zinc oxide was conventionally added reagent into the rubber to reduce vulcanization time during the manufacture of tires.

The upgradation of CTPO caused a drastic reduction in the oxygenates from 7.01% to 2.93%, which reduces the NHR. Fig. 6.7 and Fig. 6.8 represents the rate of pressure rise of CTPO and StTPO blends with diesel. The variation in the rate of pressure rise and net heat release of CTPO and StTPO blends was higher than diesel. There is a gradual rise in the pressure variation inside the cylinder, increasing the blend ratio of CTPO<sub>xx</sub> and StTPO<sub>xx</sub> due to longer ignition delay. Due to the longer ignition delay of CTPO and StTPO blends, some quantity of fuel may be deposited in the surface of cylinder walls, which may result in a steeper rise in the pressure



perturbations at a higher blend ratio of CTPO and StTPO, which again supported with literature (Kumaravel et al. 2016).

### 6.3.3 Rate of pressure rise (RPR)

The rate of pressure rises in CTPO100 at full load results in unstable vibration of engine parts during the experimental investigations due to higher cylinder pressure and rate of pressure rise compared to other fuel blends. However, there are no such perturbations in-cylinder pressure was observed for upgraded oils. The maximum heat release of CTPO100, StTPO100, and diesel are 51.76 J/°CA at 372°CA, 50.43 J/°CA at 371 °CA, and 27.08 J/°CA at 365 °CA. It can be observed that the ignition delay lessens after the upgradation of CTPO due to an improvement in the cetane index. Thus, the ignition delay of CTPO100, StTPO100 is found to be longer than diesel by 7 °CA and 6 °CA, respectively. However, the ignition delay of lower CTPO and StTPO blend ratios (say, CTPO20 and StTPO20) are found to be matched with diesel fuel. Fig. 6.6 represents the benzene derivatives identified in CTPO by GC×GC TOF-MS

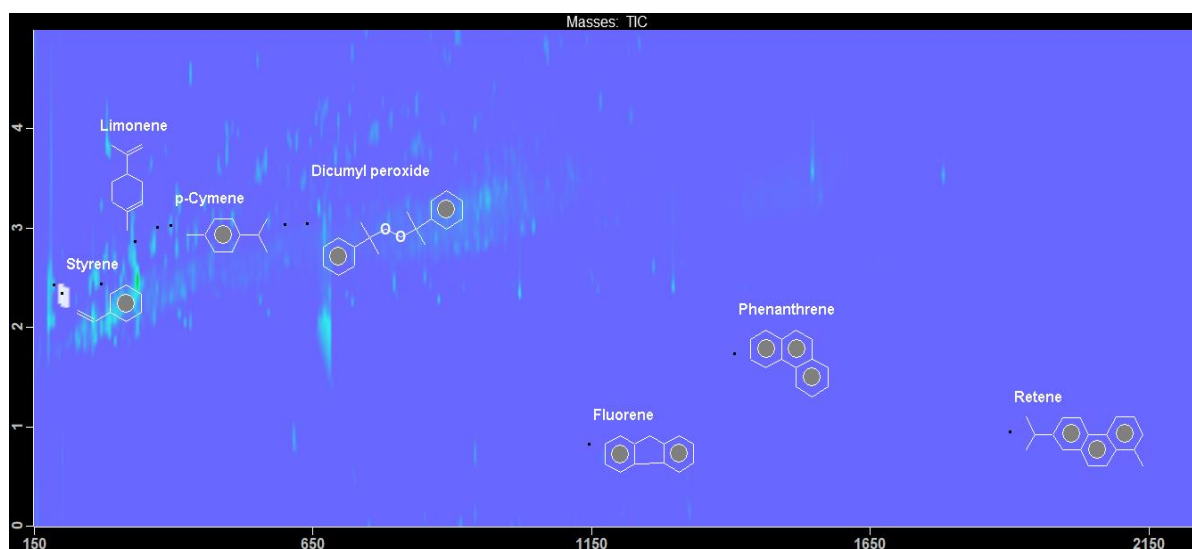


**Fig. 6.6 Selective benzene derivatives (ring type structures) identified in CTPO**

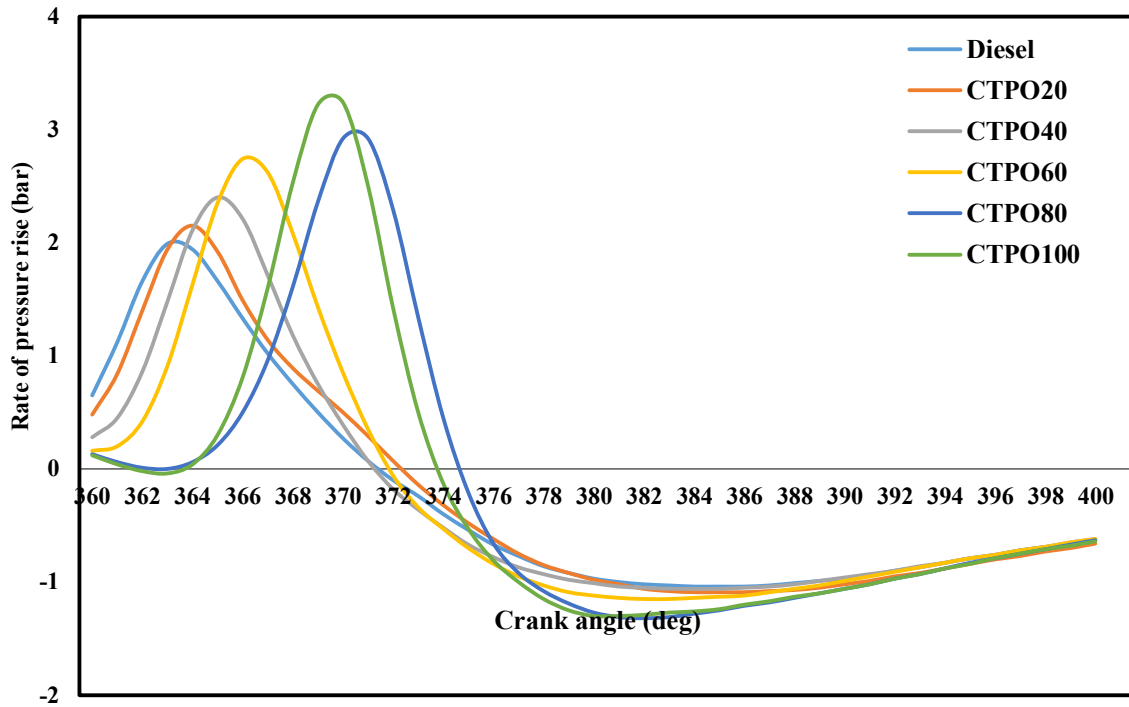


Fig. 6.7 Variation of the rate of pressure rise of CTPOxx blends with diesel

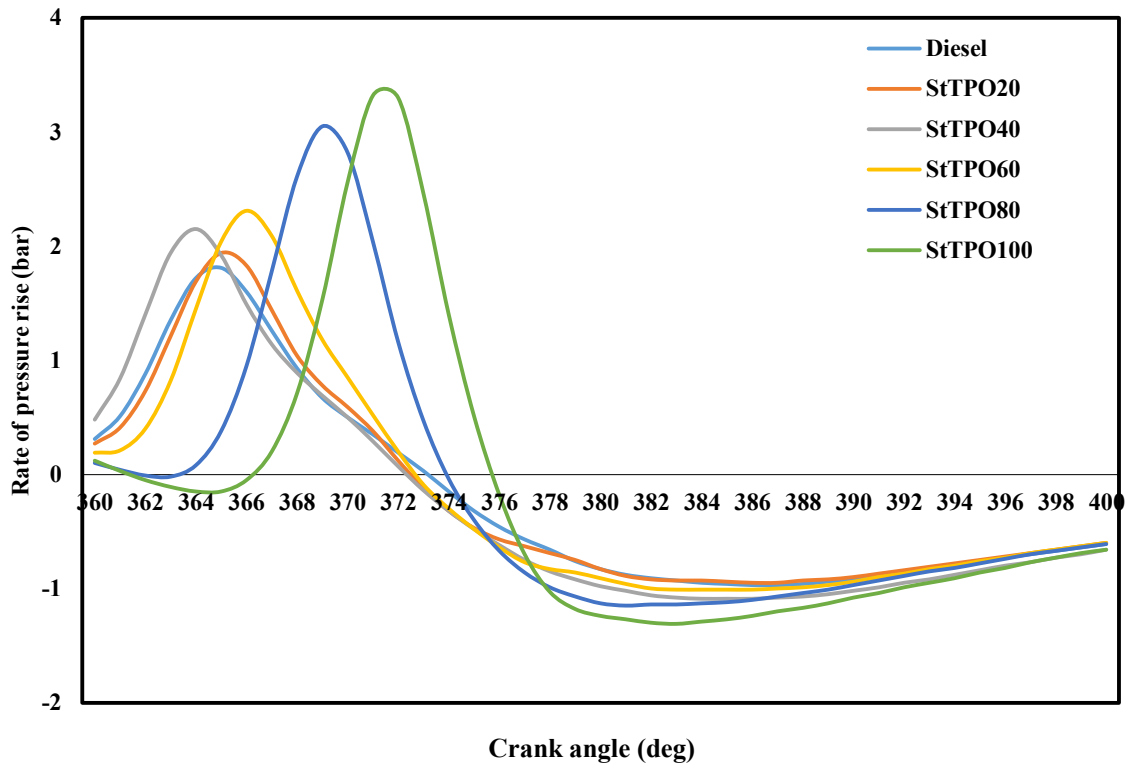


Fig. 6.8 Variation of the rate of pressure rise of StTPOxx blends with diesel

## 6.4 Emission characteristics

### 6.4.1 Nitrous oxide emissions

Nitrogen oxides (NO<sub>x</sub>) are formed due to the splitting of nitrogen molecule into nitrogen atoms, which then binds with oxygen molecules at high temperatures. The major factors which affect NO<sub>x</sub> formation are in-cylinder combustion temperature, fuel injection strategy, compression ratio, operating speed, and the physicochemical properties of fuel (Brunt et al. 1999, Ilkilic et al. 2011, Vihar et al. 2015, Uyumaz et al. 2019). There is no single explanation for the formation of nitrous oxide in a single-cylinder diesel engine, and further studies need to be conducted to investigate all other factors which affect the formation of NO<sub>x</sub> (Hossain et al. 2020). The NO<sub>x</sub> formation is favored at higher in-cylinder temperatures and high oxygen content of fuels (Ashok et al. 2019). The factors affecting nitrous oxide emissions from the tailpipe of diesel engines are air to fuel ratio, oxygen concentration, cylinder temperature, cetane index, nitrogen content, residence time, adiabatic flame temperature, injection timing, and ignition delay, etc. (Verma et al. 2018, Simsek et al. 2020). The fundamental mechanism behind the formation of NO<sub>x</sub> are thermal, prompt, and fuel bound nitrogen. The thermal NO<sub>x</sub> is categorized as the most dominant mechanism in engine combustion compared to others. Thermal NO<sub>x</sub> is formed by the oxidation of nitrogen at a temperature of 1427 °C and requires sufficient residence time for its formation. The formation of NO<sub>x</sub> in the combustion chamber of a single-cylinder diesel engine can be explained by the Zeldovich mechanism (Agarwal et al. 2004).



Fig. 6.9 portrays NO<sub>x</sub> emission variation from CTPO<sub>xx</sub> and StTPO<sub>xx</sub> from the engine's tailpipe before and after upgradation. It can be inferred that the NO<sub>x</sub> emissions are comparatively scaled-down after the upgradation strategy. The NO<sub>x</sub> emissions from CTPO20, CTPO40, CTPO60, CTPO80 and CTPO100 are recorded as 535, 605, 650, 700, 800 ppm respectively whereas the emission from StTPO20, StTPO40, StTPO60, StTPO80 and StTPO100 are found to be 338, 313, 260, 213 and 201 ppm respectively. Among all fuel blends, StTPO20 has the lowest NO<sub>x</sub>, and values increase as an increase in the concentration of CTPO and StTPO. Similar results for CTPO are reported in literature (Murugan et al. 2008). The NO<sub>x</sub> emission from fuel blends StTPO20 and StTPO40 was reduced by 38.54% and 43.09% due to

the batch scale upgradation process compared with diesel. However, the emission levels are slightly higher than the neat diesel. This tremendous drop in the amount of aromatic fraction after upgradation lowers the flame propagation speed inside the combustion chamber, evident from Fig. 6.7 and Fig. 6.8. Exhaust gas temperature is found to increase with the rise in load and is shown in Fig. 6.10.

The latent heat of upgraded oil evaporation is higher than CTPO (Murugan et al. 2008, Hossain et al., 2020). Frigo et al. (2014) reported that the reduction in cetane number of CTPO-DF blends lowers ignition delay with an increase in CTPO fraction. Thus, the combustion was confined in a larger volume with lower pressure and temperature results in lower nitrous oxide formation. In another study reported by (Ilkilic et al. 2015), the nitrogen oxides were lessened due to the low cetane number of tire-derived fuel, which delayed the combustion and caused a decrease in the in-cylinder temperature. The studies reported by (Tudu et al. 2016) said that lower peak pressure and in-cylinder temperature are reasons for low nitrous oxide formation from light fraction tire pyrolysis oil.

StTPO is a multi-component mixture consisting of aliphatic, aromatics, aldehydes, and carboxylic acid functionalities. In this present study, the compounds present in StTPO100 with broader boiling-point range compared to diesel reduces the in-cylinder temperature and pressure in the combustion chamber (Murugan et al. 2008). Nitrous oxide formation mainly depends upon the temperature inside the combustion chamber. Thus,  $\text{NO}_x$  and EGT in StTPO100 were found to be lower than diesel. Another reason behind the lower  $\text{NO}_x$  and EGT of StTPO100 is variation in StTPO and diesel cetane index. The lower cetane index of StTPO100 caused delayed combustion in the combustion chamber and decreased in-cylinder temperature and pressure (Arya et al. 2020). Thus, the combustion in a larger volume, low pressure and temperature lead to lower nitrous oxide formation (Frigo et al. 2014).

In the present research study, the low cetane index (40) and higher density (0.8682 g/mL) of StTPO than diesel causes inferior combustion and higher heat of vaporization occurred inside the engine cylinder, which reduces the pressure and temperature, leading to lower nitrous oxide formation. Similar reasons for light fraction tire pyrolysis oil were reported in literatures (Verma et al. 2018, Tudu et al. 2017, and Koc et al. 2014). Other reasons are due to the presence of oxygen-containing compounds in tire-derived oil such as CaO, ZnO, TiO, stearic acid, CuO, and antioxidants (oxygen-containing additives) added during tire production, which imparts a cooling effect in the combustion chamber and reduces the in-cylinder temperature and low

nitrous oxide formation. The major additives added during tire production are detailed in Table 6.1.

**Table 6.1 Additives and their functions during tire production (Jain et al. 2016)**

S. No.	Additives	Functions
1.	CaO	Improves strength and durability
2.	ZnO, TiO	Accelerates vulcanization process
3.	CuO	Bonding agent
4.	ZnO, Stearic acid	Aids vulcanization and enhances physical property
5.	Antioxidants	Prevent deterioration of rubber complexes

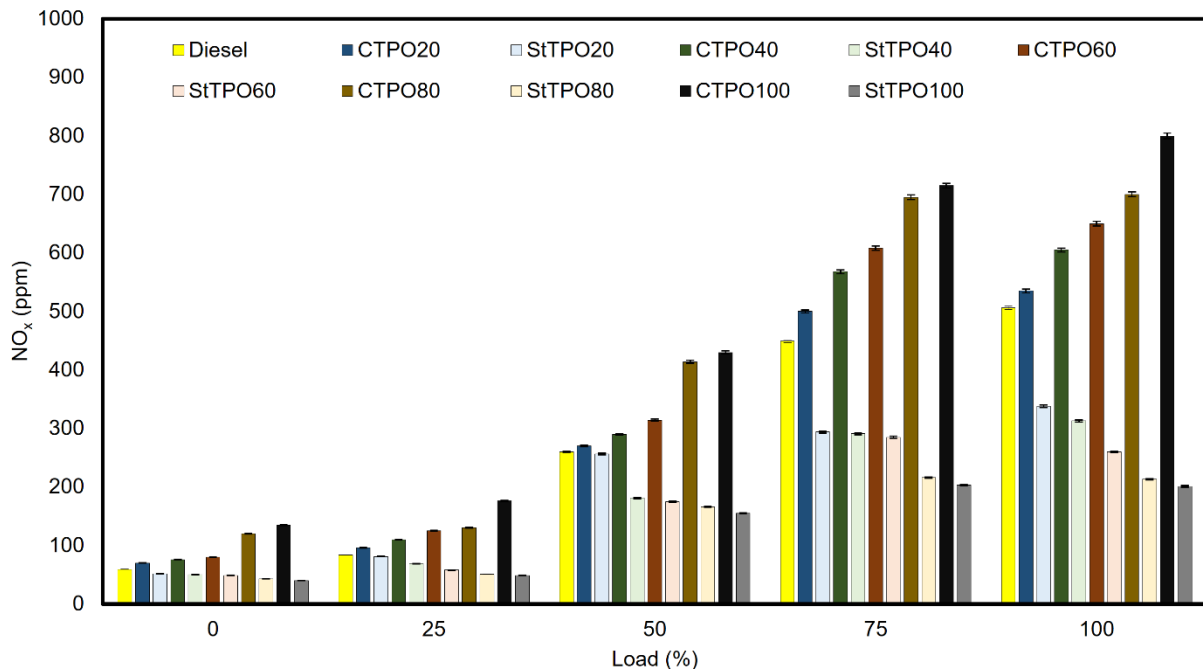


**Fig. 6.9 Variation of nitrous oxide emission of CTPO<sub>xx</sub> and StTPO<sub>xx</sub> with load**

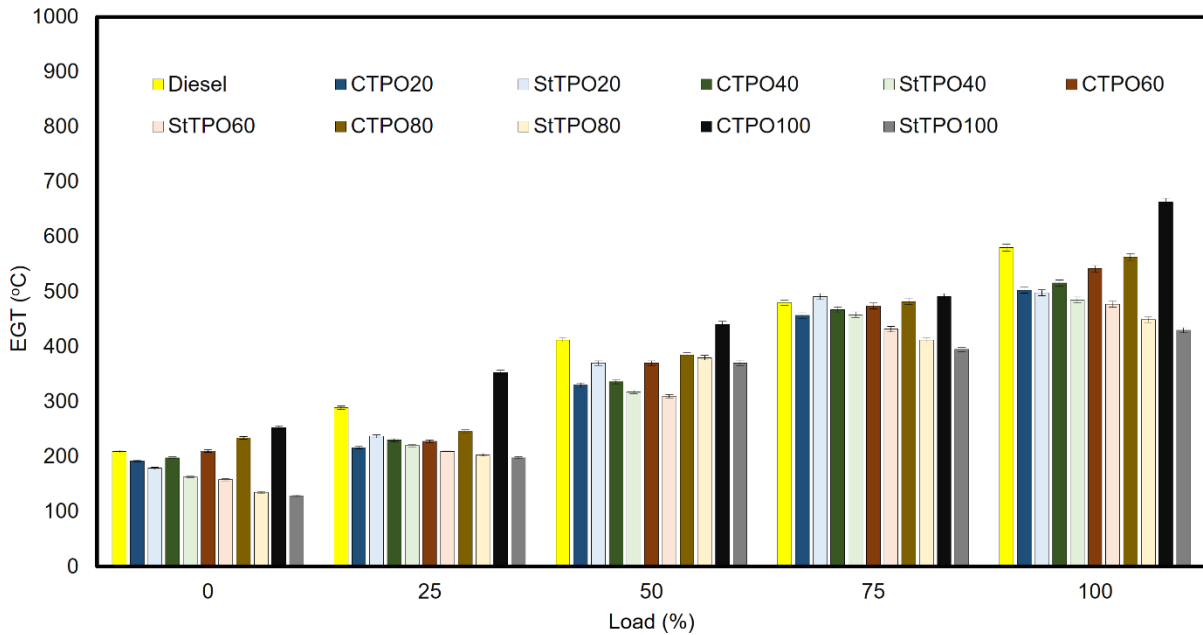


**Fig. 6.10 Variation of exhaust gas temperature of CTPOxx and StTPOxx with load**

#### 6.4.2 Carbon monoxide emissions

Carbon monoxide emissions are formed due to incomplete combustion of carbon and oxygen atoms inside the combustion chamber, which results in the formation of deposits on the surface of piston and cylinder surfaces. The prominent factors that affect the formation of incomplete combustion are high viscosity of fuel blends, retardation in ignition timing, the high carbon content in fuel, air to fuel ratio of fuel, air-fuel density, fuel bound oxygen, etc. (Verma et al. 2018). Fig. 6.11 shows carbon monoxide variation with engine load from 0 to 100% for various fuel blends. It can be seen that carbon monoxide emissions are increased gradually with an increase in CTPO and StTPO. The CO emissions from CTPO20, CTPO40, CTPO60, CTPO80 and CTPO100 are 0.55, 0.78, 0.88, 0.98, and 1% respectively but the CO emissions from StTPO20, StTPO40, StTPO60, StTPO80 and StTPO100 are recorded as 0.35, 0.45, 0.59, 0.69 and 0.7%.

With an increase in the ratio of CTPO and StTPO in fuel blend, there is a dramatic rise in the carbon monoxide emissions from engines comparable with diesel (0.3%). Similar results of CTPO were reported elsewhere (Wamankar et al. 2014, Murugan et al. 2008, Tudu et al. 2016). Among the tested fuel blends, the carbon monoxide emissions from StTPO20 are the lowest (0.35%) compared with neat diesel. The carbon monoxide emission from StTPO20 reduces by 36.36% in comparison with CTPO20. However, the emission levels are slightly higher than diesel (0.30%) for a higher blend's ratio of StTPOxx and CTPOxx (1% for CTPO100 and 0.7% for StTPO100). Due to the high amount of CTPO and StTPO blends, the lower air to fuel ratio

(high density and higher viscosity in the case of CTPO) inside the combustion chamber leads to leaner formations fraction inside the combustion chamber (Ilkiliç et al. 2011). Due to the leaner mixture formation, some fuel may not propagate to the fuel mixtures near cylinder walls and crevices, resulting in incomplete combustion resulting in soot-like deposits (Murugan et al. 2008). The carbon monoxide emission was reduced after upgradation due to low viscosity and high volatility of StTPO-DF blends compared with CTPO-DF blends. Similar reasons were reported in literature (Murugan et al. 2008).

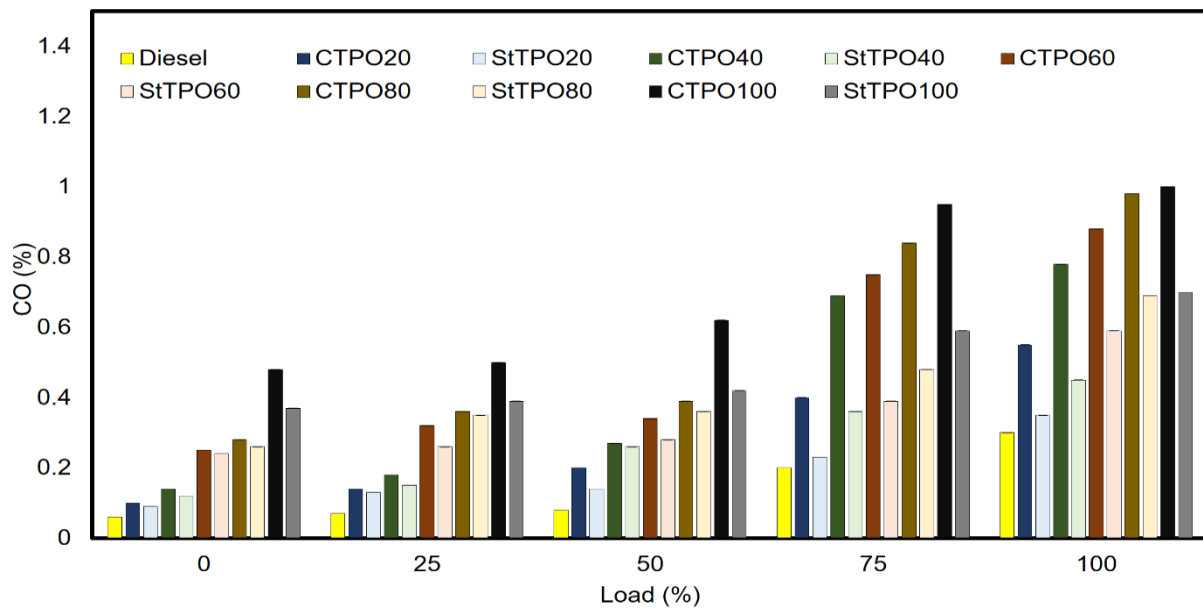


**Fig. 6.11 Variation of carbon monoxide emissions of CTPO<sub>xx</sub> and StTPO<sub>xx</sub> with load**

### 6.4.3 Carbon dioxide emissions

Carbon dioxide emissions indicate the oxidation tendency of carbon atoms in fuel blends insufficient oxygen quantity inside the combustion chamber. The significant factors affecting carbon dioxide emissions are air to fuel ratio, oxygen content, carbon content, density, viscosity, etc. Fig. 6.12 represents the carbon dioxide variation of various fuel blends for the different loads. It can be noted that the carbon dioxide emissions from the tailpipe of the engine gradually rise to load variation from low to peak load. Diesel has the highest carbon dioxide emission from the fuel tested due to its low density than other fuel blends. The lowest carbon dioxide emission from CTPO100 is due to the higher density of CTPO compared to different fuel blends. The higher density of fuel causes more fuel consumption on a mass basis from the fuel injector, which results in lower air to fuel ratio, resulting in less CO<sub>2</sub> production (Verma et al. 2018). A similar trend of CO<sub>2</sub> from CTPO was reported in literatures (Uyumaz et al. 2019, Tudu et al. 2016, Verma et al. 2018).

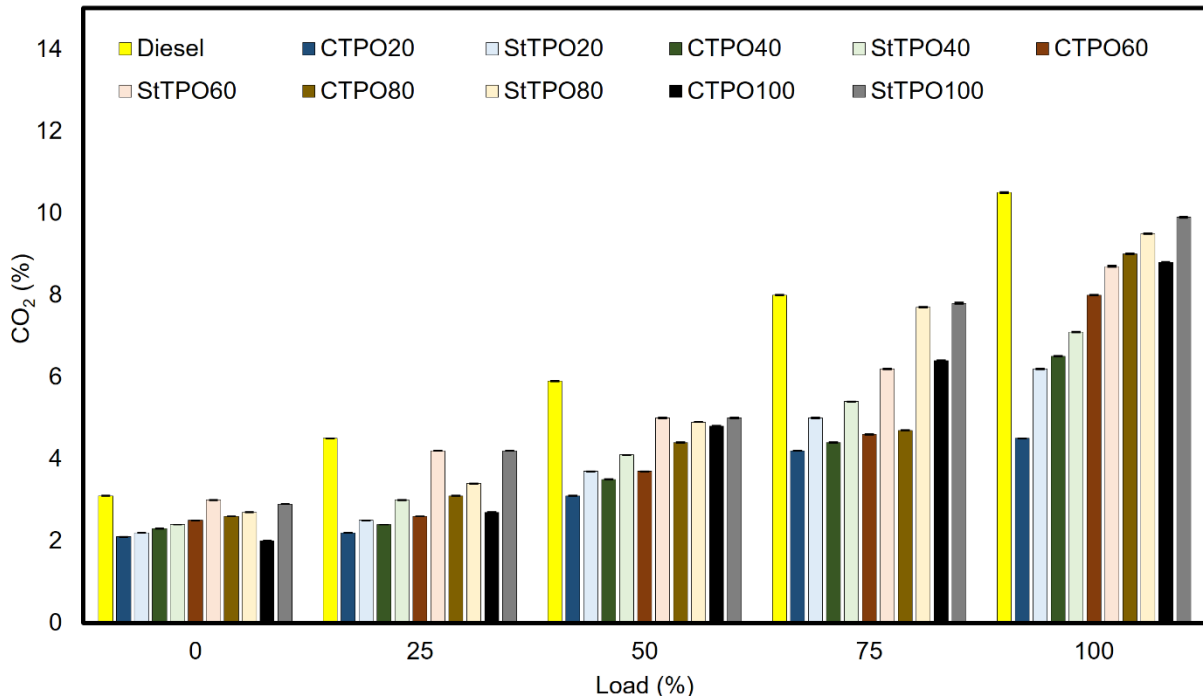


**Fig. 6.12 Variation of carbon dioxide emissions of CTPOxx and StTPOxx with load**

#### 6.4.4 Unburned hydrocarbon emissions (UBHC)

UBHC is formed due to the incomplete combustion of fuel molecules inside the combustion chamber. Literature about studies on the application of waste tire-derived oils in engine showed that volatility, viscosity, cetane index, availability of oxygen, sulfur content, air to fuel ratio are some of the factors leads to the formation of hydrocarbons (Tudu et al. 2016, Verma et al. 2018, Murugan et al. 2008, Wamankar et al. 2014). Fig. 6.13 displays the variation of hydrocarbon emission with the load. It has been noticed that the concentration of hydrocarbons decreases with the engine load varies from 0 to 100% load (Odaka et al. 1991, Wamankar et al. 2014). Murugan et al. (2008) argued that the presence of unsaturated hydrocarbons (alkenes, alkyne fractions) is the reason for the drastic rise in unburned hydrocarbons from CTPO and distilled TPO blends.

High hydrocarbons for CTPO are due to the high viscosity, density, and presence of polyaromatic hydrocarbons (Kumaravel et al. 2016). In contrast to general findings reported in the literature on CTPO by Frigo et al. 2014, the lower viscosity of CTPO than diesel results in better combustion inside the cylinder due to the presence of aliphatic and aromatic hydrocarbons, which aids in better atomization of fuel molecules. Karagoz et al. (2020) proposed that the addition of tire pyrolysis oil reduced the hydrocarbon emission at all loads due to the increase in viscosity and volatility of test fuels. This ensures the uniform mixing of



air-fuel mixture and lowers hydrocarbon emissions. The hydrocarbon content is found to be reduced as an increase in CTPO due to high hydrogen content.

Among the fuel tested, the hydrocarbon emission from upgraded tire pyrolysis oil is significantly lowered by the refinement of CTPO by silica gel and petroleum ether. For example, the release of hydrocarbons from StTPO40 was reduced by 10% compared to CTPO20, but emissions from StTPOxx blends are slightly greater than diesel. During the production of tires, aromatic oils are enriched with compounds like chrysene, retene, chamazulene, benzopyrene, benzoanthracene, benzofluoranthene, dibenzo anthracene, and naphthalene were added to the raw tire, which acts as a cushion between the molecular chains of rubber to improve its lubricity. These polycyclic aromatic hydrocarbons (PAHs) are relatively higher in CTPO than StTPO and diesel. These PAH's are partially downstream during the combustion process inside the cylinder, resulting in more volatile hydrocarbons at the cylinder's centre. The crevice volume is left unburned, which develops a non-homogeneous air-fuel mixture inside the cylinder leads to the formation of UBHC.

In the case of upgraded tire pyrolysis oil, the viscosity is found to be lower than diesel. Although the fuel-air mixture burns completely, the presence of unsaturated hydrocarbons leads to higher emissions in CTPO. Still, in the case of upgraded tire pyrolysis oil, the hydrocarbon emissions are found to be lowered due to the reduction in polyaromatic hydrocarbon fractions (27.79 %) than CTPO. Similar results of CTPO were reported in literatures (Murugan et al. 2008, Verma et al. 2018, and Kumaravel et al. 2016).

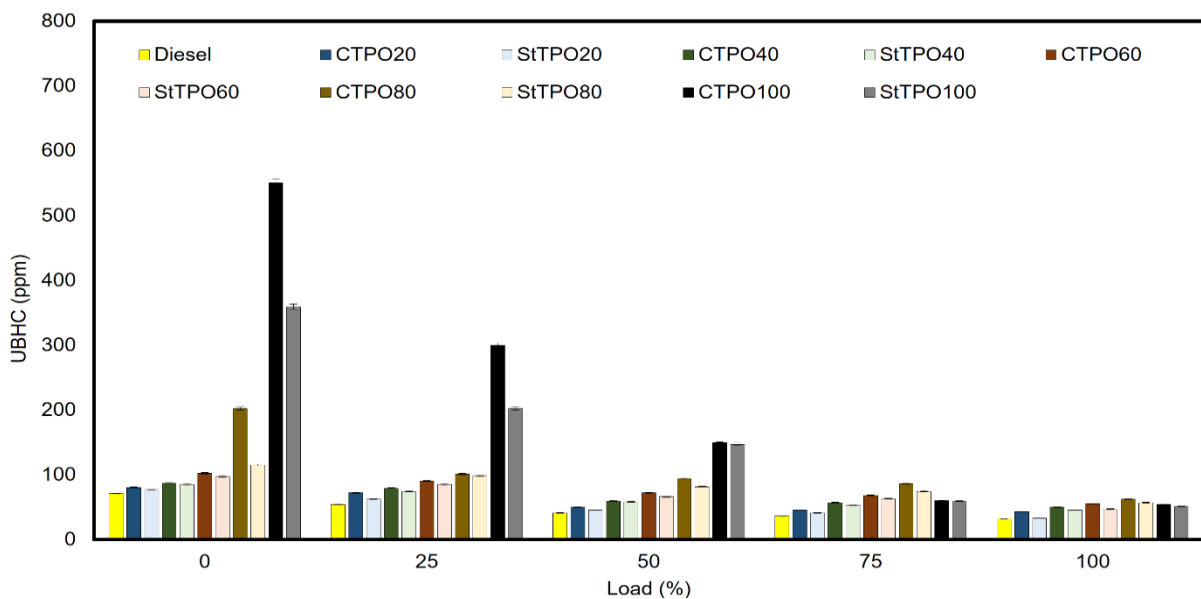


**Fig. 6.13 Variation of unburned hydrocarbons of CTPOxx and StTPOxx with load**

## 6.5 Conclusions

The present chapter focused on the effect of StTPO on combustion, performance, and emission from a direct-injected single-cylinder diesel engine. The most significant conclusions obtained from the research study are presented as follows.

1. The addition of upgraded tire pyrolysis oil into diesel significantly changed the fuel's physical and chemical properties.
2. StTPO40 is an optimum blend in terms of better performance, combustion, and emissions than diesel.
3. The brake thermal efficiency of StTPO40 at full load (26.76%) is found to be comparable with CTPO40 (27.50%) diesel but slightly lesser than diesel (32.50%).
4. With an increment in TPO in diesel, heat release from CTPO and StTPO blends is higher than diesel due to the high number of aromatics, benzene derivatives, and naphthalene.
5. Hydrocarbon emission from StTPO40 is lowered by 10% than CTPO40 and seems similar to diesel.
6. Ignition delay of CTPO40 is longer than StTPO40 by 1°CA
7. NO<sub>x</sub> emission from StTPO20 and StTPO40 is lowered by 38.54% and 43.09% than diesel.
8. CO emissions are higher in StTPO20 and StTPO40 than diesel.
9. It can be concluded that the upgraded tire pyrolysis oil can be utilized as a fuel in a single-cylinder diesel engine as a partial substitute with diesel fuel. Besides, the usage of StTPO in diesel engines seems significant in terms of "waste management" and "waste to energy concepts."

The upgraded crude tire pyrolysis oil (StTPO) and its blends with diesel were successfully utilized in a single-cylinder diesel engine to study the performance, emission and combustion characteristics and compared with CTPO. The studies corroborate that the upgraded tire pyrolysis oil-diesel blends showed superior performance, combustion and emissions than CTPO due to the diesel-range properties of StTPO. However, the net heat release, unburnt hydrocarbons and carbon monoxides are relatively higher than diesel due to the aromatic fractions in upgraded oil. To improve the combustion quality and emission to a maximum extent, a novel biomass-derived fuel additive needs to be found out.

## CHAPTER 7

### EXPERIMENTAL STUDY ON EFFECT OF ETHYL LEVULINATE ON SINGLE CYLINDER DIESEL ENGINE FUELLED WITH UPGRADED TIRE PYROLYSIS OIL-DIESEL TERNARY BLENDS

#### 7.1 Introduction

This chapter highlights using an ethyl levulinate (biomass-derived fuel additive) to reduce the nitrous oxide emission, oxides of carbon and unburnt hydrocarbons from single-cylinder diesel engines. The specific reason for the selection of ethyl levulinate as an additive in the presence of a high amount of oxygenates. The present investigation evaluates the effect of ethyl levulinate as a bio-diluent in a single-cylinder diesel engine fuelled with StTPOxx blends to study the performance, combustion, and emission characteristics. The various fuel blends were prepared on a volumetric basis by blending various StTPO and diesel percentages by adding 10% ethyl levulinate. Fuel blends are named StTPOxxEL10, where xx denotes the percentage of upgraded tire pyrolysis oil in the ternary mixture and the remaining is diesel. The prepared fuel blends were named as diesel, StTPO20EL10, StTPO40EL10, StTPO60EL10, StTPO80EL10, StTPO90EL10, StTPO100 and CTPO100.

#### 7.2 Fuel properties of StTPOxxEL10 blends

Few literatures are available on the study of ethyl levulinate as an additive to study the performance, combustion and emission characteristics in the single-cylinder diesel engine. To the best of our knowledge, no reviews were reported on the effect of ethyl levulinate as a bio-diluent in StTPOxx blends. The various ternary fuel blends were prepared by the blending of StTPO, EL, and diesel using a lab-scale stirrer at a rotational speed of 500 rpm for 1h. The prepared blends were stored in a separate glass beaker to study the phase separation through a six-month visual inspection technique. It has been noticed that there was no phase separation was observed in the stored glass containers. The prepared fuel blends properties are determined as per ASTM standards, and the tested fuel properties are detailed in Table 7.1. It can be evident that density and viscosity of fuel blends decrease with 10% EL into the StTPO. However, there is a significant reduction in gross calorific value and cetane index with EL in StTPO. Furthermore, the flashpoint of StTPOxxEL10 was found to be increased with the addition of 10%EL. The pour point (PP) of StTPO was found to be -50 °C, whereas the PP of StTPOEL10 marginally increased to -45 °C. This observation is in line with literature data (Unlu et al. 2018)

where the addition of EL increases the PP to a small extent, possibly due to the higher melting point (ca. 25 °C) of EL. However, the cold-flow properties are not only determined by pour point (PP) but also other parameters such as cloud point (CP) are equally important. The cloud point of EL-blended fuels is generally improved due to better miscibility of EL with various fuel components (Joshi et al. 2011). The solubility of ethyl levulinate in diesel is a major technical constraint regarding the commercialization of EL as an additive in deployment at a larger scale. However, the EL in StTPO showed better miscibility without any separation due to more polar fractions (mostly oxygenates and alcohol) in StTPO than diesel. Fig. 7.1 shows the cleanliness and compatibility studies of StTPOxxEL10 blends.

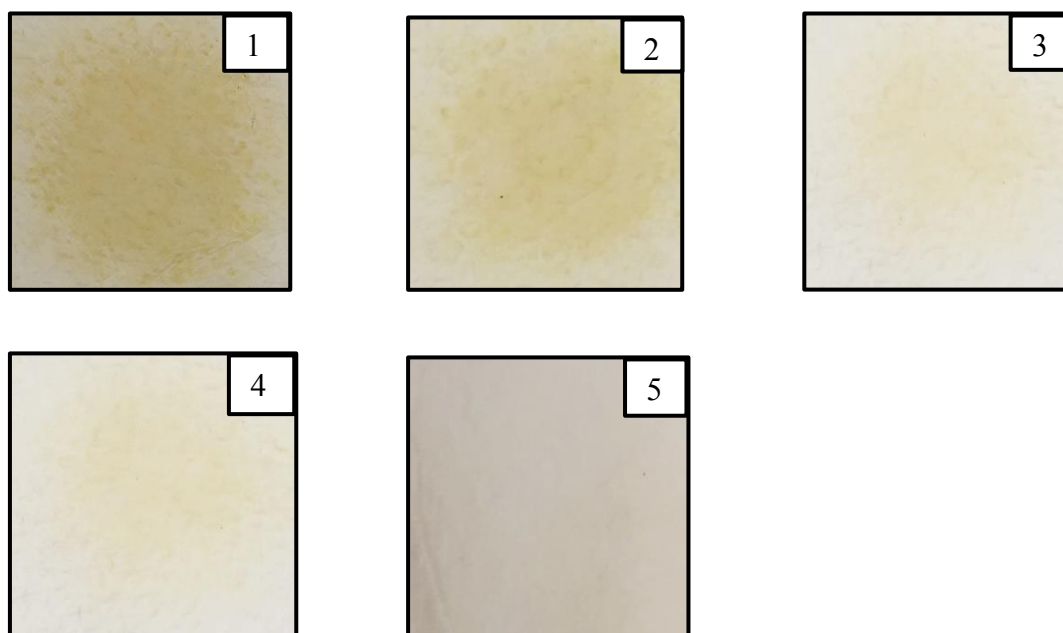


**Fig. 7.1 Cleanliness and compatibility studies of StTPOxxEL10 ternary blends by spot test (1-StTPO20EL10, 2-StTPO40EL10, StTPO60EL10, StTPO80EL10, StTPO90EL10)**

**Table 7.1 Physical properties of StTPOxxEL10 ternary fuel blends**

Fuel blends	Density (g/m <sup>3</sup> )	Flashpoint (°C)	Kinematic viscosity (cSt)	GCV (MJ/kg)	CCI
StTPO20EL10	0.8353	62	2.33	40.595	39.80
StTPO40EL10	0.8541	60	2.45	39.778	37.59
StTPO60EL10	0.8749	59	2.51	37.965	32.72

StTPO80EL10	0.8809	50	2.61	37.530	28.65
StTPO90EL10	0.8909	44	2.63	37.095	24.50
StTPO100	0.8682 <sup>#</sup>	40 <sup>#</sup>	2.54 <sup>#</sup>	41.760 <sup>#</sup>	40.00 <sup>#</sup>
CTPO100	0.907 <sup>#</sup>	32 <sup>#</sup>	3.83 <sup>#</sup>	42.980 <sup>#</sup>	33.00 <sup>#</sup>
Diesel	0.830 <sup>*</sup>	50 <sup>*</sup>	2-4 <sup>*</sup>	43.800 <sup>*</sup>	50 <sup>*</sup>

<sup>#</sup>Mohan et al. (2019), <sup>\*</sup>Tudu et al. (2016)

### 7.3 Performance characteristics

#### 7.3.1 Variation of BTE with load

The brake thermal efficiency of diesel, StTPO20EL10, StTPO40EL10, StTPO60EL10, StTPO80EL10, StTPO90EL10, StTPO100 and CTPO100 are found to be 32.5%, 29%, 28.10%, 27.10%, 26.76%, 26.50%, 27%, 29% respectively. Fig. 7.2 shows the variation of brake thermal efficiency with engine load. The average decrease in brake thermal efficiency in comparison with diesel for StTPO20EL10, StTPO40EL10, StTPO60EL10, StTPO80EL10, StTPO90EL10, StTPO100 and CTPO100 are 0.10%, 0.13%, 0.16%, 0.17%, 0.18%, 0.16%, and 0.10%. Brake thermal efficiency of CTPO40, StTPO40 and StTPO40EL10 is found to be 31.00%, 29.95% and 28.10% respectively. BTE showed a reduction in performance by upgradation and addition of EL as an additive.

It can be seen that the addition of 10% EL in StTPO results in a reduction in brake thermal efficiency, which can be ascribed due to the lower heating value of ethyl levulinate. Lower heating value consumes more fuel during engine combustion. Higher latent heat of evaporation induces a cooling effect inside the combustion chamber, which results in a lower heat release rate. Among the fuel tested, diesel consumes less fuel. Similar reasons were found in literature, where they utilized higher alcohol as a fuel additive in compression ignition engines. Similar concepts were reported in literatures (Atmanli et al. 2018, Yilmaz et al. 2017, Kumar et al. 2015). Brake specific energy consumption is the most reliable parameter to access fuel consumption when two different fuels with different densities and calorific values are blended (Lei et al. 2016). The variation of brake specific energy consumption (BSEC) with load is shown in Fig. 7.3. BSEC was calculated based on the specific fuel consumption and lower heating value of the fuel for all fuel blends. The average decrease in BSEC compared to diesel were 2 mJ/kWh, 4 mJ/kWh, 6.9 mJ/kWh, 8.31 mJ/kWh and 10.11 mJ/kWh for StTPO20EL10, StTPO40EL10, StTPO60EL10, StTPO80EL10 and StTPO90EL10. It can be noticed that the increase in BSEC with the addition of 10%EL in StTPO due to a lower heating value of EL

(24 MJ/kg) than StTPO100 (41.76 MJ/kg) and diesel (43.80 MJ/kg). Similar findings were reported in literatures (Hayes et al. 2008, Wang et al. 2012).

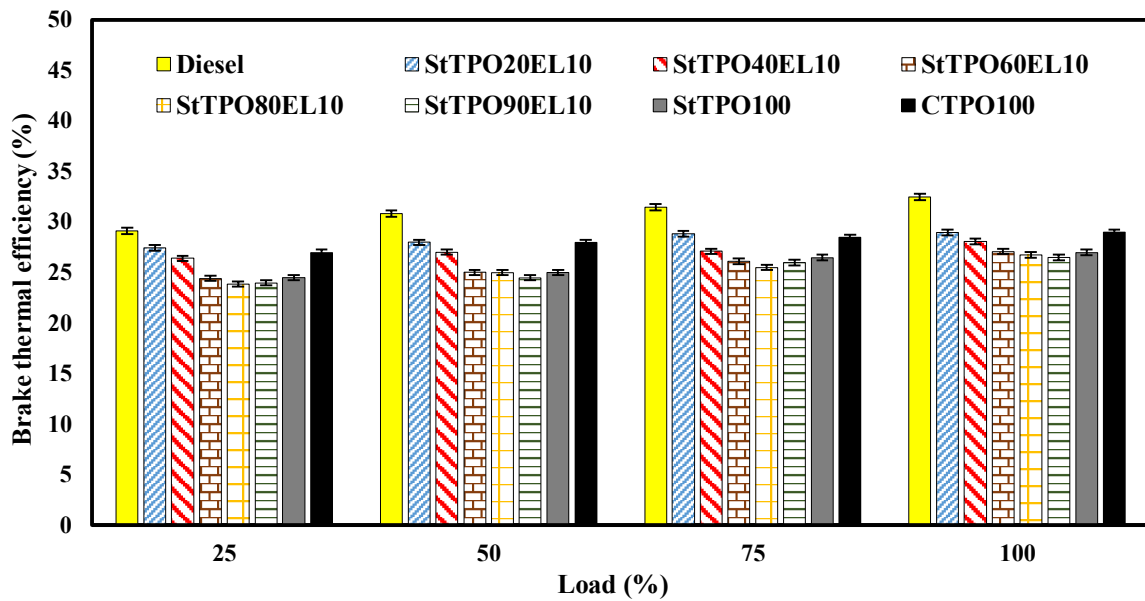


Fig. 7.2 Variation of brake thermal efficiency with load

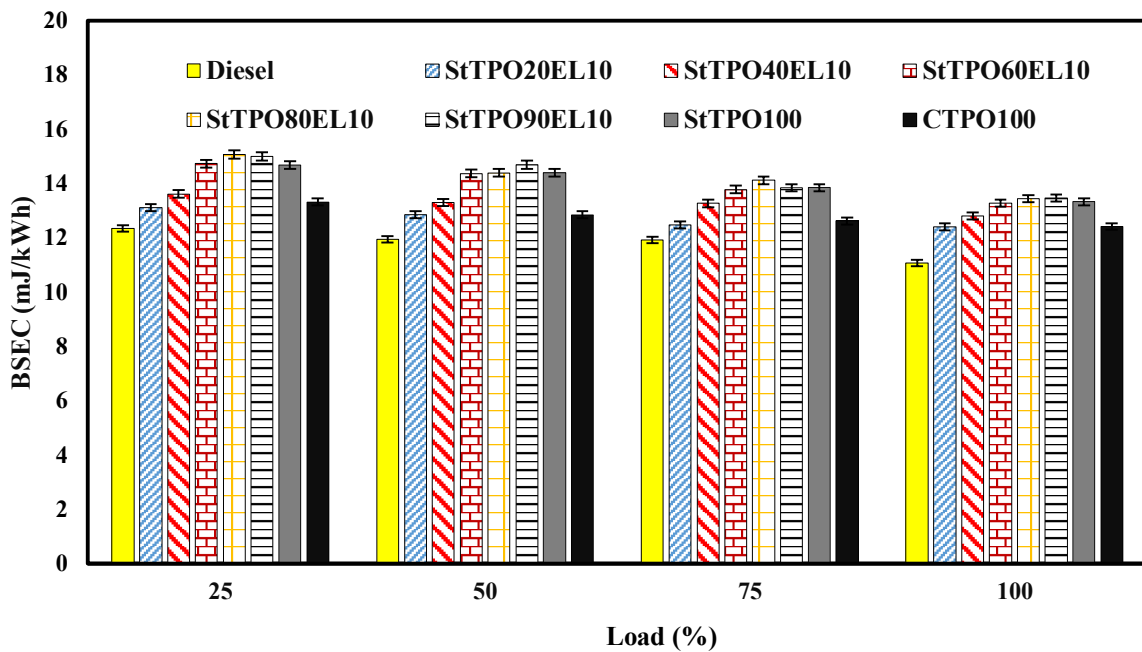


Fig. 7.3 Variation of brake energy fuel consumption with load

## 7.4 Combustion characteristics

### 7.4.1 Variation of in-cylinder pressure with load

The maximum in-cylinder pressure in compression ignition engines gives valuable information regarding the ignition delay, fuel mixture preparation, and combustion rate at initial

combustion stages, reported by Hariharan et al. (2013). The maximum in-cylinder pressure for StTPO20EL10, StTPO40EL10, StTPO60EL10, StTPO80EL10, StTPO90EL10, StTPO100, CTPO100 and diesel is recorded as 41 bar at 374 °CA, 41.87 at 374 °CA, 42.33 at 375 °CA, 43.05 at 375 °CA, 44.28 at 377 °CA, 46.38 at 378 °CA, 47.4 at 377 °CA and 40.48 at 374 °CA (Fig. 7.4). The in-cylinder pressure of CTPO40, StTPO40 and StTPO40EL10 is reported by 43.89 bar, 43.20 bar and 41.87 bar, respectively. The cylinder pressure was lowered after the upgradation and addition of EL as an additive in StTPO. The addition of 10% EL in StTPO caused a longer ignition delay due to the lower cetane index of StTPO90EL10 than StTPO100. However, the ignition delay is reduced at a lower blend of StTPOxxEL10 due to the convergence of the cetane index towards the diesel range.

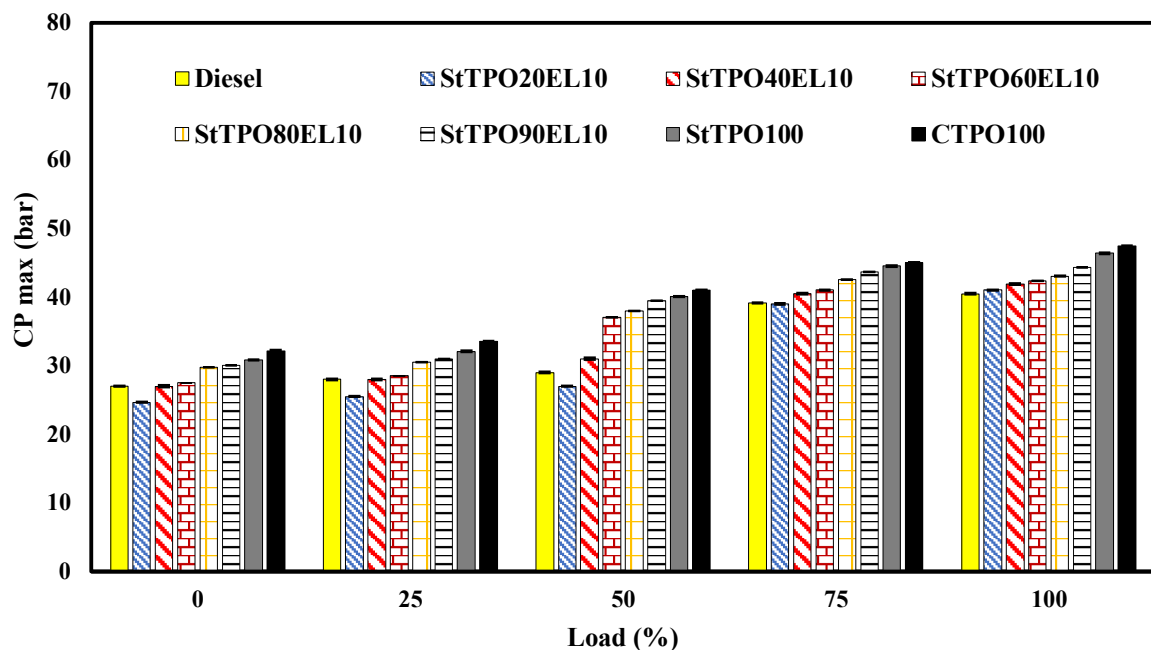


**Fig. 7.4 Variation of maximum in-cylinder pressure with load**

#### 7.4.2 Variation of net heat release with load

The net heat release curve gives insights into the combustion phenomena like ignition timing, heat release, combustion duration in the engine. Fig. 7.5 shows the maximum heat release rate of diesel, StTPO20EL10, StTPO40EL10, StTPO60EL10, StTPO80EL10, StTPO90EL10, StTPO100 and CTPO100 are 25.77 J/°CA, 27.79 J/°CA, 31.14 J/°CA, 35.15 J/°CA, 43.06 J/°CA, 47.79 J/°CA, 50.43 J/°CA, and 51.76 J/°CA. Net heat release data of CTPO40, StTPO40 and StTPO40EL10 is given by 32.27 J/°CA, 27.79 J/°CA and 31.14 J/°CA respectively. The net heat release was observed to be reduced with refining and addition of EL in StTPO.

It can be noticed that the addition of ethyl levulinate ester reduced the heat release rate due to the cooling effect produced in the engine cylinder due to the presence of more oxygenates in EL (33%). Furthermore, the heat release from CTPO is predominantly higher than StTPO due to higher aromatic content than CTPO. The presence of aromatic compounds in CTPO alleviates the net heat release due to the high ignition delay compared to CTPO. Due to higher ignition delay and aromatics in CTPO induces a competitive effect inside the combustion chamber, a steep rise in heat release and pressure rises inside the cylinder. Similar explanations for CTPO were documented in literatures (Murugan et al. 2008, Hossain et al. 2020, Kalargaris et al. 2017). The maximum heat release of StTPO100, StTPO90EL10, and diesel are recorded as 50.41 J/°CA at 371 °CA, 47.79 J/°CA at 372 °CA, and 27.08 J/°CA at 365 °CA. It can be seen that the ignition delay is longer for StTPOxxEL10 blends than diesel due to the reduction in the cetane index. The ignition delay of StTPO100 and StTPO90EL10 is longer by 6 °CA and 7 °CA than diesel. However, the ignition delay of a lower blend percentage (say StTPO20 and StTPO20EL10) was matched with diesel. The rate of pressure rises for CTPO, StTPO, and StTPO with additives blends is shown in Fig. 7.6. The heat release data supported with the pressure rise rate signifies the higher ignition delay of CTPO, StTPO, and StTPO with EL blends are due to a lower cetane number than diesel.

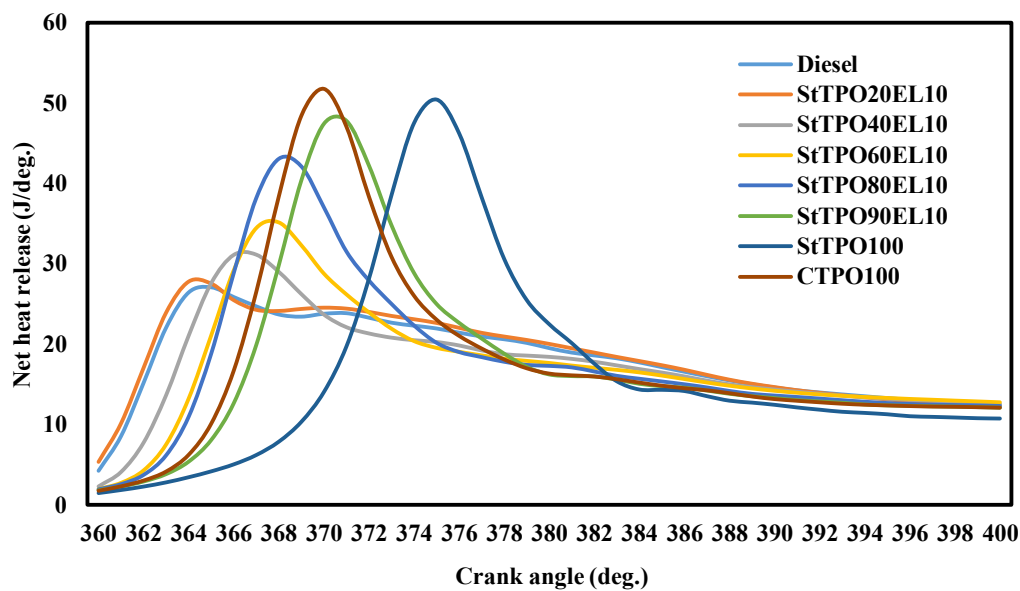


**Fig. 7.5 Variation of net heat release with load**



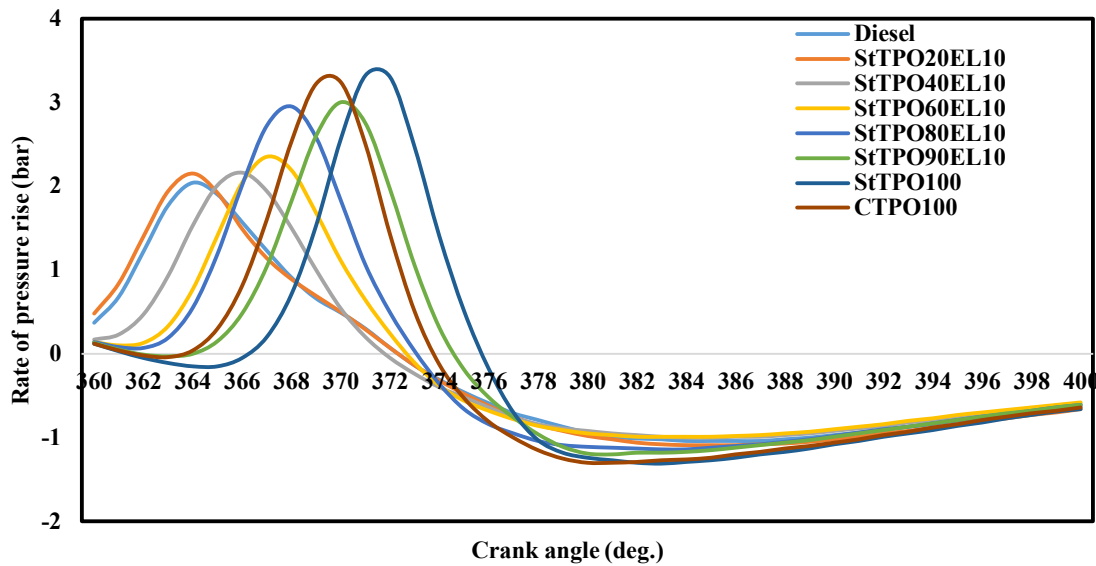


**Fig. 7.6 Variation of the rate of pressure rise with load**

## 7.5 Emission characteristics

### 7.5.1 Variation of nitrous oxide emission with load

The variation of  $\text{NO}_x$  and exhaust gas temperature with engine load was shown in Fig. 7.7 and Fig. 7.8. Nitrous oxide emission from CTPO40, StTPO40 and StTPO40EL10 is reported by 605 ppm, 313 ppm and 305 ppm, respectively. Nitrous oxide emission was found to be lessened after refining and addition of EL in StTPO. The blending of 10% ethyl levulinate in StTPO40 reduces the  $\text{NO}_x$  emission by 44.54% compared with diesel due to the cooling effect produced by ethyl levulinate (high oxygen content). Interestingly, the higher latent heat evaporation of EL (307 kJ/kg) than diesel (270 kJ/kg) also cools the combustion chamber leads to low nitrous oxide formation (Lei et al. 2016). The  $\text{NO}_x$  emissions are found to increase with a rise in the load gradually. Engine studies conducted by Lei and co-authors argued that an increase in ethyl levulinate ester (above 10%) in diesel oil induces more oxygenates to the engine cylinder supersedes the cooling effect. Also, the oxygen content in CTPO and StTPO is higher than diesel, but increased nitrogen fraction in CTPO and StTPO lowers the cooling effect, leading to more  $\text{NO}_x$  than diesel. Similar results of CTPO were reported in literature (Murugan et al. 2008). Kovisto et al. (2015) proposed that low  $\text{NO}_x$  emission from ethyl levulinate compared with butyl levulinate can be explained by heat release in the expansion stroke of diesel engine due to high cylinder volume. The variation of  $\text{NO}_x$  formation is due to the competition between

the cooling effect (reduction in an activation energy barrier, low calorific value, and high latent heat of evaporation) of EL additive and opposing effect of low cetane number and high ignition delay during premixed combustion. This variation can be a shift on one side or another, depending on the operating conditions of engine. A similar concept was reported in literature (Cork well et al. 2003). The variation of exhaust gas temperature with load was showed a similar trend as the same as NO<sub>x</sub> emission.

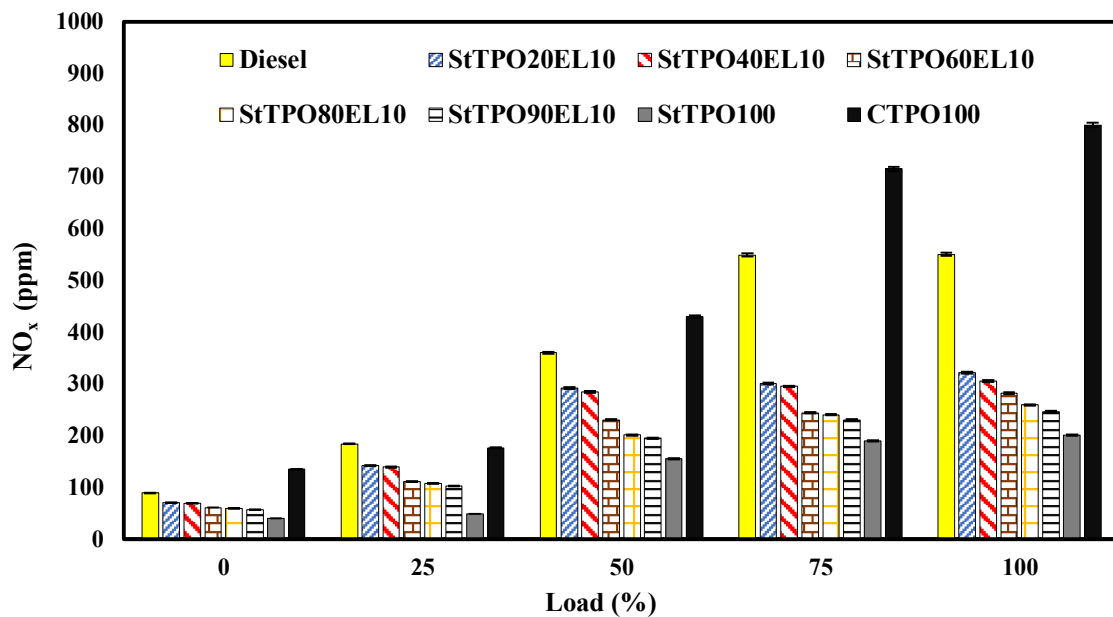


**Fig. 7.7 Variation of nitrous oxide emission with load**

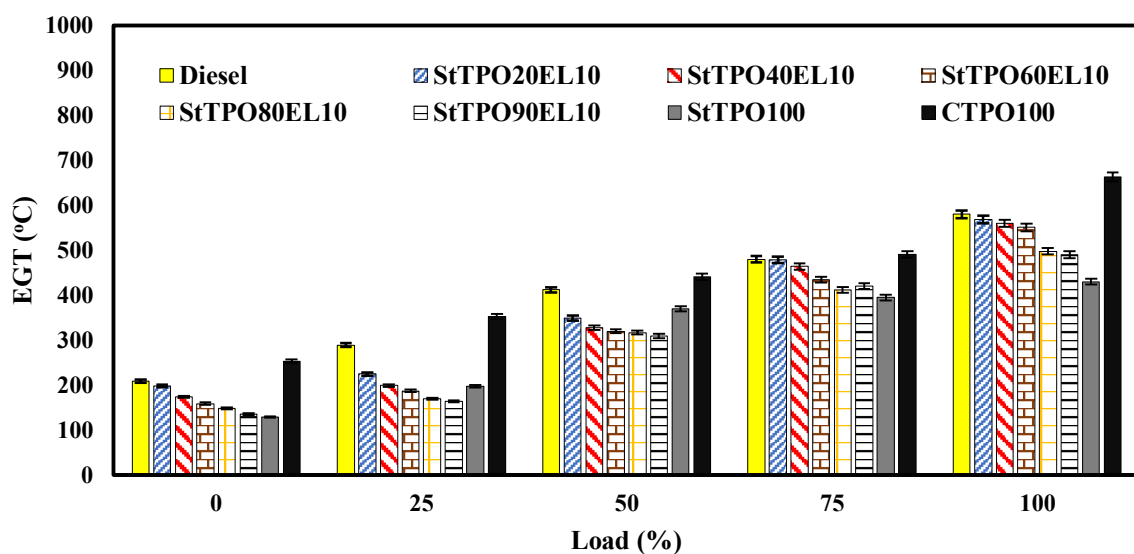


**Fig. 7.8 Variation of exhaust gas temperature with load**

### 7.5.2 Variation of oxides of carbon with load

The addition of 10% ethyl levulinate with StTPO blends showed a significant amount of carbon monoxide reduction compared to CTPO, but there is a slight increase in neat diesel. Fig. 7.9 and Fig. 7.10 shows the variation of CO and CO<sub>2</sub> emissions from StTPO-EL blends and comparative study with StTPO and diesel. The CO emission from diesel, StTPO20EL10, StTPO40EL10, StTPO60EL10, StTPO80EL10, and StTPO90EL10, StTPO100 are found to be 0.3%, 0.31%, 0.33%, 0.45%, 0.56%, 0.60% and 0.70%. Carbon monoxide emission from CTPO40, StTPO40 and StTPO40EL10 is recorded by 0.78%, 0.45% and 0.31% respectively. The carbon monoxide emission was reduced with the upgradation and addition of EL as an additive in StTPO.

52.85% reduction in CO by adding 10% EL as a diluent in StTPO40 is due to the presence of a higher amount of oxygenates in EL (C<sub>7</sub>H<sub>12</sub>O<sub>3</sub>) than CTPO100. The oxygen atoms in EL results in the oxidation of a greater number of carbon atoms forming a homogeneous air-fuel mixture inside the combustion chamber, which leads to lower CO emissions. There are many attempts to reduce carbon monoxide emissions from waste tire-derived fuels using biodiesel, dimethyl carbonate, diethyl ether, etc. (Tudu et al. 2014). Studies conducted using 10% diethyl ether as an additive in crude tire pyrolysis oil resulted in a 66% reduction in CO (Tudu et al. 2016). They have pointed that excess oxygen content in diethyl ether is responsible for lower CO formation, similar to the present investigations. Like CO emissions, the complete oxidation of a carbon atom leads to more CO<sub>2</sub> (Verma et al. 2018). Another interesting reason in the present investigation for reducing CO in StTPO<sub>xx</sub> blends than StTPO100 can be explained with the carbon content in EL, StTPO, CTPO, and diesel (Table 7.2). The less carbon content in EL lowers the CO emission and release more CO<sub>2</sub> emissions than CTPO. Still, the CO emission is slightly higher than diesel.

**Table 7.2 Carbon content in ethyl levulinate, StTPO, CTPO, and diesel**

Fuel/Additive	Formulae	Carbon (%)	Reference
EL	C <sub>7</sub> H <sub>12</sub> O <sub>3</sub>	58.00	Pullen et al. (2014)
StTPO	C <sub>83.26</sub> H <sub>11.34</sub> N <sub>1.77</sub> O <sub>2.93</sub> S <sub>0.70</sub>	83.52	Mohan et al. (2019)
CTPO	C <sub>85.67</sub> H <sub>10.04</sub> O <sub>2.02</sub> S <sub>1.12</sub> N <sub>1.15</sub>	85.67	Islam et al. (2016)
Diesel	C <sub>5</sub> H <sub>32</sub> O <sub>3</sub>	85.00	Pullen et al. (2014)

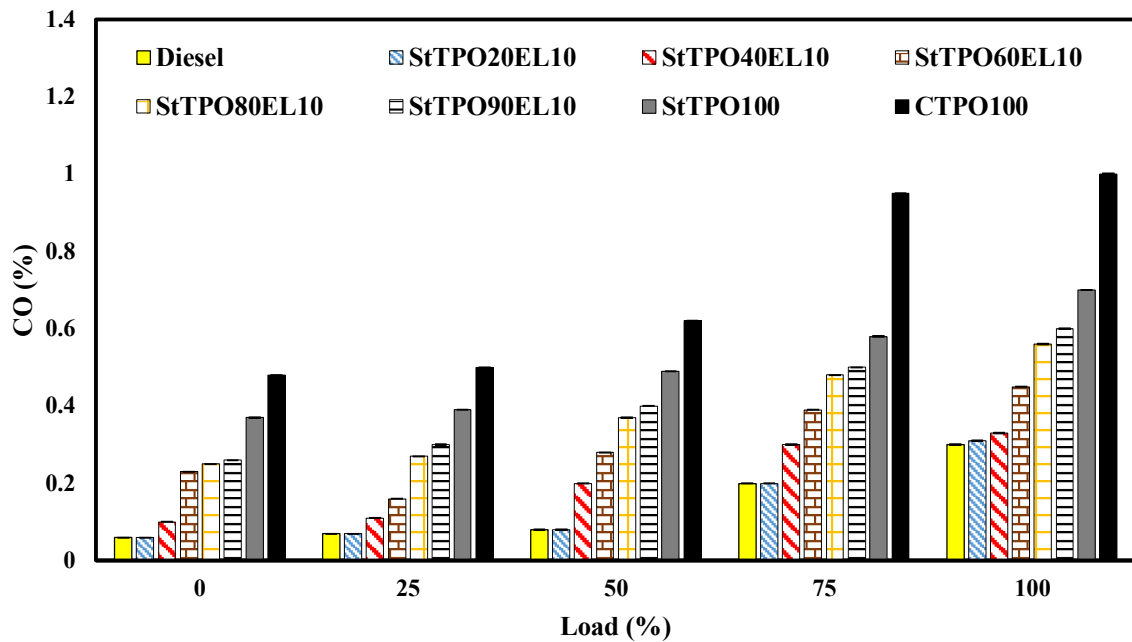


Fig. 7.9 Variation of carbon monoxide with load

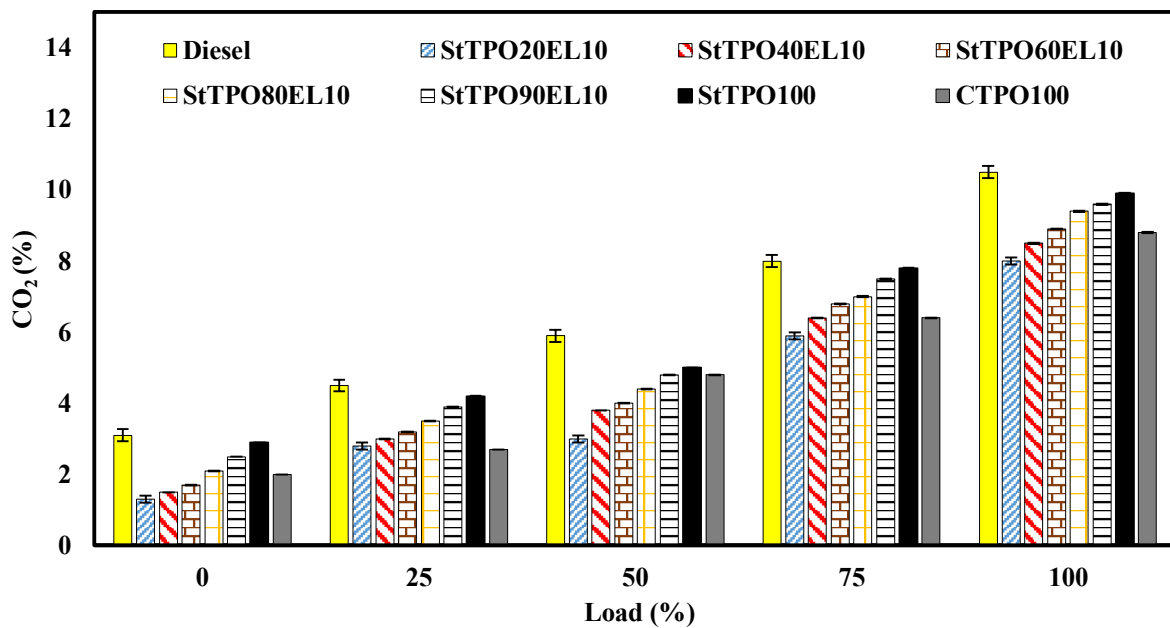
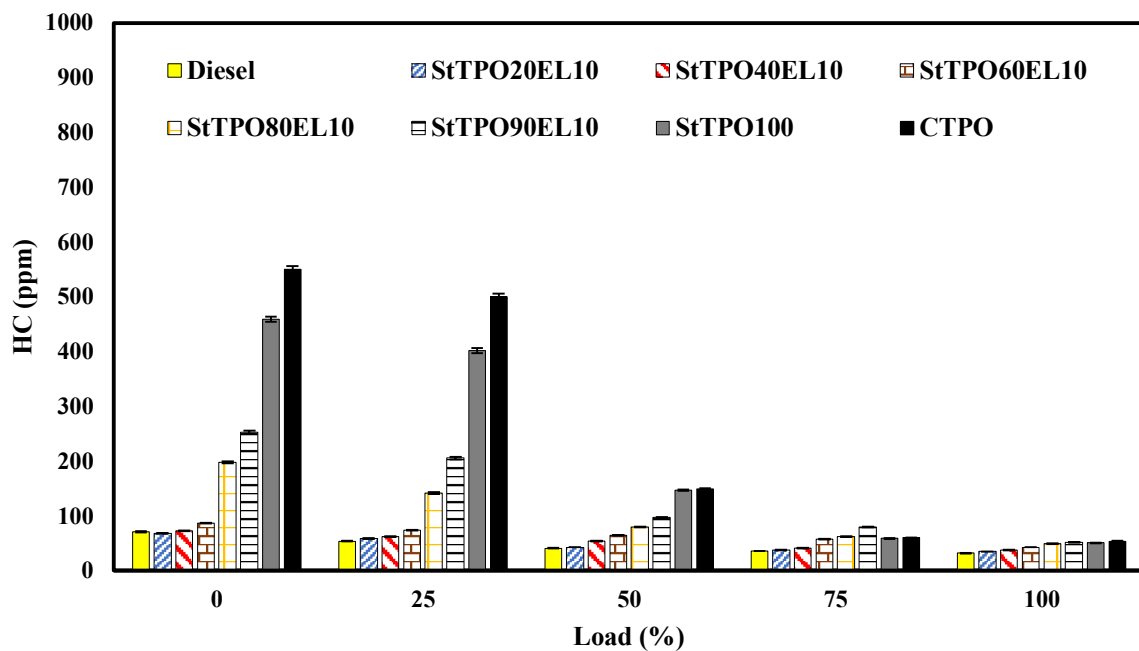


Fig. 7.10 Variation of carbon dioxide with load

### 7.5.3 Variation of hydrocarbon emissions with load

The addition of ethyl levulinate in StTPO blends lowers the hydrocarbon emissions. Fig. 7.11 displays the variation of hydrocarbon emission of StTPO-EL blends concerning variation in load. Hydrocarbon emission decreases with a rise in load for all fuel blends. Unburnt

hydrocarbons from CTPO40, StTPO40 and StTPO40EL10 are given by 50 ppm, 45 ppm, and 38 ppm. The UBHC emission was observed to be lessened with the upgradation and addition of EL as an additive in StTPO. The hydrocarbon emissions from StTPO40 was reduced by 15.55% in comparison with CTPO40. The reduction in hydrocarbons is mainly due to the better combustion inside the engine cylinder due to the presence of high oxygenates in EL compared to StTPO100. The presence of ethyl levulinate promotes complete oxidation of carbon atoms, which may reduce the release of hydrocarbons from the engine. Due to the presence of ketone and ester functionalities on the carbon chain of EL can readily produce stable intermediates during auto-oxidation process in diesel engine (Lei et al. 2016, Prasad et al. 2012). Thus the formation of stable intermediates lower the reaction rate leads to low HC formation (Tudu et al. 2016, Tian et al. 2017). Table 7.3 summarises the trend of performance, combustion and emission characteristics of various fuel blends with respect to CTPO



**Fig. 7.11 Variation of hydrocarbon emission with load**

S. No.	Fuel blends	BTE (%)	BSEC (mJ/kWh)	CP (bar)	NHR (J/°CA)	NO <sub>x</sub> (ppm)	CO (%)	CO <sub>2</sub> (%)	HC (ppm)
1.	Diesel	32.50	11.07	40.48	25.77	550	0.30	10.50	32
2.	CTPO20	31.85	11.30	43.19	27.79	535	0.55	4.50	43
3.	StTPO20	↓	↑	↓	↓	↓	↓	↑	↓
4.	StTPO20EL10	↓	↑	↓	↓	↓	↓	↑	↓
5.	CTPO40	31.00	11.61	43.89	32.27	605	0.78	6.50	50
6.	StTPO40	↓	↑	↓	↓	↓	↓	↑	↓
7.	StTPO40EL10	↓	↑	↓	↓	↓	↓	↑	↓
8.	CTPO60	30.56	11.77	45.48	45.48	650	0.88	8.00	55
9.	StTPO60	↓	↑	↓	↓	↓	↓	↑	↓
10.	StTPO60EL10	↓	↑	↓	↓	↓	↓	↑	↓
11.	CTPO80	30.00	11.99	46.40	46.40	700	0.98	9.00	62
12.	StTPO80	↓	↑	↓	↓	↓	↓	↑	↓
13.	StTPO80EL10	↓	↑	↓	↓	↓	↓	↑	↓

**Table 7.3 Summary of the performance, combustion and emission characteristics of various fuel blends with diesel**

↓ Decreasing trend w.r.t CTPO ↑Increasing trend w.r.t CTPO

### **7.6 Effect of ethyl levulinates on performance, emission, and combustion from diesel engine fuelled with StTPOxxDF blends**

Ethyl levulinate has shown a versatile chemical in single-cylinder diesel engines due to its multifunctional groups like ketone and ester, inherent fuel properties such as high lubricity, improved flow, low sulfur content, improved flashpoint, and stability. Firstly, the performance parameters like BTE and BSFC studies revealed that the lower heating value of EL consumes more fuel results in higher BSFC with lower BTE.

Secondly, the combustion characteristics like in-cylinder pressure, heat release rate, and pressure rise explain low heat release and cylinder pressure by adding 10% EL to StTPO100, which can be attributed to the low heating value and cetane index of StTPOxxEL10 blends

compared to StTPO100. The ignition delay of StTPOxxEL10 combinations is higher than StTPO due to the lower cetane index of ethyl levulinate than StTPO.

Thirdly, the emission components like NO<sub>x</sub>, CO, CO<sub>2</sub>, and HC were significantly improved after the upgradation of CTPO due to the oxygen-containing functional groups and high latent heat evaporation of EL. The increased oxygen content enhances combustion. High latent heat of evaporation removes heat from the combustion chamber and creates a cooling effect inside the combustion chamber, which lowers NO<sub>x</sub> formation.

The addition of 10% EL in StTPO40 reduces the CO by 14.28% compared to StTPO100, but the value is slightly higher than diesel. The lower carbon content in EL is a prominent reason for reducing CO compared to other fuel blends. The NO<sub>x</sub> emission from StTPO40EL10 is dropped by 44.54% regarding diesel due to stable intermediates and high LHE of EL compared to diesel. Phase stability and fuel compatibility of StTPOxxEL10 blends are similar to diesel due to better miscibility of EL in StTPO and diesel.

Finally, it can be concluded that fuel blends with a lower percentage of EL can be utilized in a single-cylinder diesel engine due to its superior fuel properties and less toxicity compared to other fuel additives. Due to the presence of high oxygen content in StTPOxxEL10 blends from stearic acid and zinc oxide (curing agents added during tire vulcanization) and the presence of oxygenates in EL promotes auto-oxidation reaction inside the engine cylinder.

The decomposition pathway of EL under the auto-oxidation process in a diesel engine is shown in Fig. 7.12. In the proposed scheme of EL auto-oxidation by (Thion et al. 2015), oxidation reactions are initiated by hydroxyl and methyl radicals through  $\beta$ -scission and hydrogen abstraction reactions. It can be seen that the attraction of oxygen atom towards carbon makes the bond more potent than C-C and C-H bond in ethyl levulinate, which may cause the C-H and C-C bonds are found to be the most preferred sites for initial radical reaction and hydrogen abstraction reactions.

Ethyl acrylate and ethyl vinyl ketone are the primary products of EL auto-oxidation reactions. Therefore, it can be concluded that the reaction lowers the activation energy barrier by forming stable intermediates of ethyl levulinate, which may result in lower cylinder temperature in the engine with lower emissions from single-cylinder diesel engines. Thion and co-authors reported similar discussions for methyl levulinate esters.

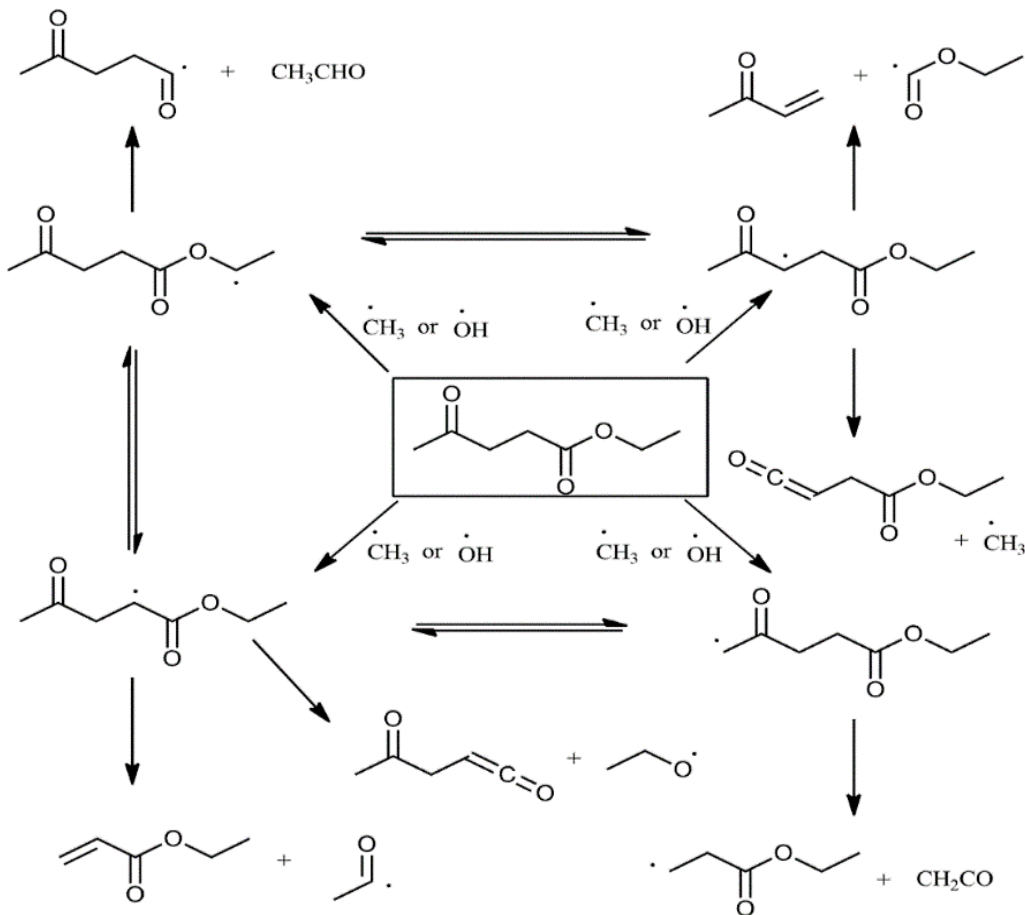


**Fig. 7.12 Proposed pathway of autoxidation mechanism of EL in the combustion chamber**

## 7.7 Conclusion

To sum up, in the present chapter, the effect of ethyl levulinate as a fuel additive in StTPO was carried out to study the performance, combustion and emissions from a single-cylinder diesel engine. The following inferences are made based on the obtained results.

1. The addition of EL in StTPO induces a significant reduction in emissions and lowers the performance of diesel.
2. StTPO40EL10 is found to be an optimal blend in terms of performance, combustion, and emissions from the direct-injected single-cylinder diesel engine.
3.  $\text{NO}_x$  emission from StTPO40 was lessened with the addition of 10%EL by 44.54% in comparison with diesel.
4. The addition of 10% EL in StTPO40 lowers the carbon monoxide emissions by 52.85% compared to StTPO100.



5. Hydrocarbon emission was found to be lowered by 15.55% in StTPO40EL10 in comparison with StTPO40.
6. Spot test supported with phase stability studies revealed that the StTPOxxEL10 (xx represents various fraction StTPO in ternary blend mixture with EL and diesel) blends are stable without any phase separation or characteristic creaming.
7. Heat release from StTPOxxEL10 was higher than diesel and lower than CTPO due to higher amounts of polyaromatic hydrocarbons, benzene derivatives, and naphthalene.
8. EL was found to be a better additive in reducing emissions due to a high oxygenates.

## CHAPTER 8

### SUMMARY AND CONCLUSIONS

Thermal depolymerization of scrap tires under optimum reaction conditions in a pyrolysis reactor yields crude tire pyrolysis oil, carbon black, and steel wires. Crude tire pyrolysis oil is a dark black coloured syrupy liquid consisting of C<sub>6</sub>-C<sub>24</sub> with various classes of compounds such as aliphatics, olefins, terpenes, aromatics, nitrogen, sulfur, and oxygen-containing compounds. The oil cannot be directly used in diesel engines due to its inferior properties such as low calorific value, high viscosity, unpleasant odour, high acidity, low thermal stability, and poor storage stability. There are various methods available for the upgradation of CTPO, such as distillation, hydrotreating, hydroprocessing, esterification, desulfurization, etc. However, these processes are energy-intensive and need huge capital investment for deployment on a pilot scale. The present study was focused on developing a cost-effective method for refining CTPO. Accordingly, the objectives of the current work were framed in fourfold: (i) pyrolysis of scrap tires in a 10-ton rotating autoclave reactor in optimum reaction conditions and the extensive characterization of CTPO using various analytical techniques (ii) different upgradation strategies for refining CTPO into diesel range fuels and comprehensive characterization of refined oils and comparison with CTPO and diesel (iii) performance, combustion and emission studies of upgraded tire pyrolysis oil in a single-cylinder diesel engine and comparison with CTPO and diesel as reference fuels (iv) scrutinize the effect of ethyl levulinate as a bio-diluent on performance, combustion, and emission from the single-cylinder diesel engine and comparative study with upgraded oil, CTPO, and diesel.

The CTPO obtained from a rotating autoclave reactor is extensively characterized to understand the detailed chemistry, physical and thermal properties using various sophisticated analytical techniques. One dimensional gas chromatography-mass spectrometry (1D GC-MS) espoused with Fourier transform infrared spectroscopic data suggest that nitrogen, sulfur, and oxygen-containing compounds are present in CTPO. NMR spectra revealed that aliphatic compounds are predominant (71.10%) than aromatics, oxygenates, aldehydes and ketones. Further, the data obtained from nuclear magnetic resonance spectrometry confirms that aldehyde peak at 9.6 ppm and heteroaromatic peak above eight ppm are responsible for high acid content (11.54) in crude tire pyrolysis oil. The long-term storage of CTPO in the pyrolysis industry's storage tank leads to gummy deposits due to the polymerization of olefins, which is again confirmed by thermo gravimetric data and stability analysis.

CTPO obtained from the 10-ton rotating autoclave reactor was upgraded using column-based and mechanically stirring-based refining strategies. The mechanically stirring-based approach was then scaled-up using a batch reactor fitted with an overhead stirrer, membrane-based filtration system, and laboratory chiller for condensing the solvent during rotary evaporation. The mechanically stirring-based strategy effectively removed polar oxygenates due to the higher contact area of CTPO with silica gel.

The upgraded oil was then extensively characterized for detailed physical, thermal, chemical, and stability analysis. The loss of oil from a batch scale upgradation strategy was observed to be 5% compared to laboratory-scale techniques. Sulfur content in the batch scale upgradation process was significantly reduced by 48.86%. Sulfur content in CTPO is mainly due to the presence of sulfides, disulfides, and mercaptans. The polyaromatic hydrocarbons and naphthalene content were lowered by 27.72% and 43.69%. The linear alkanes in StTPO were increased by 20.22% after the mechanically stirred strategy due to the longer contact time of CTPO with silica gel.

Benzene fraction has a prominent role in combustion chemistry to determine the cylinder pressure and heat release from diesel engines. The primary reason for reducing benzene derivatives (25.68%) is the escape of benzene due to continuous heating and cooling operation during the refining strategy. The StTPOxx blends were thermally stable for whole engine experiments without any creaming or phase separation. UV-visible spectra supported with fluorescence spectra confirm that extender oil, stearic acid, and aromatic oil are the primary reasons for fluorescence emission from CTPO. However, the fluorescence was significantly reduced due to the adsorption of polyaromatics by silica gel due to its characteristic pore size of 40-60 Å and surface area of 350-450 m<sup>2</sup>/gm.

The study emphasized the extensive characterization of CTPO, StTPO, and diesel samples by physical, thermal, and chemical analysis before engine tests. Results from experimental investigations found that the CTPO and StTPO (20%, 40%, 60%, 80%, and 100%) can be fully utilized in the engine without any seizing or injector blockage. GC×GC TOF-MS analysis revealed that the polyaromatics and naphthalenes are significantly reduced by 27.79% and 43.69%. StTPO40 is found to be the best blend in terms of performance, combustion, and emissions.

There is no significant change in the BTE after upgradation, but the BTE is slightly lower than diesel. The ignition delay of CTPOxx and StTPOxx blends is higher than diesel due to higher

heat release during premixed combustion. The tailpipe emissions like CO, CO<sub>2</sub>, HC, and CO are significantly lowered after upgrading due to removing impurities and carbon particles. NO<sub>x</sub> emission from StTPO40 is reduced by 43.09% than diesel due to oxygen content in StTPO. Hydrocarbon emission from StTPO40 is comparable with diesel. Phase stability studies supported with spot tests reveal that the tested samples show no phase separation or creaming. Thus, a lower percentage of StTPO-DF blends can be utilized in a diesel engine without further modifications.

Ethyl levulinate is a potential diesel additive due to its inherent oxygen content and anti-knock properties. The present objective mainly focused on ethyl levulinate on performance, emission, and combustion from the single-cylinder direct-injected diesel engine. EL in pure StTPO significantly lowers the cylinder pressure due to the absorption of heat of combustion by EL due to its high LHE, which results in a cooling effect inside the engine cylinder. StTPO40EL10 is found to be an optimal blend in terms of performance, combustion, and emissions.

BTE of StTPO<sub>xx</sub>EL10 blends were lower than StTPO and diesel due to lower calorific value and cetane index. Nitrous oxide emission from StTPO40EL10 was reduced by 44.54% by the addition of 10%EL in StTPO due to high oxygen content. The carbon monoxide and hydrocarbon from StTPO40EL10 were comparable with diesel due to their better chemical reactivity during autoxidation reactions. Phase stability studies supported with spot tests suggested that the tested blends were much stable than CTPO and formed no phase separation or creaming. Thus, it can be concluded that StTPO40EL10 can be utilized in a single-cylinder diesel engine without any external modification. Still, the higher StTPO percentage can be suitable for marine engines, burners, and boiler applications.

The highlights of the present study are summarized as follows:

1. Extensive characterization of CTPO, StTPO, and diesel to understand the fuel chemistry and to identify the value-added compounds present in the oil.
2. The loss of oil from a batch scale upgradation strategy is reduced by 5% compared to the lab-scale approach.
3. GC×GC results show that polyaromatics, naphthalene, and sulfur are reduced by 27.79%, 43.69%, and 48.86% after upgradation.

4. The engine can run up to 100% CTPO and 100% StTPO without any modifications. The tailpipe emissions are increased with load compared to loads for a higher blend ratio (60-100%) than diesel.
5. The addition of EL as a potential diesel additive caused an improvement in the emissions due to its higher oxygen content. NO<sub>x</sub> emission is lowered by 44.54% compared to diesel.
6. The optimum fuel blend found in this research was StTPO40EL10 (i.e., 40 vol% StTPO, 10 vol% EL, 50 vol% Diesel) in terms of performance, combustion, and emissions.

### **Scope of future work**

Although the present work included the characterization of CTPO, StTPO and recommended an up gradation method to utilize tire pyrolysis oil as a liquid fuel for diesel engines, some improvements can still be made. Some interesting research topics which are worth investigating further are listed below.

1. One of the limitations of the current study is the loss of oil during Millipore filtration methods and stirring processes (adsorption of oil by silica gel) during batch scale refining strategy. This can be further improved by passing the solution of CTPO and petroleum ether through a series of packed columns filled with silica gel in a continuous regime. The contact time of CTPO with silica gel in the glass columns can be modified by monitoring the flow rate and the number of columns used in the scale-up studies.
2. Thermal pyrolysis of natural rubber and scrap tire produces a limonene yield of 18.4 wt.% and 4.3 wt.%, respectively (Januszewicz et al. 2020). Quantification and recovery of odoriferous compounds (limonene) in CTPO and upgraded tire pyrolysis oil can be carried out.
3. Scale-up of batch scale refining strategy to a field-scale refining unit in a tire pyrolysis plant remains a challenge. The process modelling and techno-economic analysis of the refining system need to be carried out to deploy field units.
4. In the present study, only limited experiments on performance, combustion, and emissions using CTPO<sub>xx</sub>, StTPO<sub>xx</sub>, and StTPO<sub>xx</sub>EL10 in a single-cylinder direct-injected diesel engine were carried out. Further studies can be planned on the

tribological behaviour of CTPO and StTPO in a single-cylinder diesel engine by carrying out the endurance test.

5. There is scarce literature available on the combustion diagnostics of tire-derived oil in a single-cylinder diesel engine. Thus, detailed combustion studies of CTPO<sub>xx</sub>, StTPO<sub>xx</sub>, and StTPO<sub>xx</sub>EL10 can be carried out using a spray chamber.
6. There is no literature available on the application of upgraded tire pyrolysis oil as a fuel in furnaces and cook stoves. The quantification of suspended particulate matter, smoke sampling, heavy metals, sulfur dioxides, ammonia, hydrogen sulfide, Poly Aromatic Hydrocarbons (PAH) in the indoor environment is important to study the effect on humans health. Therefore, performance, emission, and modelling studies using StTPO as a fuel in traditional and modern cook stoves need to be carried out.
7. The genotoxic and carcinogenic potency of crude and upgraded tire pyrolysis oil on human health need to be studied to understand the effect of pyrolysis oil.

## REFERENCES

Abdallah, R., Juaidi, A., Assad, M., Salameh, T., Agugliaro, F. M. (2020). "Energy recovery from waste tires using pyrolysis: Palestine as case of study." *Energies*, 13, 1817.

Abdulkadir, A., Recep, Y. (2016). "Production of gasoline and diesel-like fuels from waste tire oil by using catalytic pyrolysis." *Energy*, 103, 456-468.

Abdulkadir, A., Recep, Y. (2016). "Rotary kiln and batch pyrolysis of waste tire to produce gasoline and diesel-like fuels." *Energy Convers. Manag.*, 111, 261-270.

Agarwal, A. K., Singh, S. K., Sinha, S., Shukla, M. K. (2004). "Effect of EGR on the exhaust gas temperature and exhaust opacity in compression ignition engine." *Sadhana- Academic Proceedings in Engineering Sciences*, 29(3), 275-284.

Agarwal, A. K., Bijwe, J., Das, L. M. (2003). "Effect of biodiesel utilization of wear of vital parts in compression ignition engine." *J. Eng. Gas Turbines Power*, 125, 604-611.

Agrawal A. K. (2007). "Biofuels (alcohols and biodiesel) applications as fuels for internal combustion engines." *Energy and Combustion Science*, 33, 233–71.

Agarwal, R., Gooty, R. T. (2020). "Misconceptions about efficiency and maturity of distillation." *AIChE*, 66, 1-11.

Agbulut, U., Yesilyurt, M. K., Saridemir, S. (2021). "Waste to energy: Improving the poor properties of waste tire pyrolysis oil with waste cooking oil methyl ester and waste fusel alcohol – A detailed assessment on the combustion, emission and performance characteristics of a CI engine." *Energy*, 222, 119-942.

Alsaleh, A., Sattler, M. L. (2014). "Waste tire pyrolysis: Influential parameters and product properties." *Current Sustainable Renewable Energy Reports*, 1, 129-135.

Almeida, T. M., Bispo, M. D., Cardoso, A. R. T., Migliorini, M. V., Schena, T., De Campos, M. C. V., Machado, M. E., López, J. A., Krause, L. C., & Caramão, E. B. (2013). "Preliminary

studies of bio-oil from fast pyrolysis of coconut fibers." *J. Agric. Food Chem*, 61(28): 6812–6821.

Ambrosewicz-Walacik, M., & Piętak, A. (2016). "Spectrofluorometric Characterization of Oil From Pyrolysis of Scrap Tires." *J. KONES*, 23(1), 25–30.

Amfo-otu, R., Agyenim, J. B., Adzraku, S. (2014). "Meat contamination through singeing with scrap tires in Ghana." *Applied Research Journal*, 1(1), 12-19.

Andrea U., Luca R., Marco F., Piero F. (2014) "Upgraded fuel from microwave-assisted pyrolysis of the waste tire." *Fuel*, 115, 600-608.

Antoniou, N., Zabaniotou, A. (2013). "Features of an efficient and environmentally attractive used tire pyrolysis with energy and material recovery." *Renew. Sustain. Energy Rev*, 20, 539-558.

Arabiourrutia, M., Lopez, G., Artexe, M., Alvarez, J., Bilbao, J. (2020). "Waste tire valorization by catalytic pyrolysis." *Renew. Sustain. Energy Rev*, 129, 109:932.

Arai, M. (2012). "Physics behind sprays" 12<sup>th</sup> Triennial International Conference on liquid atomization and spray systems, Heidelberg, Germany on September 2-6.

Arya, S., Sharma, A., Rawat, M., Agarwal, A. (2020). "Tire pyrolysis oil as an alternate fuel: A review", *Material Today: Proceedings*." 28(4), 2481-2484.

Ashok, B., Jeevanantham, A. K., Nanthagopal, K., Saravanan, B., Senthil Kumar, M., Johny, A., Mohan, A., Kaisan, M. U., & Abubakar, S. (2019). "An experimental analysis on the effect of n-pentanol- Calophyllum Inophyllum Biodiesel binary blends in CI engine characteristics." *Energy*, 173, 290–305.

Ashok, B., Nanthagopal, K. (2019). "Eco-friendly biofuels for CI engine applications." *Advances in eco fuel for a sustainable environment*, 407-440.



Atmanli, A., & Yilmaz, N. (2018). "A comparative analysis of n-butanol/diesel and 1-pentanol/diesel blends in a compression ignition engine." *Fuel*, 234(5), 161–169.

Ayanoglu, A., Yumrutas, R. (2016). "Production of gasoline and diesel-like fuels from waste tire oil by using catalytic pyrolysis." *Energy*, 103, 456-468.

Aydin, H., Ilkilic, C. (2012). "Optimization of fuel production from waste vehicle tires by pyrolysis and resembling to diesel fuel by various desulfurization methods." *Fuel*, 2012, 102, 605-612.

Aylón E., Fernández-Colino A., Murillo R., Navarro M.V., García T., Mastral A.M. "Valorization of waste tire by pyrolysis in a moving bed reactor." *Waste Manag.*, 30, 1220–1224.

Aya, F.C., Nwite, J.N. (2016). "Roasting goat with tire on human health and environment in Abakaliki, Ebonyi state, Nigeria." *Journal of Pollution Effects and Control*, 4, 153

Babu, R., Anand, R. (2019). "Biodiesel-diesel-alcohol blend as an alternative fuel from DIC engine." *Advanced biofuels*, 978-0-08-102791-2, 337-367.

Baškovič, U. Z., Vihar, R., Seljak, T., & Katrašnik, T. (2017). "Feasibility analysis of 100% tire pyrolysis oil in a common rail Diesel engine." *Energy*, 137, 980–990.

Banar, M., Aksun, O., Cokaygil, Z., Onay, O. (2012). "Characterization of pyrolytic oil obtained from pyrolysis of tire-derived fuel." *Energy convers. Manag*, 62, 22-30.

Banar, M. (2015). "Life cycle assessment of waste tire pyrolysis." *Frensenius Environ. Bull.*, 24(4).

Barlaz, M.A., Eleazar, W.E., Whittle, D.J. (1993). "Potential to use waste tire as a supplement fuel in paper and pulp mill boilers, cement kiln, and road pavement." *Waste Manage. Res.*, 11(6), 463-80.

Bell, S. (1999). *A beginners guide to uncertainty of measurement*. National Physical Laboratory, United Kingdom.

Benzouk, A., Douzane, O., Langlet, T., Mezreb, K., Roucoult, J.M., Queneudec, M. (2007). "Physio-chemical properties and water absorption of cement composite containing shredded rubber waste." *Cem Concr Compos.*, 29, 732-40.

Bockstal, L., Berchen, T., Schmetz, Q., Richel, A. (2019). "Devulcanisation and reclaiming of tires and rubber by physical and chemical process: A review.", *J. Clean. Prod*, 239, 117-574.

Bodisco, T. A., Rahman, S. M. A., Hossain, F. M., & Brown, R. J. (2019). "On-road NOx emissions of a modern commercial light-duty diesel vehicle using a blend of tire oil and diesel." *Energy Rep.*, 5, 349–356.

Boggavarapu, P., Ravikrishna, R. V. (2013). "A review on atomization and sprays of biofuels for internal combustion engine applications." *International Journal of Spray and Combustion Dynamics*, 5(2), 85-121.

Brunt, M., Platts, K. (1999). "Calculation of heat release indirect injection diesel engine." *SAE Transactions*, 108, 161-175.

Chakravarthy, R., Acharya, C., Savalia, A., Naik, G. N., Das, A. K., Saravanan, C., Verma, A., & Gudasi, K. B. (2018). "Property Prediction of Diesel Fuel Based on the Composition Analysis Data by two-Dimensional Gas Chromatography." *Energy Fuels*, 32(3), 3760–3774.

Chaturvedi, B., Handa, R. R. (2017). *Report on Circulating tires in the economy- A waste to wealth approach to old tires*, Chintan Environmental and Action Group.

Chen, J., Ma, X., Yu, Z., Deng, T., Chen, X., Chen, L., Dai, M. (2019). "A study on catalytic co-pyrolysis of kitchen waste with tire waste over ZSM-5 using TG-FTIR and Py-GC-MS.", *Bioresour. Technol*, 289, 121-585.

Chen, L., Ma, X., Tang, F., Li, Y., Yu, Z., Chen, X. (2020). "Comparison of catalytic effect on upgrading bio-oil derived from co-pyrolysis of water hyacinth and scrap tire over multilamellar MFI nanosheets and HZM-5.", *Bioresour. Technol.*, 312, 123-592.

Christensen, E., Yanowitz, J., Ratcliff, M., & McCormick, R. L. (2011). "Renewable oxygenate blending effects on gasoline properties." *Energy Fuels*, 25(10), 4723–4733.

Chumpitaz, G. R. A., Coronado, C. J. R., Carvalho, J. A., Andrade, J. C., Mendiburu, A. Z., Pinto, G. M., & de Souza, T. A. (2019). "Design and study of a pure tire pyrolysis oil (TPO) and blended with Brazilian diesel using Y-Jet atomizer." *J. Braz. Soc. Mech. Sci. & Eng.*, 41(3).

Costa, G.A., Santos, R.G.D. (2019). "Fractionation of tire pyrolysis oil into light fuel fraction by steam distillation." *Fuel*, 249, 558-563.

Czajczynska, D., Czajka, K., Krzyzyska, R., Jouhara, H. (2020). "Waste tire pyrolysis- Impact of process and its products on the environment." *Therm. Sci. Eng.*, 20(1), 100-690.

Czajczynska, D., Krzyzyska, R., Jouhara, H., Spencer, N. (2017). "Use of pyrolytic gas from waste tire as a fuel: A review, *Energy*, 134, 1121-31.

Dai, L., Fan, L., Duan, D., Ruan, R., Wang, Y., Liu, Y., Zhao, Y., Yu, Z. (2017). "Microwave-assisted catalytic fast pyrolysis of soap stock and waste tire for bio-oil production." *J Anal Appl Pyrolysis*, 125, 304-309.

Davanlou, A., Lee, J. D., Basu, S., Kumar, R. (2015). "Effect of viscosity and surface tension on breakup and coalescence of bio component sprays." *Chemical Engineering Science*, 131, 243-255.

Debek, C., Walendziewoki, J. (2015). "Hydro refining of oil from pyrolysis of the whole tire for passenger car and van." *Fuel*, 159, 659-65.

Dick, D. T., Agboola, O., Ayeni, A. O. (2020). "Pyrolysis of waste tires for high-quality fuel products – A review, *AIMS Energy*, 8(5), 869-895.

Dijkhuis, K. (2008). "Recycling of vulcanized EPDM rubber, Ph.D. Thesis, University of Twente, Enschede, Netherlands.

Dizay, B. I. A. (2016). "Fuel spray deposit and real driving emission analysis of heavy truck using used cooking oil as fuel." PhD. A thesis submitted at the University of Leeds, London.

Dogan, O., Celik, M.B., Ozdalyon, B. (2012). "The effect of tire derived fuel blends utilization on diesel performance and emissions.", *Fuel*, 95, 340-346.

Dutriez, T., Courtiade, M., Thiébaud, D., Dulot, H., Bertoncini, F., Vial, J., & Hennion, M. C. (2009). "High-temperature two-dimensional gas chromatography of hydrocarbons up to nC60 for analysis of vacuum gas oils." *J. Chromatogr. A*, 1216(14), 2905–2912.

Ejim, C. E., Fleek, B. A., Amirfezli, A. (2007). "Analytical study for atomization of biodiesel and their blends in a typical injector: surface tension and viscosity effects." *Fuel*, 86, 1534-1544.

Frigo, S., Seggiani, M., Puccini, M., & Vitolo, S. (2014). "Liquid fuel production from waste tire pyrolysis and its utilization in a Diesel engine." *Fuel*, 116, 399–408.

Han, Y., Stankovikj, F., Perez, M.G. (2017). "Co-hydro treatment of tire pyrolysis oil and vegetable oil for the production of transportation fuels." *Fuel Process. Technol*, 159, 328-339.

Hariharan, S., Murugan, S., & Nagarajan, G. (2013). "Effect of diethyl ether on Tyre pyrolysis oil fueled diesel engine." *Fuel*, 104, 109–115.

Hariadi, D., Saleh, S. M., Yamin, R. A., Aprilia, S. (2021). "Utilization of LDPE plastic waste on the quality of pyrolysis oil as an asphalt solvent alternative." *Therm. Sci. Eng*, 23(1), 100-872.

Heywood, J. B. (1988). "Internal Combustion Engine Fundamentals." Mc-Graw-Hill Series in Mechanical Engineering.

Hita I., Palos R., Arandes J. M., Hill J. M., Castano P. (2016) "Petcock derived functionalized activated carbon as support in a bi-functional catalyst for tire oil hydroprocessing." *Fuel Process. Technol.*, 144, 239-247.

Hita, I. (2015). "Upgrading model compounds and scrap tire pyrolysis oil on hydrotreating Ni-Mo catalyst with tailored supports." *Fuel*, 145, 158-169.

Hita, I., Gutierrez, A., Olzar, M., Bilbao, J., Arandes, J. M., Castano, P. (2015) "Upgrading model compounds and scrap tires pyrolysis oil on hydro-treating Ni-Mo catalyst with tailored supports." *Fuel*, 145, 158-169.

Hita, I., Palos R., Arandes, J. M., Hill, J. M., Castano, P., (2016). "Petcock derived functionalized activated carbon as support in a bi-functional catalyst for tire oil hydroprocessing." *Fuel Process. Technol.*, 144, 239-247.

Hoang, A. T., Le, A. T., Pham, V. V. (2019). "A core correlation of spray characteristics, deposit formation and combustion of a high-speed engine fuelled with *Jatropha* oil and diesel, *Fuel*, 2019, 244, 159-175.

Hossain, F. M., Nabi, M. N., Rainey, T. J., Bodisco, T., Bayley, T., Randall, D., Ristovski, Z., & Brown, R. J. (2020). "Novel biofuels derived from waste tires and their effects on reducing oxides of nitrogen and particulate matter emissions." *J. Clean. Prod.*, 242, 118-463.

Hughey, C. A., Hendrickson, L., Rodgers, R. P., Marshall, A. G. (2001). "Elemental composition analysis of processed and unprocessed diesel fuel by electron spray ionization fourier transform ion cyclotron resonance mass spectrometry." *Energy Fuels*, 15(5), 1186-1193.

Ilkiliç, C., & Aydin, H. (2011). "Fuel production from waste vehicle tires by catalytic pyrolysis and its application in a diesel engine." *Fuel Process. Technol.*, 92(5), 1129–1135.

Islam, M.R., Haniu, H., Beg, M.R.A. (2008). "Liquid fuels and chemicals from pyrolysis of motorcycle tire waste: Product yield, composition, and related properties." *Fuel*, 87, 3112-3122.

Jain, A. (2016). "Report on compendium of technologies for the recovery of materials or energy from end of life tires", Regional resource centre for Asia and the Pacific.

Januszewicz, K., Kazimierski, P., Suchocki, T., Kardas, D., Lewandowski, W., Radziemska, E. K., Luczak, J. (2020). "Waste rubber pyrolysis: product yield and limonene concentration." *Materials*, 13(19), 4435.

Joseph, A., George, B., Madhusoodanan, K., & Alex, R. (2015). "Current status of sulfur vulcanization and devulcanization chemistry: process of vulcanization." *Rubber Science*, 28(1), 82–121.

Joshi, H., Moser, B. R., Toler, J., Smith, W. F., & Walker, T. (2011). "Ethyl levulinate: A potential bio-based diluent for biodiesel which improves cold flow properties." *Biomass Bioenergy*, 35(7), 3262–3266.

Junqing, X., Yu, J., Xu, J., Sun, C., He, W., Huang, J., Li, G. (2020). "High-value utilization of waste tires: A review with focus on modified carbon black from pyrolysis." *Sci. Total Environ.*, 742, 140-235.

Kalargaris, I., Tian, G., & Gu, S. (2017). "Combustion, performance, and emission analysis of a DI diesel engine using plastic pyrolysis oil." *Fuel Process. Technol*, 157, 108–115.

Kalargaris, I., Tian, G., & Gu, S. (2017). "Experimental evaluation of a diesel engine fuelled by pyrolysis oils produced from low-density polyethylene and ethylene–vinyl acetate plastics." *Fuel Process. Technol*, 161, 125–131.

Karagoz, M. (2020). "Investigation of performance and emission characteristics of a CI engine fuelled with diesel-waste tire oil-butanol blends", *Fuel*, 280,118-872.

Karagoz, M., Agbulut, U., Saridemir, S. (2020). "Waste to energy: production of waste tire pyrolysis oil and comprehensive analysis of its usability in diesel engine", *Fuel*, 275, 117-844.

Kawaharada, N., Thimm, L., Dageforde, T., Groger, K., Hasen, H., Dinkelacker, F. (2020). "Approaches for detailed investigations on transient flow and spray characteristics during high-pressure fuel injection, *Applied Sciences*, 10, 4410.

Kidoguchi, Y., Yang, C., & Miwa, K. (2000). "Effects of fuel properties on combustion and emission characteristics of a direct-injection diesel engine." *SAE Tech. Pap.*, 21, 469–475.

Kim, H. Y., Ge, J. C., Choi, N. J. (2020). "Effects of ethanol-diesel on the combustion and emissions from a diesel engine at low ideal speed." *Applied Sciences*, 10, 4153.

Kiss, A. A. (2014). "Distillation technology – still young and full of break through opportunities." *J. Chem. Technol.*, 89(4), 479-498.

Khaleque, M., Islam, M.R., Hossain, M.S., Khan, M., Rahman, M.S., Haniu, H. (2015). "Upgrading of waste tire pyrolysis oil to be used in diesel engine, *Proc. Int. Conference on Mechanical Engineering and Renewable Energy*, Chittagong, Bangladesh.

Khan, M. Z. H., Hossain, M. (2016). "Fuel properties of pyrolytic tire oil and its blend with diesel fuel- towards waste management." *Int J Environ Waste Manag*, 18(4), 335-348.

Koc, A.B, Abdullah, A. (2014). "Performance of a four cylinder diesel engine running on tire oil-biodiesel-diesel blend, *Fuel Process. Technol*, 118, 264-269.

Krishania, N., Rajak, U., Verma, T.N., Birru, A.K., Pughazendhi, A., "Effect of microalgae, tire pyrolysis oil and Jatropha enriched with diesel fuel on performance and emission characteristics of compression ignition engines", *Fuel*, 2020, 278, 118-252.

Kumaravel, S. T., Murugesan, A., & Kumaravel, A. (2016). "Tyre pyrolysis oil as an alternative fuel for diesel engines - A review." *Renew. Sustain. Energy Rev*, 60, 1678–1685.

Kumaravel, S.T., Murugesan, A., Vijayakumar, C., Thenmozhi, M. (2019). "Enhancing the fuel properties of tire oil diesel blends by doping nanoadditives for green environments." *J. Clean. Prod.*, 240, 118-128.

Laresgoiti, M. F., Caballero, B. M., Marco, I. D., Torres, A., Cabrero, M. A., Chomon, M. J. (2004). "Characterization of the liquid products obtained in tire pyrolysis." *J Anal Appl Pyrolysis*, 71(2), 917-934.

Lefebvre, A. H., McDonell, V. G. (2017). "Atomization and Sprays." Taylor and Francis, CRC Press.

Lewandowski, W.M., Januszewicz, K., Kosakowski, W. (2019). "Efficiency and proportions of waste tire pyrolysis products depending on the reactor type – A review." *J Anal Appl Pyrolysis*, 140, 25-53.

Lehto, J., Oasmaa, A., Solantausta, Y., Kytö, M., & Chiaramonti, D. (2013). *Fuel oil quality and combustion of fast pyrolysis bio-oils*, VTT Publications, 87-79.

Lei, T., Wang, Z., Chang, X., Lin, L., Yan, X., Sun, Y., Shi, X., He, X., & Zhu, J. (2016). "Performance and emission characteristics of a diesel engine running on optimized ethyl levulinate-biodiesel-diesel blends." *Energy*, 95, 29–40.

Lei, T., Wang, Z., Li, Y., Li, Z., He, X., & Zhu, J. (2013). "Performance of a diesel engine with ethyl levulinate-diesel blends: A study using grey relational analysis." *Bioresources*, 8(2), 2696–2707.

Leyan, J. M., Tormos, B., Salvador, B., Garger, K. (2009). "Comparative analysis of a direct-injected diesel engine fuelled with biodiesel blends during the European MVEG-A cycle: Preliminary study." *Biomass and Bioenergy*, 33(6-7), 941-947.

LHeywood, J. B. (2010). *Internal combustion engine fundamentals*. McGraw-Hill series in mechanical engineering.



- Li, W., Huang, C., Li, D., Huo, P., Wang, M., Han, L., Chen, G., Li, H., Li, X., Wang, Y., Wang, M. (2016). "Derived oil production by catalytic pyrolysis of scrap tire." *CHINESE J CATAL*, 37, 526-532.
- Lim, J. (2011). "Hedonic scaling : A review of methods and theory." *Food Qual Prefer*, 22, 733-747.
- Lindstrom, M. (2009). "Injector nozzle hole parameters and their influence on real direct-injected diesel engine performance." A graduate thesis submitted at KTH Industrial Engineering and Management, Stockholm.
- Liu, X.J., Wang, F., Zhai, L.L., Xu, Y.P., Xie, L.F., Duan, P.G. (2019). "Hydro-treating of waste engine oil and scrap tire blend for production of liquid fuel." *Fuel*, 249, 418-426.
- Lloyd, J. B. F. (1975). "Characterisation of rubbers, rubber contact traces, and tire prints by fluorescence spectroscopy." *Analyst*, 100(1187), 82-95.
- Ma, F., Zhao, C., Zhang, F., Zhao, Z., Zheng, Z., Xie, Z., Wang, H. (2015). "An experimental investigation on the combustion and heat release characteristics of an opposed-piston folded crank train diesel engine." *Energies*, 8, 6365-6381.
- Mahallawy, F. E. (2002). "Fundamentals and technology of combustion." Elsevier.
- Martínez, J. D., Lapuerta, M., García-Contreras, R., Murillo, R., & García, T. (2013). "Fuel properties of tire pyrolysis liquid and its blends with diesel fuel". *Energy Fuels*, 27(6), 3296-3305.
- Martinez, J.D., Veses, A., Montral, A.M., Murillo, R., Navarvo, M.V., Pug, N., Artigues, A., Bartrolli, J., Garcia, T. (2014). "Co-pyrolysis of biomass with waste tires: Upgrading of liquid biofuel." *Fuel Process. Technol*, 119, 263-271.
- Mascal, M., & Nikitin, E. B. (2010). "Co-processing of carbohydrates and lipids in oil crops to produce hybrid biodiesel." *Energy Fuels*, 24(3), 2170-2171.

Mastral, A.M., Murillo, R., Callen, M.S., Garcia, T., Snape, C.E. (2000). "Influence of process variable on oils from tire pyrolysis and hydrolysis in a swept fixed bed reactor." *Energy Fuels*, 14, 739-44.

McMurry, J. E., Fay, R. C., Chemistry, 978-0-321-94317, Pearson publications.

Miandad, R., Barakat, M.A., Rahaman, M., Aburiazaiza, A.S., Gardy, J., Nizami, A.S., "Effect of advanced catalyst on tire waste pyrolysis oil." *PROCESS SAF ENVIRON*, 2018, 116, 542-552.

Mohan, A., Dutta, S., & Madav, V. (2019). "Characterization and upgradation of crude tire pyrolysis oil (CTPO) obtained from a rotating autoclave reactor." *Fuel*, 250, 339-351.

Murphy, M. J., Taylor, J. D., & McCormick, R. L. (2004). *Compendium of Experimental Cetane Number Data*. National Renewable Energy Laboratory, August, 1–48.

Murugan, S., Ramaswamy, M. C., & Nagarajan, G. (2008). "The use of tire pyrolysis oil in diesel engines." *Waste Manage.*, 28(12), 2743–2749.

Murugan, S., Ramaswamy, M. C., & Nagarajan, G. (2014). "Erratum: A comparative study on the performance, emission, and combustion studies of a di diesel engine using distilled tire pyrolysis oil-diesel blends." *Fuel*, 87, 2111-2121.

Murugan, Sivalingam, Ramaswamy, M. R. C., & Nagarajan, G. (2008). "Influence of distillation on performance, emission, and combustion of a di diesel engine, using tire pyrolysis oil diesel blends." *Therm. Sci.*, 12(1), 157–167.

Mustafa, K. (2020). "Investigation on performance and emission characteristics of CI engine fuelled with diesel-waste tire oil-butanol blends." *Fuel*, 282, 118-872.

Muzyka, V., Veimer, S., & Schmidt, N. (1998). "Particle-bound benzene from diesel engine exhaust." *Scand. J. Work Environ. Health*, 24(6), 481-485.

Muzenda, E. (2014). "A discussion of waste tire utilization options." *Int. Conference on Research in Science, Engineering and Technology*, Dubai, UAE.

Muzenda, E. (2014). "A comparative review of waste tire pyrolysis, gasification and liquefaction process, Int. Conference on Chemical Engineering and Advanced Computational Technologies, Pretoria, South Africa.

Navarro, F.J., Partal, P., Martinez-Boza, F.J., Gallegos, C. (2010). "Novel recycled polyethylene/ground tire rubber/bitumen blends for use in roofing applications: thermomechanical properties." *Polymer Test.*, 29, 588-95.

Ngxangxa, S., Villiers, A. de, & Tredoux, A. (2016). "Development of GC-MS methods for the analysis of tire pyrolysis oils." Mtech thesis, Stellenbosch University, South Africa.

NIIR Board of consultant and Engineers, *Complete book on rubber processing and compound technology*, Asia Pacific Business Press Inc.

Obadiah, M., Alfayo, M., Leonard, M. (2017). "Characterization and evaluation of distilled tire pyrolysis oil and its potential as a supplement to diesel fuel." *Energy Sources*, 39, 51-57.

Odaka, M., Koike, N., Tsukamoto, Y., Narusawa, K., & Yoshida, K. (1991). "Effects of EGR with supplemental manifold water injection to control exhaust emissions from heavy-duty diesel-powered vehicles." *SAE Tech. Pap.*

Onorevoli, B., Machado, M. E., Polidoro, A. S., Corbelini, V. A., & Jacques, A. (2017). "Pyrolysis of Residual Tobacco Seeds : Characterization of Nitrogen Compounds in Bio-oil Using Comprehensive Two-Dimensional Gas Chromatography with Mass Spectrometry Detection." *Energy Fuels*, 31(9):9402-9407.

Pakdel, H., Roy, C. (1994). "Simultaneous gas chromatographic- fourier transform infrared spectroscopic- mass spectrometric analysis of synthetic fuel derived from used tire vacuum pyrolysis oil, naphtha fraction." *J. Chromatogr. A*, 683(1), 203-14.

Kidoguchi, Y., Yang, C., Kato, R., Miwa, K. (2000). "Effects of fuel cetane number and aromatics on the combustion process and emission process of a direct-injection diesel engine, *JSAE Review*, 21, 469-475.

Prasad, L., Pradhan, S., Das, L. M., & Naik, S. N. (2012). "Experimental assessment of toxic phorbol ester in oil, biodiesel and seed cake of *Jatropha curcas* and biodiesel in a diesel engine." *Appl. Energy*, 93, 245–250.

Pundlik Shivaji Ware. (2015). "Pyrolysis of waste tires and future." *Chem.*, 1(1), 1–9.

Quek, A., Balasubramanian, R. (2016). "Liquefaction of waste tire by pyrolysis for oil and chemicals – A review," *J Anal Appl Pyrolysis*, 101, 1-16.

Rajesh, Kumar, B., & Saravanan, S. (2015). "Effect of exhaust gas recirculation (EGR) on performance and emissions of a constant speed di diesel engine fueled with pentanol/diesel blends." *Fuel*, 160, 217–226.

Rao, G.V., Dutta, R. K. (2006). "Compressibility and strength behavior of sand-tire chip mixtures." *Geotech. Geol. Eng.*, 24(3), 711-724.

Rao, P. V., Rao, B. V. A. (2018). "Heat release rate, performance and vibrational analysis of diesel engine operating with biodiesel-triacetin additive blend fuels." *International Journal of Automobile Engineering Research and Development*, 8(2), 11-22.

Report on global ELT management – A global state of knowledge on collection rates, recovery routes and management methods, World Business Council for Sustainable Development, 2018.

*Report on revised technical guidelines on environmentally sound management of used tires, Basel Convention*, United Nations Environmental Programme, 2008.

Robler, M., Koch, T., Janzer, T., Olzmann, M. (2017). "Mechanism of NO<sub>x</sub> formation in diesel engines, *MTZ worldwide*, 78, 70-75.

- Sathiskumar, C., & Karthikeyan, S. (2019). "Recycling of waste tires and its energy storage application of by-products –a review." *SM&T*, 22, e00125.
- Schwarzenegger, A., Lloyd, A. C. (2006). *Report on Evaluation and economic analysis of waste tire pyrolysis, gasification and liquefaction*, Integrated Waste Management Board, University of California, Riverside, California.
- Sienkiewicz, M., Kucinska-Lipka, J., Janik, H., Balas, A. (2012). "Progress in used tire management in European Union: A review, *Waste Manage.*, 32, 1742-51.
- Sindhu, R., Rao, G. A. P., Murthy, K. M. (2018). "Effective reduction of NO<sub>x</sub> emission from a diesel engine using split injection, *Alexandria Engineering Journal*, 57, 1379-1392.
- Shahir, V. K., Jawahar, C. P., Vinod, V., & Suresh, P. R. (2020). "Experimental investigations on the performance and emission characteristics of a common rail direct injection engine using tire pyrolytic biofuel." *J. King Saud Univ. Eng. Sci.*, 32(1), 78–84.
- Sharma, A., (2017). "Investigation of a direct injected diesel engine run on non-petroleum fuel blends." PhD Thesis, National Institute of Technology Rourkela, Odisha.
- Sharma, V. K, Mincarini, M., Fortuna, F., Cognini, F., Cornacchia, G. (1998). "Disposal of waste tires for energy recovery and safe environment – review, *Energy Convers. Manag.*, 39, 511-528.
- Sharma, A., Murugan, S. (2015). "Potential for using a tire pyrolysis oil-biodiesel blend in a diesel engine at different compression ratios." *Energy Convers. Manag.*, 93, 289–297.
- <sup>a</sup>Sharma, A., <sup>b</sup>Sharma, A., Joshi, J. B., Jain, R. K., Kasilingam, R. K. (2021). "Application of high grade carbon produced from tire waste using advanced thermochemical technology." *Mater. Today*, <https://doi.org/10.1016/j.matpr.2021.01.589>.
- Shin, J., Kim, D., Seo, J., Park, S. (2020). "Effects of the physical properties of fuel on spray characteristics from a gas turbine nozzle." *Energy*, 205, 118090.
- Siddique, R., Naik, T.R., (2004). "Properties of concrete containing scrap tire rubber-an overview." *Waste Manage.*, 24, 563-9.

Simsek, S., Uslu, S., Costu, R. (2020). "A novel approach to study the effect of motor silk-added pyrolysis tire oil on performance and emission characteristics of a diesel engine." *Fuel*, 119-668.

Somri, S. (2018). "Upgrading of pyrolysis oil." Degree Project in Chemical Science and Engineering, KTH Royal Institute of Technology, Sweden.

Spitz, N. (2010). "Review, examination and comparison of alternatives for thermochemical conversion of municipal solid waste and scrap tire." Israel Ministry for Environmental Protection.

Strydom, R. (2017). "Enhanced waste tire pyrolysis for the production of hydrocarbon and petrochemicals, Ph.D. Thesis, Cape Peninsula University of Technology, Cape Town.

Tian, M., McCormick, R. L., Luecke, J., de Jong, E., van der Waal, J. C., van Klink, G. P. M., & Boot, M. D. (2017). "Anti-knock quality of sugar derived levulinic esters and cyclic ethers." *Fuel*, 202, 414–425.

Timpanaro, A. (2019). "Reduction of NO<sub>x</sub> emissions in a single-cylinder diesel engine using SNCR with an in-cylinder injection of aqueous urea, Graduate thesis and dissertations, University of North Florida.

Tretel, B. (2020). "Re-evaluating the jet breakup regime diagram." *Atomization and Sprays*, 30, 1-28.

Toraman, H. E., Dijkmans, T., Djokic, M. R., Van Geem, K. M., & Marin, G. B. (2014). "Detailed compositional characterization of plastic waste pyrolysis oil by comprehensive two-dimensional gas-chromatography coupled to multiple detectors." *J. Chromatogr. A*, 1359(x), 237–246.

Tonini, S., Gavaises, M., Theodorakakos, A. (2009). "The role of droplet fragmentation in high pressure evaporating diesel sprays." *International Journal of Thermal Sciences*, 48, 554-572.

Tudu, K., Murugan, S., & Patel, S. K. (2014). "Light oil fractions from a pyrolysis plant-An option for energy use." *Energy Procedia*, 54, 615–626.

Tudu, K., Murugan, S., & Patel, S. K. (2016a). "Effect of diethyl ether in a DI diesel engine run on a tire-derived fuel-diesel blend." *J. Energy Inst.*, 89(4), 525–535.

Tudu, K., Murugan, S., & Patel, S. K. (2016b). "Effect of the tire-derived oil-diesel blend on the combustion and emissions characteristics in a compression ignition engine with internal jet piston geometry." *Fuel*, 184, 89–99.

Tzanetakakis, T., Ashgriz, N., James, D. F., & Thomson, M. J. (2008). "Liquid fuel properties of a hardwood-derived bio-oil fraction." *Energy Fuels*, 22(4), 2725–2733.

Tziourtzioumis, D. N., Stamatelos, A. M. (2017). "Experimental investigation of the effect of biodiesel blend on direct-injected diesel engines injection and combustion." *Energies*, 10, 970.

Ucar, S., Karagoz, S. (2007). "Upgrading scrap tire-derived oil using activated carbon-supported metal catalyst." *Energy Sources, Part A: Recovery, Utilization and Environmental Effects*, 29: 425-437.

Ucar, S., Karagoz, S., "co-pyrolysis of pine nut with scrap tire." *Fuel*, 2014, 137, 85-93.

Ucar, S., Karagoz, S., Ozkan, A. R., Yanik, J. (2005). "Evaluation of two different scrap tire as hydrocarbon source by pyrolysis, *Fuel*, 84 (14-15), 1884-1892.

Umeki, E. R., Oliveira, C. F. D., Torres, R. B., Santos, R. G. D., "Physico-chemistry properties of fuel blends compared of diesel and tire pyrolysis oil." *Fuel*, 185, 236-242.

Undri, A., Rosi, L., Frediani, M., Frediani, P. (2014). "Upgraded fuel from microwave-assisted pyrolysis of the waste tire." *Fuel*, 2014, 115, 600-8.

Unlu, D., Boz, N., Ilgen, O., Hilmioglu, N. (2018). "Improvement of fuel properties of biodiesel with bio additive ethyl levulinate." *Open Chem.*, 2018, 16, 647-652.

Uyumaz, A., Aydoğan, B., Solmaz, H., Yılmaz, E., Yeşim Hopa, D., Aksoy Bahtli, T., Solmaz, Ö., & Aksoy, F. (2019). "Production of waste tire oil and experimental investigation on combustion, engine performance, and exhaust emissions." *J. Energy Inst.*, 92(5), 1406–1418.

Verduzco, L. F. R., Rodriguez, J. E. R., Jacob, A. D. R. J. "Predicting cetane number, kinematic viscosity, density and higher heating value of biodiesel from its fatty acid methyl ester composition, *Fuel*, 2012, 91, 102-111.

Verma, P., Zare, A., Jafari, M., Bodisco, T. A., Rainey, T., Ristovski, Z. D. & Brown, R. J. (2018). "Diesel engine performance and emissions with fuels derived from waste tires." *Sci. Rep.*, 8(1),1–13.

Vihar, R., Seljak, T., Rodman Oprešnik, S., & Katrašnik, T. (2015). "Combustion characteristics of tire pyrolysis oil in turbocharged compression ignition engine." *Fuel*, 150, 226–235.

Vozka, P., & Vrtis, D. (2019). "Impact of Alternative Fuel Blending Components on Fuel Composition and Properties in Blends with Jet A." *Energy Fuels*, 33, 3275-3289.

Wamankar, A. K., & Murugan, S. (2014). "Experimental investigation of carbon black-water-diesel emulsion in a stationary DI diesel engine." *Fuel Process. Technol.*, 125, 258–266.

Wang, X., Cheng, V. W., Li, Z., Chen, Z., Wang, Y. (2021). "Co-pyrolysis of sewage sludge and organic fraction of municipal solid waste: synergistic effects on biochar properties and environmental risk of heavy metals." *J. Hazard. Mater.*, 412, 125-200.

Ware, R. L., Rowland, S. M., Lu, J., Rodgers, R. P., & Marshall, A. G. (2018). "Compositional and Structural Analysis of Silica Gel Fractions from Municipal Waste Pyrolysis Oils." *Energy Fuels*, 32, 7752–7761.

Walacik, M. A., Pietak, A. (2016). "Spectrofluorometric characterization of oil from pyrolysis of scrap tires, *Journal of KONES*, 23(1).



Williams, P. T., Brindle, A. J. (2002). "Catalytic pyrolysis of tire : Influence of catalyst temperature" *Fuel*, 81, 2425-2434.

Williams P.T., Brindle A.J. (2003). "Fluidized bed pyrolysis and catalytic pyrolysis of scrap tires." *Environ. Technol*, 24, 921-929.

Williams, P. T. (2013). "Pyrolysis of waste tires: A review." *Waste Manage.*, 33(8), 1714–1728.

Williams, P. T., & Taylor, D. T. (1993). "Aromatization of tire pyrolysis oil to yield polycyclic aromatic hydrocarbons." *Fuel*, 72(11), 1469–1474.

Williams, P. T., Beseler, S. (1995). "Pyrolysis thermo-gravimetric analysis of tires and tire components." *Fuel*, 74, 1277-1283.

Xin, J., Ricert, L., Reitz, R. D. (2014). "Computer modelling of diesel spray atomization and combustion." *Combustion Science and Technology*, 137 (1-6), 171-194.

Yilmaz, N., & Atmanli, A. (2017). "Experimental evaluation of a diesel engine running on the blends of diesel and pentanol as a next-generation higher alcohol." *Fuel*, 210 (8), 75–82.

Yuwapornpanit, R., Jitkarnka (2015). "Cu-doped catalyst and their impacts on tire-derived oil and sulfur removal." *J Anal Appl Pyrolysis*, 111, 200-8.

Ziadat, A. H., Sood, E. (2014). "An environmental impact assessment of open burning of scrap tires, *J. Appl. Sci.*, 14(21), 2695-2703.

## Web references

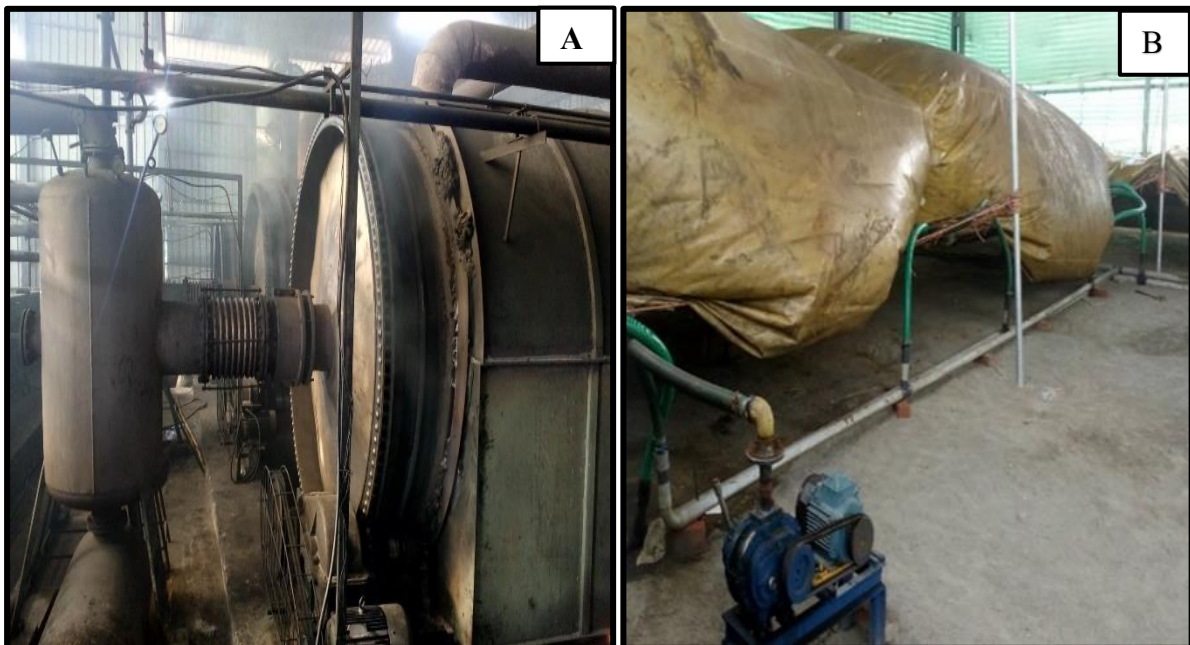
- URL 01 <https://shaktifoundation.in/report/roadmap-standards-labelling>  
Road map for Standards and Labelling Programmes for Tires in India.
- URL 02 <https://www.lobachemie.com/>  
Properties of Silica gel and Petroleum ether
- URL 03 <https://www.sigmaaldrich.com/>  
Properties of Ethyl Levulinate
- URL 04 [http://petroleum.nic.in/sites/default/files/ipngstat\\_0.pdf](http://petroleum.nic.in/sites/default/files/ipngstat_0.pdf)  
Indian Petroleum and Natural gas Statistics 2017-2018.
- URL 05 [http://ipindia.gov.in/writereaddata/Portal/IPOJournal/1\\_4811\\_1/Part-2.pdf](http://ipindia.gov.in/writereaddata/Portal/IPOJournal/1_4811_1/Part-2.pdf)  
Patent on Method, System and Apparatus for upgrading Tire Pyrolysis oil.

## APPENDIX I

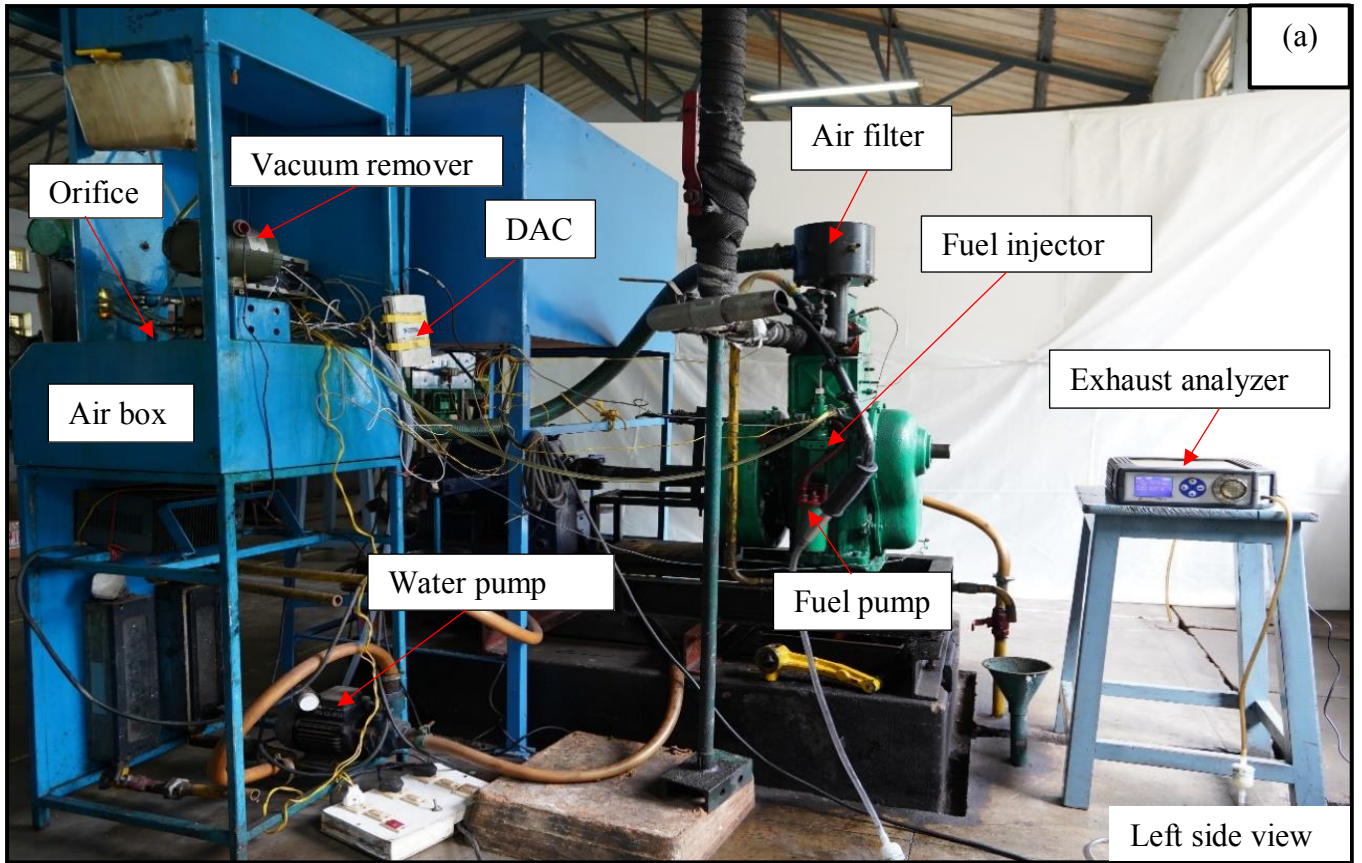
### Photographs and experimental setup used in present study



**Fig. I-1 Photograph of 10-ton tire pyrolysis plant**



**Fig. I-2 (a) Rotating autoclave reactor (b) Gas storage facility**



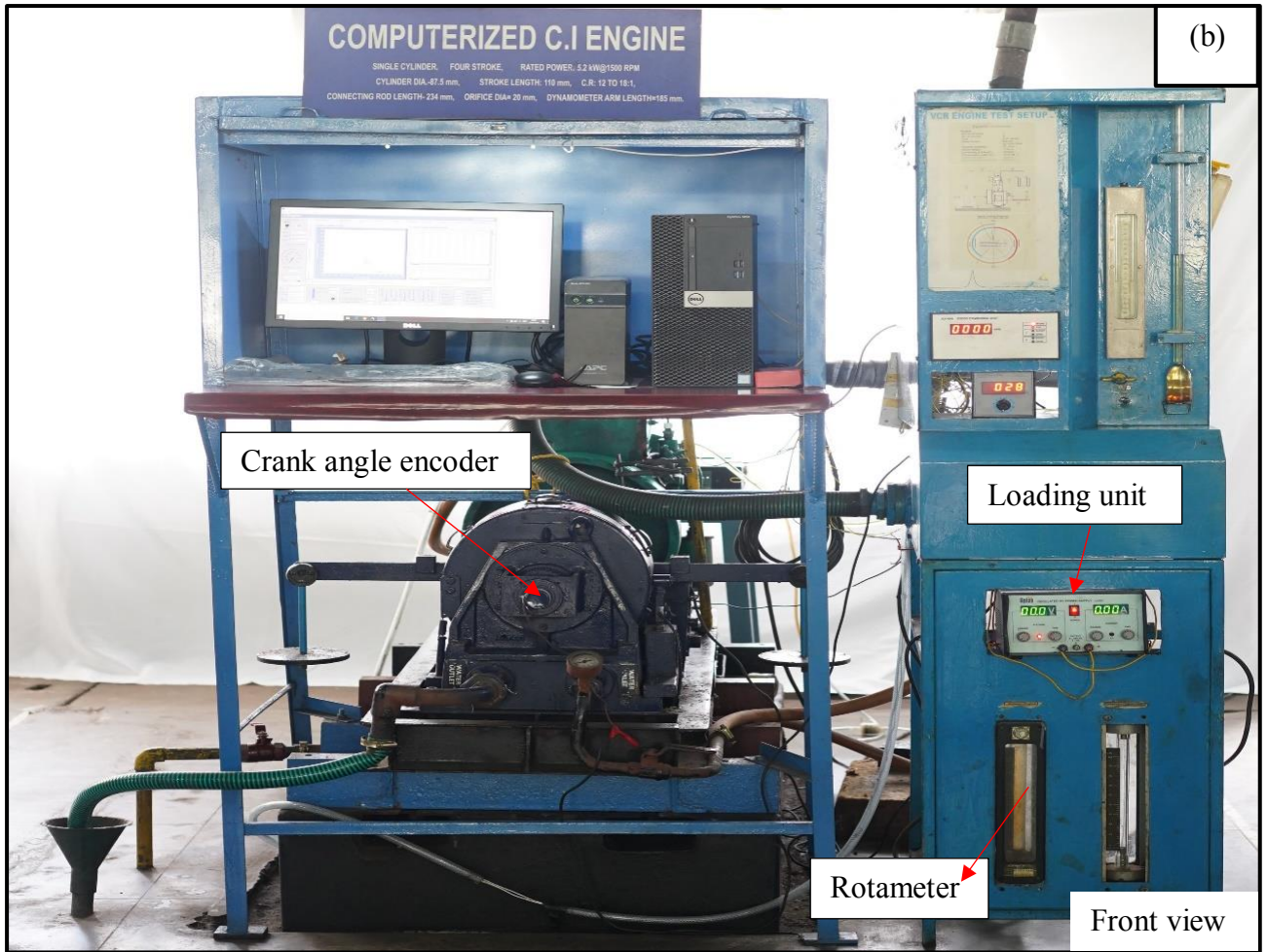


Fig. I-3 (a) Left side view and (b) front view of single cylinder diesel engine test facility

## APPENDIX II

### LIST OF TABLES

**Table II-1 Major compounds detected in CTPO using GC-MS**

<b>Molecular formula</b>	<b>Retention time (R.T)</b>	<b>Identified compounds</b>	<b>Peak area percentage (%)</b>
C <sub>8</sub> H <sub>10</sub>	4.9	1,3- Dimethyl benzene	2.99
C <sub>9</sub> H <sub>20</sub>	5.35	n-Nonane	4.98
C <sub>10</sub> H <sub>22</sub>	7.53	Decane	4.98
C <sub>10</sub> H <sub>16</sub>	8.34	Limonene	7.606
C <sub>11</sub> H <sub>24</sub>	9.66	Undecane	5.037
C <sub>12</sub> H <sub>26</sub>	11.65	Dodecane	3.761
C <sub>17</sub> H <sub>36</sub>	11.83	Tetradecane	0.247
C <sub>15</sub> H <sub>36</sub>	11.97	n-pentadecane	0.247
C <sub>16</sub> H <sub>34</sub>	15.22	Hexadecane	4.112
C <sub>17</sub> H <sub>36</sub>	16.66	Heptadecane	4.97
C <sub>17</sub> H <sub>36</sub>	16.84	2,6,10 trimethyltetradecane	3.377
C <sub>17</sub> H <sub>36</sub>	17.06	2,6,10-trimethyltetradecane	10.918
C <sub>16</sub> H <sub>34</sub> S	18.35	Tert-hexadecanethiols	0.33
C <sub>27</sub> H <sub>56</sub>	19.81	Heptaacosane	5.31
C <sub>21</sub> H <sub>44</sub>	21.24	Heneicosane	5.31
C <sub>8</sub> H <sub>10</sub>	22.91	1,3- Dimethyl benzene	2.99
C <sub>9</sub> H <sub>20</sub>	23.14	n-Nonane	4.98
C <sub>10</sub> H <sub>22</sub>	25.17	Decane	4.98
C <sub>11</sub> H <sub>24</sub>	27.57	Undecane	5.037

**Table II-2 Major compounds detected in CoTPO using GC-MS**

<b>Molecular formula</b>	<b>Retention time (R.T)</b>	<b>Identified compounds</b>	<b>Peak area percentage (%)</b>
C <sub>8</sub> H <sub>10</sub>	6.05	Ethyl benzene	1.32
C <sub>8</sub> H <sub>10</sub>	6.27	Ethyl benzene	1.32
C <sub>9</sub> H <sub>9</sub> BrO	6.77	Benzene propanoyl bromide	2.161
C <sub>12</sub> H <sub>20</sub> O <sub>2</sub>	7.67	Isopulegol acetate	1.317
C <sub>10</sub> H <sub>16</sub>	8.06	Limonene	0.642
C <sub>9</sub> H <sub>12</sub>	8.28	Benzene,1-ethyl-3-methyl	2.079
C <sub>10</sub> H <sub>18</sub> O	8.64	3,6-octadien-1-ol	2.925
C <sub>12</sub> H <sub>20</sub> O <sub>2</sub>	9.73	Cyclohexane	2.056
C <sub>12</sub> H <sub>20</sub> O <sub>2</sub>	10.88	6-isopropenyl-3-methoxymethoxy-3methyl-cyclohexane	1.708
C <sub>18</sub> H <sub>28</sub> O <sub>2</sub>	11.36	10,12-Octadecadiynoic acid	10.83
C <sub>13</sub> H <sub>18</sub> O	12.32	Oxacyclotetradeca-4,11-diyne	1.303
C <sub>11</sub> H <sub>14</sub>	13.19	Benzene,1-methyl-3-91-methyl-2-propenyl	4.207
C <sub>17</sub> H <sub>24</sub> O	15.57	Falcarinol	0.741
C <sub>14</sub> H <sub>20</sub>	16.46	Oct-3-ene-1,5-diyne	2.409
C <sub>18</sub> H <sub>24</sub> O <sub>2</sub>	17.44	5,8,11- Heptadecatriynoic acid, methyl ester	3.249
C <sub>18</sub> H <sub>24</sub> O <sub>2</sub>	17.95	5,8,11- Heptadecatriynoic acid, methyl ester	3.249
C <sub>13</sub> H <sub>14</sub>	19.11	3-(2-methyl-propenyl)-1H-indene	21.284
C <sub>18</sub> H <sub>24</sub> O <sub>2</sub>	19.39	5,8,11-Heptadecatriynoic acid	1.553
C <sub>33</sub> H <sub>54</sub> O <sub>3</sub>	20.89	Cholest-22-ene-21-ol,3,5-dehydro-6-methoxy	1.274

**Table III-3 Major compounds detected in StTPO using GC-MS**

<b>Chemical Formulae</b>	<b>Retention time (R.T)</b>	<b>Compound</b>	<b>Peak area %</b>
C <sub>7</sub> H <sub>8</sub>	4.27	Toluene	0.843244985
C <sub>8</sub> H <sub>10</sub>	6.17	Ethyl benzene	1.542131347
C <sub>9</sub> H <sub>10</sub>	6.41	p-xylene	2.332892484
C <sub>9</sub> H <sub>10</sub>	6.99	p-xylene	1.313354103
C <sub>9</sub> H <sub>12</sub>	7.71	Benzene(1-methylethyl)	1.094468925
C <sub>12</sub> H <sub>20</sub> O <sub>2</sub>	8.08	Isopulegol acetate	0.601258225
C <sub>9</sub> H <sub>12</sub>	8.55	Benzene, 1-methyl-3 methyl	1.256140296
C <sub>9</sub> H <sub>12</sub>	8.83	Benzene, 1-methyl-3 methyl	2.024109246
C <sub>14</sub> H <sub>20</sub> O	9.25	Cyclopentanol, (1-methylene 2-propenyl)	1.600520956
C <sub>9</sub> H <sub>12</sub>	9.7	Benzene, 1,3,5-trimethyl	11.85896143
C <sub>12</sub> H <sub>20</sub> O <sub>2</sub>	10.62	Cyclohexene 4-isopropenyl-1-methoxymethoxymethyl	11.85896143
C <sub>12</sub> H <sub>20</sub> O <sub>2</sub>	11.32	6-Isopropenyl-3 methoxymethoxy-3methyl-cyclohexene	1.70656674
C <sub>10</sub> H <sub>16</sub>	12.08	3- Carene	1.70656674
C <sub>10</sub> H <sub>12</sub>	12.3	Benzene, 4-ethenyl-1,2-dimethyl	0.653517938
C <sub>13</sub> H <sub>18</sub> O	13.91	Oxacyclotetradeca- 4,11-diyne	1.55305138
C <sub>11</sub> H <sub>14</sub>	14.83	Benzene, 1-methyl-3-(1-methyl-2-propenyl)	0.515857043
C <sub>11</sub> H <sub>14</sub>	15.05	Benzene, 1-methyl-3-(1-methyl-2-propenyl)	0.945629436
C <sub>17</sub> H <sub>24</sub> O	18.2	Flacarinol	1.520802606
C <sub>14</sub> H <sub>20</sub>	19.36	Oct-3-ene-1,5-diyne,3-t-butyl-7,7-dimethyl	41.3980
C <sub>22</sub> H <sub>32</sub> O <sub>2</sub>	21.3	Retinol, acetate	1.400638829
C <sub>13</sub> H <sub>14</sub>	22.83	3-(2-methyl-propenyl)-1H-indene	1.062860372
C <sub>17</sub> H <sub>36</sub>	25.31	Tetradecane-2,6,10-trimethyl	0.153456643
C <sub>15</sub> H <sub>17</sub> BrO	26.43	4a-10a-methanophenanthren-9-β-ol,11-syn-bromo-1,2,3,4,4a,9,10,10a-octahydro	0.916261883
C <sub>13</sub> H <sub>16</sub> N <sub>4</sub> O <sub>6</sub>	40.52	2-Acetoxyptental 2,4-dinitrophenyl hydrazine	0.577910299



APPENDIX III  
LIST OF FIGURES

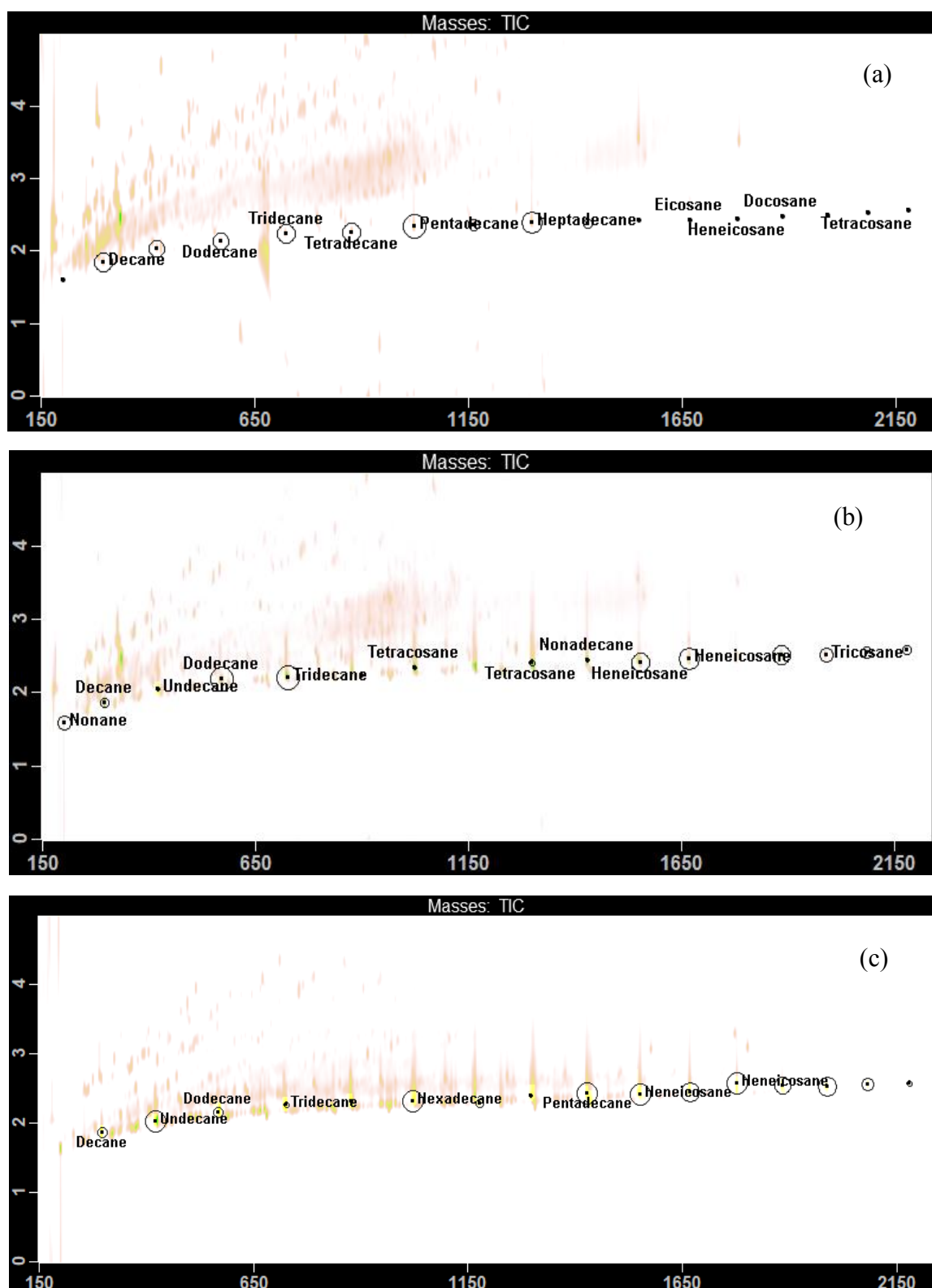


Fig. III-1 Chromatogram of saturates (n-alkanes) in (a) CTPO, (b) StTPO and (c) diesel

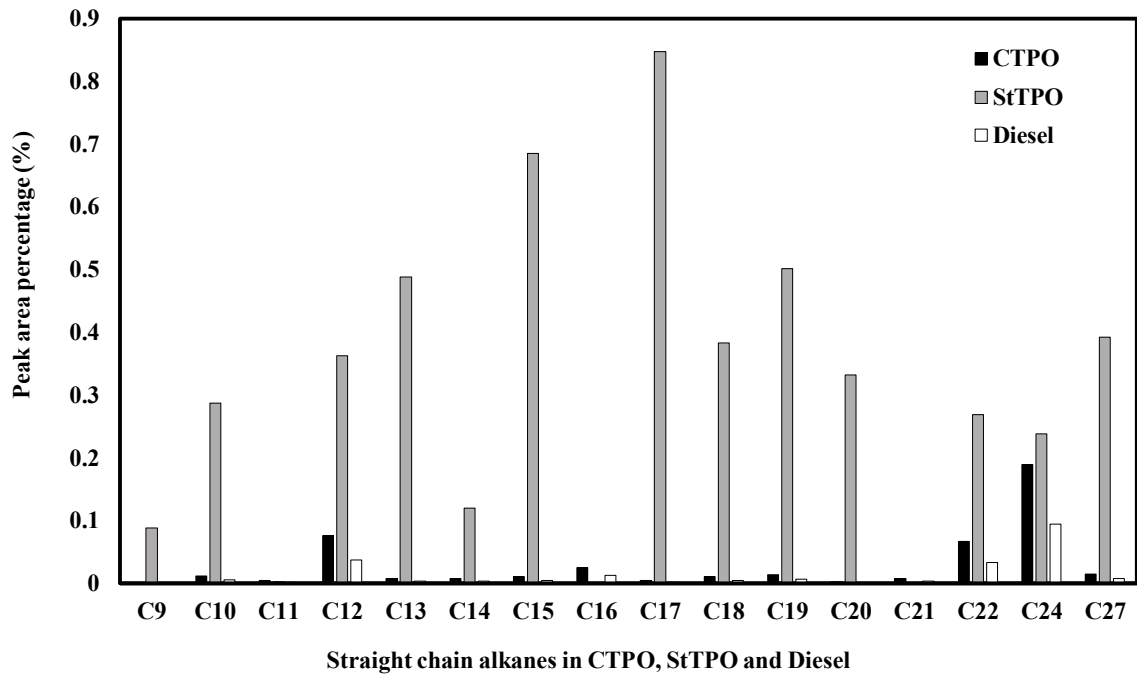


Fig. III-2 Peak area percentage of carbon atoms in StTPO and diesel

**LIST OF PUBLICATIONS BASED ON Ph.D. RESEARCH WORK**

<b>Sl. No.</b>	<b>Title of the paper</b>	<b>Authors (in the same order as in the paper. Underline the Research Scholar's name)</b>	<b>Name of the Journal/ Conference, Vol., No., Pages</b>	<b>Month, Year of Publication</b>	<b>Category *</b>
1.	Method, system and apparatus for upgrading tire pyrolysis oil	<u>Akhil Mohan</u> , Saikat Dutta, Vasudeva Madav	<a href="https://ipindiaservices.gov.in/publicsearch">https://ipindiaservices.gov.in/publicsearch</a> (Patent No. 347787)	September, 2020	1
2.	Characterization and upgradation of crude tire pyrolysis oil from a rotating autoclave reactor	<u>Akhil Mohan</u> , Saikat Dutta, Vasudeva Madav	Fuel (DOI: 10.1016/j.fuel.2019.03.139), 250, 339-351 (IF – 5.578)	April, 2019	1
3.	Liquid fuel from waste tires: Novel Refining, Advanced Characterization and Utilization in engines with ethyl levulinate as an additive	<u>Akhil Mohan</u> , Saikat Dutta, Saravanan Balusamy, Vasudeva Madav	RSC Advances (DOI: 10.1039/d0ra08803j) 11, 9807-9826 (IF – 3.119)	March, 2021	1
4.	Novel upgrading of tire pyrolysis oil into diesel range fuels: process scale up and study of fuel properties	<u>Akhil Mohan</u> , Saikat Dutta, Vasudeva Madav	National Conference on Energy and Chemicals from Biomass (NCECB), Pondicherry Engineering College, Pondicherry	October, 2019	4
5.	Studies on the chemical composition and physicochemical characterization of upgraded tire pyrolysis oil for application in engine and furnace	<u>Akhil Mohan</u> , Saikat Dutta, Vasudeva Madav	9 <sup>th</sup> International Conference on IGCC and XtL Technologies, Freiberg, Institute of Energy Process Engineering and Chemical Engineering, Germany	June, 2018	4

6.	Studies on the chemical composition and physicochemical properties of tire pyrolytic oil for its application in furnace and engines	<u>Akhil Mohan</u> , Saikat Dutta, Vasudeva Madav	International Conference on Energy and Environment, National Institute of Technology, Calicut	March, 2018	4
----	---	---	---	-------------	---

\*Category: 1: Journal paper, full paper reviewed 2: Journal paper, Abstract reviews 3: Conference / Symposium paper, full paper reviewed 4: Conference /Symposium paper, abstract reviewed 5: Others (including papers in Workshops, NITK Research Bulletins, Short notes etc.).

## BIO-DATA

**Name** : AKHIL MOHAN  
**Date of Birth** : 19-06-1992  
**Residence address** : S/O Mohanan Pillai S  
: Sivodayam house  
: Puthoor P.O  
: Kollam – 691507  
**Phone Number** : +91-7349765162  
**E-mail ID** : [akhil.177me001@nitk.edu.in](mailto:akhil.177me001@nitk.edu.in)  
[akhilmohanmechanical1@gmail.com](mailto:akhilmohanmechanical1@gmail.com)



### Education

Programme	Department/Specialization	Institute	University	CGPA
B-Tech	Mechanical Engineering	YCET, Kollam	Kerala	8.22
M-Tech	Energy Systems Analysis and Design	GEC, Calicut	KTU	8.68
Ph.D.	Waste to energy	NITK, Surathkal	NITK	9.08

### Research interests

Waste to Energy conversion, Pyrolysis of polymers, Biofuels, IC Engine, Particulate studies and Emission control, Catalysis, Carbon dioxide capture, Radiofrequency pyrolysis, Photo catalysis.

### Awards and Recognition

1. “**Innovative Researcher in Pyrolysis 2020**” is awarded by International Research Leadership Award, World Research Council
2. **Best oral presentation award** for the paper entitled “Novel upgrading of crude tire pyrolysis oil to diesel range fuels: Process scale up and study of fuel properties”, presented at AICTE sponsored National Conference on Energy and Chemicals from Biomass, held during 10-11<sup>th</sup> October 2019, organized by Department of Mechanical Engineering and Department of Chemical Engineering, Pondicherry Engineering College, Pondicherry